Load Modelling for Steady-State and Transient Analysis of Low Voltage dc Systems

Einar Pálmi Einarsson
Bengt-Olof Wickbom

CHALMERS

Thesis for the Degree of Master of Science, November 2004

Department of Electric Power Engineering
Chalmers University of technology
Göteborg, Sweden

ISSN 1401-6184
M.Sc. No. 109E

Title

Load Modeling for Steady-State and Transient Analysis of Low Voltage dc Systems

Title in swedish

Lastmodellering för stationär och transient analys av likströmsbaserade lågspänningsnät

Authors

Einar Pálmi Einarsson
Bengt-Olof Wickbom

Publisher

Chalmers University of Technology
Department of Electric Power Engineering
SE-41296 Göteborg, Sweden

ISSN

1401-6184

M.Sc. Thesis No.

109E

Subject

Power Systems

Examiner

Ambra Sannino

Date

November 18, 2004

Printed by

Chalmers University of Technology
SE-41296 Göteborg, Sweden

Abstract

In this thesis, common loads used in low-voltage residential and commercial power systems are investigated when supplied with dc. There steady-state and transient behavior is characterized, in order to build simple models suitable for computer simulation with PSCAD/EMTDC.

Laboratory measurements were carried out on various loads that were categorized in resistive, rotating and electronic loads. From these measurements it was possible to characterize the steady-state behavior of loads. To indicate how much the load disturbs the network, the frequency spectrum was analyzed. To be able to analyze the transient response of the loads, a voltage reduction circuit was designed and constructed. The loads were subjected to several voltage steps in order to derive a simple dynamic model.

Another objective of this work was to study the load sensitivity to voltage variations, in particular voltage dips, with dc supply and then compare the result to the same voltage variation in ac.

The models developed in this thesis can be used for load flow, voltage dip and short circuit current calculations in a low voltage dc distribution system.

Keywords: Load modeling, low-voltage power dist system, direct current (dc), voltage dip (sag), load tolerance, domestic appliances, electro magnetic trans simulation.

Acknowledgements

This work has been carried out at the Department of Electric Power Engineering, Chalmers University of Technology in Göteborg.

We would like to thank our supervisors Ass. Prof. Ambra Sannino and Daniel Nilsson for their support and encouragement during the work, despite their busy schedule. Thanks for all the Friday, after five, meetings. We also wish to thank Massimo Bongiorno for all the help and support.

We like specially to thank Göran Wennerström at Wennerström Ljuskontroll AB, for his generous contributions, Mats Barkell at Telamp AB for his contribution and Jan-Olof Lantto at the Department of Electric Power Engineering for his contributions.

We like to thank Prof. Gunnar Engered at the Department for Radio and Space Science for his help and Stefan Svensson at SP for his help on the measuring techniques.

We wish to thank Jan Hendén and Jonas Nordström for all the fun lunch sessions and also František Kinčeš and Cai Rong for their patience having us in the same office.

Final we like to thank each other for the work well done and wish each other a prosperous working life.

Einar Pálmi Einarsson would like to thank his father Einar Pálmi Jóhannsson for his moral support.

Bengt-Olof Wickbom would like to thank his family and specially his fiance Aranzazu Muñoz Luengo for all the support throughout the years.

Contents

List of Tables

List of Figures

Chapter 1

Introduction

This chapter will give a general description about the role of direct current in today's power systems, present briefly the background to this thesis and explain the outline of the thesis.

1.1 Background

In the end of the 19th century, direct current, dc, was replaced by alternating current, ac, for normal commercial power transmission. The main reasons were the possibility to transform the voltage to higher levels used for long-distance transmission and the invention of three-phase generators and motors [1] [2]. In the 1960's the thyristor was invented. Power semiconductor technology solved the problem of inefficient transformation between voltage levels in dc. Furthermore the price of these devices have gone down rapidly in recent years, which makes it more interesting from an economical point of view [3].

Today, due to recent developments, the electric power industry clearly indicates an increasing usage of dc at end-user equipment level, see Fig. 1.1 [4]. In an ac distribution system, generation units like solar- and fuel cells, that generate energy at dc, can be connected to the ac power grid via inverters. Other generation units like micro turbines generate ac but needs a two-stage (ac/dc and dc/ac) conversion in order match the grid frequency.

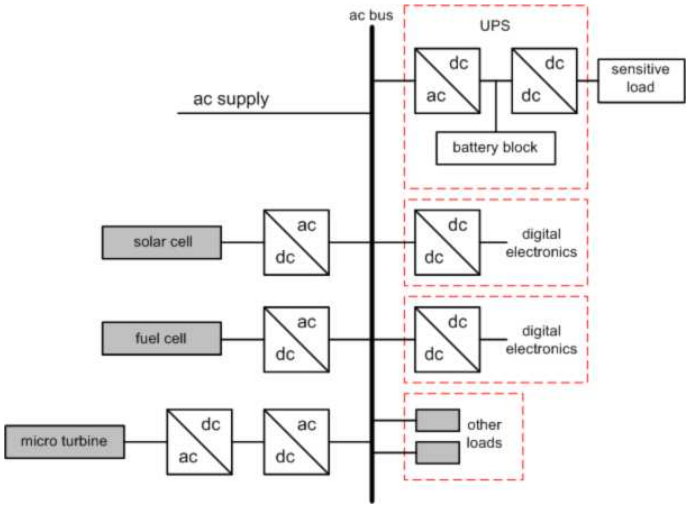

Figure 1.1: Scheme of existing ac low-voltage distribution system.

Most office and household loads have a single phase rectifier converting ac to dc that causes disturbances to the ac grid. From a power quality perspective disturbances in a power grid should be kept at minimum level. An example of improving the power quality and reliability is a Uninterruptible Power System (UPS). This device consists of a rectifier, a battery block and an inverter which will keep sensitive loads operational when interruption occurs, thereby providing so called uninterruptible power [5].

A Ph.D. project is currently carried out at the Department of Electric Power Engineering at Chalmers University of Technology, which concerns the analysis of dc systems. The aspects under study are choice of voltage levels, voltage control, transformation between different voltage systems (dc/ac, ac/dc) etc. With a dc distribution system, see Fig. 1.2, it may be possible to achieve a more efficient use of electricity at end-user equipment, easier incorporation of renewable energy sources and reduction in losses among other things [6].

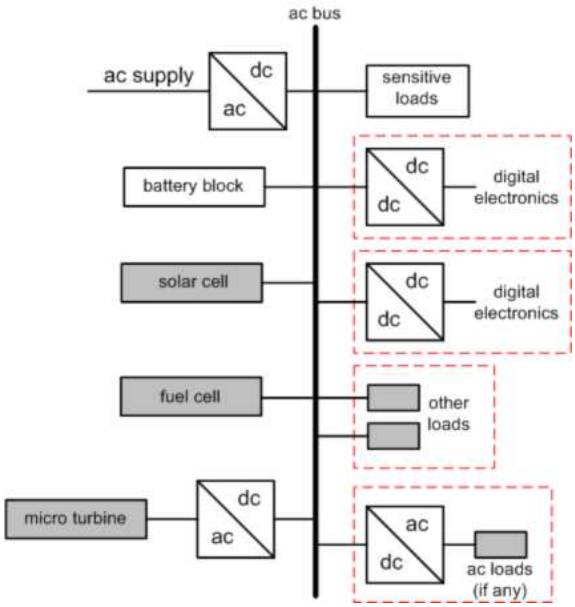

Figure 1.2: A possible dc distribution system.

In order to construct a suitable model for the analysis of a dc distribution system, it is necessary to have accurate models of the loads. These models should describe both steady-state and transient behavior when the load is supplied with dc.

1.2 Objectives

The purpose of this M.Sc. thesis is to test a number of commonly used loads found in households and offices in order to determine whether they would function satisfactory when supplied with dc, characterize the steady-state and transient behavior of the loads and build simple and suitable models for computer simulation with PSCAD/EMTDC which describe this behavior. Another objective of this work was to study the load sensitivity to voltage variations, in particular voltage dips, with dc supply and then compare the result to the same voltage variation in ac.

The loads tested in this thesis are tabulated in Table 1.1.

Load	Amount
Battery recharger (Mobile)	3
Blender	1
Clock radio	1
Coffee machine	2
Computer	4
Curling iron	1
Electric stove	1
Electric whisk	2
Electronic transformer for halogen lamps	2
Energy saving lamp	8
Fan	1
Fluorescent lamp with chock ballast	2
Fluorescent lamp with electronic ballast	3
Hair dryer	2
Hair trimmer	2
Incandescent lamp	26
Ip telephone	1
Juice press	1
Kettle	2
Loud speakers	1
Monitor (CRT)	1
Monitor (LCD)	1
Printer (Inkjet)	2
Refrigerator/freezer	1
Sandwich maker	2
Satellite receiver	1
Steam iron	1
Tungsten halogen lamp	2
TV	1
Vacuum cleaner	3

Table 1.1: List of loads tested.

1.3 Methodology

The research methodology used in this master thesis was literature reviews of published research papers found in databases such as Inspec and IEEE as well as theses, standards, books and other reliable information found on the internet. Interviews and consultations about specific topics related to the work have been made with personal at the Department of Electric Power Engineering. Data acquisition was done with an oscilloscope through the measurement configuration described in Chapter 2. Devices used to obtain measurements of transient behavior and sensitivity tests of the loads were designed and built by the authors of this thesis. The data processing and analysis was done with MATLAB 6.5. The simulations performed throughout the work were based on models developed and realized in EMTDC, which is a Fortran-based power-network simulation program.

1.4 Outline

The outline of this thesis is as follows:

Chapter 1 (this chapter) gives an introduction to this work.

Chapter 2 describes the theory background, the measurement setup and procedure.

Chapter 3 consists of the measurement results and models for steady-state and transient behavior of the resistive loads.

Chapter 4 describes the measurement and modelling result for steady-state and transient behavior of the rotating loads.

Chapter 5 presents the result of the measurement and modelling result for steady-state and transient behavior of the electronic loads.

Chapter 6 gives the result of the sensitivity measurements and analysis.

Chapter 7 presents the conclusions drawn of this thesis.

Chapter 2

Measurements and Analysis

This chapter will cover the measurement and data analysis procedures used for this thesis. It will also describe the different measurement setups and the equipment used for obtaining the data.

2.1 Measuring Procedure

All the loads were first tested on ac, i.e under normal operation conditions. From that it was estimated if they would function properly on dc. The loads which were determined to work on dc, were subjected to dc input voltage of different magnitudes in order to determine a relation between current and voltage. The frequency spectrum of the loads was analyzed under steady-state condition with nominal voltage. At last the loads were subjected to a fast voltage reduction to determine the transient behavior. The following subsections will describe how the measurement data was retrieved for each load for each test mentioned above.

The instruments used for the measurements are listed in Table 2.1 together with their rated error according to their manufacturer [7] [8]. The inaccuracies have been taken into account throughout the work.

Instrument	Quantity	Accuracy	Range
LeCroy Current Probe AP011	Current	±1%	dc−120 kHz
LeCroy Differential Probe AP032	Voltage	±2%	dc−15 MHz
Fluke 77	Voltage	±0.3%	-
Fluke 87	Current	±0.2%	-

Table 2.1: Measurement accuracy and frequency range for the instruments used.

The oscilloscope used throughout the work was a LeCroy 9304 CM with a bandwidth of 200 MHz, which gives a maximum sample rate of 100 MS/s. The data was then transmitted via a data communication cable to a computer which could also control the oscilloscope.

2.1.1 AC Measurements

The scope of these measurements is to determine whether the loads would operate satisfactory supplied with dc. There are loads whose major requirement to function is a variable

field, for instance transformers or single phase induction motors etc. These would otherwise saturate in dc, lose their operation principle which may lead to failure, i.e short circuit, or simply not perform their function. One way to estimate if the loads would function properly on dc is to measure the true power factor, PF, and the displacement power factor, DPF, of the load. Those are defined according to

$$PF = \frac{I_{s1}}{I_s}\cos(\phi_1) \tag{2.1}$$

$$DPF = \cos(\phi_1) \tag{2.2}$$

where the angle ϕ_1 is the angle between the fundamental component of voltage and the current, i.e. at 50 Hz. I_{s1} is the RMS value of the fundamental frequency component of the current and I_s is the total RMS current. Equation 2.1 is called the true power factor while Eq. (2.2) is called the displacement power factor [3] [9]. If the displacement power factor is close to unity, then the load is assumed to function on dc.

The voltage and current was measured using the measuring setup show in Fig. 2.1.

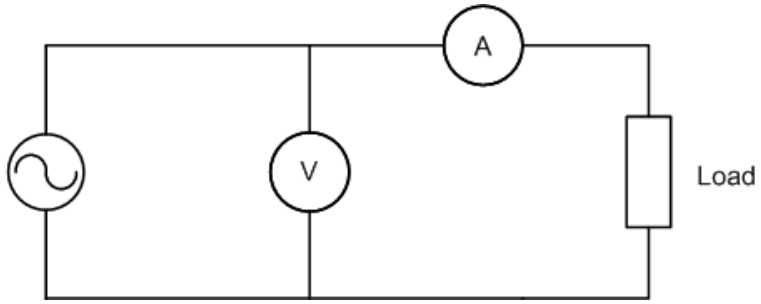

Figure 2.1: Measurement setup for ac measurements.

Furthermore the total harmonic distortion, THD, was calculated which is defined as

$$THD = \frac{\sqrt{\sum_{k=2}^{n} x_k^2}}{X_1} \cdot 100\ \% \qquad \text{where } k = 2, 3, \ldots, n \tag{2.3}$$

where x_n is the n^{th} frequency component and X_1 is the fundamental frequency component. This expression holds for both voltage and current signals. This quantity indicates how much the loads are disturbing the system [10].

2.1.2 DC Steady-State Measurements and Characterization

To characterize the loads, relation between current and voltage was measured. First the loads were categorized according to their operation principle and of which components they were made of. These categories are resistive loads, e.g. simple resistors, rotating loads, e.g. motors, and electronic loads, which consists of passive and active components. The measurement setup is shown in Fig. 2.2, where the dc source is variable. In this measurement setup the Fluke 77 and Fluke 87 were used for voltage and current measurements respectively. Two capacitors of 3300 µF each were shunt connected to the source for smoothing the voltage. To obtain the current relation to the voltage, the voltage was varied from 50 V to 380 V and the values measured by the two Flukes were recorded. The voltage range was not applicable to all the loads, simply because some of them either shut off, restarted or drew a very high current which could lead to malfunction.

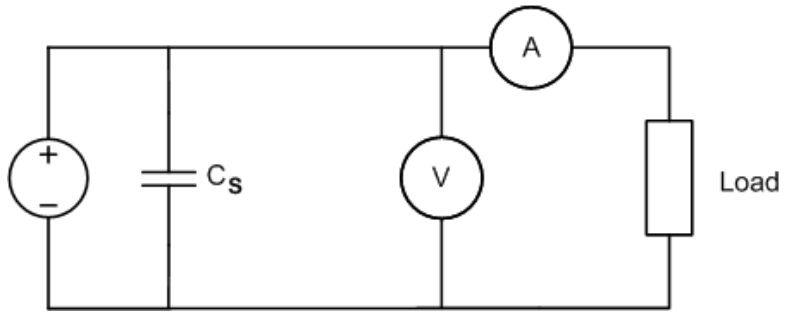

Figure 2.2: Measurement setup used for characterization and steady-state measurements.

2.1.3 Frequency Spectrum Measurements

The steady-state measurements were done to see how the loads behave in their normal operation when the voltage and current are constant. The measurement setup is the same as the setup used for the characterization measurements, except that the voltage and current meters have been replaced by the probes listed in Table 2.1.

The voltage level was chosen to be 230 V dc which the loads were subjected to for 1 s and 0.1 s that results in the frequency resolution of 1 Hz and 10 Hz respectively. When higher frequency components are expected, due to the specification or the nature of the load, e.g. rotating loads, the 10 Hz resolution was used.

Unavoidably the measurement will be affected by different external disturbances. Common mode disturbances, i.e. disturbances that are present in both the phase and the return conductor, are reduced by twisting the cables around a ferrite. The common mode will try to change the flux in the ferrite, that will resist by creating a flux in the opposite direction. In order to reduce the low frequency disturbances caused by surrounding wires of mostly 50 Hz, the loop area has to be minimized. This is achieved by twisting the cables around each other.

Finally, to reduce the disturbances even more, the phase is twisted around the current probe which will increase the current with multiplication factor equal to the number of turns that the phase is twisted around the probe. This measured current will later be divided with the same factor in Matlab and thereby the disturbance will be reduced by the same factor.

This measured data will be used to test the steady state performance of the obtained load models.

2.1.4 Transient Measurements

To determine the transient behavior of the loads, they were subjected to a fast voltage reduction. The measurement setup is described in Fig. 2.3. The design and analysis of the voltage reduction circuit and its performance can be found in Appendix D. The shunt connected capacitors were removed for this test.

Each load was subjected to four steps of different magnitudes, ranging from $0.4 - 0.9$ p.u., from the nominal voltage of 230 V. Ten steps were done for each step in magnitude to get a better statistical result, so in total each load was subjected to 40 steps. The voltage at the input terminals of the load and current were recorded over a period of 100 ms, but in some cases it was decided to record the data for a longer period of time if it was required to fully capture the load behavior.

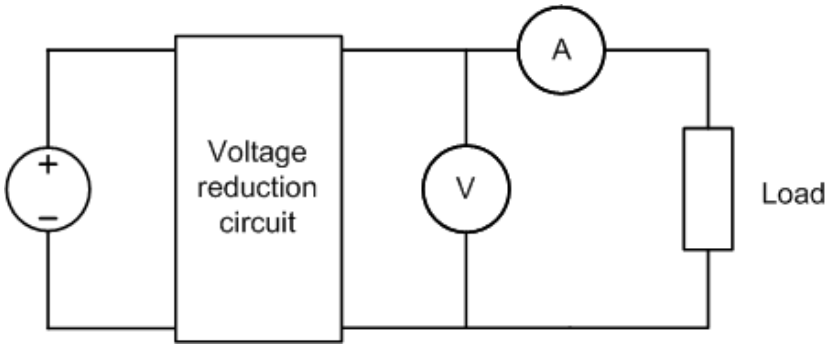

Figure 2.3: Measurement setup for transient measurements.

2.2 Measurement Analysis

This section will describe how the analysis of the measured data was done together with the necessary theory. The computer softwares utilized for the analysis were Matlab v.6.5.1, EMTDC v.3.0.8 together with Fortran.

2.2.1 Load Characterization

A load model is in this thesis a mathematical representation of the relationship between voltage and current or power and voltage. This is done be measuring the current at different voltage levels as described earlier. Then the voltage relation with the current can be described by

$$U(I) = R_{p2}I^2 + R_{p1}I + R_{p0} \tag{2.4}$$

where $R_{p0} = 0$ in most cases (except constant power) [5]. For those cases where the load always draws the same current as the voltage changes, Eq. (2.4) is not valid. Then the current vs. the voltage is considered and the model can be described as

$$I(U) = Y_{p2}U^2 + Y_{p1}U + Y_{p0} \tag{2.5}$$

where Y_{p0} gives the current that the load consumes.

From the voltage and current measurements the power can be calculated. The power voltage relation can be modelled as

$$P(U) = A_{p2}U^2 + A_{p1}U + A_{p0} \tag{2.6}$$

Equation (2.6) gives the power relation to the voltage characteristics for a specific load, that is if it is a quadratic model the load is said to be a constant resistance load, when it is linear the load is said to be constant current and if it is a constant then the load is constant power [11]. This formula can also be realized in p.u. or as

$$\frac{P(U)}{P_0} = a_2\left(\frac{U}{U_0}\right)^2 + a_1\frac{U}{U_0} + a_0 \tag{2.7}$$

This should give $a_2 + a_1 + a_0 = 1$ as the parameter indicate how the power is divided into constant power, constant current and constant resistance loads [11]. One question is how to choose the values of P_0, U_0 in Eq. (2.7). One option is to consider the rated RMS voltage and the rated power by the manufacturer. Otherwise the measured power

at 230 V could be used, if the rated power is not known or if the difference between the two values is significant.

The method of least squares can be used to determine the coefficients in Eqs. (2.4), (2.5) and (2.6), see Appendix B.

To determine the accuracy of these models, the relative absolute error is calculated for each measuring point and then the average is taken over the whole error interval as

$$\varepsilon = \text{mean} \left| \frac{\text{measured value} \; - \; \text{model value}}{\text{measured value}} \right| \tag{2.8}$$

The error for each model described in Eqs. (2.4), (2.5) and (2.6) are denoted by the subscript "R", "Y" and "P" respectively.

2.2.2 Frequency Spectrum Analysis

The voltage and current signals obtained by the measurements are still quite noisy, although measures have been taken to reduce the noise. To further reduce the disturbance the signals are run through a moving average filter with 50 samples in a single average. This will also get rid of random spikes in the signals. To obtain the correct magnitudes at the correct frequency components the voltage and current signals are then multiplied with a Bartlett window which is defined as

$$w_t[n] = 1 - \frac{|2n - N + 1|}{N + 1}, \qquad 0 \leq n \leq N - 1 \tag{2.9}$$

where N is the total number of samples of the signal [12]. The discrete time and frequency response of the window is shown in Fig. 2.4.

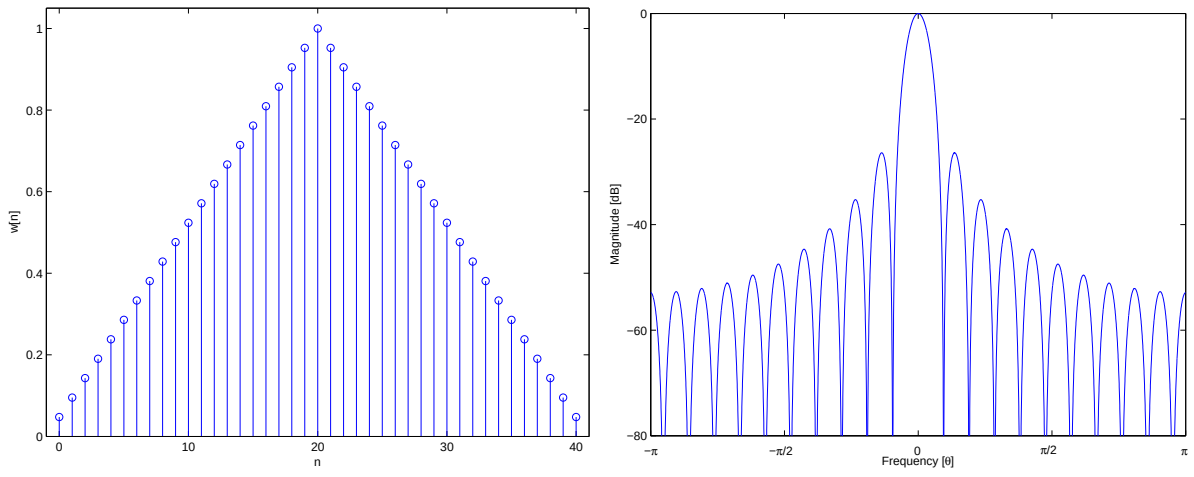

(a) Time-domain. (b) Frequency-domain.

Figure 2.4: Bartlett window, N = 41: (a) time-domain plot; (b) frequency-domain plot.

The width of the main lobe in the frequency response of the window will cause unwanted frequencies near the dc component due to its high magnitude compared to the rest of the signal. This is of course dependent on the frequency resolution and the number of samples of the signal that is to be windowed.

After windowing the signals the frequency components of the signals are found using a FFT algorithm [12]. The frequency components of the ten largest magnitudes are then

picked out to see whether they exceed the inaccuracy of the probes [12]. If any of the components exceed this limit a distortion factor [9] is calculated, defined as

$$DF = \frac{\sqrt{\sum(\text{Magnitudes of the frequency components})^2}}{\text{Mean value of the signal}} \tag{2.10}$$

where the magnitude of the frequency components is their RMS values.

This analysis was done for both the measurements and the results obtained via the simulation of the steady state model of each load. The simulation was done in EMTDC using the measured voltage as the input voltage and the current was then recorded.

2.2.3 Transient Analysis

The results from the characterization of the loads are used as models to estimate the current consumption of the loads, when the voltage was stepped down. The models were realized in EMTDC to simulate the voltage step as well. First, with an ideal voltage step that matches the measured one was applied, and then the measured voltage was fed to the model to see how it acts to a realistic step, with all of its noise. In many cases the steady-state model was enough to describe the response to a step change, but there were additional transient phenomena, which were modeled by adding more components.

Chapter 3

Resistive Loads

The resistive loads can be divided into two categories, heating and lighting. The loads that were measured and fall into this category are

Loads	
Heaters	Coffee machine
	Curling iron
	Kettle
	Sandwich maker
	Stove
Lighting	Incandescent lamp
	Tungsten halogen lamp

Table 3.1: Resistive loads acquired.

The heaters are loads where the thermal loss of the resistor is utilized for different purposes, i.e. heating and cooking.

Most of these heaters have a thermostat which breaks the current when certain temperature is reached, and closes it again when the temperature goes down. The heaters is also equipped with a thermal fuse for protection. The construction of the thermal fuse is shown in Fig. 3.1 gotten from [13].

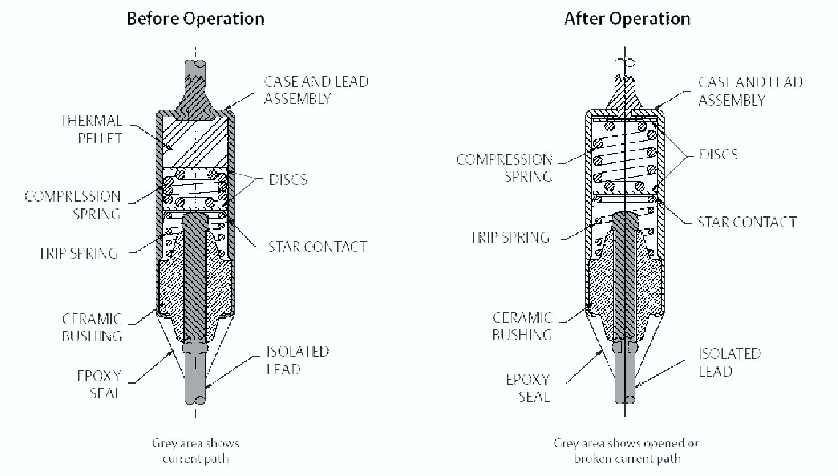

Figure 3.1: Operating principle of a thermal fuse.

The active trigger mechanism of the thermal fuse in Fig. 3.1 works in the following way

- In the fuse there is an electrically nonconductive pellet. Under normal operating temperatures, the solid pellet holds the spring-loaded contacts closed.
- When a predetermined temperature is reached, the pellet melts, allowing the compression spring to relax. The trip spring then slides the contact away from the lead and the circuit is opened.

The thermostat did not work properly to break the dc current that the load required. This resulted in that the heating element heated up above normal operation temperature and the thermal fuse tripped. Once this occurs the thermal fuse has to be replaced in order to make the load operational again [13].

The heaters are designed to consume a certain amount of current at the voltage that is used in the system. In Europe this voltage is 230 V RMS. The current varies with the voltage and if the load is supplied with another voltage than rated, the heating power will be in direct proportion to that. For example if the coffee machine is supplied with 0.5 p.u., the water flow will be significantly less than if the supply is 1 p.u. and vice versa if the supply is 1.5 p.u., the water flow will be too much and the coffee will be slightly "tea-ish".

There are basically two types of lamps for indoor lighting that fall into this resistive category. These are incandescent lamps and tungsten halogen lamps. Incandescent lamps are thermal radiators in an enclosed bulb filled with gas. An electric current is passed through a filament of tungsten wire to make it glow. With this method of generating light only about 5 % of the energy consumed is converted into light, the rest is lost as heat. To make the filament glow, the temperature must exceed 500 °C [14]. Adding halogens turns conventional light bulbs into halogen lamps. "Things simply look better in the brilliant light generated by these lamps", that is the halogen lamps are a more efficient light source than the conventional ones as the temperature of the filament is kept well above 1000 °C, depending of the type of halogen used in the lamp [14].

The light output is proportional to the voltage over the lamp, so to be safe it is suggested that the rated voltage is used to ensure the same light output in dc as in ac. The drawback of supplying these lamps with dc is that the filament can polarize, due to the high temperature, thereby shortening the lifetime of the lamp.

3.1 Load Characterization

To characterize the loads the voltage was varied from 50 to 380 V in 10 V steps. For each step, both voltage and current were recorded. Measurement setup and procedure have been described in Chapter 2.

From the measurements, it was found that the heaters could be considered as constant resistors, for which Ohm's law can be applied directly, while the lamps showed a strong temperature dependency.

For the heaters, Eq. (2.4) should be applied with $R_{p2} = R_{p0} = 0$, where the temperature dependency of the load is neglected. Equation (2.6) can be rewritten as $P = U \cdot I$ and it can be shown that $A_{p2} = R_{p1}^{-1}$.

When the temperature dependency of the load is considered, Ohm's law cannot be applied directly. The load is still considered as a resistance, but its value is dependent on the current as the current in turn influences the temperature of the filament. Equation (2.4) can be modified according to

$$R = R_{p2} \cdot I + R_{p1} \tag{3.1}$$

yielding

$$U = R_{p2} \cdot I^2 + R_{p1} \cdot I \tag{3.2}$$

This means that Eq. (2.6) is not valid since we have a varying resistor. To derive a more meaningful expression for the power, Eq. (3.2) can be solved with respect to I, with U known, and results in

$$P(U) = U \cdot I = U \cdot \left(\pm \sqrt{\frac{U}{R_{p2}} + \frac{R_{p1}^2}{4R_{p2}^2}} - \frac{R_{p1}}{2R_{p2}} \right) \tag{3.3}$$

The negative solution is neglected as it will give a negative result. It is necessary to consider the current dependent resistance when R_{p2} in Eq. (2.4) is large enough compared to R_{p1} so that it can not be neglected. This would be the case for the loads that are used for lighting.

For each model, the relative amplitude error defined, as in Chapter 2, was calculated for both the error of the resistance and the error in power, called ε_R and ε_P respectively.

3.1.1 Heaters

Coffee Machine (Butler)

The rated power of the coffee machine is obtained from the nameplate and is 1000 W at the rated voltage of 230 V. According to Ohm's law the resistance is calculated to be 52.9 Ω.

The characteristics of the Butler coffee machine with dc supply are plotted in Fig. 3.2. Fig. 3.2(a) shows how the voltage varies with the current. The method of least squares, described in Appendix B, is used to obtain a linear and a quadratic model as described in Eq. (2.4). The linear model describes the load as a constant resistor and the quadratic model is used to detect the temperature dependency of the load.

Fig. 3.2(b) describes how the power varies with the voltage. The linear model is obtained from Ohm's law, where $P = U^2/R_{p1}$. When the temperature variation is considered, Eq. (3.3) is used to obtain the power.

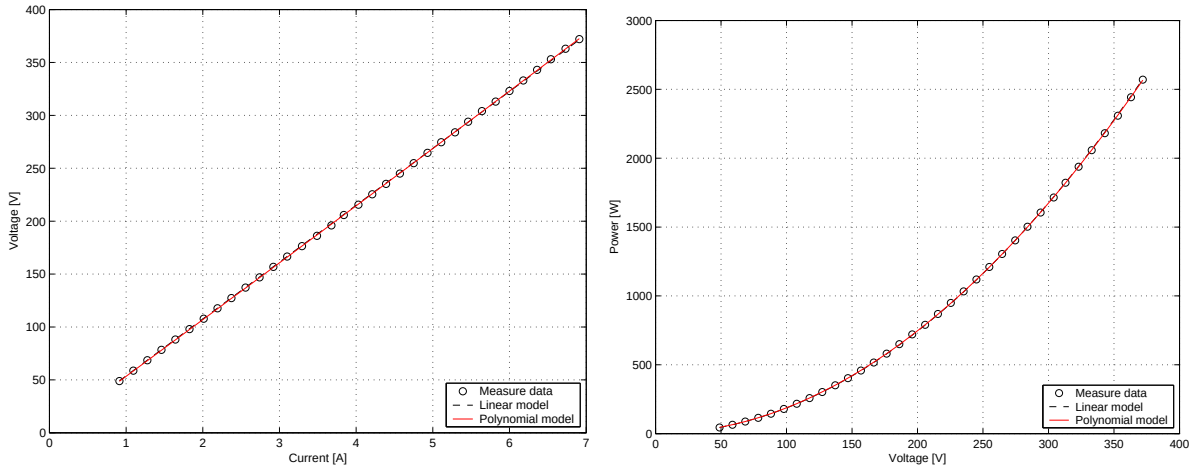

(a) Voltage vs. Current (b) Power vs. Voltage

Figure 3.2: Characteristics of coffee machine (Butler).

Table 3.2 shows the parameters obtained from the models as described above. R_{p2}, R_{p1} and R_{p0} are the coefficients obtained when the least square method is applied on the measured data, setting first $R_{p2} = R_{p0} = 0$ to obtain a linear model and then only $R_{p0} = 0$ to obtain a quadratic model. A_{p2}, A_{p1} and A_{p0} are the coefficients gotten from the least square method when the voltage is said to vary linearly with current, with $A_{p0} = 0$. When the voltage is assumed to vary quadratically with the current, Eq. (3.3) is used and the method of least squares cannot be used directly. For each model the error is calculated according to Eq. (2.8).

	R_{p2}	R_{p1}	R_{p0}	ε_R [%]	A_{p2}	A_{p1}	A_{p0}	ε_P [%]
quadratic model:	0.0956	53.25	0	0.24	-	-	-	0.24
linear model:	0	53.76	0	0.27	0.0186	0	0	0.27

Table 3.2: Model parameters for coffee machine (Butler).

For the linear model $R_{p1} = A_{p2}^{-1} = 53.76\ \Omega$ and the error is 0.27 %. This value of resistance is only 1.62 % higher than the rated resistance obtained from the nameplate data. The quadratic model shows that $R_{p2} \ll R_{p1}$ so R_{p2} can be neglected. The coffee machine is thereby a constant resistive load and the rated values give a quite accurate model. The model is

$$\boxed{R = 52.9\ \Omega \pm 1.62\ \%}$$

Coffee Machine (Philips)

The rated power of the coffee machine is obtained from the nameplate and is 850 W at the rated voltage of 230 V. According to Ohm's law the resistance is calculated to be 62.24 Ω. The characteristic is plotted in Fig. 3.3 and the model parameters are tabulated in Table 3.3.

Table 3.3 shows that the coffee machine can be modelled as a constant resistive load, where $R_{p1} = A_{p2}^{-1} = 61.04\ \Omega$ and the error is ≈ 2 %. The value of the resistance is 1.92 % lower than the rated resistance. The model is

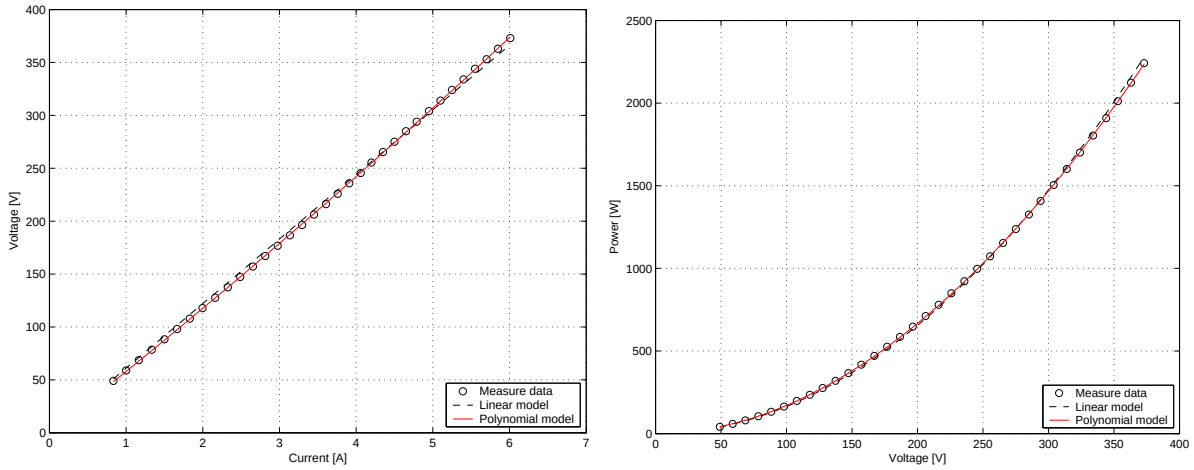

(a) Voltage vs. Current (b) Power vs. Voltage

Figure 3.3: Characteristics of coffee machine (Philips).

	R_{p2}	R_{p1}	R_{p0}	ε_R	A_{p2}	A_{p1}	A_{p0}	ε_P
quadratic model:	0.8599	57.09	0	0.43	-	-	-	0.41
linear model:	0	61.04	0	2.13	0.01638	0	0	2.08

Table 3.3: Model parameters for coffee machine (Philips).

$$\boxed{R = 62.24\ \Omega \pm 2.13\ \%}$$

Curling Brush (XL Concept)

The rated power of the curling brush is obtained from the nameplate and is 11 W at the rated voltage of 230 V. According to Ohm's law the resistance is calculated to be 4809.1 Ω. The characteristic is plotted in Fig. 3.4 and the model parameters are tabulated in Table 3.4.

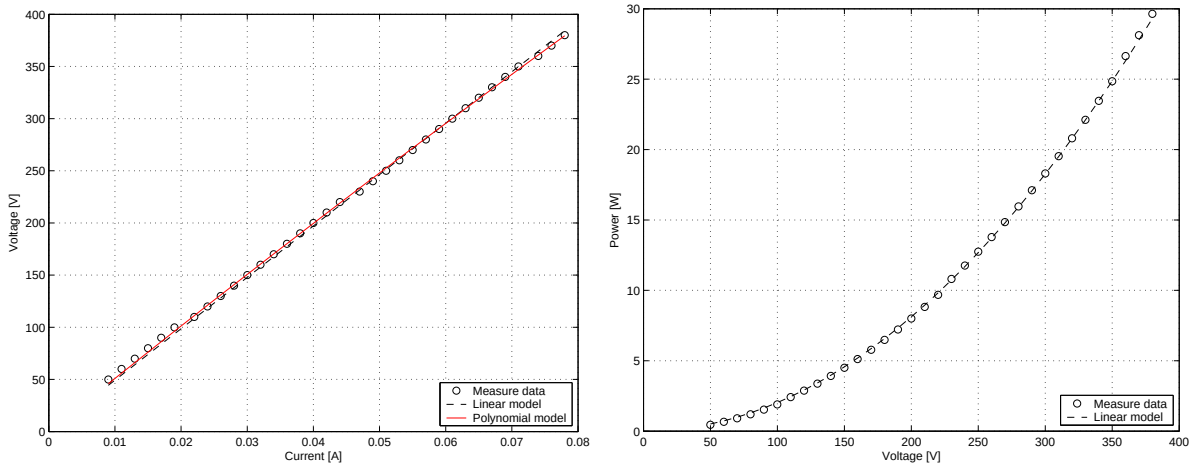

(a) Voltage vs. Current (b) Power vs. Voltage

Figure 3.4: Characteristics of curling brush (XL Concept).

	R_{p2}	R_{p1}	R_{p0}	ε_R	A_{p2}	A_{p1}	A_{p0}	ε_P
quadratic model:	-3305.1	5122.3	0	1.41	-	-	-	4819
linear model:	0	4926.8	0	2.18	$2.03 \cdot 10^{-4}$	0	0	2.33

Table 3.4: Model parameters for curling brush (XL Concept).

Table 3.4 shows that the curling brush can be modelled as a constant resistive load, where $R_{p1} = A_{p2}^{-1} = 4926.8\ \Omega$ and the error is $\approx 2\ \%$. The quadratic model gives a very strange result because R_{p2} is negative and Eq. (3.3) is not valid. The value of the resistance is 2.45 % higher than the rated resistance. The model is

$$\boxed{R = 4809.1\ \Omega \pm 2.45\ \%}$$

Kettle (Elram)

The rated power of the kettle is gotten from the nameplate and is 2000 W at the rated voltage of 230 V. According to Ohm's law the resistance is calculated to be 26.45 Ω. The characteristic is plotted in Fig. 3.5 and the model parameters are tabulated in Table 3.5.

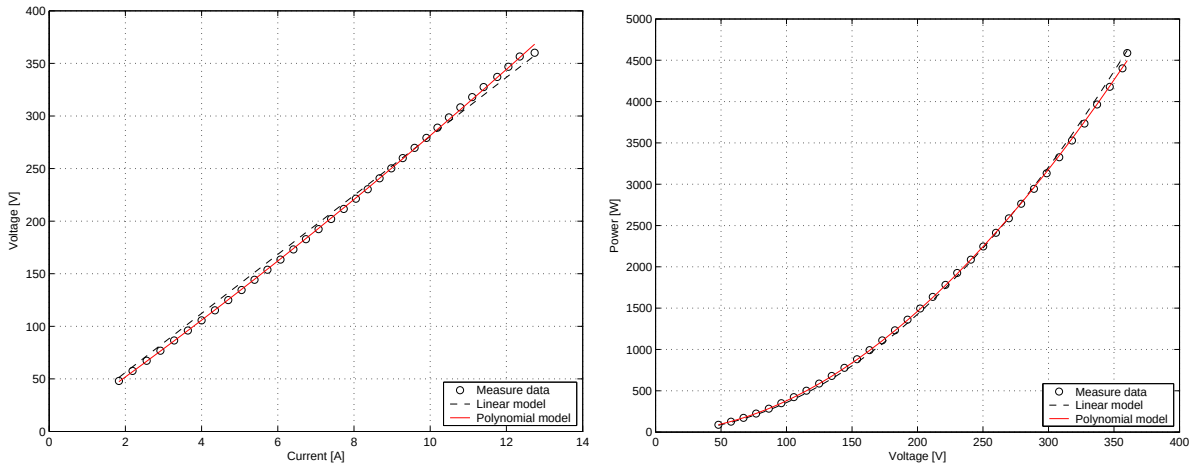

(a) Voltage vs. Current

(b) Power vs. Voltage

Figure 3.5: Characteristics of kettle (Elram).

	R_{p2}	R_{p1}	R_{p0}	ε_R	A_{p2}	A_{p1}	A_{p0}	ε_P
quadratic model:	0.2796	25.342	0	0.50	-	-	-	0.47
linear model:	0	28.06	0	3.41	0.03564	0	0	3.28

Table 3.5: Model parameters for kettle (Elram).

Table 3.5 shows that the kettle can be modelled as a constant resistive load, where $R_{p1} = A_{p2}^{-1} = 28.06\ \Omega$ and the error is $\approx 3.4\ \%$. The value of the resistance is 6.09 % lower than the rated resistance. The difference is so high probably due to extensive use and age. The model is then

$$\boxed{R = 26.45\ \Omega \pm 6.09\ \%}$$

Kettle (Solingmüller)

The rated power of the kettle is obtained from the nameplate and is 2025 W at the rated voltage of 230 V. According to Ohm's law the resistance is calculated to be 26.12 Ω. The characteristic is plotted in Fig. 3.6 and the model parameters are tabulated in Table 3.6.

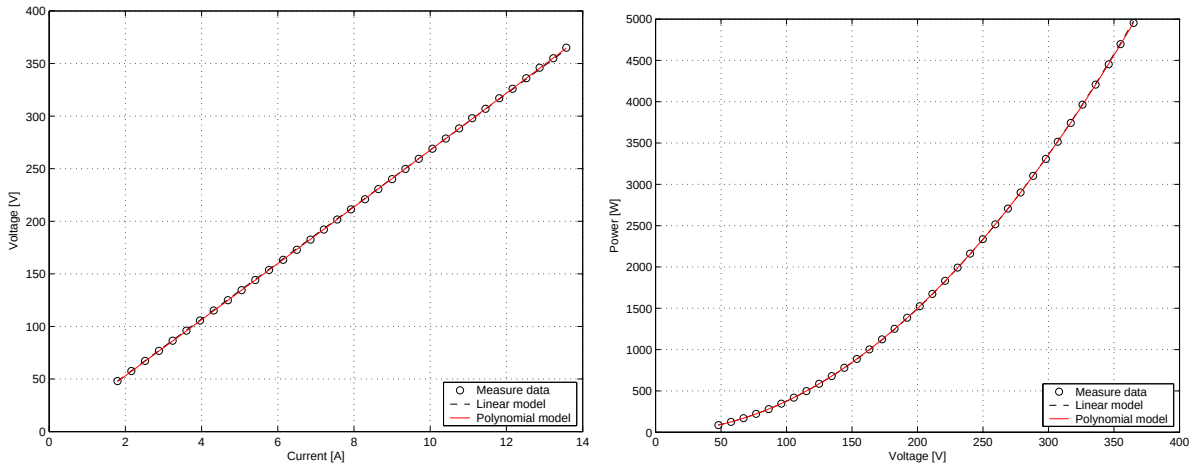

(a) Voltage vs. Current (b) Power vs. Voltage

Figure 3.6: Characteristics of kettle (Solingmüller).

	R_{p2}	R_{p1}	R_{p0}	ε_R	A_{p2}	A_{p1}	A_{p0}	ε_P
quadratic model:	0.03113	26.45	0	0.19	-	-	-	0.19
linear model:	0	26.77	0	0.35	0.03735	0	0	0.35

Table 3.6: Model parameters for kettle (Solingmüller).

Table 3.6 shows that the kettle can be modelled as a constant resistive load, where $R_{p1} = A_{p2}^{-1} = 26.77\ \Omega$ and the error is $\approx 0.3\ \%$. The value of the resistance is 2.48 % lower than the rated resistance. The model is then

$$\boxed{R = 26.12\ \Omega \pm 2.48\ \%}$$

Sandwich Maker (Mirabelle)

The rated power of the sandwich maker is obtained from the nameplate and is 800 W at the rated voltage of 230 V. According to Ohm's law the resistance is calculated to be 66.13 Ω. The characteristics are plotted in Fig. 3.7 and the model parameters are tabulated in Table 3.7.

	R_{p2}	R_{p1}	R_{p0}	ε_R	A_{p2}	A_{p1}	A_{p0}	ε_P
quadratic model:	-0.03759	62.55	0	0.80	-	-	-	66051
linear model:	0	62.38	0	0.74	0.01603	0	0	0.74

Table 3.7: Model parameters for sandwich maker (Mirabelle).

Table 3.7 shows that the sandwich maker can be modelled as a constant resistive load, where $R_{p1} = A_{p2}^{-1} = 26.77\ \Omega$ and the error is $\approx 0.7\ \%$. The quadratic model gives a very

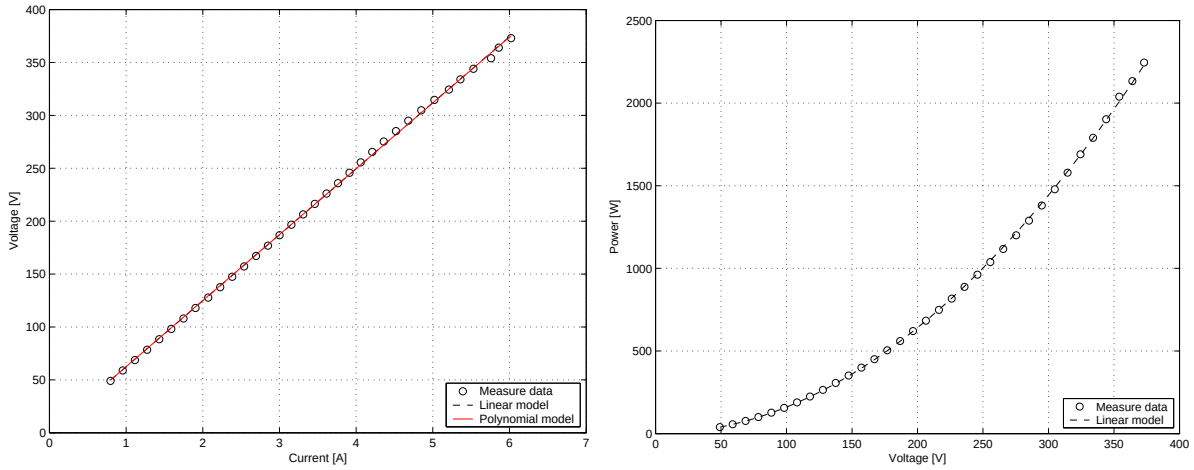

(a) Voltage vs. Current (b) Power vs. Voltage

Figure 3.7: Characteristics of sandwich maker (Mirabelle).

strange result because R_{p2} is negative and then Eq. (3.3) is not valid. However, the value of R_{p2} is anyway quite small. The value of the resistance is 5.66 % higher than the rated resistance. The difference is so high probable due to extensive use. The model is

$$\boxed{R = 66.13\ \Omega \pm 5.66\ \%}$$

Sandwich Maker (AFK)

The rated power of the sandwich maker is gotten from the nameplate and is 700 W at the rated voltage of 230 V. According to Ohm's law the resistance is calculated to be 75.57 Ω. The characteristic is plotted in Fig. 3.8 and the model parameters are tabulated in Table 3.8.

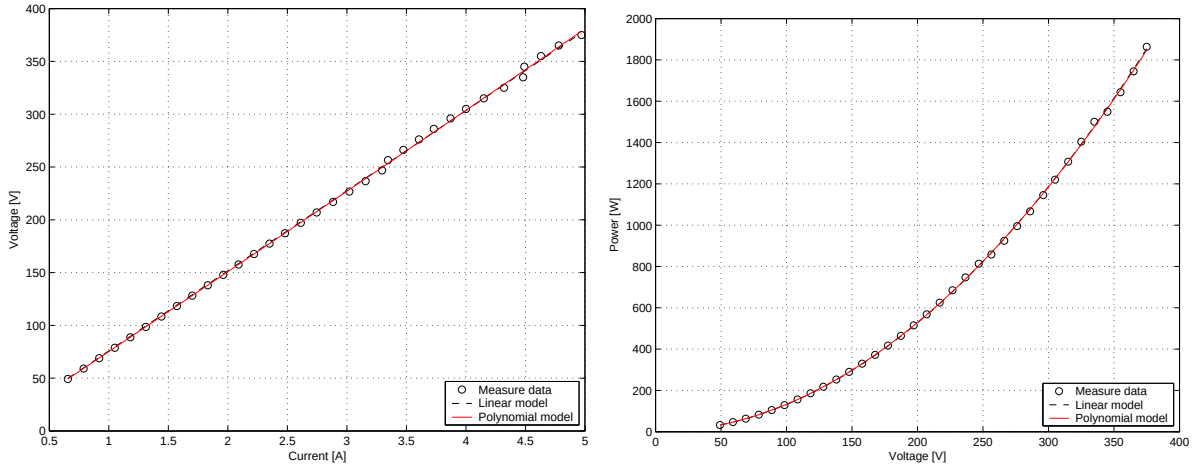

(a) Voltage vs. Current (b) Power vs. Voltage

Figure 3.8: Characteristics of sandwich maker (AFK).

Table 3.8 shows that the sandwich maker can be modelled as a constant resistive load, where $R_{p1} = A_{p2}^{-1} = 75.86\ \Omega$ and the error is ≈ 0.9 %. The value of the resistance is

	R_{p2}	R_{p1}	R_{p0}	ε_R	A_{p2}	A_{p1}	A_{p0}	ε_P
quadratic model:	0.2363	74.98	0	0.51	-	-	-	0.51
linear model:	0	75.86	0	0.86	0.01318	0	0	0.85

Table 3.8: Model parameters for sandwich maker (AFK).

0.39 % higher than the rated resistance. The small difference is probably due to the fact that it is brand new. The model is

$$\boxed{R = 75.57\ \Omega \pm 0.86\ \%}$$

Stove (Siemens)

The rated power of the stove is unknown. Only one plate of the stove was used at full heat to obtain the model because of its high current consumption. The characteristic is plotted in Fig. 3.9 and the model parameters are tabulated in Table 3.9.

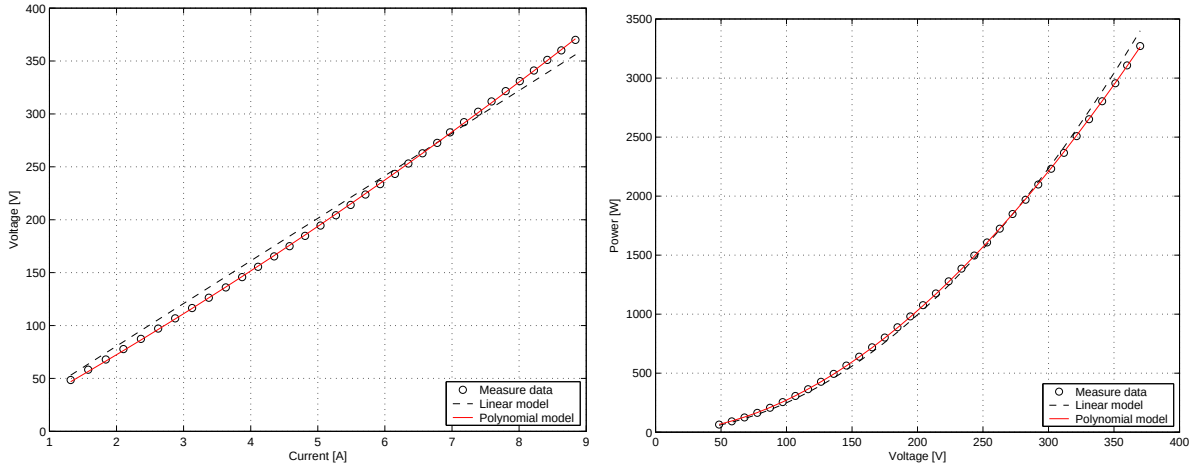

(a) Voltage vs. Current

(b) Power vs. Voltage

Figure 3.9: Characteristics of stove (Siemens).

	R_{p2}	R_{p1}	R_{p0}	ε_R	A_{p2}	A_{p1}	A_{p0}	ε_P
quadratic model:	0.8433	34.52	0	0.61	-	-	-	0.58
linear model:	0	40.26	0	4.67	0.02484	0	0	4.43

Table 3.9: Model parameters for stove (Siemens).

Table 3.9 shows that the stove can be modelled as a constant resistive load, where $R_{p1} = A_{p2}^{-1} = 40.26\ \Omega$ and the error is $\approx 4.7\ \%$. The model is

$$\boxed{R = 40.26\ \Omega \pm 4.67\ \%}$$

3.1.2 Lighting

Incandescent Lamps

A number of 26 incandescent lamps of 5 different power levels from 5 different manufacturers were tested. The rated power of the lamps were obtained from their nameplates at the rated voltage of 230 V. According to Ohm's law the resistance is calculated and reported in Table 3.10.

P [W]	25	40	60	75	100
R [Ω]	2116.0	1322.5	881.7	705.3	529.0

Table 3.10: Calculated resistances for lamps at 230 V.

The model parameters are tabulated in Table 3.11 for all lamps. Note that it is always $R_{p0} = 0$ in Eq. (2.4) and $a_{p1} = a_{p0} = 0$ in Eq. (2.6).

The characteristics for the lamps are plotted for each power level in Figs. 3.10 to 3.14. Remaining plots can be found in Appendix H.

		Model	R_{p2}	R_{p1}	ε_R	A_{p2}	ε_P
25 W	Lamp 1	quadratic:	16966.2	128.4	1.59	-	0.81
		linear:	0	2132.6	28.3	$4.69 \cdot 10^{-3}$	19.48
	Lamp 2	quadratic:	16871.3	131.8	1.51	-	0.77
		linear:	0	2128.9	28.2	$4.69 \cdot 10^{-3}$	19.4
	Lamp 3	quadratic:	17020.5	121.2	1.50	-	0.76
		linear:	0	2132.0	28.3	$4.7 \cdot 10^{-4}$	19.5
	Lamp 4	quadratic:	16682.8	111.5	1.64	-	0.83
		linear:	0	2105.8	28.4	$4.7 \cdot 10^{-4}$	19.5
	Lamp 5	quadratic:	17511.7	102.0	1.59	-	0.79
		linear:	0	2150.8	28.5	$4.65 \cdot 10^{-4}$	19.6
40 W	Lamp 1	quadratic:	7010.2	133.7	1.42	-	0.74
		linear:	0	1399.8	27.4	$7.14 \cdot 10^{-3}$	19.1
	Lamp 2	quadratic:	7071.6	120.8	1.4	-	0.75
		linear:	0	1398.2	27.7	$7.15 \cdot 10^{-4}$	19.2
	Lamp 3	quadratic:	6695.1	148.0	1.29	-	0.68
		linear:	0	1378.1	27.1	$7.26 \cdot 10^{-4}$	19.0
	Lamp 4	quadratic:	6294.9	143.7	1.35	-	0.71
		linear:	0	1336.2	27.2	$7.48 \cdot 10^{-4}$	19.0
	Lamp 5	quadratic:	6706.8	137.4	1.34	-	0.71
		linear:	0	1373.0	27.3	$7.28 \cdot 10^{-4}$	19.0
	Lamp 6	quadratic:	6624.7	145.8	1.37	-	0.73
		linear:	0	1367.0	27.2	$7.30 \cdot 10^{-4}$	19.0
60 W	Lamp 1	quadratic:	2925.8	113.5	1.27	-	0.68
		linear:	0	919.9	26.8	$1.1 \cdot 10^{-3}$	18.8
	Lamp 2	quadratic:	3046.9	115.9	1.27	-	0.68
		linear:	0	938.8	26.8	$1.1 \cdot 10^{-3}$	18.8
	Lamp 3	quadratic:	2956.0	117.1	1.16	-	0.63
		linear:	0	926.5	26.7	$1.08 \cdot 10^{-3}$	18.7
	Lamp 4	quadratic:	3285.6	106.5	1.33	-	0.71
		linear:	0	966.5	27.1	$1.04 \cdot 10^{-4}$	18.9
	Lamp 5	quadratic:	3922.5	3.98	1.82	-	0.88
		linear:	0	992.65	29.5	$1.01 \cdot 10^{-3}$	20.0
	Lamp 6	quadratic:	3867.6	1.93	2.05	-	0.98
		linear:	0	984.3	29.6	$1.02 \cdot 10^{-3}$	20.0
	Lamp 7	quadratic:	3889.2	2.91	1.87	-	0.90
		linear:	0	987.6	29.6	$1.01 \cdot 10^{3}$	20.0
	Lamp 8	quadratic:	3805.5	1.65	1.73	-	0.83
		linear:	0	976.3	29.5	$1.02 \cdot 10^{-3}$	20.0
75 W	Lamp 1	quadratic:	1709.5	106.7	1.23	-	0.68
		linear:	0	714.7	26.2	$1.4 \cdot 10^{-3}$	18.5
	Lamp 2	quadratic:	1685.3	103.5	1.24	-	0.68
		linear:	0	708.2	26.3	$1.4 \cdot 10^{-3}$	18.6
	Lamp 3	quadratic:	1853.2	101.7	1.14	-	0.62
		linear:	0	738.8	26.4	$1.35 \cdot 10^{-3}$	18.6

		Model	R_{p2}	R_{p1}	ε_R	A_{p2}	ε_P
100 W	Lamp 1	quadratic:	994.5	87.6	1.12	-	0.62
		linear:	0	548.5	25.9	$1.82 \cdot 10^{-3}$	18.35
	Lamp 2	quadratic:	997.1	92.5	1.20	-	0.67
		linear:	0	551.9	25.7	$1.81 \cdot 10^{-3}$	18.25
	Lamp 3	quadratic:	968.1	83.9	1.25	-	0.69
		linear:	0	539.6	26.0	$1.9 \cdot 10^{-3}$	18.4
	Lamp 4	quadratic:	992.8	83.0	1.22	-	0.67
		linear:	0	545.3	26.0	$1.8 \cdot 10^{-3}$	18.4

Table 3.11: Model parameters for incandescent lamps.

The plots that describe the voltage-current relation in Figs. 3.10 to 3.14 clearly show that the light bulbs cannot be modelled as a constant resistance and Table 3.11 shows that $R_{p2} \gg R_{p1}$, when the data is curve fitted with a quadratic model. Since the model is not linear, it is not enough to know the rated power consumption at rated voltage to determine a realistic model. It has to be done by measurements.

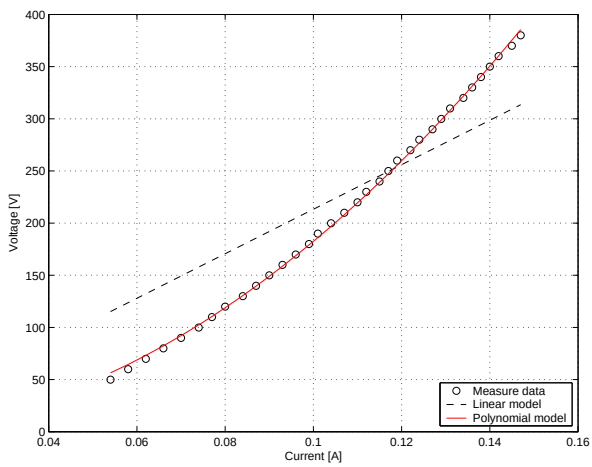

(a) Lamp 1: Voltage vs. Current.

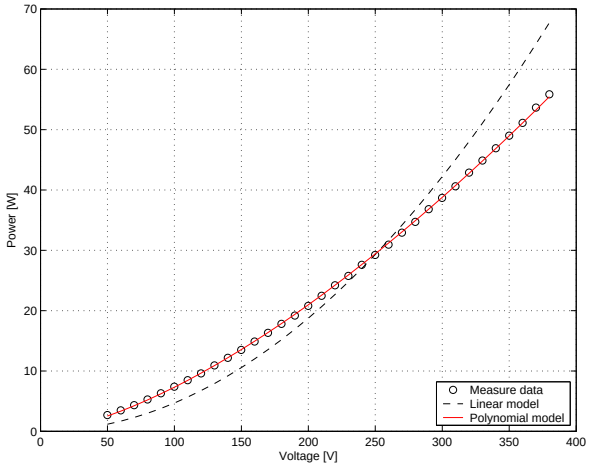

(b) Lamp 1: Power vs. Voltage.

Figure 3.10: Characteristics of a 25 W incandescent lamp.

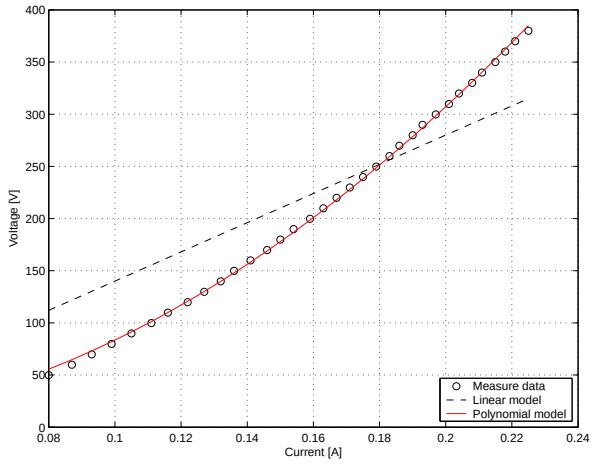

(a) Lamp 1: Voltage vs. Current.

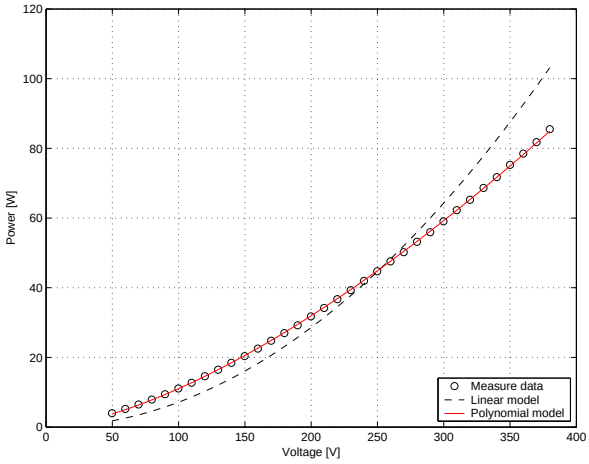

(b) Lamp 1: Power vs. Voltage.

Figure 3.11: Characteristics of a 40 W incandescent lamp.

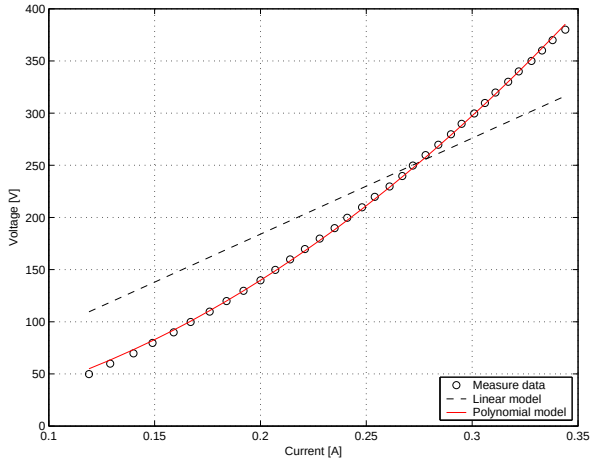

(a) Lamp 1: Voltage vs. Current.

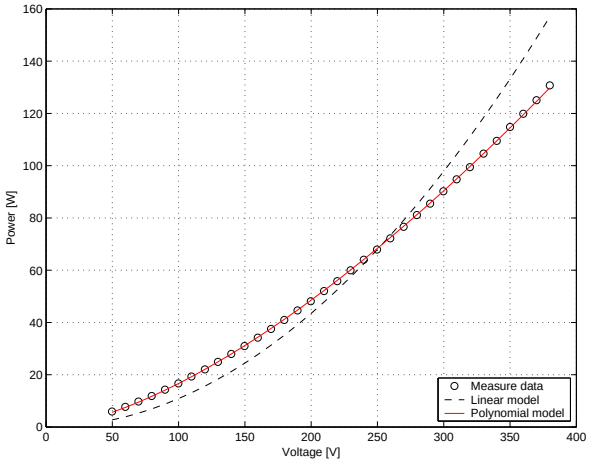

(b) Lamp 1: Power vs. Voltage.

Figure 3.12: Characteristics of a 60 W incandescent lamp.

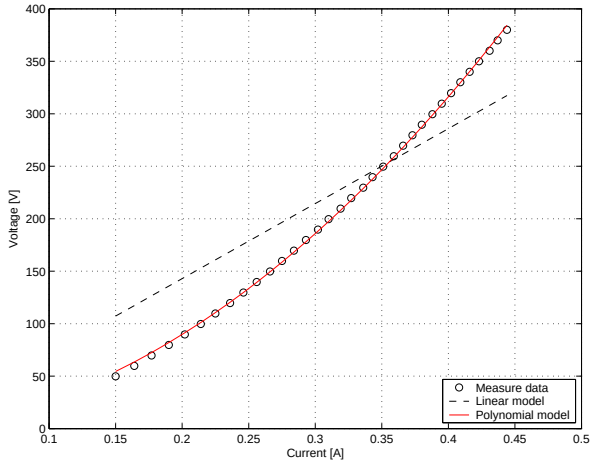

(a) Lamp 1: Voltage vs. Current.

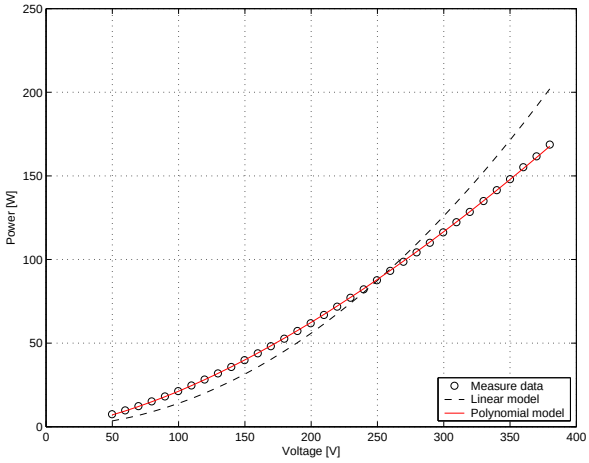

(b) Lamp 1: Power vs. Voltage.

Figure 3.13: Characteristics of a 75 W incandescent lamp.

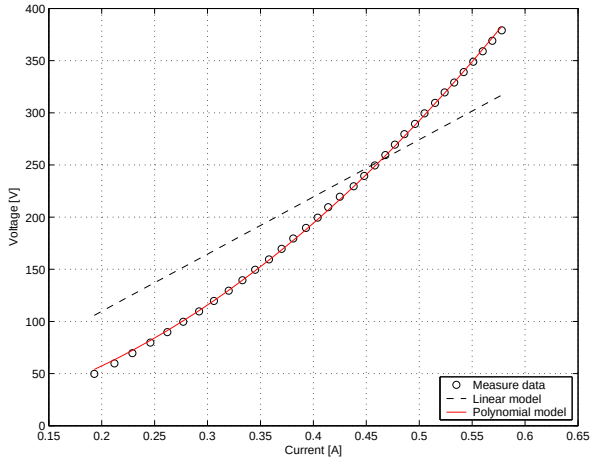

(a) Lamp 1: Voltage vs. Current.

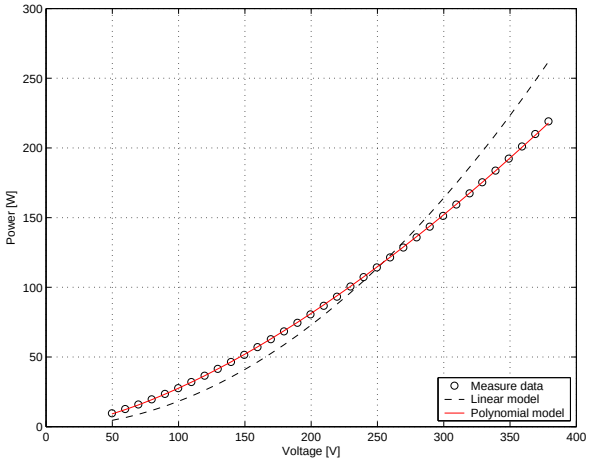

(b) Lamp 1: Power vs. Voltage.

Figure 3.14: Characteristics of a 100 W incandescent lamp.

Tungsten Halogen Lamp (150 W, 1)

The rated power of the lamp is obtained from the nameplate and is 150 W at the rated voltage of 230 V. The characteristic is plotted in Fig. 3.15 and the model parameters are tabulated in Table 3.12.

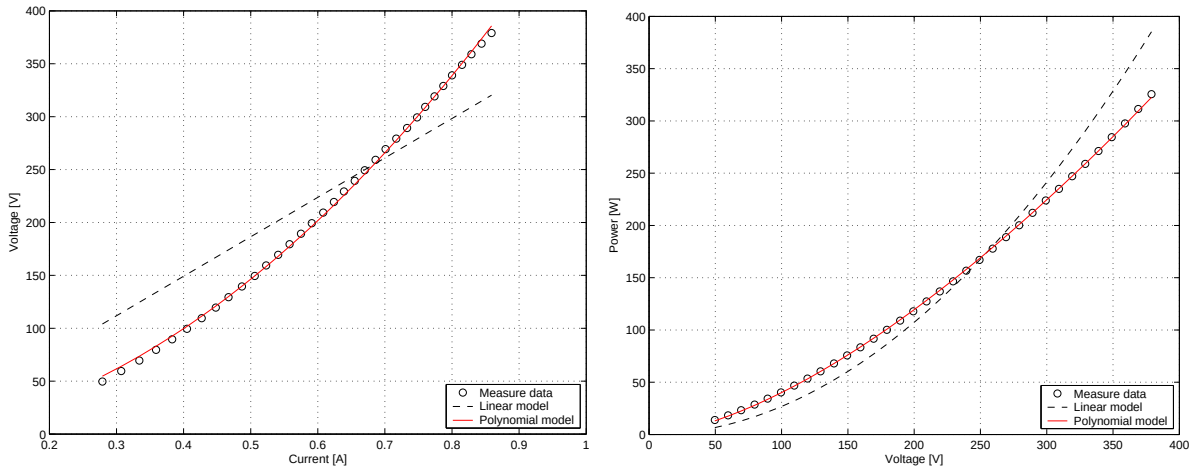

(a) Voltage vs. Current.

(b) Power vs. Voltage.

Figure 3.15: Characteristics of tungsten halogen lamp (150 W, 1).

	R_{p2}	R_{p1}	R_{p0}	ε_R	A_{p2}	A_{p1}	A_{p0}	ε_P
quadratic model:	435.9	74.67	0	1.68	-	-	-	0.96
linear model:	0	372.8	0	25.2	$2.68 \cdot 10^{-3}$	0	0	17.9

Table 3.12: Model parameters for tungsten halogen lamp (150 W, 1).

Table 3.12 shows that the quadratic model obtained from Eq. (2.4) fits best and it behaves exactly as a normal incandescent lamp. The model can be assumed to be

$$\boxed{R = 435.9 \cdot I + 74.7\ \Omega \pm 1.68\ \%}$$

Tungsten Halogen Lamp (150 W, 2)

The rated power of the lamp is obtained from the nameplate and is 150 W at the rated voltage of 230 V. The characteristic is plotted in Fig. 3.16 and the model parameters are tabulated in Table 3.13.

	R_{p2}	R_{p1}	R_{p0}	ε_R	A_{p2}	A_{p1}	A_{p0}	ε_P
quadratic model:	441.5	72.88	0	1.65	-	-	-	0.93
linear model:	0	373.8	0	25.4	$2.68 \cdot 10^{-3}$	0	0	18.1

Table 3.13: Model parameters for tungsten halogen lamp (150 W, 2).

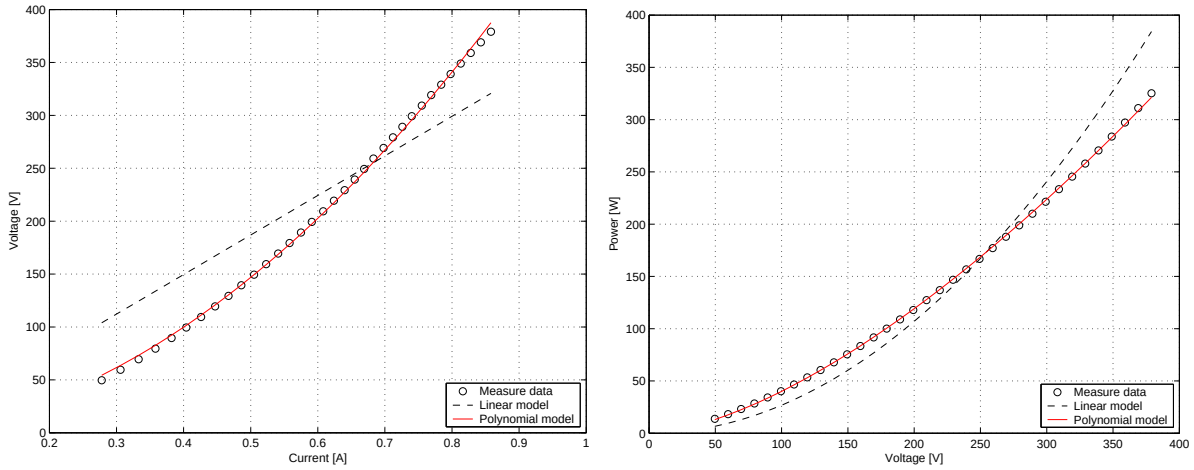

(a) Voltage vs. Current.

(b) Power vs. Voltage.

Figure 3.16: Characteristics of tungsten halogen lamp (150 W, 2).

Table 3.13 shows that the model can be assumed to be

$$\boxed{R = 441.5 \cdot I + 72.9\ \Omega \pm 1.65\ \%}$$

3.1.3 Summary

The results of the characterization of the resistive loads is tabulated in Table 3.14 with the estimated error of the models.

Heaters		Model [$R =$]	error [%]
Coffee Machine (Butler)		52.90 Ω	±1.62
Coffee Machine (Philips)		62.24 Ω	±3.13
Curling Brush (XL Concept)		4809.1 Ω	±2.45
Kettle (Elram)		26.45 Ω	±6.1
Kettle (Solingmüller)		26.12 Ω	±2.48
Sandwich Maker (Mirabelle)		26.12 Ω	±2.48
Sandwich Maker (AFK)		75.57 Ω	±0.86
Stove (Siemens)		40.26 Ω	±4.67
Lighting		**Model [$R =$]**	**error [%]**
25 W	Lamp 1	$16966.2 \cdot I + 128.4$ Ω	±1.59
	Lamp 2	$16871.2 \cdot I + 131.8$ Ω	±1.51
	Lamp 3	$17020.5 \cdot I + 121.2$ Ω	±1.50
	Lamp 4	$16682.8 \cdot I + 111.5$ Ω	±1.64
	Lamp 5	$17511.7 \cdot I + 102.0$ Ω	±1.59
40 W	Lamp 1	$7010.2 \cdot I + 133.7$ Ω	±1.42
	Lamp 2	$7071.6 \cdot I + 120.8$ Ω	±1.40
	Lamp 3	$6695.1 \cdot I + 148.0$ Ω	±1.29
	Lamp 4	$6294.9 \cdot I + 143.7$ Ω	±1.35
	Lamp 5	$6706.8 \cdot I + 137.4$ Ω	±1.34
	Lamp 6	$6624.7 \cdot I + 145.8$ Ω	±1.37
60 W	Lamp 1	$2925.8 \cdot I + 113.5$ Ω	±1.27
	Lamp 2	$3046.9 \cdot I + 115.9$ Ω	±1.27
	Lamp 3	$2956.0 \cdot I + 117.1$ Ω	±1.16
	Lamp 4	$3285.6 \cdot I + 106.5$ Ω	±1.33
	Lamp 5	$3922.5 \cdot I + 4.0$ Ω	±1.82
	Lamp 6	$3868.0 \cdot I + 1.9$ Ω	±2.05
	Lamp 7	$3889.2 \cdot I + 2.9$ Ω	±1.87
	Lamp 8	$3805.5 \cdot I + 1.7$ Ω	±1.73
75 W	Lamp 1	$1709.5 \cdot I + 106.7$ Ω	±1.23
	Lamp 2	$1685.3 \cdot I + 103.5$ Ω	±1.24
	Lamp 3	$1853.2 \cdot I + 101.7$ Ω	±1.14
100 W	Lamp 1	$994.5 \cdot I + 87.6$ Ω	±1.12
	Lamp 2	$997.1 \cdot I + 92.5$ Ω	±1.20
	Lamp 3	$968.1 \cdot I + 83.9$ Ω	±1.25
	Lamp 4	$992.8 \cdot I + 83.0$ Ω	±1.22
Tungsten Halogen Lamp 1		$435.9 \cdot I + 74.7$ Ω	±1.68
Tungsten Halogen Lamp 2		$441.5 \cdot I + 72.9$ Ω	±1.65

Table 3.14: Model parameters of the resistive loads and estimated error.

From Table 3.14 it is clear that heaters can be considered as constant resistors and it is a good estimation to use the rated values that are given on their nameplates to calculate the resistance. The lamps can be modelled as a variable resistor as described in Eq. (3.1), due to the high temperature dependency of the filament. To obtain the model parameters for the lamps it is necessary to conduct experiments on the lamps as their nameplate data do not indicate anything about the parameters. Table 3.14 shows that the parameters for the lamps are inversely dependent on the power, i.e. the parameters decrease as the power increases.

3.2 Frequency Spectrum Analysis

The models realized for the characterization of the loads are used as a base for the frequency spectrum analysis. Each load was supplied with 230 V dc as described in Section 2.2.2. The analysis was done from both simulated results and measurements in order to compare.

3.2.1 Heaters

The results from the measurements and simulations are listed in Table 3.15.

	Measurements				Simulations			
	Magnitude		Distortion Factor		Magnitude		Distortion Factor	
Load	Voltage [V]	Current [A]	Voltage [%]	Current [%]	Voltage [V]	Current [A]	Voltage [%]	Current [%]
Coffee Machine (Butler)	222.88	4.20	3.39	3.38	222.88	4.21	3.39	3.39
Coffee Machine (Philips)	223.01	3.82	3.38	3.37	223.01	3.58	3.38	3.38
Curling Brush (XL Concept)	228.25	0.047	3.39	3.41	228.25	0.047	3.39	3.39
Kettle (Elram)	218.59	8.26	3.39	3.39	218.59	8.26	3.39	3.39
Kettle (Solingmüller)	217.90	8.46	3.38	3.37	217.90	8.34	3.38	3.38
Sandwich Maker (Mirabelle)	222.67	3.67	3.39	3.41	222.67	3.37	3.39	3.39
Sandwich Maker (AFK)	224.32	3.01	3.35	3.38	224.32	2.97	3.35	3.35
Stove (Siemens)	219.68	6.07	3.39	3.39	219.68	5.46	3.39	3.39

Table 3.15: Frequency spectrum analysis results from measurement and simulation of heaters.

From the results tabulated in Table 3.15 it is clear that the heaters do not cause any distortion. The distortion factor measured is about 3.4 % for all loads and occurs in both voltage and current. The maximum difference detected in the distortion factor was 0.03 % and is neglected, because it is much lower than the measurement errors given from the probes, see Chapter 2. The frequency components causing this distortion are 3 Hz and 5 Hz respectively. These two components are results of the windowing of the measured signals, see Section 2.2.2.

3.2.2 Lighting

The results from measurements and simulations listed in Table 3.16 indicate that the lamps do not cause any distortion either. The frequency components causing the distortion are not caused by the load but by the analysis procedure, as for the heaters above. This has been described more thoroughly in Chapter 2.

		Measurements				Simulations			
		Magnitude		Distortion Factor		Magnitude		Distortion Factor	
		Voltage	Current	Voltage	Current	Voltage	Current	Voltage	Current
Incandescent		[V]	[A]	[%]	[%]	[V]	[A]	[%]	[%]
25 W	Lamp 1	224.37	0.111	3.39	3.39	224.37	0.102	3.39	3.40
	Lamp 2	227.60	0.112	3.39	3.39	227.60	0.103	3.39	3.38
	Lamp 3	230.17	0.113	3.39	3.39	230.17	0.104	3.39	3.39
	Lamp 4	230.30	0.114	3.38	3.38	230.30	0.105	3.38	3.40
	Lamp 5	228.23	0.111	3.38	3.38	228.23	0.104	3.38	3.39
40 W	Lamp 1	227.70	0.171	3.39	3.39	227.70	0.163	3.39	3.41
	Lamp 2	227.50	0.171	3.38	3.38	227.50	0.166	3.38	3.39
	Lamp 3	228.93	0.175	3.39	3.39	228.93	0.170	3.39	3.38
	Lamp 4	230.24	0.175	3.38	3.38	230.24	0.165	3.38	3.38
	Lamp 5	230.11	0.180	3.42	3.40	230.11	0.164	3.42	3.38
	Lamp 6	228.20	0.175	3.38	3.38	228.20	0.167	3.38	3.37
60 W	Lamp 1	226.84	0.260	3.41	3.40	226.84	0.253	3.41	3.40
	Lamp 2	226.39	0.254	3.36	3.37	226.39	0.247	3.36	3.36
	Lamp 3	227.97	0.259	3.37	3.38	227.97	0.251	3.39	3.39
	Lamp 4	227.31	0.255	3.37	3.38	227.31	0.247	3.37	3.37
	Lamp 5	226.89	0.249	3.37	3.38	226.89	0.247	3.37	3.40
	Lamp 6	226.52	0.251	3.39	3.39	226.52	0.257	3.39	3.33
	Lamp 7	227.05	0.251	3.38	3.38	227.05	0.251	3.38	3.35
	Lamp 8	226.83	0.253	3.38	3.38	226.83	0.262	3.38	3.31
75 W	Lamp 1	228.08	0.335	3.39	3.39	228.08	0.328	3.39	3.38
	Lamp 2	227.91	0.338	3.39	3.39	227.91	0.331	3.39	3.38
	Lamp 3	228.95	0.325	3.38	3.38	228.95	0.318	3.38	3.38
100 W	Lamp 1	227.69	0.437	3.38	3.38	227.69	0.426	3.38	3.39
	Lamp 2	227.53	0.434	3.38	3.38	227.53	0.425	3.38	3.39
	Lamp 3	229.60	0.446	3.40	3.39	229.60	0.433	3.40	3.39
	Lamp 4	229.67	0.441	3.38	3.38	229.67	0.428	3.38	3.38
Tungsten Halogen									
150 W	Lamp 1	226.89	0.651	3.37	3.38	226.89	0.641	3.37	3.38
	Lamp 2	226.34	0.652	3.38	3.38	226.34	0.638	3.38	3.38

Table 3.16: Frequency spectrum analysis results from measurement and simulation of lamps.

3.3 Transient Behavior

The models realized from the characterization of the loads are used as a base to estimate how the load will react to a sudden voltage reduction. Each load was subjected to four steps in magnitude and the procedure is described in detail in Section 2.1.4.

3.3.1 Heaters

In general for all resistive loads the resistance is assumed to be constant and so as the voltage is reduced the current should reduce by the same amount, according to Ohm's law. This was tested with EMTDC where the models where subjected to a simulated step, as well as to the measured voltage step. Fig. 3.17 shows the typical transient recorded for a coffee machine (Butler). The curve denoted as "measured" comes from the measurements, the one called "modelled" is obtained from EMTDC with a simulated voltage step at the input, and the one called "simulated" is obtained from EMTDC, but using the measured voltage step as input to the model. All four steps are shown. From Fig. 3.17, the Butler coffee machine behaves as a constant resistance load, the current drops by the same amount as the voltage. The model is in total agreement to the measurement. The results for all other heaters can be found in Appendix G.

From those figures it can be seen that the models generally agree with the measurements, but in some there are some errors. The errors are generally a mixture of measurement error and model error. In some cases it is due to the age and extensive usage of the load.

The conclusion is that constant resistive loads behave exactly like Ohm's law predicts, when they are subjected to a sudden voltage step. A constant resistance can also be used as transient model.

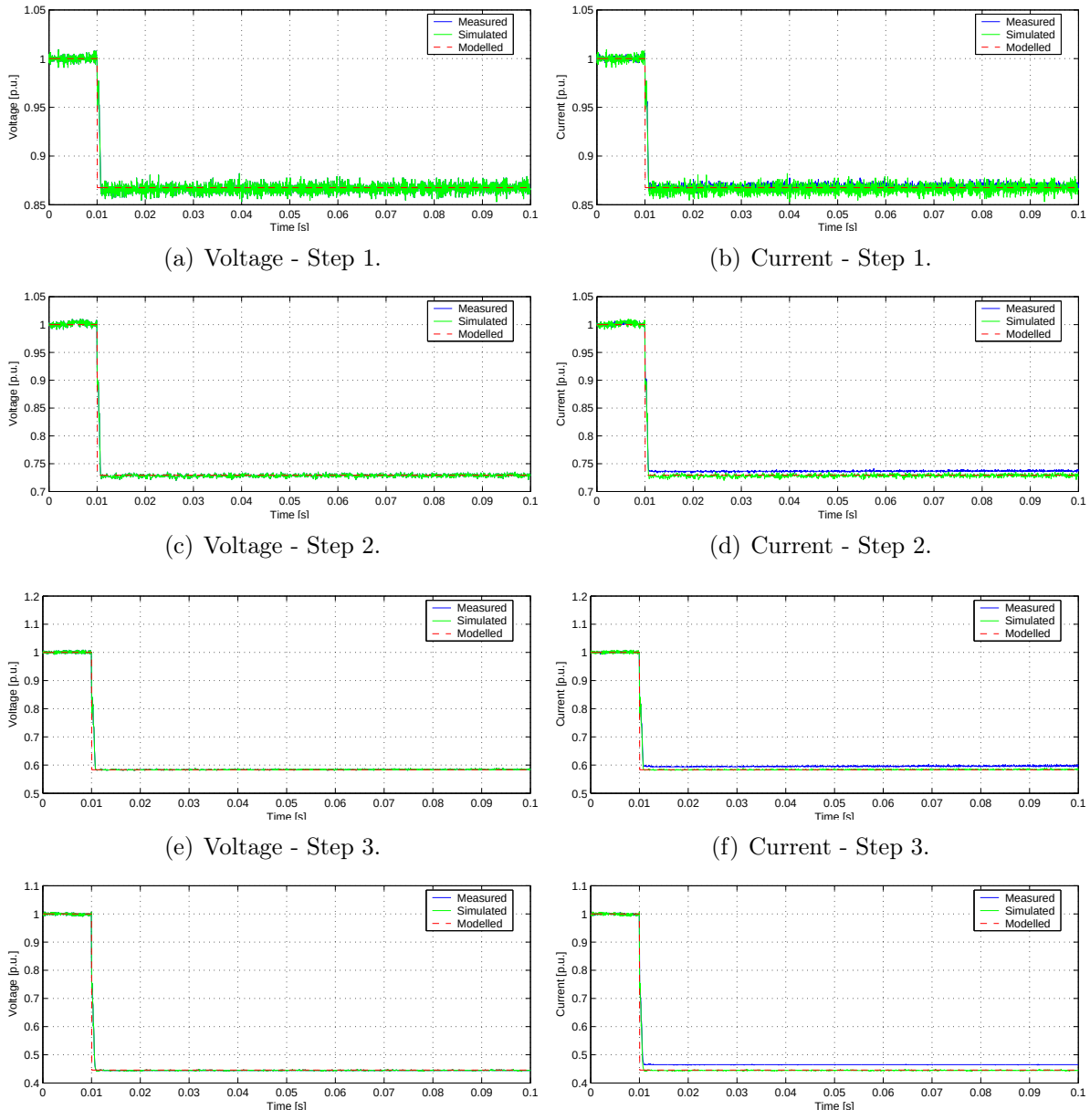

(a) Voltage - Step 1.

(b) Current - Step 1.

(c) Voltage - Step 2.

(d) Current - Step 2.

(e) Voltage - Step 3.

(f) Current - Step 3.

(g) Voltage - Step 4.

(h) Current - Step 4.

Figure 3.17: Transient behavior of coffee machine (Butler).

3.3.2 Lighting

As stated above, the lamps have a much higher temperature coefficient than the heaters and therefore the resistance is modelled as a variable resistor. Because of this, when a sudden voltage reduction is applied, the current first drops about the same amount as the voltage and then gradually increases to the new steady-state value. To model this behavior, the impedance during the step is said to change exponentially, to the new

steady-state value, and that can be realized in discrete time as

$$\hat{R}(k+1) = \hat{R}(k) + \frac{\tau}{\Delta t}(R(k+1) - \hat{R}(k)) \tag{3.4}$$

where τ is the time constant, Δt the time step of the simulation, k the discrete time and $R(k)$ is the steady-state resistance from the load characterization. Since this equation is in discrete time it can easily be implemented in EMTDC, using Fortran [5].

To estimate the time constant τ in Eq. (3.4) all four transient tests for each load were analyzed. The time from when the step is applied to the point when the current had reached 63 % of the steady-state value after the step, is said to be the time constant for that step. To determine the time constant τ, which describes how the current goes from 0 p.u. to 1 p.u. exponentially, the method of least squares is applied to the data, i.e. the time constant τ is assumed to be linearly dependent on the retained voltage after the step, see Fig. 3.18. As the figure suggests, the time constant τ for the load should then be the value where the line crosses the y-axis, that is the retained voltage is 0 p.u. To estimate how far this time constant is from the real values, measured for each step, Eq. (2.8) is used to estimate the error, called ε_τ.

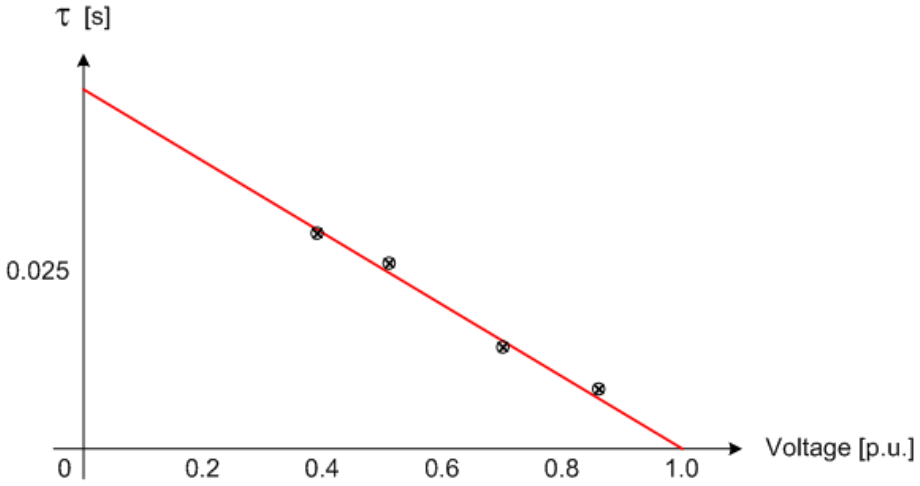

Figure 3.18: Time constant τ versus retained voltage after the step in p.u. The dots are measured points and the line is obtained with the method of least squares.

The results from the τ approximation is listed in Table 3.17 for all the lamps. The table shows that there is a strong relation between the time constant and the rated power of the lamp, which is not surprising since the lamp is very temperature dependent. The correlation was found to be logarithmic, in sense that the time constant could be estimated as $\tau = A\ln(P) + B$, where $A = 0.0151$ and $B = -0.0112$. The result from this estimation, donated by τ_{est}, is also tabulated in Table 3.17. The tungsten halogen lamps were not considered in the estimation as they are, as stated earlier, a bit different from a normal incandescent lamp. The relation is then shown in Fig. 3.19.

The model according to Eq. (3.1) were simulated in EMTDC, applying both a simulated step and the step gotten from the measurements. In Figs. 3.20 to 3.25, a typical transient is shown for six different lamps, one for each power level. The other transient measurements are reported in Appendix H. Besides the measured voltage and current (denoted as "measured"), the plots also show the model response to a simulated voltage step (denoted by "modelled") and to the actual measured voltage step (denoted as "simulated"). All four steps are shown for each load.

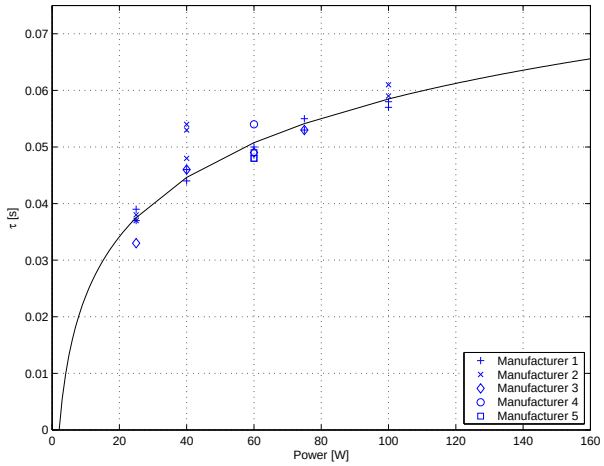

Figure 3.19: Time constant τ vs. rated power of lamps. The solid line is obtained from the model $\tau = A\ln(P) + B$.

Incandescent Lamps		τ [s]	ε_τ [%]	τ_{est}
25 W	Lamp 1	0.0390	±9.72	0.0375
	Lamp 2	0.0370	±2.09	
	Lamp 3	0.0380	±0.67	
	Lamp 4	0.0370	±3.91	
	Lamp 5	0.0330	±11.63	
40 W	Lamp 1	0.0440	±1.47	0.0446
	Lamp 2	0.0460	±2.20	
	Lamp 3	0.0480	±2.61	
	Lamp 4	0.0530	±2.00	
	Lamp 5	0.0540	±11.67	
	Lamp 6	0.0460	±2.66	
60 W	Lamp 1	0.0500	±3.67	0.0508
	Lamp 2	0.0500	±2.92	
	Lamp 3	0.0490	±2.15	
	Lamp 4	0.0538	±0.69	
	Lamp 5	0.0480	±2.46	
	Lamp 6	0.0491	±0.54	
	Lamp 7	0.0479	±4.39	
	Lamp 8	0.0478	±0.92	
75 W	Lamp 1	0.0530	±3.21	0.0541
	Lamp 2	0.0550	±1.07	
	Lamp 3	0.0530	±1.32	
100 W	Lamp 1	0.0570	±1.27	0.0585
	Lamp 2	0.0580	±3.12	
	Lamp 3	0.0610	±5.14	
	Lamp 4	0.0590	±1.82	
Tungsten halogen Lamps				
150 W	Lamp 1	0.0564	±4.01	-
	Lamp 2	0.0565	±3.65	-

Table 3.17: Estimated time constant τ for lamps and error.

From those figures it is clear that the simulations agree well with the measurements made on the lamps. The current obtained from the simulations follows the current from the measurements quite well, with the values of τ_{est} given in Table 3.17. For every lamp and every step, the current obtained from the measurements does not step down by the same amount as the voltage, but a little bit more. That means that in that instant the resistance of the lamps changes, and then gradually decreases. This behavior is neglected in the model and that is why the current from the model is always a little bit lower than the measurement directly after the step.

25 W Incandescent Lamp

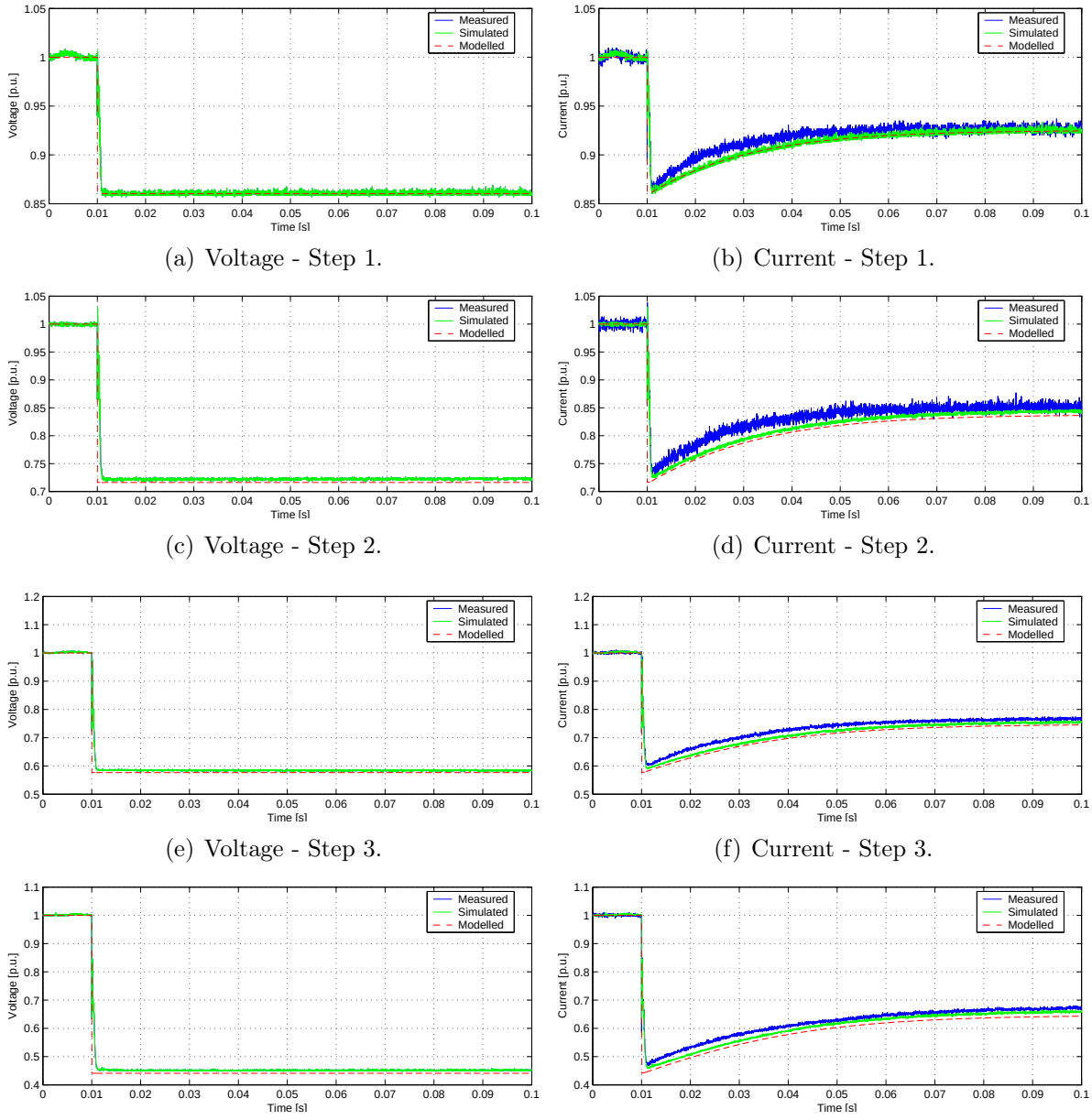

(a) Voltage - Step 1.

(b) Current - Step 1.

(c) Voltage - Step 2.

(d) Current - Step 2.

(e) Voltage - Step 3.

(f) Current - Step 3.

(g) Voltage - Step 4.

(h) Current - Step 4.

Figure 3.20: Transient behavior of 25 W incandescent lamp 1.

40 W Incandescent Lamp

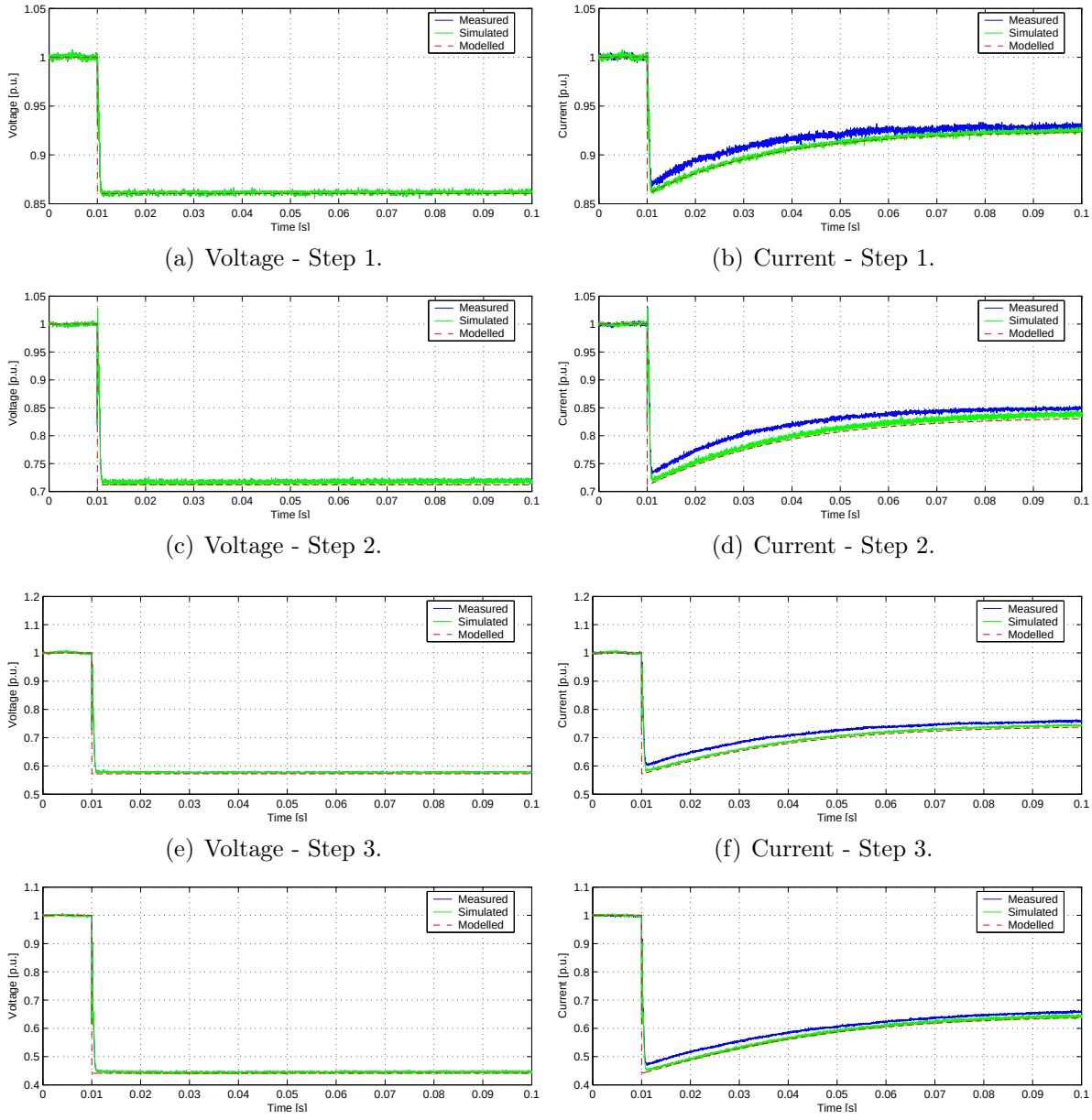

(a) Voltage - Step 1.

(b) Current - Step 1.

(c) Voltage - Step 2.

(d) Current - Step 2.

(e) Voltage - Step 3.

(f) Current - Step 3.

(g) Voltage - Step 4.

(h) Current - Step 4.

Figure 3.21: Transient behavior of 40 W incandescent lamp 1.

60 W Incandescent Lamp

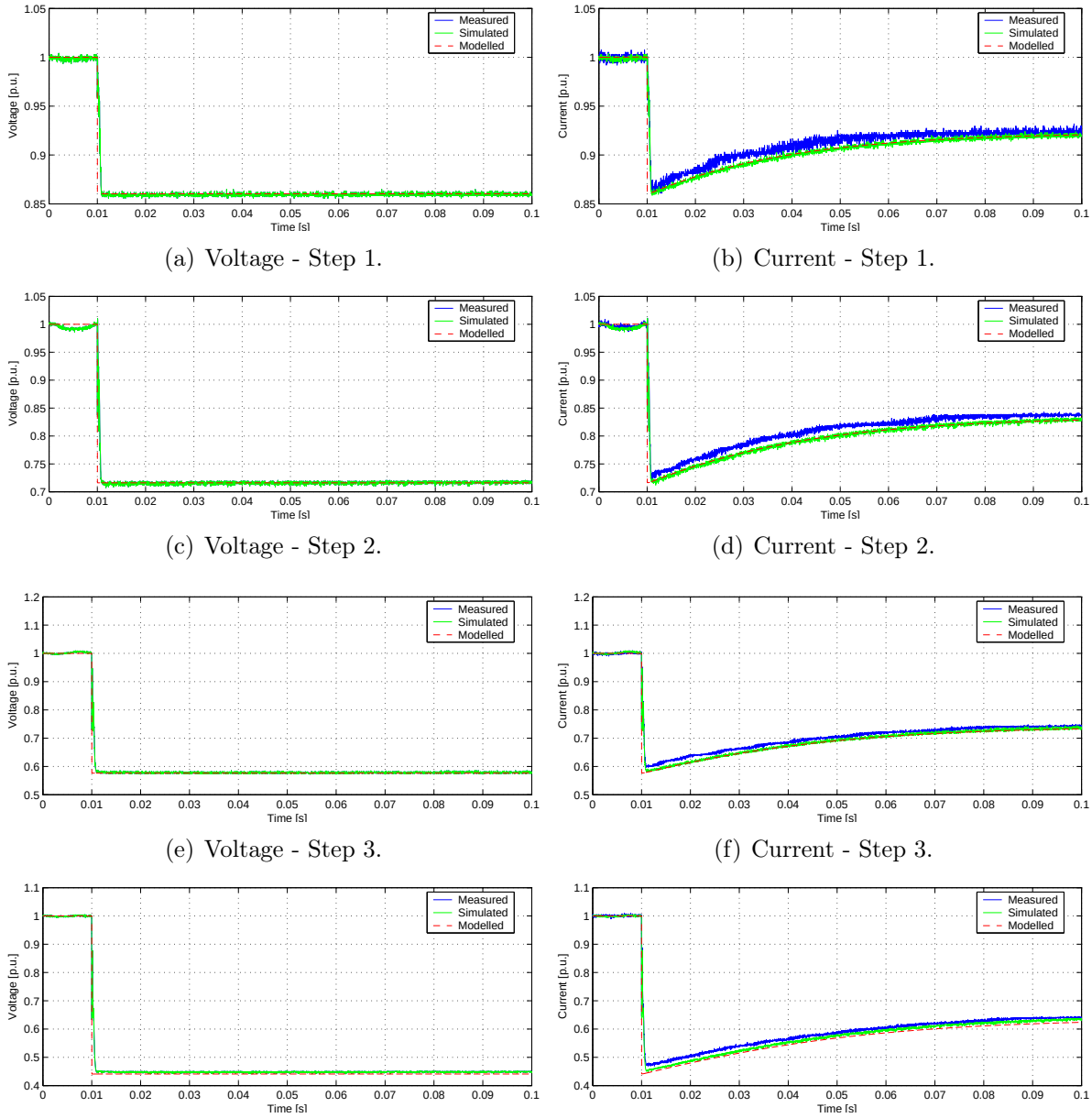

(a) Voltage - Step 1.

(b) Current - Step 1.

(c) Voltage - Step 2.

(d) Current - Step 2.

(e) Voltage - Step 3.

(f) Current - Step 3.

(g) Voltage - Step 4.

(h) Current - Step 4.

Figure 3.22: Transient behavior of 60 W incandescent lamp 1.

75 W Incandescent Lamp

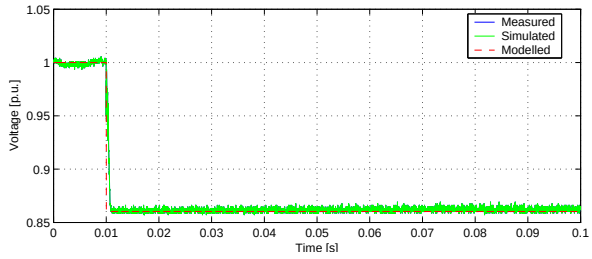

(a) Voltage - Step 1.

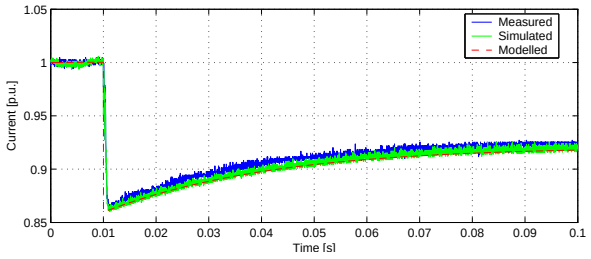

(b) Current - Step 1.

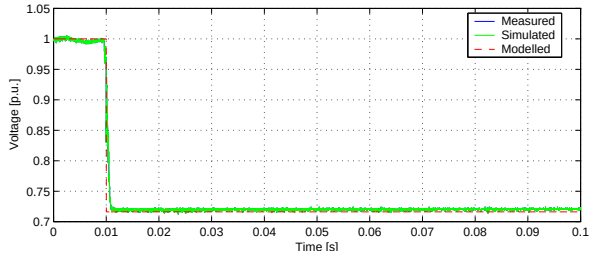

(c) Voltage - Step 2.

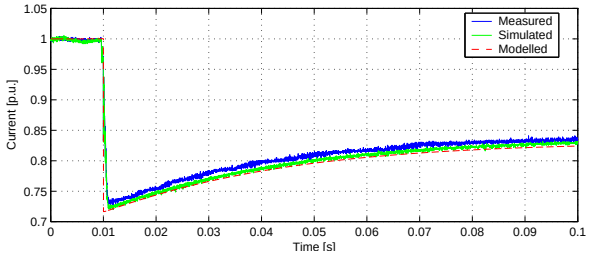

(d) Current - Step 2.

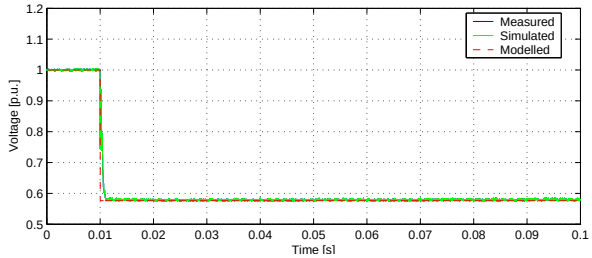

(e) Voltage - Step 3.

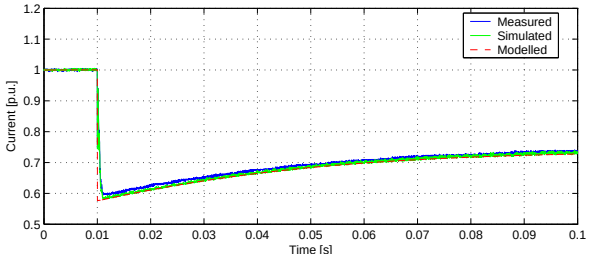

(f) Current - Step 3.

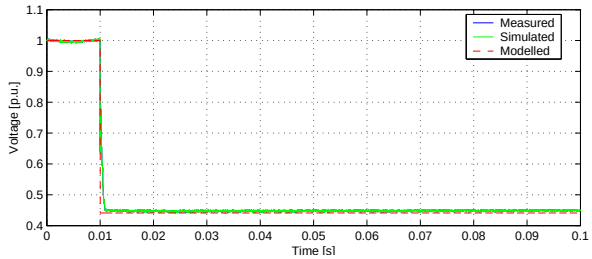

(g) Voltage - Step 4.

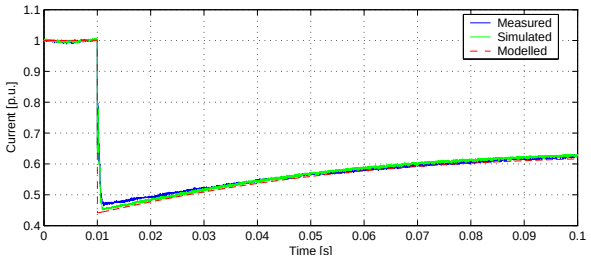

(h) Current - Step 4.

Figure 3.23: Transient behavior of 75 W incandescent lamp 1.

100 W Incandescent Lamp

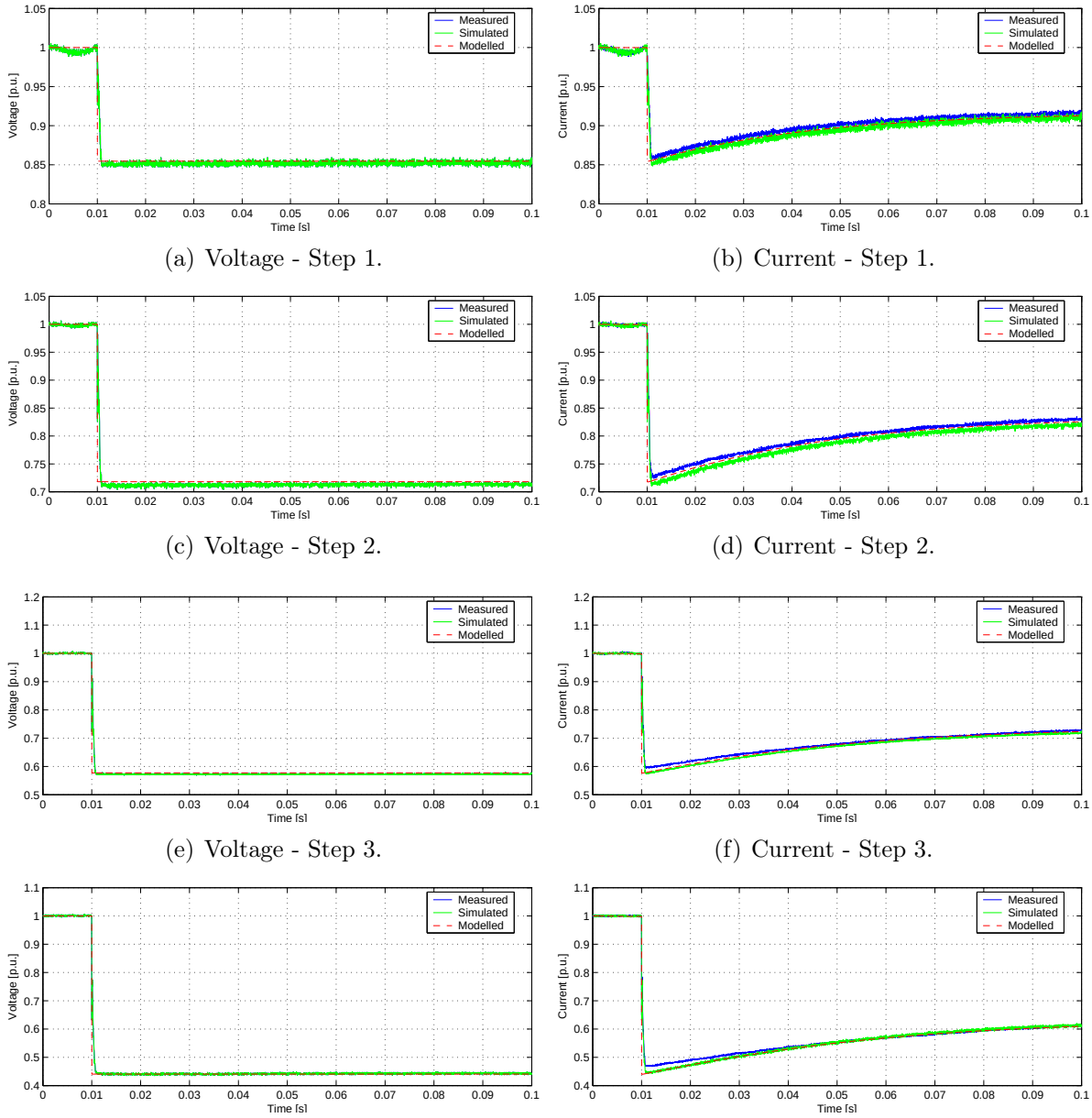

(a) Voltage - Step 1.

(b) Current - Step 1.

(c) Voltage - Step 2.

(d) Current - Step 2.

(e) Voltage - Step 3.

(f) Current - Step 3.

(g) Voltage - Step 4.

(h) Current - Step 4.

Figure 3.24: Transient behavior of 100 W incandescent lamp 1.

150 W Tungsten Halogen Lamp

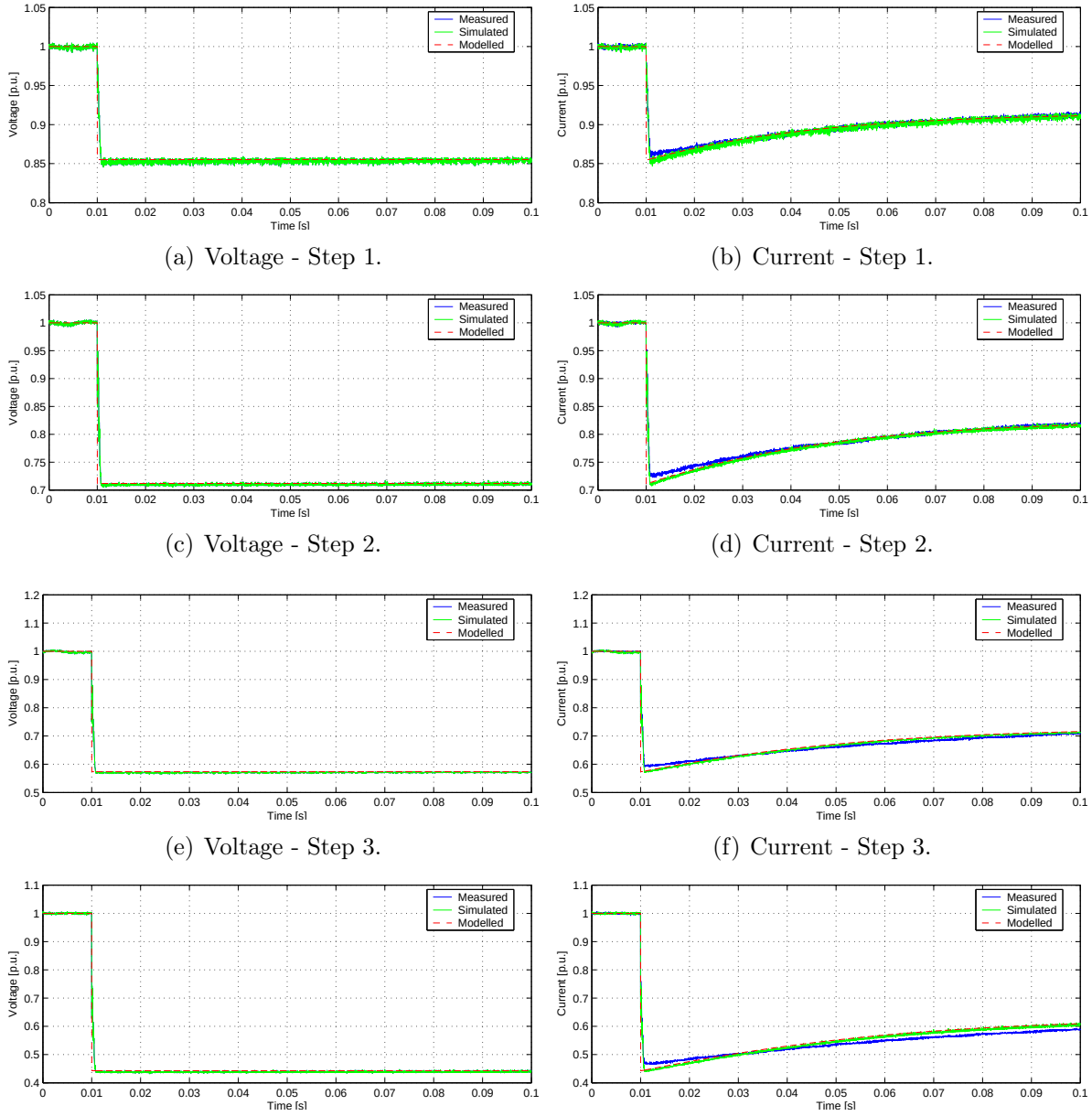

(a) Voltage - Step 1.

(b) Current - Step 1.

(c) Voltage - Step 2.

(d) Current - Step 2.

(e) Voltage - Step 3.

(f) Current - Step 3.

(g) Voltage - Step 4.

(h) Current - Step 4.

Figure 3.25: Transient behavior of 150 W tungsten halogen lamp 1.

3.4 Summary

The resistive loads were divided into to groups. Loads that should behave according to Ohm's law, or as constant resistance loads, and loads that where highly temperature dependent and needed to be modelled as a variable resistor, according to Eq. (3.1). The conclusion from that assumption is tabulated in Table 3.18. From there it can be seen that the models that are constant resistive are those loads used for thermal purposes. The loads that needed to be modelled as a variable resistor are used for lighting due to the fact that the temperature of the filament is quite high.

In steady-state it was expected that the loads would not cause any distortion in the grid. The loads where measured and it was proven that simple resistors do not cause any distortion in dc.

When the loads were subjected to a sudden voltage step the magnitude of the current was proportional to the retained voltage, that is it follows Ohm's law. That is the case for the heaters, but the resistance of the lamps is current dependent and the magnitude of the current will therefore not be in proportion to the retained voltage. Also the resistance of the lamp does not change instantly. That is due to the temperature of the filament. The resistance goes down exponentially and a method of estimating the time constant τ was presented. The results from that are also tabulated in Table 3.18. This τ_{est} gives a good result to the measurements obtained.

Heaters

	Rated Power [W]	Model [$R =$]	error [%]	τ [s]	error [%]	τ_{est} [s]
Coffee Machine (Butler)	1000	52.90 Ω	±1.62	-	-	-
Coffee Machine (Philips)	850	62.24 Ω	±3.13	-	-	-
Curling Brush (XL Concept)	11	4809.1 Ω	±2.45	-	-	-
Kettle (Elram)	2000	26.45 Ω	±6.1	-	-	-
Kettle (Solingmüller)	2025	26.12 Ω	±2.48	-	-	-
Sandwich Maker (Mirabella)	800	66.13 Ω	±2.48	-	-	-
Sandwich Maker (AFK)	700	75.57 Ω	±0.86	-	-	-
Stove (Siemens)	unknown	40.26 Ω	±4.67	-	-	-

Lighting

	Rated Power [W]	Model [$R =$]	error [%]	τ [s]	error [%]	τ_{est} [s]
Incandescent Lamp 1	25	$16966.2 \cdot I + 128.4$ Ω	±1.59	0.0390	±9.72	0.0375
Incandescent Lamp 2		$16871.2 \cdot I + 131.8$ Ω	±1.51	0.0370	±2.09	
Incandescent Lamp 3		$17020.5 \cdot I + 121.2$ Ω	±1.50	0.0380	±0.67	
Incandescent Lamp 4		$16682.8 \cdot I + 111.5$ Ω	±1.64	0.0370	±3.91	
Incandescent Lamp 5		$17511.7 \cdot I + 102.0$ Ω	±1.59	0.0330	±11.63	
Incandescent Lamp 1	40	$7010.2 \cdot I + 133.7$ Ω	±1.42	0.0440	±1.47	0.0446
Incandescent Lamp 2		$7071.6 \cdot I + 120.8$ Ω	±1.40	0.0460	±2.20	
Incandescent Lamp 3		$6695.1 \cdot I + 148.0$ Ω	±1.29	0.0480	±2.61	
Incandescent Lamp 4		$6294.9 \cdot I + 143.7$ Ω	±1.35	0.0530	±2.00	
Incandescent Lamp 5		$6706.8 \cdot I + 137.4$ Ω	±1.34	0.0540	±11.67	
Incandescent Lamp 6		$6624.7 \cdot I + 145.8$ Ω	±1.37	0.0460	±2.66	
Incandescent Lamp 1	60	$2925.8 \cdot I + 113.5$ Ω	±1.27	0.0500	±3.67	0.0508
Incandescent Lamp 2		$3046.9 \cdot I + 115.9$ Ω	±1.27	0.0500	±2.92	
Incandescent Lamp 3		$2956.0 \cdot I + 117.1$ Ω	±1.16	0.0490	±2.15	
Incandescent Lamp 4		$3285.6 \cdot I + 106.5$ Ω	±1.33	0.0538	±0.69	
Incandescent Lamp 5		$3922.5 \cdot I + 4.0$ Ω	±1.82	0.0480	±2.46	
Incandescent Lamp 6		$3868.0 \cdot I + 1.9$ Ω	±2.05	0.0491	±0.54	
Incandescent Lamp 7		$3889.2 \cdot I + 2.9$ Ω	±1.87	0.0479	±4.39	
Incandescent Lamp 8		$3805.5 \cdot I + 1.7$ Ω	±1.73	0.0478	±0.92	
Incandescent Lamp 1	75	$1709.5 \cdot I + 106.7$ Ω	±1.23	0.0530	±3.21	0.0541
Incandescent Lamp 2		$1685.3 \cdot I + 103.5$ Ω	±1.24	0.0550	±1.07	
Incandescent Lamp 3		$1853.2 \cdot I + 101.7$ Ω	±1.14	0.0530	±1.32	
Incandescent Lamp 1	100	$994.5 \cdot I + 87.6$ Ω	±1.12	0.0570	±1.27	0.0585
Incandescent Lamp 2		$997.1 \cdot I + 92.5$ Ω	±1.20	0.0580	±3.12	
Incandescent Lamp 3		$968.1 \cdot I + 83.9$ Ω	±1.25	0.0610	±5.14	
Incandescent Lamp 4		$992.8 \cdot I + 83.0$ Ω	±1.22	0.0590	±1.82	
Tungsten Halogen Lamp 1	150	$435.9 \cdot I + 74.7$ Ω	±1.68	0.0564	±4.01	-
Tungsten Halogen Lamp 2	150	$441.5 \cdot I + 72.9$ Ω	±1.65	0.0565	±3.65	-

Table 3.18: Model parameters for resistive loads.

The main conclusion drawn from the analysis is that a model for the constant resistive loads, the heaters, can be realized from the nameplate of the load, that are actually the parameters given in Table 3.18. This is not possible for loads where the resistance is temperature dependent, and thereby current dependent. This is the case for the lamps, the nameplate values give no hint of how the model should be realized. That can only be found via measurements. This is also the case for the time constant τ_{est}.

Chapter 4

Rotating Loads

Rotating loads are those loads that perform their work by rotation. For domestic use, many types of machines are used. For instance induction motors and universal motors.

Induction motors are commonly used in domestic appliances. There are two types. First there are induction motors used in variable speed drives, like in new washing machines and refrigerators. They are usually inverter based, and convert the single phase ac input to dc and then to three-phase ac. Those drives should work fine with dc but are expensive.

Second type of induction motors are single phase and do not require such a complicated system, they are widely used in todays refrigerators. The system consists of a relay, one or two capacitors and the motor. When the motor is started the capacitor is connected between the start winding and the run winding to create a phase shift between them which makes the rotor rotate. Than after about 30 ms, the capacitor is disconnected by the relay, see Fig. 4.1. The motor can operate with a run capacitor between the phases (capacitive start, capacitive run or CSCR) or without (capacitive start, inductive run or CSIR). The main purpose of this capacitor is to improve the efficiency of the motor and is mainly used in motors with higher power ratings. These motors require alternating current to run [15] [16].

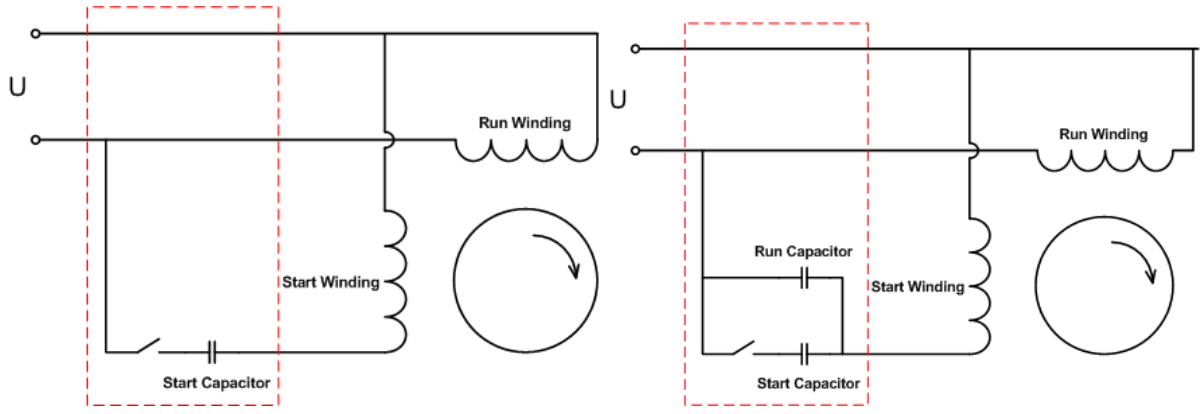

(a) CSIR motor (b) CSCR motor

Figure 4.1: Equivalent circuit for single phase induction motors, (a) capacitive start, inductive run, (b) capacitive start capacitive run.

The universal motor is also widely used in todays domestic appliances mainly because of its wide speed range. These motors are series dc motors, i.e. the field winding is connected in series with the armature winding, but they can also be used with alternating

current, hence the term universal motor [17]. That is, the equivalent circuit should be the same for the dc motor and the universal motor or as Fig. 4.2 shows.

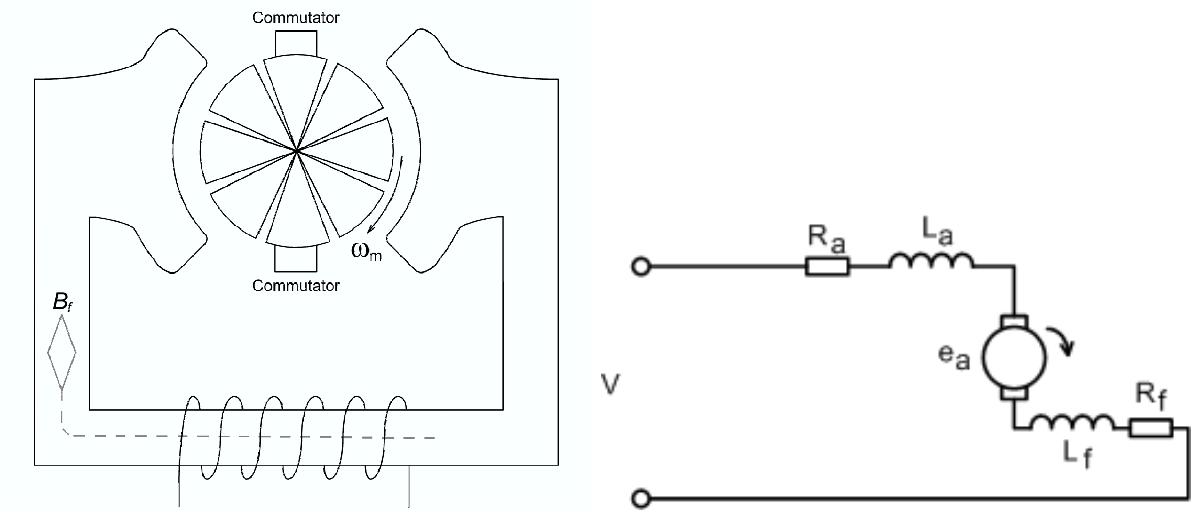

(a) Structure (b) Circuit

Figure 4.2: Structure and circuit diagram of a dc motor (universal motor).

The equivalent circuit shows the conversion between electrical and mechanical power. This is given by the following

$$V_a = e_a + R_{eq} I_a + L_{eq} \frac{\mathrm{d}I_a}{\mathrm{d}t} \tag{4.1}$$

where $R_{eq} = R_a + R_f$ is the equivalent resistance of the armature and the field windings, $L_{eq} = L_a + L_f$ the equivalent inductance and e_a the back emf. The equivalent inductance can be neglected if only small changes in voltage and current are considered (steady-state). The rotational speed, ω_m, of the motor is proportional to the back emf e_a, and the torque, T_e, is proportional to the current I_a, yielding

$$e_a = k_E \omega_m \tag{4.2}$$

$$T_e = k_T I_a \tag{4.3}$$

where $k_E = k_T$ and are usually considered as constants. Physically $k_E = k_T = n_a \cdot l \cdot r/(2 \cdot a) \cdot \Phi_f$ where n_a is the number of conductors on the armature, l is the length of each conductor, r is the radius, a is the cross sectional area of the conductor and Φ_f is the uniform flux in the stator [16]. Since the field winding is connected in series with the armature, Eqs. (4.2) and (4.3) can be rewritten as

$$e_a = k_e \Phi_f \omega_m \tag{4.4}$$

$$T_e = k_t \Phi_f I_a \tag{4.5}$$

The flux Φ_f is directly related to the field current and since that current is the same as the armature current and magnetic linearity is assumed, Eqs. (4.4) and (4.5) can be rewritten as

$$e_a = k_m I_a \omega_m \tag{4.6}$$

$$T_e = k_m I_a^2 \tag{4.7}$$

From Eq. (4.7) it is clear that the motor operates under alternating current because it produces a unipolar torque, but it will be pulsating with twice the frequency of the current [16].

The final expression for the motor relates the change in speed to the change in torque as

$$\frac{d\omega_m}{dt} = \frac{1}{J_{eq}}(T_e - T_L) \tag{4.8}$$

where J_{eq} is the equivalent inertia of the motor and the load and T_L is the load torque [18]. From Eqs. (4.1) to (4.6) it is clear that many parameters are needed to be able to make a dynamic model of the universal motor. In short what is needed to be known is R_{eq}, L_{eq}, k_m (that is the structure of the rotor) and either the speed or torque. These parameters cannot be measured over the input terminals of the motor.

Before the load was tested on dc it was decided to see how the current shape looked when it was supplied with ac. From the shape and the power factor of the motor it is clear if it is a universal motor or an induction motor as in shown in Fig. 4.3 and the distortion and power is tabulated in Table 4.1

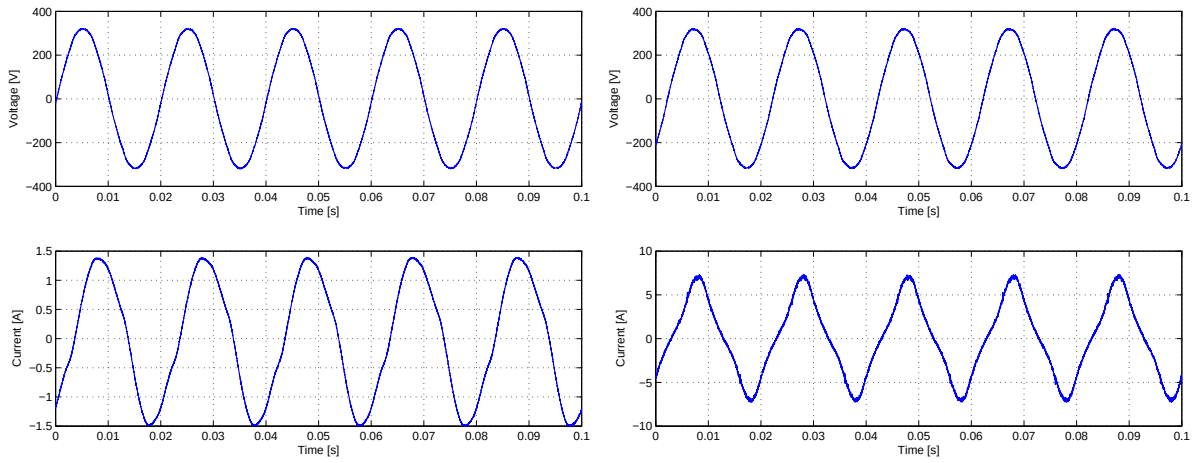

(a) induction motor

(b) universal motor

Figure 4.3: Voltage and current shapes of a refrigerator (induction motor) and a vacuum cleaner (universal motor).

The loads were then categorized accordingly and the loads that it was possible to test on are listed in Table 4.2.

	induction motor		universal motor	
Voltage	Amplitude [V]	THD [%]	Amplitude [V]	THD [%]
	227.5	1.33	226.9	1.37
Current	Amplitude [A]	THD [%]	Amplitude [A]	THD [%]
	1.00	8.01	4.33	15.81
Power factor	DPF	PF	DPF	PF
	0.52	0.52	0.98	0.96
Power	Amplitude [VA]		Amplitude [VA]	
	226.8		983.5	

Table 4.1: Characteristics of a refrigerator (induction motor) and a vacuum cleaner (universal motor).

Induction motors	Universal motors
Fan	Blender
Hair trimmer	Mixer
Refrigerator	Two hair dryers
with compressor	Three vacuum cleaners

Table 4.2: Motors acquired.

4.1 Load Characterization

To characterize the loads, the voltage was varied from 50 to 300 V in 10 V steps. The reason why the loads where not supplied at higher voltages is that the speed of the rotor is proportional to the voltage, as Eq. (4.2) shows, and due to the high speed of most of these motors their structural integrity is questionable. For each step the voltage and current were recorded with the measurement setup and procedure which were more thoroughly described in Chapter 2.

When the voltage against the current was plotted it seemed logical to characterize the loads according to Eq. (2.5). The power thus be calculated and plotted against the voltage and characterized according to Eq. (2.6). When these two equations are compared, the following can be observed:

- If current vs. voltage shows a quadratic relation, then $Y_{p2} \neq 0$, $Y_{p1} \neq 0$ and $Y_{p0} \neq 0$. Then the power vs. voltage should show a third order relation. That is the load cannot be characterized by Eq. (2.6).

- If the power vs. voltage shows a quadratic relation, then $Y_{p2} = 0$, $Y_{p1} = A_{p2}$, $Y_{p0} = A_{p1}$ and $A_{p0} = 0$. That is the voltage vs. current should show a linear relation.

When the characterization was done for the loads these two assumptions were tested, and the absolute average error is taken according to Eq. (2.8). If the loads did not follow the above, they where characterized according to Section 3.1. The loads that follow the above are grouped as universal motors and those that don't are grouped as other motors.

4.1.1 Universal Motors

Blender (Melissa)

The rated power of the blender is gotten from the nameplate and is 300 W at the nominal voltage of 230 V. The characteristic of the blender is plotted in Fig. 4.4. Fig. 4.4(a) shows how the current varies with voltage. The method of least squares is used to obtain a quadratic and a linear model as described by Eq. (2.5), with the assumptions above.

Fig. 4.4(b) shows how the power varies with the voltage. If the quadratic model from Eq. (2.5) is used the power should have a third order relation to voltage, and no curve fit is made. The linear model is then referred to the linear model in Fig. 4.4(a), that can be curve fitted according to Eq. (2.6).

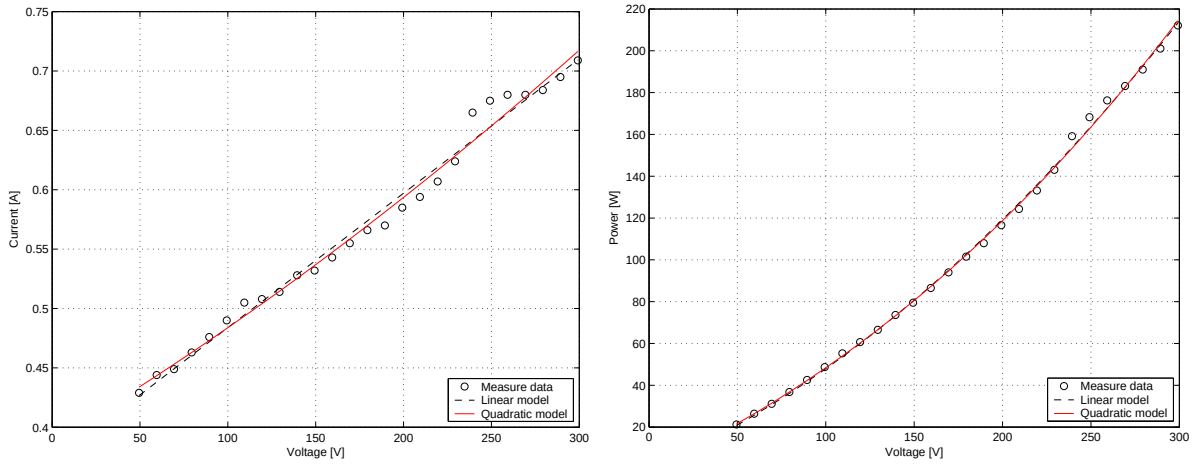

(a) Current vs. Voltage

(b) Power vs. Voltage

Figure 4.4: Characteristics of blender (Melissa).

Table 4.3 shows the parameters gotten from the models as described above. It shows that no characterization of the power has been made when the voltage vs. current relation is assumed to be quadratic. The error of the power of that assumption is still shown, that is the power is calculated directly from the model and assumed to be third order. Then in the linear model, it is clear that the power vs. voltage relation should be quadratic and the method of least squares is applied on the data to obtain the parameters together with the calculated error.

	Y_{p2}	Y_{p1}	Y_{p0}	ε_Y	A_{p2}	A_{p1}	A_{p0}	ε_P
quadratic model:	$7.1 \cdot 10^{-7}$	$8.8 \cdot 10^{-4}$	0.388	1.18	-	-	-	1.18
linear model:	0	$1.13 \cdot 10^{-3}$	0.371	1.32	$1.17 \cdot 10^{-3}$	0.362	0	1.61

Table 4.3: Model parameters for blender (Melissa).

From Table 4.3 it is clear that Y_{p2} is very small and can be neglected. It is also clear that $Y_{p1} \approx A_{p2}$ and $Y_{p0} \approx A_{p1}$ for the linear model. These parameters have nothing to do with the rated power of the motor and a model can not be realized from only knowing the power at rated voltage. The model has to be obtained from measurements and it is possible to model the blender as a controllable current source, or as

$$\boxed{i_l = 1.13 \cdot 10^{-3} u + 0.371 \pm 1.61\ \%}$$

Mixer (Ide Line)

The rated power of the mixer is 220 W at the rated voltage of 230 V. the characteristics are plotted in Fig. 4.5 and the model parameters are tabulated in Table 4.4

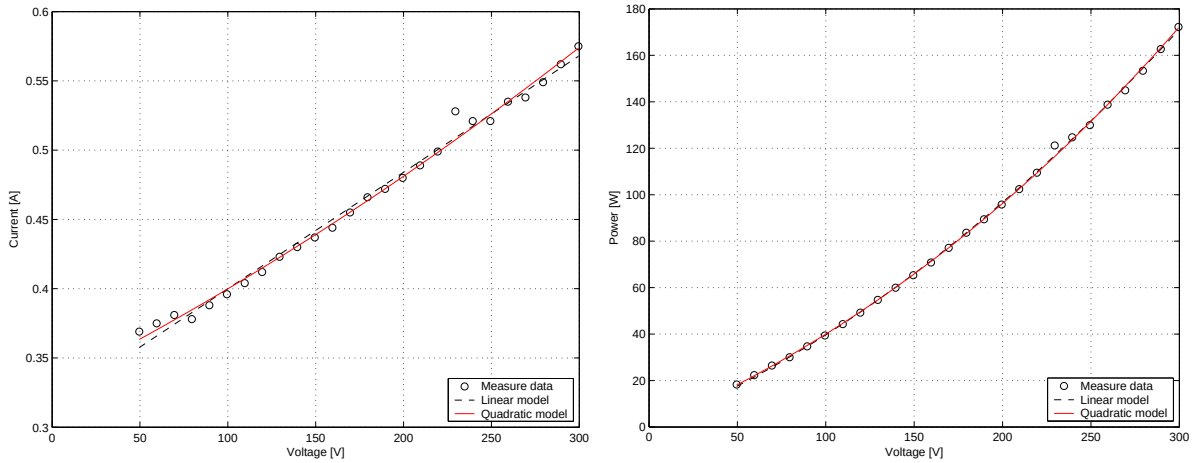

(a) Current vs. Voltage

(b) Power vs. Voltage

Figure 4.5: Characteristics of mixer (Ide Line).

	Y_{p2}	Y_{p1}	Y_{p0}	ε_Y	A_{p2}	A_{p1}	A_{p0}	ε_P
quadratic model:	$5.84 \cdot 10^{-7}$	$6.37 \cdot 10^{-4}$	0.330	0.75	-	-	-	0.75
linear model:	0	$8.4 \cdot 10^{-4}$	0.316	1.05	$8.71 \cdot 10^{-4}$	0.309	0	0.94

Table 4.4: Model parameters for mixer (Ide Line).

Table 4.4 shows that Y_{p2} is very small and can be neglected. It is also clear that $Y_{p1} \approx A_{p2}$ and $Y_{p0} \approx A_{p1}$ for the linear model. Again, the measurements show that it is possible to model the mixer as a controllable current source, or as

$$\boxed{i_l = 8.4 \cdot 10^{-4} u + 0.316 \pm 1.05\ \%}$$

Vacuum Cleaner (Electrolux)

The rated power of the vacuum cleaner is unknown. The characteristics are plotted in Fig. 4.6 and the model parameters are tabulated in Table 4.5

	Y_{p2}	Y_{p1}	Y_{p0}	ε_Y	A_{p2}	A_{p1}	A_{p0}	ε_P
quadratic model:	$1.32 \cdot 10{-}5$	0.0114	0.844	0.94	-	-	-	0.947
linear model:	0	0.0156	0.562	1.94	0.0164	0.417	0	3.07

Table 4.5: Model parameters for vacuum cleaner (Electrolux).

Table 4.5 shows that Y_{p2} can be neglected and $Y_{p1} \approx A_{p2}$ and $Y_{p0} \approx A_{p1}$ for the linear model. The model was obtained from the measurements and it is possible to model the vacuum cleaner as a controllable current source, or as

$$\boxed{i_l = 0.0156u + 0.562 \pm 3.07\ \%}$$

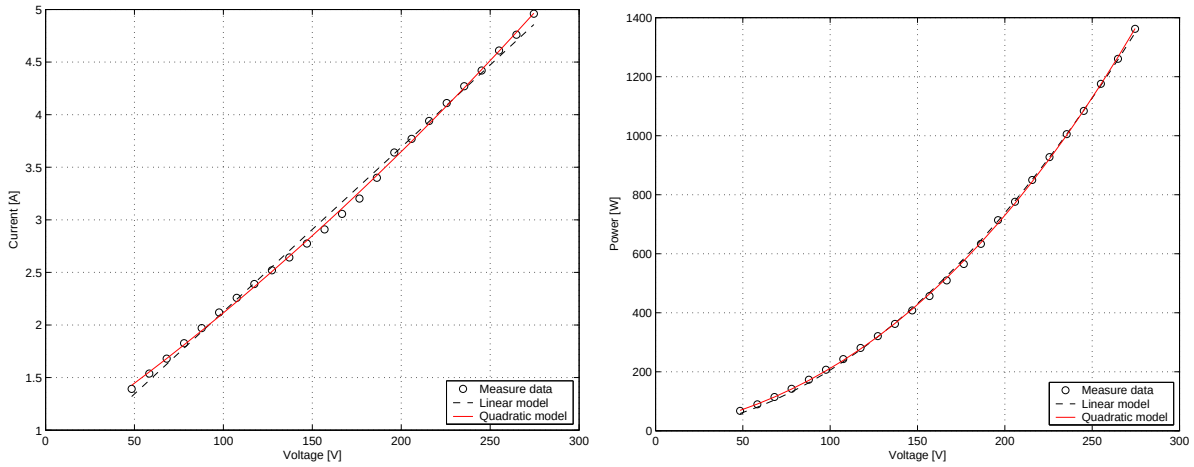

(a) Current vs. Voltage (b) Power vs. Voltage

Figure 4.6: Characteristics of vacuum cleaner (Electrolux).

Vacuum Cleaner (Euroline)

The rated power of the vacuum cleaner is 1400 W at the rated voltage of 230 V. The characteristics are plotted in Fig. 4.7 and the model parameters are tabulated in Table 4.6.

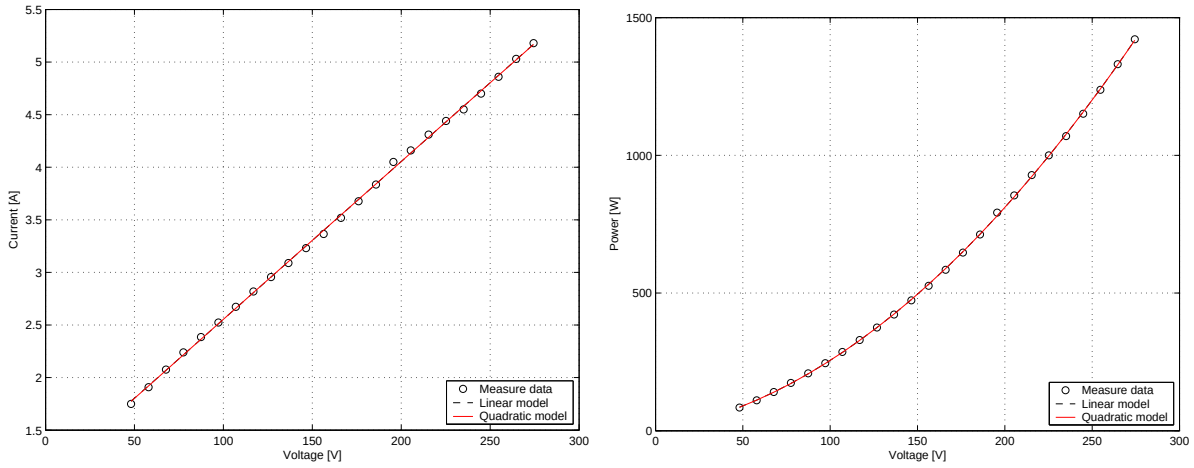

(a) Current vs. Voltage (b) Power vs. Voltage

Figure 4.7: Characteristics of vacuum cleaner (Euroline).

	Y_{p2}	Y_{p1}	Y_{p0}	ε_Y	A_{p2}	A_{p1}	A_{p0}	ε_P
quadratic model:	$-1.94 \cdot 10^{-7}$	0.0151	1.05	0.59	-	-	-	0.59
linear model:	0	0.0150	1.054	0.59	0.0150	1.054	0	0.59

Table 4.6: Model parameters for vacuum cleaner (Euroline).

Similarly to the previous case, Y_{p2} can be neglected, and $Y_{p1} \approx A_{p2}$ and $Y_{p0} \approx A_{p1}$ for the linear model. The vacuum cleaner can be modeled as a controllable current source, or as

$$\boxed{i_l = 0.0150u + 1.054 \pm 0.59\ \%}$$

Vacuum Cleaner (LG)

The rated power of the vacuum cleaner is 1300 W at the rated voltage of 230 V. The characteristics are plotted in Fig. 4.8 and the model parameters are tabulated in Table 4.7.

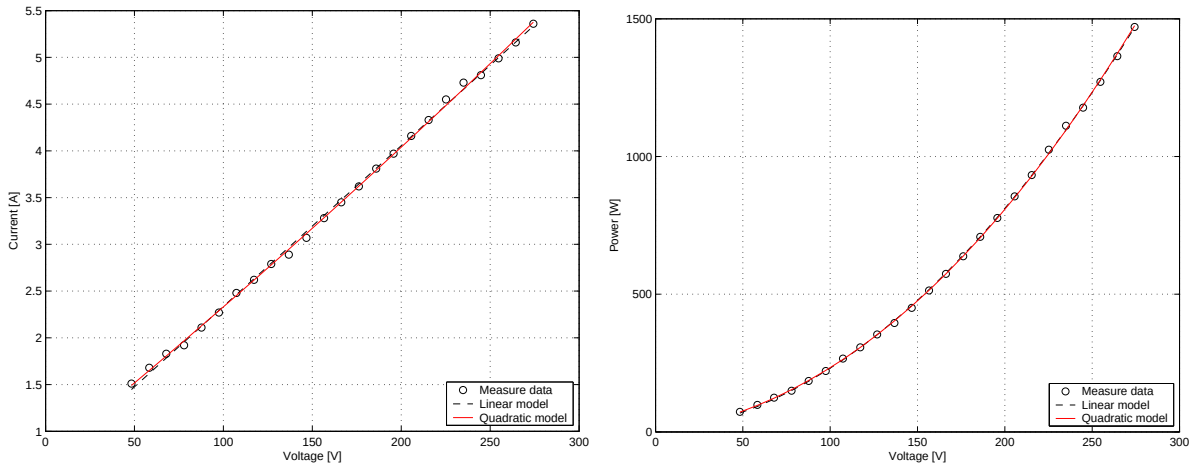

(a) Current vs. Voltage

(b) Power vs. Voltage

Figure 4.8: Characteristics of vacuum cleaner (LG).

	Y_{p2}	Y_{p1}	Y_{p0}	ε_Y	A_{p2}	A_{p1}	A_{p0}	ε_P
quadratic model:	$5.35 \cdot 10^{-6}$	0.0155	0.730	0.86	-	-	-	0.86
linear model:	0	0.0172	0.616	1.15	0.0174	0.567	0	1.25

Table 4.7: Model parameters for vacuum cleaner (LG).

Table 4.7 shows that Y_{p2} is very small and can be neglected. It is also clear that $Y_{p1} \approx A_{p2}$ and $Y_{p0} \approx A_{p1}$ for the linear model. The measurements show that it is possible to model the vacuum cleaner as a controllable current source, or as

$$\boxed{i_l = 0.0172u + 0.616 \pm 1.25\ \%}$$

4.1.2 Other Motors

The hair dryers did not show the same characteristics as the other rotating loads, and were characterized as resistive loads. That is due to the fact that, in such loads, there is a huge resistor dominating in the characteristics.

Hair Dryer (AFK, 1800W)

The rated power of the hair dryer is gotten from the nameplate and is 1800 W at the rated voltage of 230 V. According to Ohm's law the resistance is calculated to be 29.29 Ω. The characteristic is plotted in Fig. 4.9 and the model parameters are tabulated in Table 4.8.

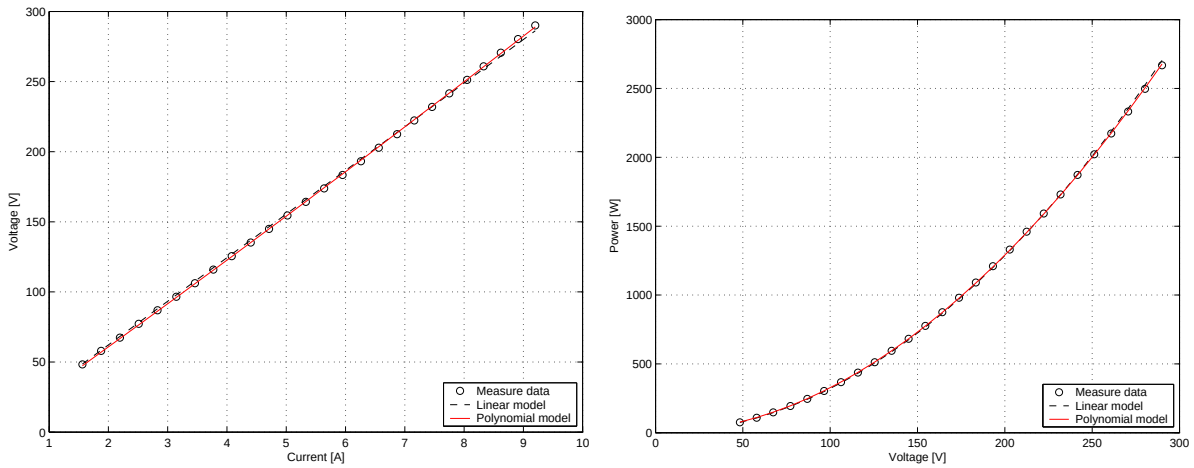

(a) Voltage vs. Current (b) Power vs. Voltage

Figure 4.9: Characteristics of hair dryer (AFK, 1800W).

	R_{p2}	R_{p1}	R_{p0}	ε_R	A_{p2}	A_{p1}	A_{p0}	ε_P
quadratic model:	0.143	30.1	0	0.44	-	-	-	0.44
linear model:	0	31.1	0	0.89	0.0321	$5.64 \cdot 10^{-16}$	0	0.88

Table 4.8: Model parameters for hair dryer (AFK, 1800W).

Table 4.8 shows that R_{p2} is very small and can be neglected. Also $R_{p1} \simeq A_{p2}^{-1} = 31.1\ \Omega$. The model gives a resistance very close to the resistance gotten from the rated power, the error is only 2.77%. The model is then

$$\boxed{R = 29.29\ \Omega \pm 2.77\ \%}$$

Hair Dryer (AFK, 1200W)

The rated power of the hair dryer is gotten from the nameplate and is 1200 W at the rated voltage of 230 V. According to Ohm's law the resistance is calculated to be 44.08Ω. The characteristic is plotted in Fig. 4.10 and the model parameters are tabulated in Table 4.9.

Table 4.9 shows that R_{p2} is very small and can be neglected, and $R_{p1} \simeq A_{p2}^{-1} = 47.6\ \Omega$. The model gives a resistance close to the resistance gotten from the rated power the error is 7.9 %. The error is that high because the resistor is less dominating the motor characteristics compared to the other hair dryer. Finally the model can be expressed as

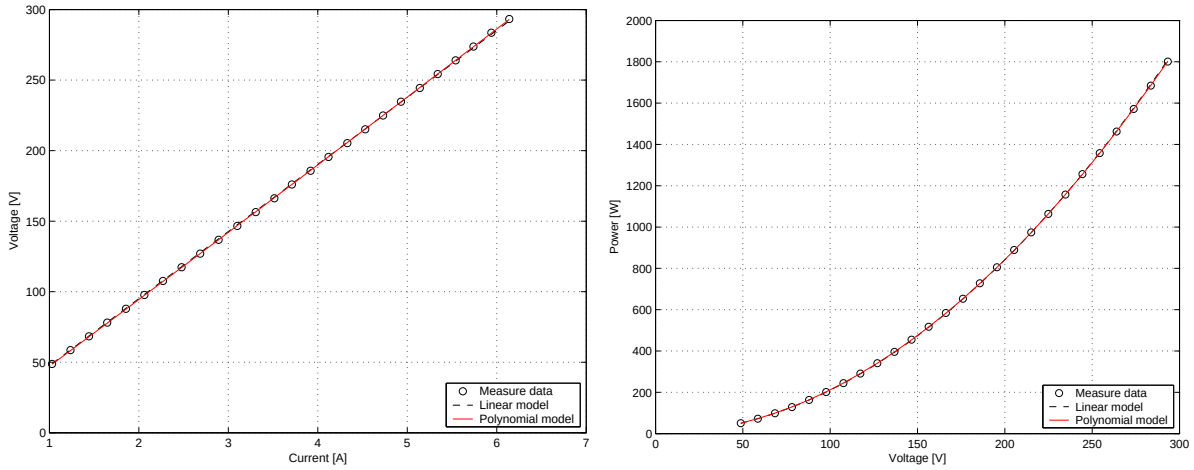

(a) Voltage vs. Current

(b) Power vs. Voltage

Figure 4.10: Characteristics of hair dryer (AFK, 1200W).

	R_{p2}	R_{p1}	R_{p0}	ε_R	A_{p2}	A_{p1}	A_{p0}	ε_P
quadratic model:	0.116	47.0	0	0.19	-	-	-	0.19
linear model:	0	47.6	0	0.31	0.0210	$-1.26 \cdot 10^{-15}$	0	0.31

Table 4.9: Model parameters for hair dryer (AFK, 1200W).

$$\boxed{R = 47.6\ \Omega \pm 7.9\ \%}$$

4.1.3 Summary

The results of the characterization of the rotating loads is tabulated in Table 4.10 with the estimated error of the models.

Universal Motors

	Model $[i_l =]$	error [%]
Blender (Melissa)	$1.13 \cdot 10^{-3}u + 0.371$	± 1.61
Mixer (Ide Line)	$8.4 \cdot 10^{-4}u + 0.316$	± 1.05
Vacuum cleaner (Electrolux)	$0.0156u + 0.562$	± 3.07
Vacuum cleaner (Euroline)	$0.0150u + 1.054$	± 0.59
Vacuum cleaner (LG)	$0.0172u + 0.616$	± 1.25

Other Motors

	Model $[R =]$	error [%]
Hair dryer (AFK, 1800W)	29.29 Ω	± 2.77
Hair dryer (AFK, 1200W)	47.6 Ω	± 7.9

Table 4.10: Model parameters for rotating loads and estimated error.

From Table 4.10 it is clear that generally universal motors can be modelled as a controllable current source, where the current is linearly related to the voltage. If these models are compared with Eq. (4.1), it is clear that it is similar if the differential part is neglected, that is if there are small variations in the voltage and the current (steady

state). Equation 4.1 can be rewritten as $I_a = V_a/R_a - e_a/R_a$, the only problem is that e_a is somehow related to the speed which is related to the supply voltage, so the constant part here is not known. The nameplate data does not contain any information about the parameters of the motors, except the rated power at rated voltage, which is not enough to construct a model that describes this behavior.

This is simpler for the hair dryers since the resistor in the load, that heats up the air that is passed through the motor, is so dominating that the load can be modelled as a constant resistor, whose value can be obtained from the nameplate data.

4.2 Frequency Spectrum Analysis

The models realized in the characterization, see Section 4.1, are used as a base for the frequency spectrum analysis. Each load was supplied with the rated voltage of 230 V. For comparing the validity of the models, their distortion factor were in turn compared to the distortion factor obtained via the measurements. A sample of the steady state-measurements, in ac and dc, of the mixer is shown in Fig. 4.11.

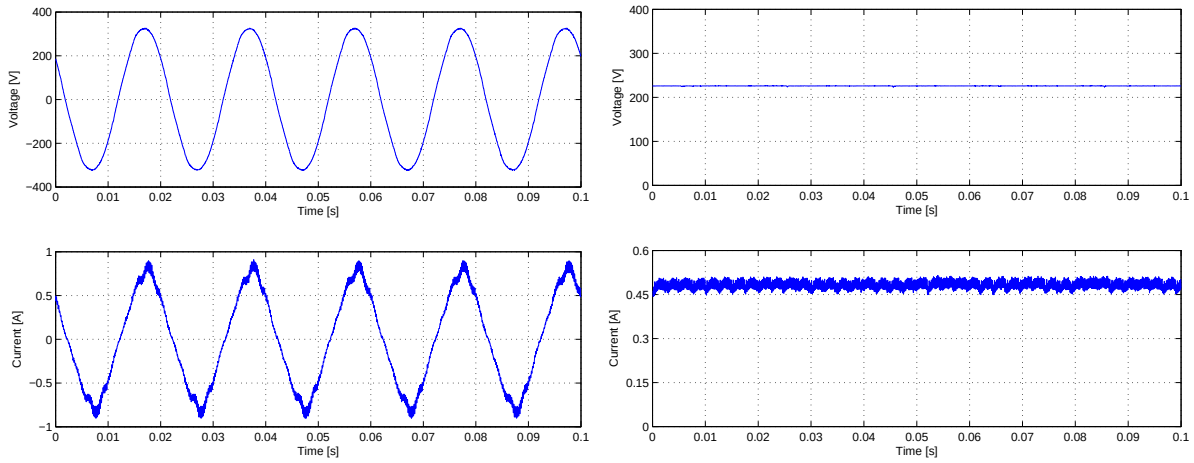

(a) ac (b) dc

Figure 4.11: Steady-state measurements of mixer (Melissa), in ac and dc.

4.2.1 Universal Motors

The results from the measurements and simulations are listed in Table 4.11.

	Measurements				Simulations			
	Magnitude		Distortion Factor		Magnitude		Distortion Factor	
Load	Voltage [V]	Current [A]	Voltage [%]	Current [%]	Voltage [V]	Current [A]	Voltage [%]	Current [%]
Blender (Melissa)	225.99	0.60	3.39	3.40	225.99	0.63	3.39	3.39
Mixer (Ide line)	226.02	0.48	3.43	3.61	226.02	0.51	3.38	3.38
Vacuum cleaner (Electrolux)	222.89	4.11	3.43	3.63	222.89	4.05	3.38	3.38
Vacuum cleaner (Euroline)	222.73	4.25	3.38	3.38	222.73	4.39	3.38	3.38
Vacuum cleaner (LG)	222.42	4.48	3.43	3.68	222.41	4.44	3.38	3.38

Table 4.11: Frequency spectrum analysis results from measurement and simulation of universal motors.

The results shown in Table 4.11 indicate that rotating loads cause approximately no distortion. The difference in distortion factor is about 0.2 % for most of the loads. This difference is due to high frequency components measured in the current for these loads and the magnitude was about 2 % of the nominal current. The blender did not show any high frequency components but this is probably due to that the magnitude was lower then the inaccuracy of the probes used for the measurements, i.e. 2 %.

The construction of the universal motor is described earlier. The origin of the frequency component is probably due that the rotor has several rotor windings displaced around the rotor and via commutators the current passes through these windings and the path is broken when the rotor poles are displaced due to the rotation. This will in turn cause some oscillations in the current and will be visible as a high frequency component in the frequency spectrum. The plots of the steady state measurements also gives an indication that higher frequency components are present, see Fig. 4.11. The rotation speed is coupled to the frequency component by:

$$f_r = \frac{n_r}{60} \cdot p \tag{4.9}$$

where f_r is the frequency component, n_r is the rotational speed in revolutions per minute and p is the number of rotor poles.

It has been observed that the rotational velocity of these loads are very high and due to the construction of the motors it has been very difficult to measure the speed. One exception is the mixer, which has two rotating shafts connected to a gear with a gear ratio of 1 : 20. This construction has made it possible to measure the rotation speed with a tachometer, placed perpendicular to the rotating shafts. The rotation speed of the mixer was measured to be about 24400 rpm and the number of poles is 12 and according to Eq. (4.9) the frequency calculated would be approx. 4880 Hz. This high frequency component was found in the frequency spectra of both ac and dc, see Fig. 4.12.

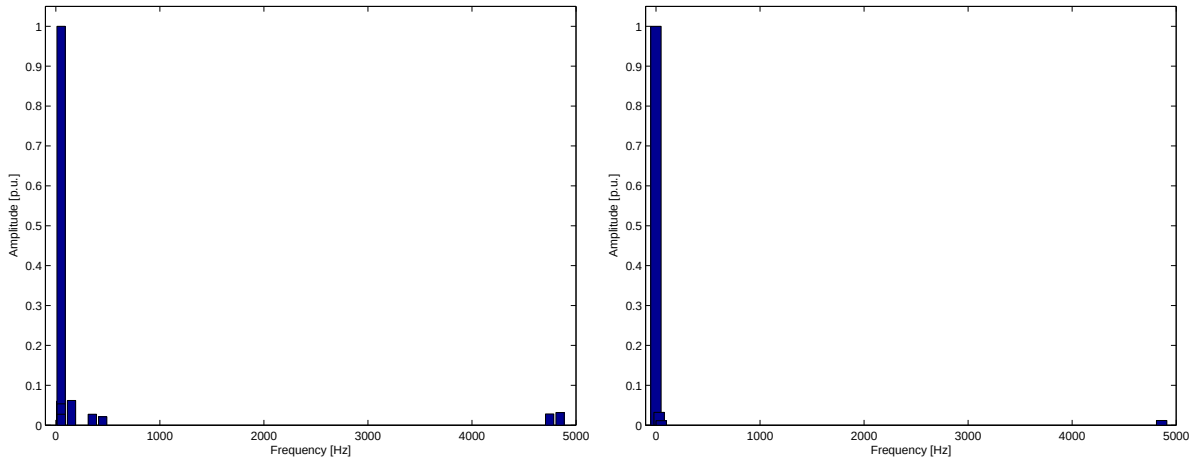

(a) ac (b) dc

Figure 4.12: Frequency spectrum of mixer (Melissa), in ac and dc.

This result indicates that the rotational speed can be detected in the frequency spectrum. These frequencies are often very high, specially for universal motors and will therefore not be modelled because these frequencies will occur naturally in the dc signals.

4.2.2 Other Motors

The results from the measurements and simulations listed in Table 4.12 give a clear indication that these loads do not cause any distortion. The resistive behavior is so dominating that these loads can be assumed to be constant resistances, see Section 4.1.

	Measurements				Simulations			
	Magnitude		Distortion Factor		Magnitude		Distortion Factor	
Load	Voltage [V]	Current [A]	Voltage [%]	Current [%]	Voltage [V]	Current [A]	Voltage [%]	Current [%]
Hair dryer (AFK, 1200W)	221.15	4.76	3.37	3.38	221.15	4.65	3.37	3.37
Hair dryer (AFK, 1800W)	219.55	7.36	3.39	3.39	219.55	7.06	3.39	3.39

Table 4.12: Frequency spectrum analysis results from measurement and simulation of other motors.

4.3 Transient Behavior

To determine the transient behavior of the motors, they where subjected to 10 voltage step of four different magnitudes (that is 40 steps in total), according to the measurement setup explained in Chapter 2. Then from that a typical step of the transient was taken and analyzed further for each load. As before, the motors are categorized into groups of universal motors and other motors.

4.3.1 Universal Motors

To fully comprehend how the universal motor reacts to a sudden voltage step a model in Simulink was built, with parameters gotten from [19]. The model was realized according to Eqs. (4.1) to (4.8) and a block scheme is shown in Fig. 4.13.

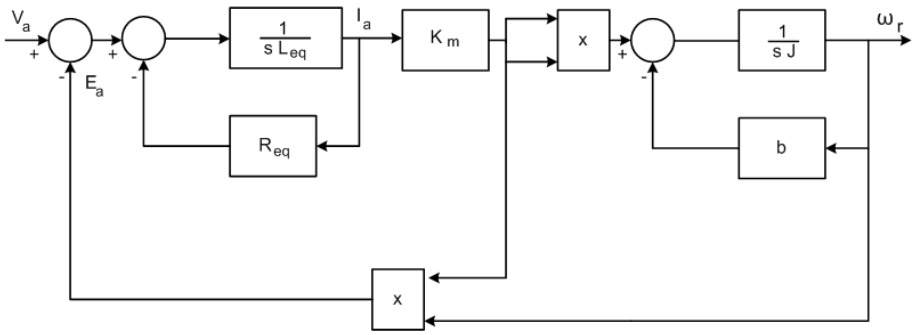

Figure 4.13: Block scheme of a universal motor, L_{eq} is the equivalent inductance, R_{eq} the equivalent resistance, k_m is the motor constant, J is the inertia and b the friction coefficient.

From the schematic it is clear that the motor has an electrical time constant R_{eq}/L_{eq} and a mechanical time constant b/J. Usually, the electrical time constant is much faster than the mechanical one, so a simulation was done over two time windows. The first lasted for 100 ms to capture the electrical transient for each step magnitude of the motor. The results from that are shown in Fig. 4.14, where the terminal voltage is V_a is plotted together with the emf E_a and the current I_a on the right, for each step in voltage. It

is clear that the electric transient is very fast lasting there for about 1 ms. Another observation can be made here that the step down in current is equal to the step down in voltage, in p.u.

Then a simulation of 2 s was analyzed and the result from that is in Fig. 4.15. The figure shows that after the step is made, the current steps down and then slowly increases. This is the mechanical response of the motor. It also shows that E_a first drops down abruptly and then slowly decays with time. It can be observed that the time constant is very long and is constant regardless of the step made.

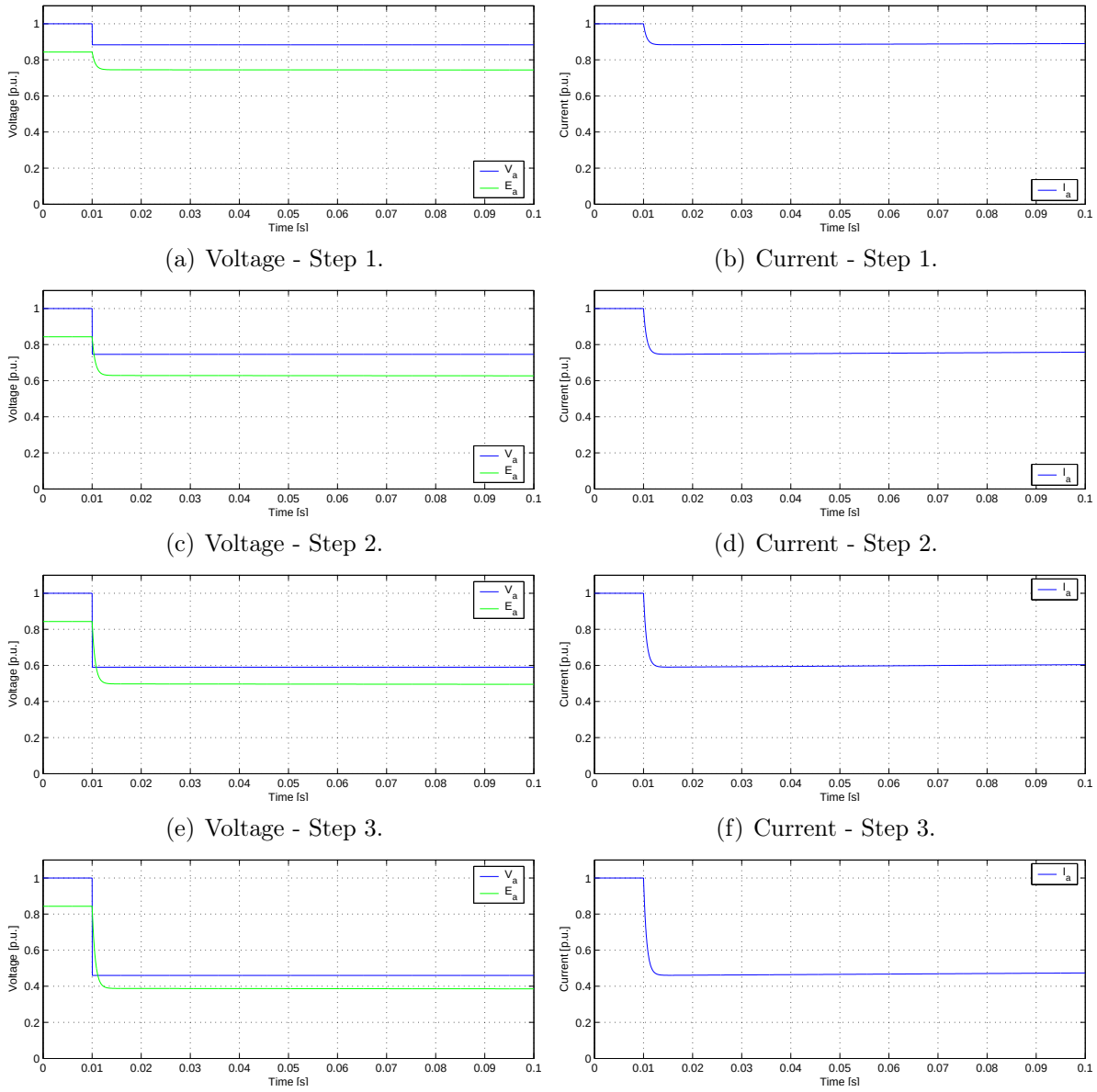

(a) Voltage - Step 1.

(b) Current - Step 1.

(c) Voltage - Step 2.

(d) Current - Step 2.

(e) Voltage - Step 3.

(f) Current - Step 3.

(g) Voltage - Step 4.

(h) Current - Step 4.

Figure 4.14: Transient behavior of the simulated motor, V_a is terminal voltage, E_a is the emf and I_a is the current. The simulation time is 100 ms.

It is clear from the block scheme in Fig. 4.13 that a complete model from having done voltage and current measurements only is impossible. Something else has to be known about the motor, e.g. the speed. In the department there were no tachometers that were able to measure the high speed of the universal motor, $10.000 - 30.000$ rpm.

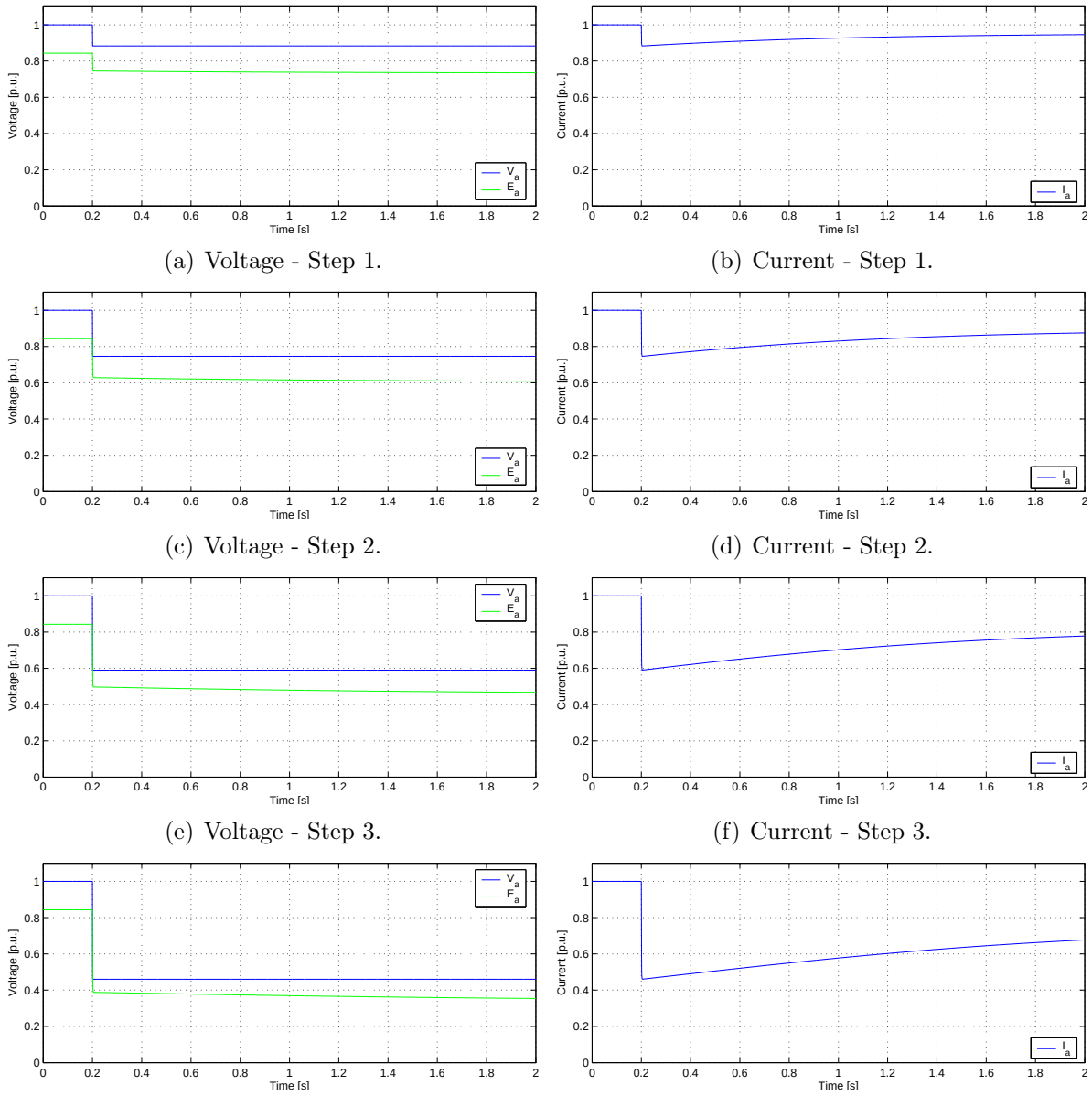

(a) Voltage - Step 1.

(b) Current - Step 1.

(c) Voltage - Step 2.

(d) Current - Step 2.

(e) Voltage - Step 3.

(f) Current - Step 3.

(g) Voltage - Step 4.

(h) Current - Step 4.

Figure 4.15: Transient behavior of the simulated motor, V_a is terminal voltage, E_a is the emf and I_a is the current. The simulation time is 2 s.

The following mathematical model was considered

$$i_l = Y_{p1} \cdot u_l + Y_{p0} + A(t) + B(t) \tag{4.10}$$

where $A(t)$ describes the electrical transient and $B(t)$ the mechanical transient, u_l is the terminal voltage and i_l is the terminal current.

For the electrical transient it was found that the time constant of that transient was not measurable as 1 ms is close to the switching off the stepper, so it is neglected, and then $A(t) = 0$.

For the mechanical transient, the time constant τ_m for each step for all loads was measured. Then the steady-state current i_{steady} and the current difference during the transient i_{diff} was measured, as in Fig. 4.16.

It was observed that the current dropped more than the voltage, directly after the step, in p.u. This phenomena was not seen in the Simulink model and it means that some

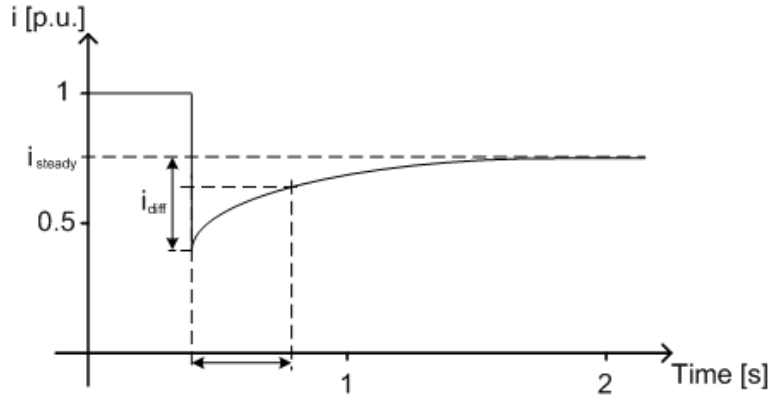

Figure 4.16: A typical transient behavior of the current for all loads.

parameters considered constant in the simulated model is in fact varying with the voltage, This might be the friction b of the motor, as the mechanical time constant τ_m was also found to be varying.

A model for the transients is assumed to be

$$i_l = Y_{p1} \cdot u_l + Y_{p0} - \kappa \mathrm{e}^{-t/\tau_m} \tag{4.11}$$

where κ and τ_m can be found in the Table 4.13. The parameter κ models the step down in current in the beginning of the transient and τ_m models the mechanical transient. Both κ and τ_m have been found to vary with the voltage, and the variation was assumed linear. The expressions of κ and τ_m as function of u_l obtained by curve fitting the data are reported in Table 4.13. By comparing Eq. (4.10) and Eq. (4.11), $B(t) = -\kappa \mathrm{e}^{-t/\tau_m}$.

The model described by Eq. (4.10), is simulated with MATLAB, for all the motors, and plotted against the measurements, in Figs. 4.17 to 4.19. The measurements where captured over 2 s, that is the time matches the simulation time, in Fig. 4.15. The figures show the same phenomena as described by the Simulink model. Fig. 4.17 to 4.19 all show that the model described by Eq. (4.11) follows the measurements quite well with the parameters κ and τ_m given in Table 4.13.

Blender (Melissa)

Step	u [pu]	i_{ss} [pu]	i_{diff} [pu]	τ_m [s]
1	0.88	1.01	0.20	0.38
2	0.74	0.94	0.31	0.38
3	0.60	0.89	0.41	0.49
4	0.47	0.81	0.44	0.62
Real parameters			$\kappa = -1.16 \cdot 10^{-3} \cdot u + 0.449$ [A]	$\tau_m = -2.56 \cdot 10^{-3} \cdot u + 0.86$
Parameters in pu			$\kappa_{pu} = -0.574 \cdot u + 0.725$ [pu]	$\tau_{m,pu} = -0.582 \cdot u + 0.86$

Mixer (Ide Line)

Step	u [pu]	i_{ss} [pu]	i_{diff} [pu]	τ_m [s]
1	0.88	0.95	0.07	0.22
2	0.74	0.89	0.13	0.45
3	0.60	0.83	0.25	0.63
4	0.46	0.75	0.34	0.73
Real parameters			$\kappa = -1.48 \cdot 10^{-3} \cdot u + 0.320$ [A]	$\tau_m = -5.55 \cdot 10^{-3} \cdot u + 1.32$
Parameters in pu			$\kappa_{pu} = -0.661 \cdot u + 0.638$ [pu]	$\tau_{m,pu} = -1.22 \cdot u + 1.32$

Vacuum cleaner (Electrolux)

Step	u [pu]	i_{ss} [pu]	i_{diff} [pu]	τ_m [s]
1	0.86	0.88	0.17	0.20
2	0.73	0.75	0.24	0.38
3	0.59	0.65	0.24	0.56
4	0.45	0.55	0.20	0.69
Real parameters			$\kappa = -1.35 \cdot 10^{-3} \cdot u + 1.33$ [A]	$\tau_m = -5.17 \cdot 10^{-3} \cdot u + 1.24$
Parameters in pu			$\kappa_{pu} = -0.0541 \cdot u + 0.250$ [pu]	$\tau_{m,pu} = -1.21 \cdot u + 1.24$

Vacuum cleaner (Euroline)

Step	u [pu]	i_{ss} [pu]	i_{diff} [pu]	τ_m [s]
1	0.86	0.90	0.09	0.27
2	0.73	0.80	0.15	0.36
3	0.59	0.70	0.19	0.46
4	0.45	0.59	0.19	0.65
Real parameters			$\kappa = -4.68 \cdot 10^{-3} \cdot u + 1.42$ [A]]	$\tau_m = -3.92 \cdot 10^{-3} \cdot u + 1.03$
Parameters in pu			$\kappa_{pu} = -0.241 \cdot u + 0.316$ [pu]	$\tau_{m,pu} = -0.893 \cdot u + 1.03$

Vacuum cleaner (LG)

Step	u [pu]	i_{ss} [pu]	i_{diff} [pu]	τ_m [s]
1	0.86	0.88	0.10	0.26
2	0.72	0.78	0.15	0.40
3	0.58	0.67	0.16	0.50
4	0.45	0.55	0.15	0.70
Real parameters			$\kappa = -2.46 \cdot 10^{-3} \cdot u + 1.028$ [A]	$\tau_m = -4.68 \cdot 10^{-3} \cdot u + 1.15$
Parameters in pu			$\kappa_{pu} = -0.122 \cdot u + 0.219$ [pu]	$\tau_{m,pu} = -1.05 \cdot u + 1.15$

Table 4.13: Measurement result of universal motors.

Blender (Melissa)

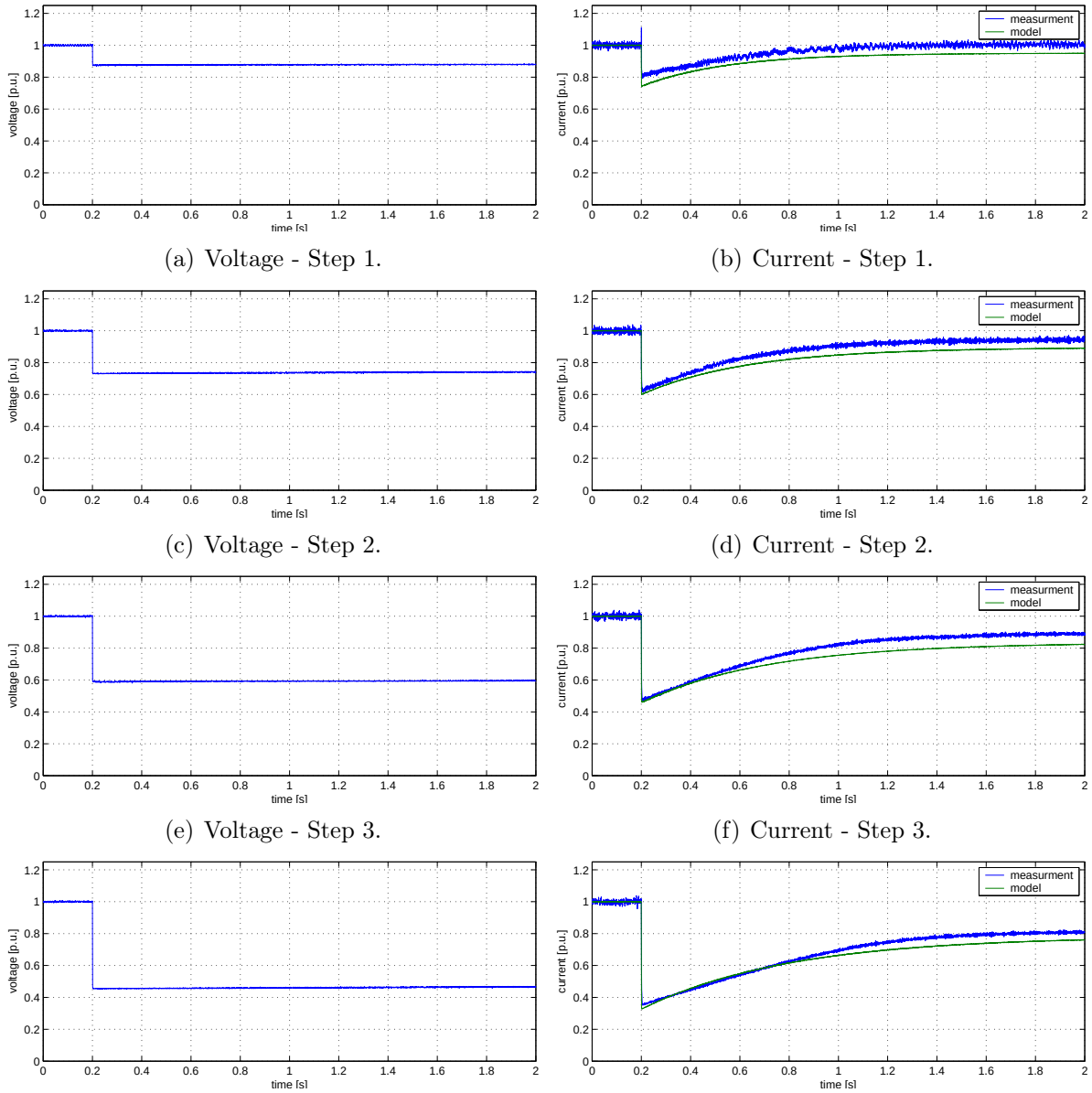

(a) Voltage - Step 1.

(b) Current - Step 1.

(c) Voltage - Step 2.

(d) Current - Step 2.

(e) Voltage - Step 3.

(f) Current - Step 3.

(g) Voltage - Step 4.

(h) Current - Step 4.

Figure 4.17: Transient behavior of blender (Melissa), measurement and model response.

Mixer (Ide Line)

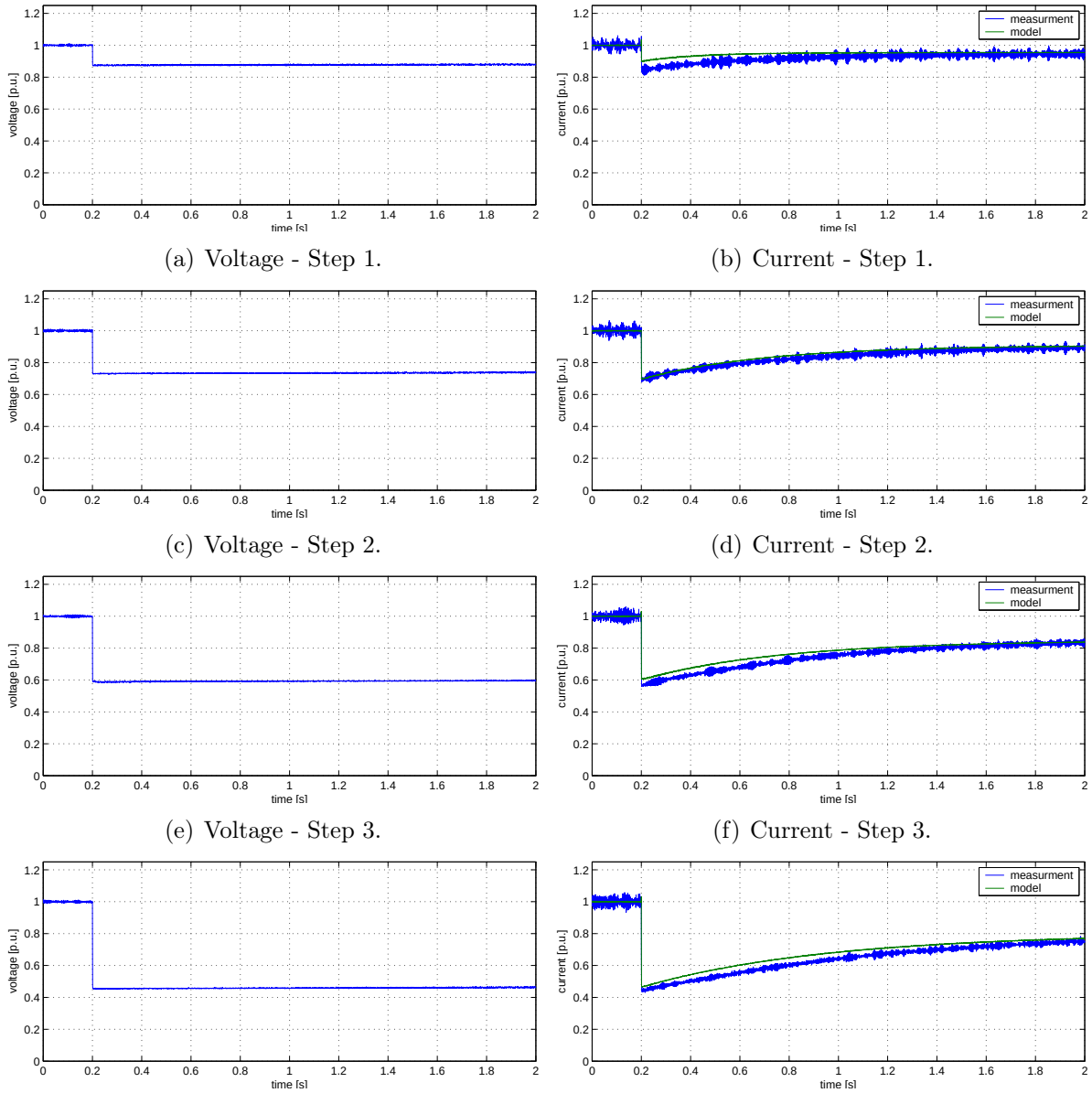

(a) Voltage - Step 1.

(b) Current - Step 1.

(c) Voltage - Step 2.

(d) Current - Step 2.

(e) Voltage - Step 3.

(f) Current - Step 3.

(g) Voltage - Step 4.

(h) Current - Step 4.

Figure 4.18: Transient behavior of mixer (Ide Line), measurement and model response.

Vacuum Cleaner (Electrolux)

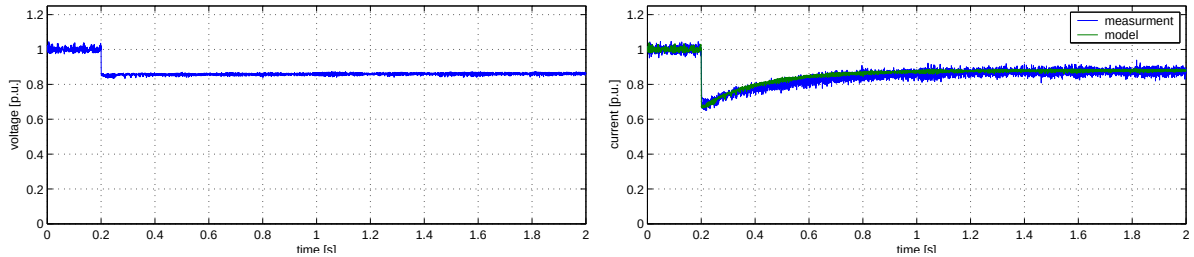

(a) Voltage - Step 1.

(b) Current - Step 1.

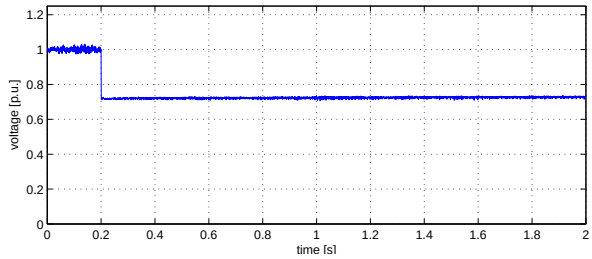

(c) Voltage - Step 2.

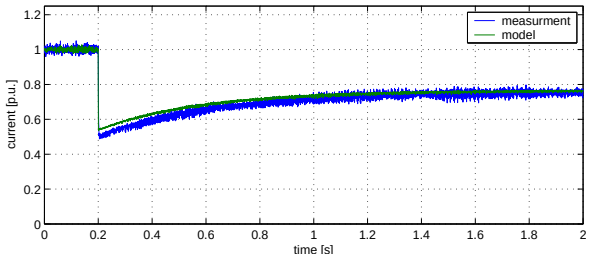

(d) Current - Step 2.

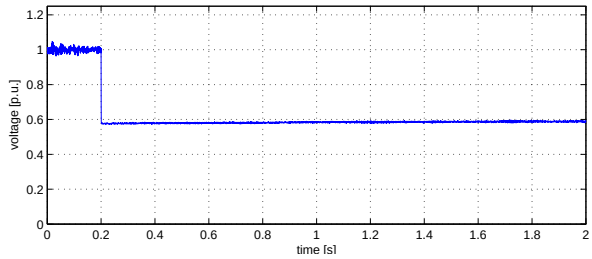

(e) Voltage - Step 3.

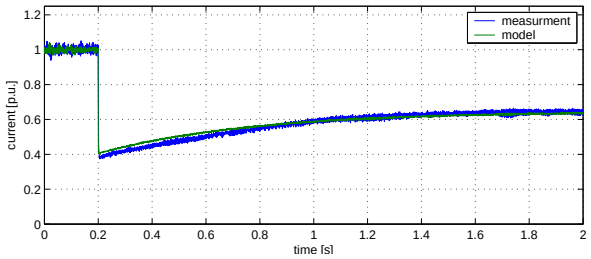

(f) Current - Step 3.

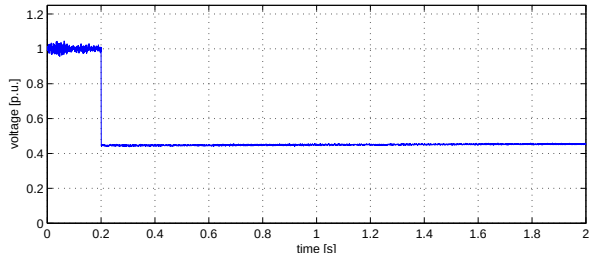

(g) Voltage - Step 4.

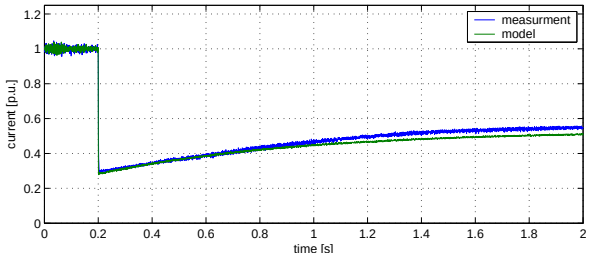

(h) Current - Step 4.

Figure 4.19: Transient behavior of vacuum cleaner (Electrolux), measurement and model response.

Vacuum Cleaner (Euroline)

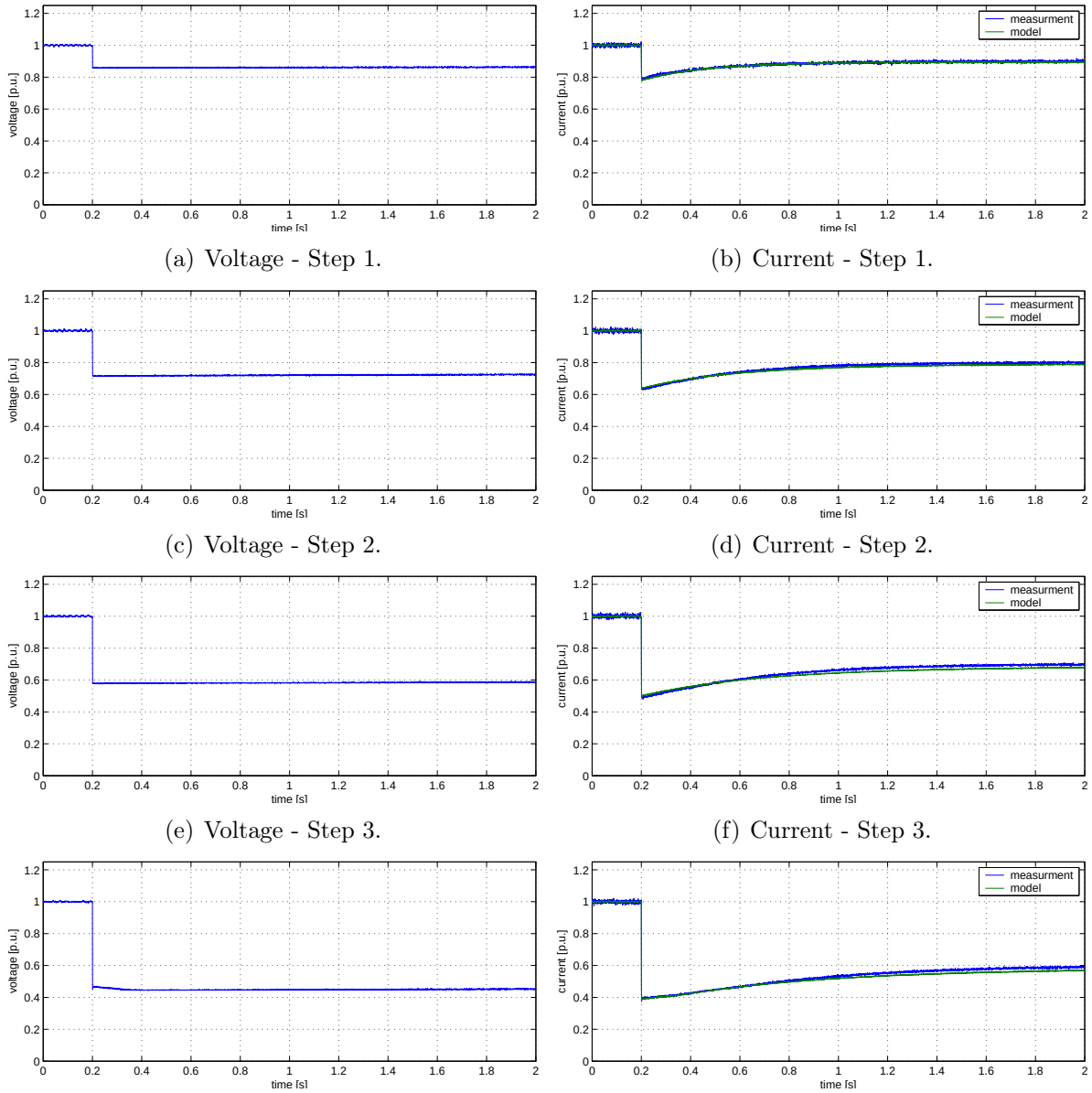

(a) Voltage - Step 1.

(b) Current - Step 1.

(c) Voltage - Step 2.

(d) Current - Step 2.

(e) Voltage - Step 3.

(f) Current - Step 3.

(g) Voltage - Step 4.

(h) Current - Step 4.

Figure 4.20: Transient behavior of vacuum cleaner (Euroline), measurement and model response.

Vacuum Cleaner (LG)

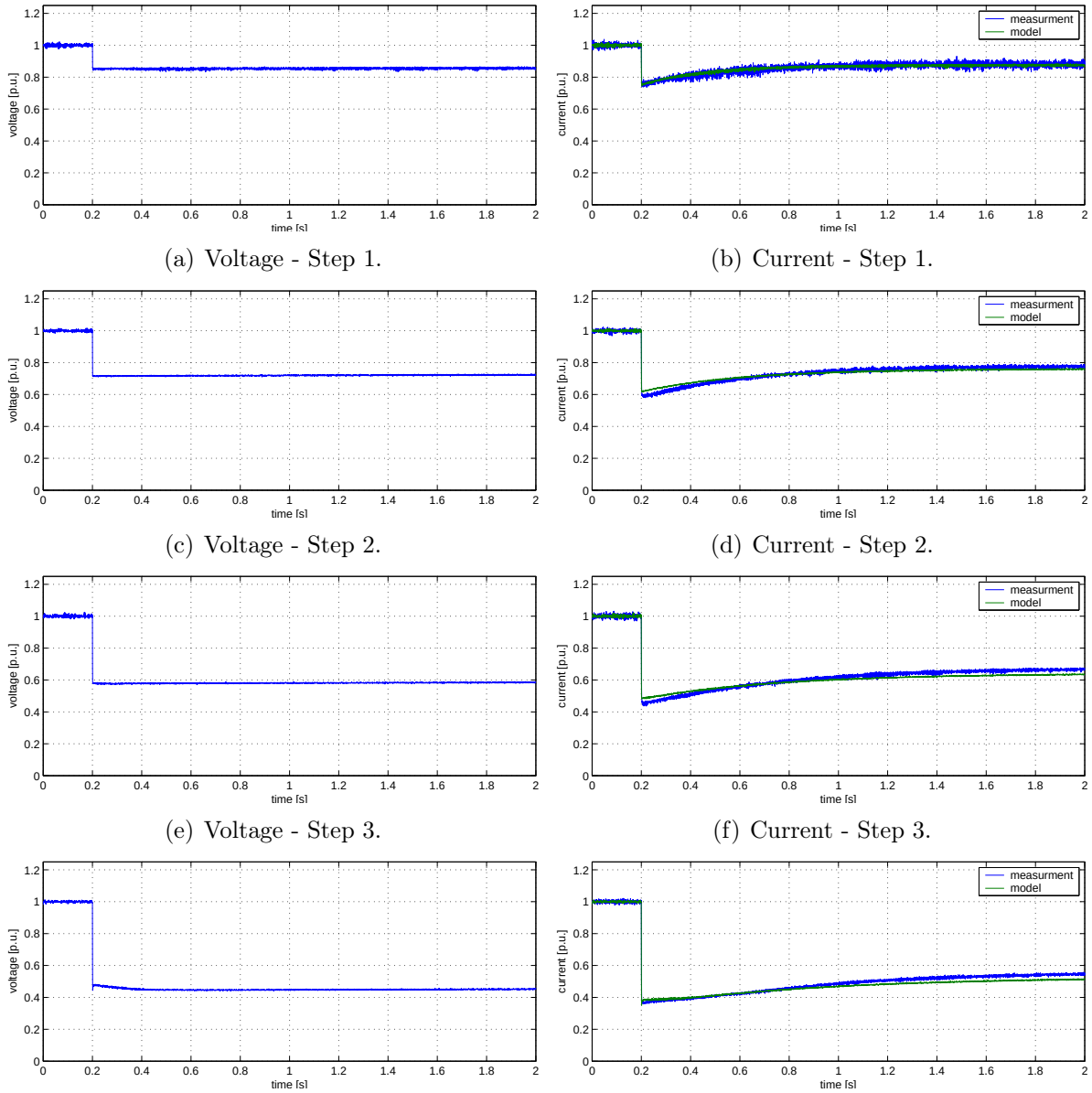

(a) Voltage - Step 1.

(b) Current - Step 1.

(c) Voltage - Step 2.

(d) Current - Step 2.

(e) Voltage - Step 3.

(f) Current - Step 3.

(g) Voltage - Step 4.

(h) Current - Step 4.

Figure 4.21: Transient behavior of vacuum cleaner (LG), measurement and model response.

4.3.2 Other Motors

Motors that have a resistive behavior, showed the same the behavior when subjected to a fast voltage reduction. That model is realized in EMTDC and simulated. The results compared with the measurements are plotted in Figs. 4.22 to 4.23.

From Fig. 4.22, the measurement result (denoted "measured"), and the model result is plotted, when both a simulated step (denoted "modelled") and the measured voltage step (denoted "simulated") is applied to the model of the load. The load behaves as a constant resistance load, the current drops by the same amount as the voltage. The model is in agreement to the measurement.

In Fig. 4.23, the load behaves as a constant resistance load, the current drops by the same amount as the voltage in step 1. In steps 2, 3 and 4 a small error can be seen between the model and the measurements because the motor of the hair dryer is causing an additional current drop as for the universal motors. It should be noted that the error of this simulation is less than the estimated error of the model parameters and therefore no additional corrections were added to the model to minimize this error.

Hair Dryer (AFK, 1800 W)

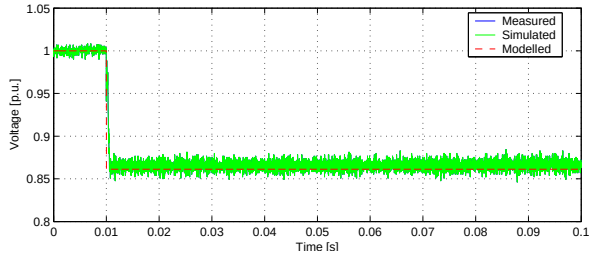

(a) Voltage - Step 1.

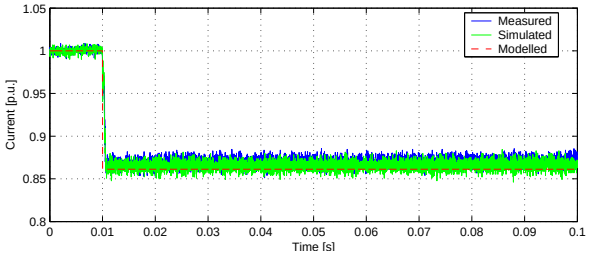

(b) Current - Step 1.

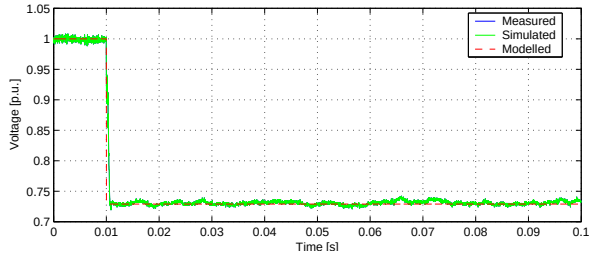

(c) Voltage - Step 2.

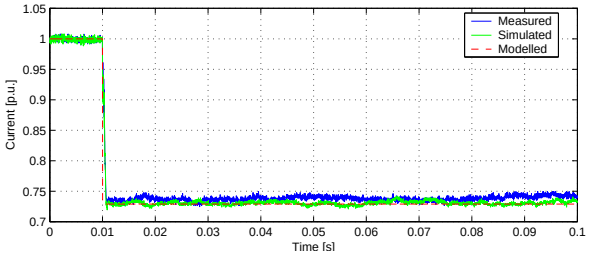

(d) Current - Step 2.

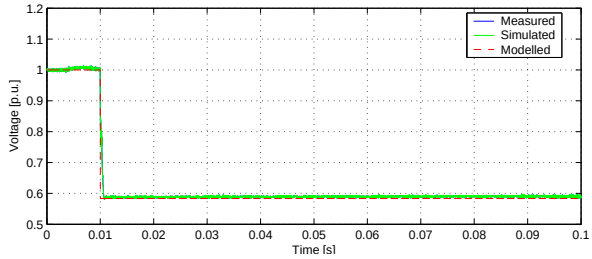

(e) Voltage - Step 3.

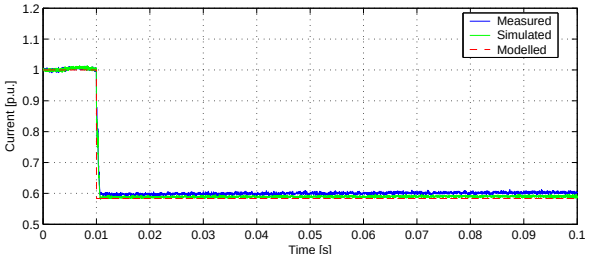

(f) Current - Step 3.

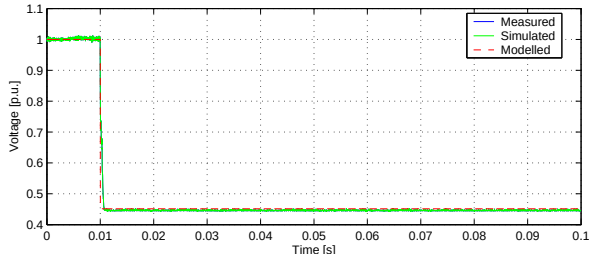

(g) Voltage - Step 4.

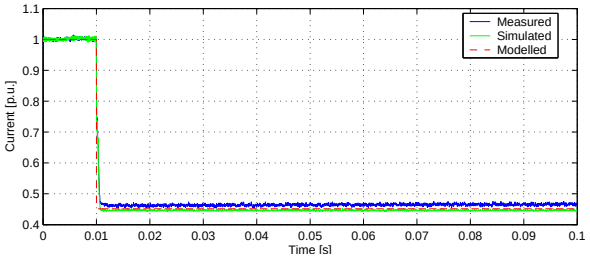

(h) Current - Step 4.

Figure 4.22: Transient behavior of hair dryer (AFK, 1800 W).

Hair Dryer (AFK, 1200 W)

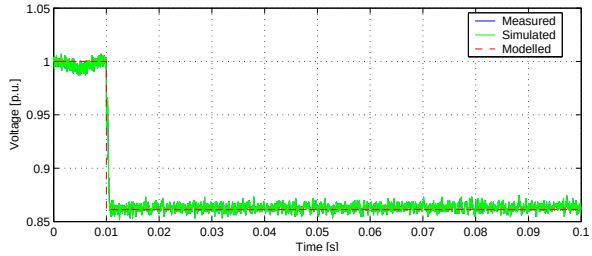

(a) Voltage - Step 1.

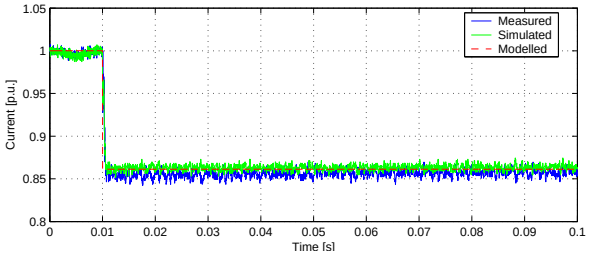

(b) Current - Step 1.

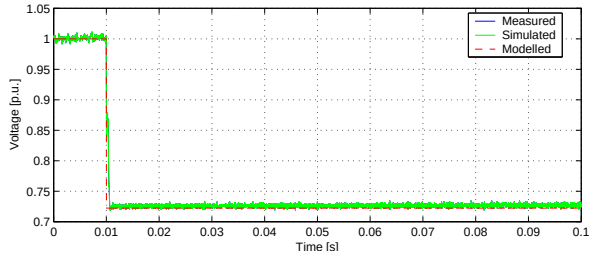

(c) Voltage - Step 2.

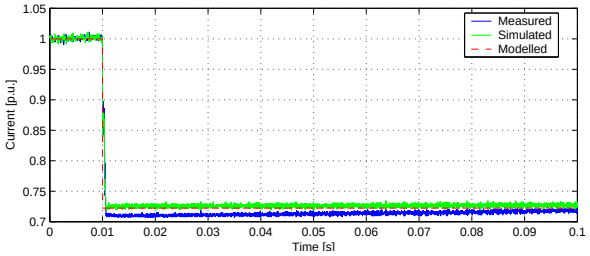

(d) Current - Step 2.

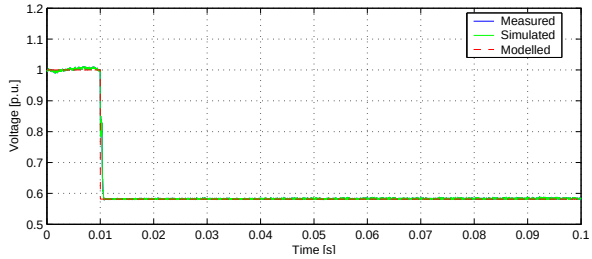

(e) Voltage - Step 3.

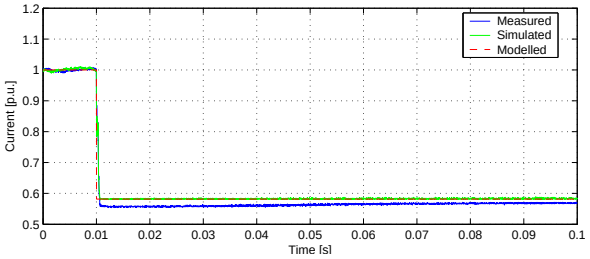

(f) Current - Step 3.

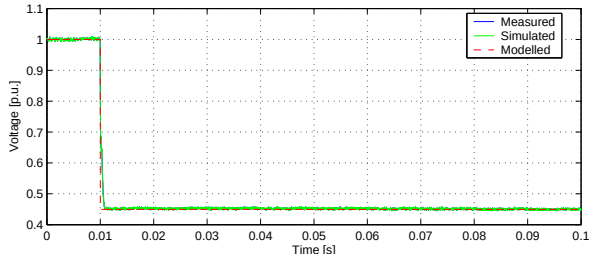

(g) Voltage - Step 4.

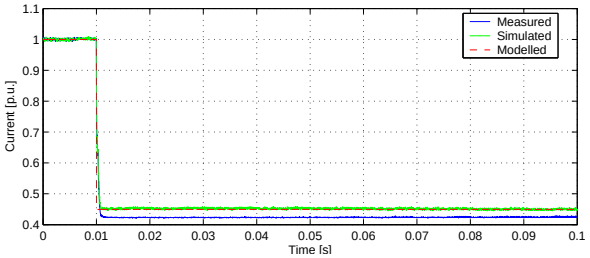

(h) Current - Step 4.

Figure 4.23: Transient behavior of hair dryer (AFK, 1200 W).

4.4 Summary

The motors tested in this thesis were divided into two groups: universal motors and other motors. The motors that fall into the second category are most likely also universal motors but they are parallel connected to a resistor that consumes more power than the actual motor. Those motors are said to have resistive behavior as described in Chapter 3. The model parameters are listed in Table 4.14.

The universal motors tested were modelled as controllable current sources as described in Section 4.1 and summarized in Table 4.14.

The steady-state analysis showed that the motors did not cause any distortion. However, high frequency components were found in the current signals. This ripple is said to be related to the speed of the motor because of the change of current path through the commutators as described in Section 4.2.

A dynamic model of a universal motor using real parameters was tested in Simulink and the same kind of behavior was found in the measurements. To build an accurate dynamic model, a number of internal parameters are needed. Since none of the parameters needed to derive a similar model are known from simple measurements of voltages and currents, for the motors tested in this thesis a mathematical approach was used as Eq. (4.11) describes, with parameters found in Table 4.13 on page 54.

Universal Motors

	Model [$i_l =$]	error [%]
Blender (Melissa)	$1.13 * 10^{-3}u + 0.371$	± 1.61
Mixer (Ide Line)	$8.4 * 10^{-4}u + 0.316$	± 1.05
Vacuum cleaner (Electrolux)	$0.0156u + 0.562$	± 3.07
Vacuum cleaner (Euroline)	$0.0150u + 1.054$	± 0.59
Vacuum cleaner (LG)	$0.0172u + 0.616$	± 1.25

Other Motors

	Model [$R =$]	error [%]
Hair dryer (AFK, 1800W)	29.29 Ω	± 2.77
Hair dryer (AFK, 1200W)	47.6 Ω	± 7.9

Table 4.14: Model parameters for rotating loads and estimated error.

Chapter 5

Electronic Loads

Electronic loads are those loads that are constructed not only from linear components, that is resistors, capacitors and inductors. These devices are the most common loads today, from clocks, radios, computers, TVs and lighting. They are in all our homes and offices and modern life would not be the same without them. These loads cause most of the disturbances in the electric system and are also the most sensitive to these disturbances.

All these loads should work fine with dc, but with one exception. If the input of the load has a low voltage transformer that transforms the system voltage to the operating voltage of the load, it will not work on dc. The transformer requires alternating current to work, otherwise it might explode. These transformers are also made to work on one frequency only, that is a transformer made for 230 V, 50 Hz system will work poorly on a 120 V, 60 Hz system and vice versa.

It is though common practice to make electronic loads work at the system voltage, both on 50 and 60 Hz systems, and then convert the voltage to the operating voltage of the loads. All these loads have one thing in common, they all consist of a rectifier that converts ac voltage to dc voltage and then the real load is operating on dc. These rectifiers all cause a lot of harmonics towards the system and draw a lot of harmonic power. If these loads were supplied with dc directly there is no need for rectification and the distortion from the load will be minimized.

These loads are split in two categories in this thesis, lighting and electronic devices for general purposes. The reason for this is manly because the behavior of these loads are somewhat different, both on how they work on ac and dc.

Lighting

The electronic devices used with lighting convert the voltage of the system to the operating voltage and frequency of the lamp. These devices usually have controllers to control the light output of the lamp, so it is difficult to say what kind of load behavior it is. There are generally two kind of devices:

- Electronic transformers for low voltage halogen lamps.
- Ballast (control gear) for fluorescent lamps.

The low voltage halogen lamp works exactly as the tungsten halogen lamp described in Chapter 3. The only difference is that they operate at another voltage and are much smaller. They all need transformers to step down the voltage, and that can be done with a traditional transformer or an electronic transformer. The trend is today to have only

electronic transformers because they have better power factor and are more compact. The ability to control the light output is also much greater.

Fluorescent lamps are discharge lamps. An electrical discharge between two electrodes in a glass tube generates UV radiation. This UV radiation, which is barely visible, causes phosphors applied to the inside of the tube to give out light. These lamps are much more efficient light source than the conventional lamps but all of them need some kind of control gear to ignite them and keep them operating [20]. This control gear is called a ballast and can either be magnetic or electronic. The magnetic ballast will not work on dc.

For the same reason as the low voltage halogen lamps, almost all ballasts today are electronic. Fluorescent lamps give much more constant light at high frequency and the output voltage of the electronic ballast is made to oscillate at $40 - 100$ kHz.

The loads that were tested within this group are:

- Three electronic ballast for florescent lamps
- Eight compact fluorescent lamps with an electronic ballast
- Two compact fluorescent lamps with a magnetic ballast*
- Two electronic transformers for low voltage halogen lamps

The control gear for tungsten halogen lamp and fluorescent lamps have all high efficiency and high power factor when the loads are supplied with ac. But this is not the case for the compact fluorescent lamps, as can be seen from Fig. 5.1 and Table 5.1, which gives the results of the the ac steady-state measurements.

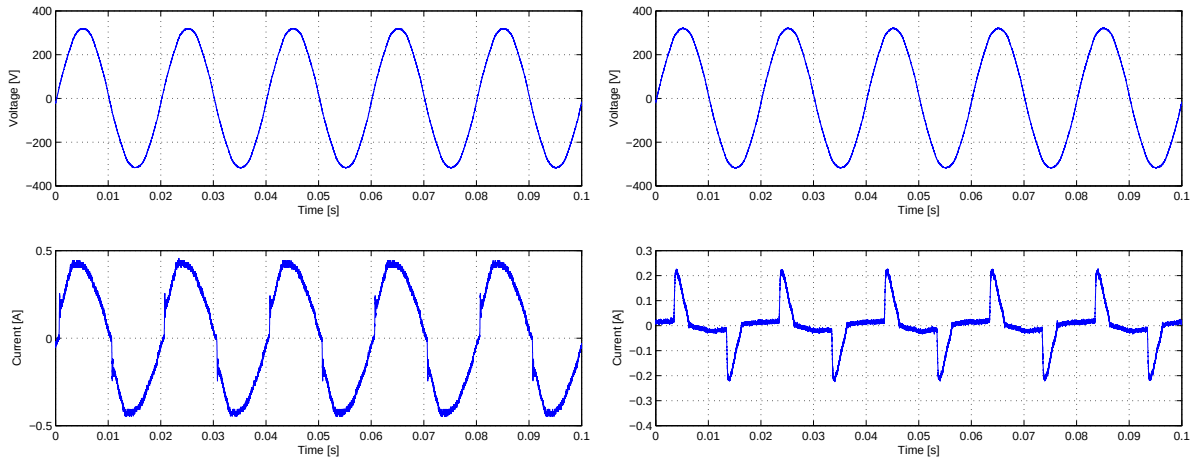

(a) Electronic ballast (b) Compact fluorescent lamp

Figure 5.1: Voltage and current shapes of a typical ballast for fluorescent lamps and a typical compact fluorescent lamp.

As can seen from Table 5.1, the ballasts do not cause much distortion in the system. This is also the case for the electronic transformer for halogen lamps. The compact fluorescent lamps are different and have much lower power factor, which is due to the design of the lamp. It is made to be compact, not efficient.

*Did not work when supplying with dc.

	Electronic Ballast		Compact fluorescent lamp	
Voltage	Amplitude [V]	THD [%]	Amplitude [V]	THD [%]
	226.9	1.27	227.5	1.19
Current	Amplitude [A]	THD [%]	Amplitude [A]	THD [%]
	0.31	<15	0.078	>90
Power factor	DPF	PF	DPF	PF
	0.99	0.99	0.92	0.66
Power	Amplitude [VA]		Amplitude [VA]	
	71.1		17.7	

Table 5.1: Characteristics of a typical ballast and a typical compact fluorescent lamp.

The ballast is very sensitive to disturbances in the network and, if they are too high, the ballast might not be able to ignite the lamp. Precautions have been taken to see to that equipment for lighting cause as little disturbance as possible, but still keeping the efficiency of the ballast as high as possible [21] [22].

Electronics for General Purposes

There are many low voltage appliances that fall into to this category, such as battery chargers, computers and general ac/dc converters, among other things. The conversion from ac to dc can be analyzed and constructed apart of the load itself and from a load construction perspective this is very suitable because the construction of the load does not depend on what the rated frequency and voltage is. There are mainly two general solutions to this problem.

The load can be connected to an adapter that feeds the load with the desired voltage and current. The adapter consists basically of a transformer, which lowers the voltage to the desired level, connected to a diode bridge rectifier and a smoothing capacitor. If the loads require such an adapter then it will not operate on dc, see Fig. 5.2.

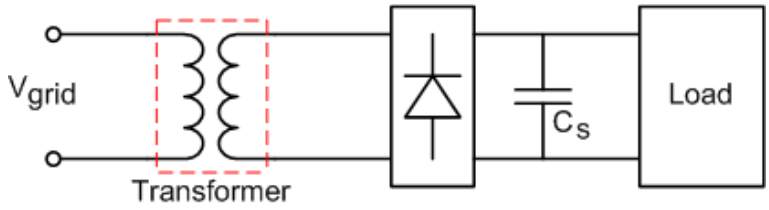

Figure 5.2: General construction for an electronic load with a transformer.

The load may have a diode bridge rectifier directly at the input and, in parallel to the rectifier, on the load side, a smoothing capacitor is connected. Towards the grid side, an EMI filter is connected to reduce high frequency disturbances caused by the load. Fig. 5.3 shows the scheme of this construction [3].

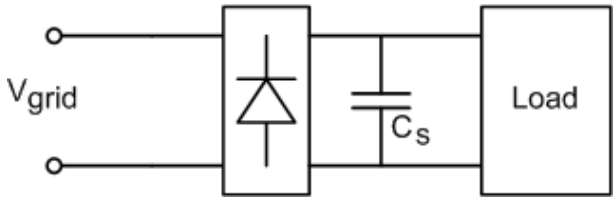

Figure 5.3: General construction for an electronic load without a transformer.

There are ways to detect whether the load has a transformer. Since the transformer consists of an iron core, the weight of the loads might indicate if the load has one transformer. An alternative and more accurate method is to analyze the voltage and current feeding the load. The transformer will cause a phase shift in the current and this will be very obvious when the power factor is calculated, see Fig. 5.4(a) and Table 5.2. If the load does not have a transformer the phase shift between the measured voltage and current will be small, see Fig. 5.4(b) and Table 5.2.

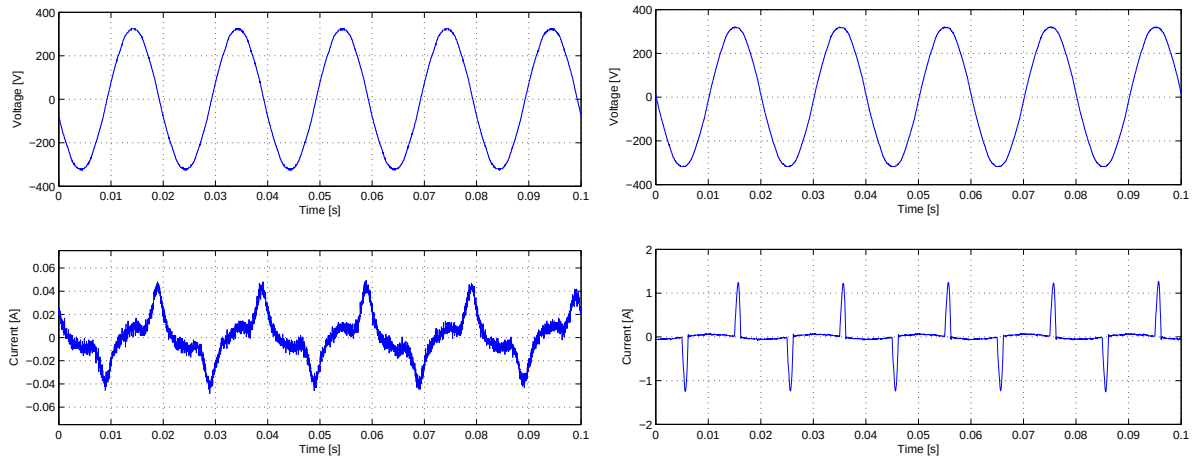

(a) With transformer

(b) Without transformer

Figure 5.4: Voltage and current shapes of typical electronic loads with and without a transformer.

	With transformer		Without transformer	
Voltage	Amplitude [V]	THD [%]	Amplitude [V]	THD [%]
	229.5	1.18	227.9	1.22
Current	Amplitude [A]	THD [%]	Amplitude [A]	THD [%]
	0.018	56.1	0.30	197.0
Power factor	DPF	PF	DPF	PF
	0.35	0.30	0.99	0.45
Power	Amplitude [VA]		Amplitude [VA]	
	4.2		68.2	

Table 5.2: Characteristics of a typical electronic load with and without a transformer.

The following electronic loads were tested:

- Four computer power supplies
- One tv **
- One satellite receiver
- One clock radio **
- Recharger for a battery driven hair trimmer **
- Three Ericsson battery rechargers
- Two printers **
- One monitor
- Speakers **
- One LCD Monitor

5.1 Load Characterization

To characterize the loads, the voltage was varied from 50 to 380 V in 10 V steps, or as long as the load was operating. For each step both the voltage and current were recorded, with the measurement setup and procedure described in Chapter 2.

Most of these loads have controllers that control how the load operates. Usually, they are controlled to take constant power, so that Eq. (2.6) should give that $A_{p2} = A_{p1} = 0$ and $P = A_{p0}$. Both voltage and current should have a quadratic relation to each other, so Eq. (2.4) should give $R_{p0} \neq 0$ and Eq. (2.5) should give $Y_{p0} \neq 0$. The simplest model for those loads is $R = U^2/A_{p0}$.

Some of these loads have other kind of relation. They can be constant current or constant resistive. When the load is constant current Eq. (2.5) together with Eq. (2.6) should give that $Y_{p0} = A_{p1}$ and the other constants in those equations should all be zero. When the load is constant resistance, the same method as in Chapter 3 can be used.

A fourth possibility of characterization is a combination of constant power, constant current, constant resistance with different characteristics in different voltage interval.

It is not possible to make any conclusion on how these loads would behave, nor in what interval they should be able to operate. This has to be decided by measurements.

**Did not work when supplying with dc.

5.1.1 Lighting

Compact Fluorescent Lamps

Six compact fluorescent lamps of different brands and power were tested. They all had different range of operation, some behaved strangely at low voltages and others shut off.

- One Eurolight lamp, rated power 9 W, operating range was 50 V to 300 V.
- One Ikea lamp, rated power 11 W, operating range was 110 V to 380 V.
- One Osram lamp, rated power 23 W, operating range was 110 V to 340 V.
- Four Philips lamps, rated power 9 W, 11 W and two 15 W, operating range was 120 V to 340 V for the 9 W and 11 W, and 140 V to 340 V for both the 15 W.
- One Sylvania lamp, rated power 10 W, operating range was 50 V to 300 V.

The Eurolight lamp behaved strangely below 100 V and a simple model in that region could not be realized. Between 100 V and 300 V the current was quite constant. The Ikea lamp behaved very strangely below 190 V and a simple model in that region is not possible either. Between 190 V and 340 V the current was quite constant. The Osram lamp would not start below 120 V. Between 120 V and 300 V the current of the lamp is quite constant. The 9 W and 11 W Philips lamps, would not start below 120 V. Between 120 V and 280 V the current was quite constant. The two 15 W Philips lamps, would not start below 140 V. These lamps do not show the same behavior as the other lamps. A simple model is not possible. As showed in Fig. 5.5 it is tried to model the lamps between 140 V and 280 V and the results from that is shown in Table 5.3. The Sylvania lamp acted strangely below 100 V. Between 100 V and 300 V the current of the lamp is quite constant as for the other lamps.

The results from the characterization are tabulated in Table 5.3

	Model	Y_{p2}	Y_{p1}	Y_{p0}	ε_Y	A_{p2}	A_{p1}	A_{p0}	ε_P
Eurolight lamp	quadratic:	$6.68 \cdot 10^{-8}$	$-1.87 \cdot 10-5$	0.0292	0.60	$2.11 \cdot 10^{-5}$	0.022	0.436	0.694
	linear:	0	$8.05 \cdot 10^{-6}$	0.0268	0.899	0	0.0302	−0.3313	1.29
Ikea lamp	quadratic:	$-3.85 \cdot 10^{-7}$	$1.99 \cdot 10^{-4}$	0.0118	1.30	$-9.63 \cdot 10^{-5}$	0.0861	−6.08	1.10
	linear:	0	$-4.41 \cdot 10^{-6}$	0.0380	2.02	0	0.0351	0.472	2.10
Osram lamp	quadratic:	$3.87 \cdot 10^{-7}$	$-1.32 \cdot 10^{-4}$	0.0765	1.33	$1.23 \cdot 10^{-4}$	0.0225	3.62	1.52
	linear:	0	$3.04 \cdot 10^{-5}$	0.0606	1.97	0	0.0742	−1.44	2.42
Philips lamp (9 W)	quadratic:	$-1.16 \cdot 10^{-8}$	$4.77 \cdot 10^{-7}$	0.0346	1.23	$-1.01 \cdot 10^{-5}$	0.0374	−0.217	1.27
	linear:	0	$-4.17 \cdot 10^{-6}$	0.0351	1.21	0	0.0334	0.162	1.16
Philips lamp (11 W)	quadratic:	$-5.76 \cdot 10^{-8}$	$1.72 \cdot 10^{-4}$	0.0339	1.69	$-1.65 \cdot 10^{-4}$	0.0973	−3.80	1.48
	linear:	0	$-5.79 \cdot 10^{-5}$	0.0556	3.11	0	0.0310	2.41	4.28
Philips lamp (15 W, 1)	quadratic:	$-1.68 \cdot 10^{-6}$	$7.817 \cdot 10^{-4}$	0.0341	2.05	$-3.09 \cdot 10^{-4}$	0.198	−16.1	2.23
	linear:	0	$6.1099 \cdot 10^{-5}$	0.0402	4.81	0	0.064	−2.26	4.31
Philips lamp (15 W, 2)	quadratic:	$-1.43 \cdot 10^{-6}$	$6.67 \cdot 10^{-4}$	−0.0226	2.89	$-2.57 \cdot 10^{-4}$	0.172	−13.3	2.93
	linear:	0	$5.07 \cdot 10^{-5}$	0.0413	4.25	0	0.0613	−1.865	3.91
Sylvania lamp	quadratic:	$1.46 \cdot 10^{-7}$	$-6.33 \cdot 10^{-5}$	0.0513	0.77	$2.09 \cdot 10^{-5}$	0.03604	0.859	0.68
	linear:	0	$-5.06 \cdot 10^{-6}$	0.0460	1.09	0	0.0444	0.0989	0.93

Table 5.3: Model parameters for compact fluorescent lamps.

From Fig. 5.5 and Table 5.3, it can be seen that the current is quite constant and a linear model can be assumed. If the linear model is looked at closer then $Y_{p0} > Y_{p1} \cdot U$ by a factor of 10 and above, so it can be neglected. The linear model also shows that $Y_{p0} \approx A_{p1}$, which makes an even stronger suggestion for a constant current model. The lamps are assumed to have a constant current behavior at the voltage interval in which the lamps functioned properly. The current that the loads consume is about 70 % to 90 % of the rated current calculated from the rated power. The model parameters are gotten from the current consumed at 230 V. The final model parameters are listed in Table 5.4

Load	Model [$R =$]	Error
Eurolight lamp	$U/0.029$	± 7.5 %
Ikea lamp	$U/0.038$	± 2.1 %
Osram lamp	$U/0.067$	± 10 %
Philips lamp (9 W)	$U/0.0351$	± 1.21 %
Philips lamp (11 W)	$U/0.0410$	± 4.28 %
Philips lamp (15 W, 1)	$U/0.057$	± 15 %
Philips lamp (15 W, 2)	$U/0.057$	± 15 %
Sylvania lamp	$U/0.046$	± 1.1 %

Table 5.4: Summary of model parameters for compact fluorescent lamps.

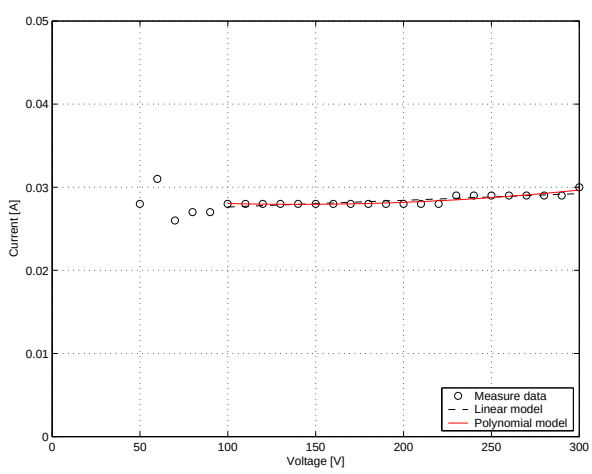

(a) Eurolight Lamp: Current vs. Voltage

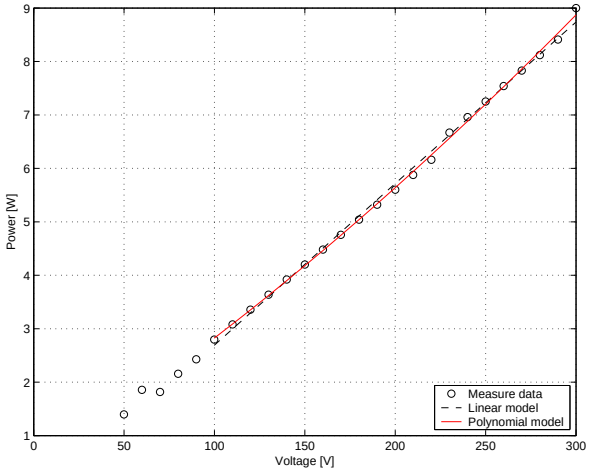

(b) Eurolight lamp: Power vs. Voltage

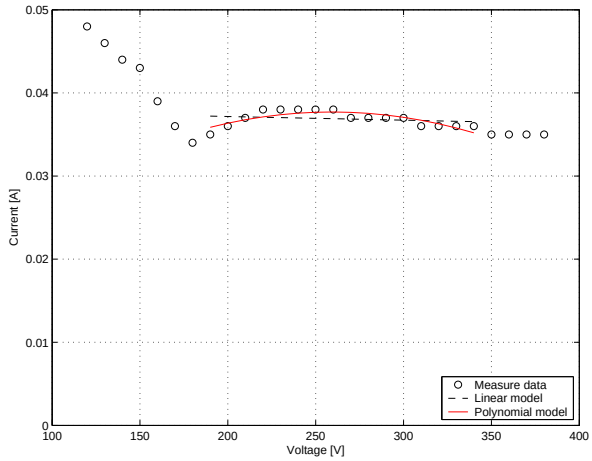

(c) Ikea lamp: Current vs. Voltage

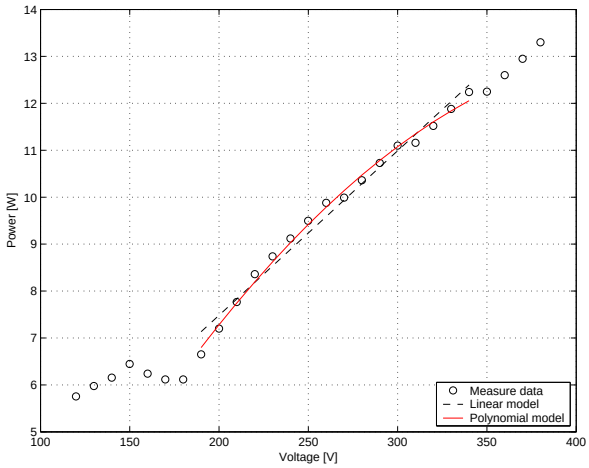

(d) Ikea lamp: Power vs. Voltage

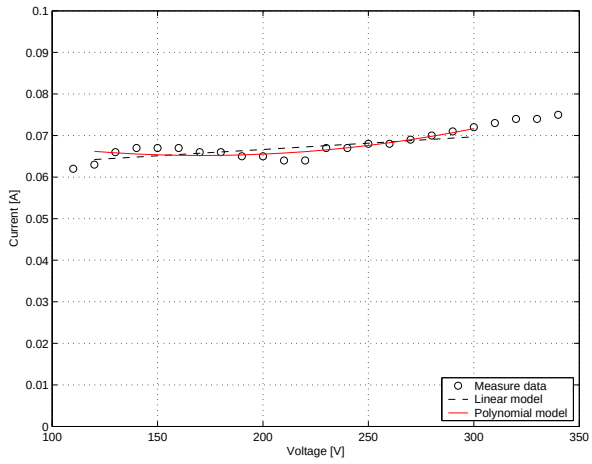

(e) Osram lamp: Current vs. Voltage

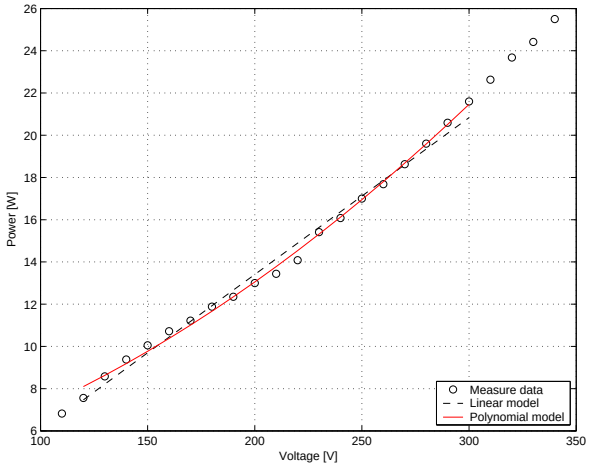

(f) Osram lamp: Power vs. Voltage

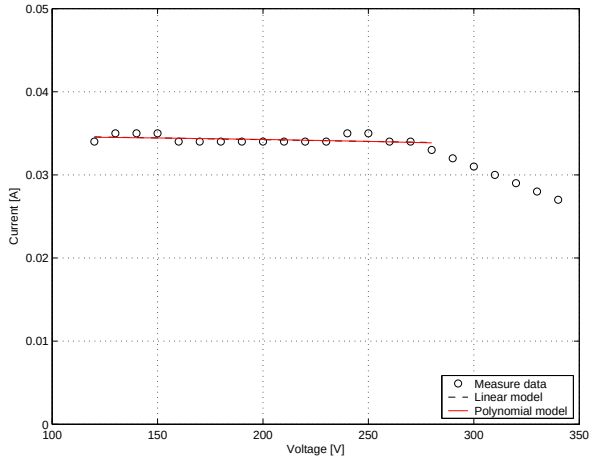

(g) Philips lamp (9 W): Current vs. Voltage

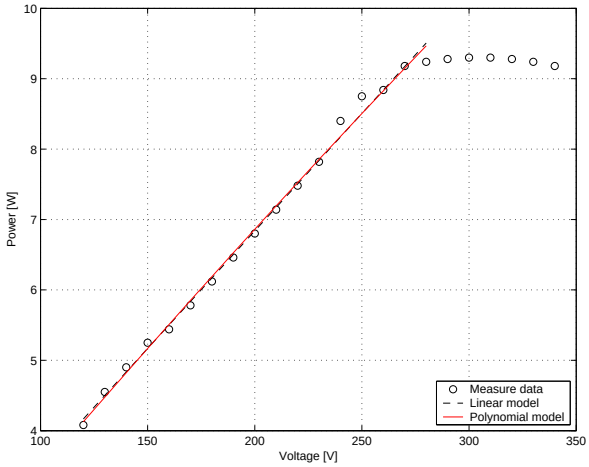

(h) Philips lamp (9 W): Power vs. Voltage

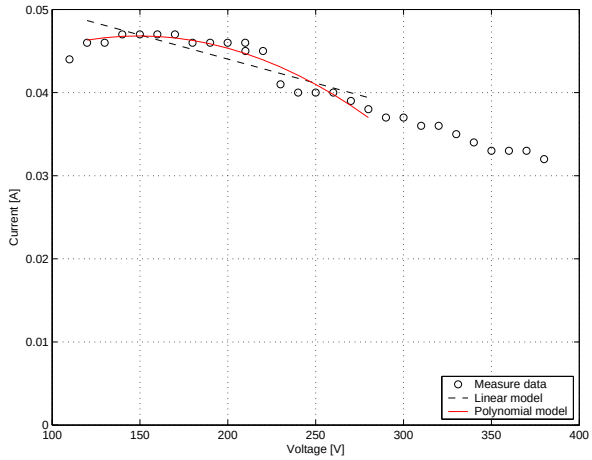

(i) Philips lamp (11 W): Current vs. Voltage

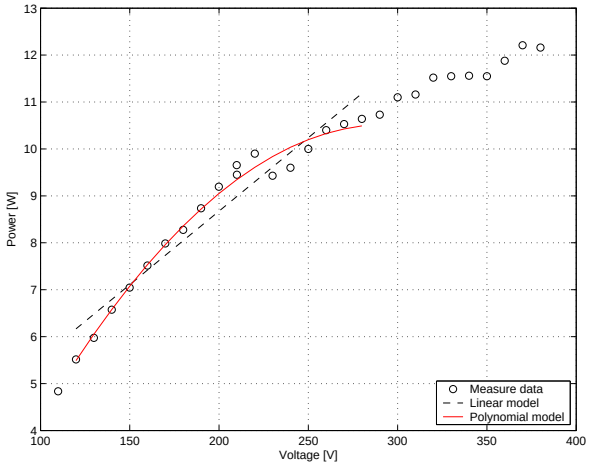

(j) Philips lamp (11 W): Power vs. Voltage

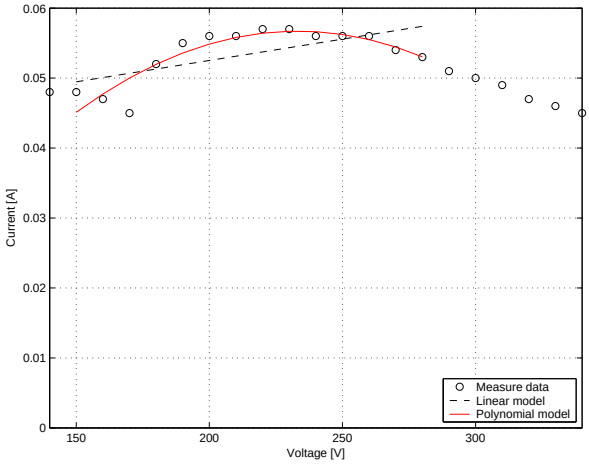

(k) Philips lamp (15 W, 1): Current vs. Voltage

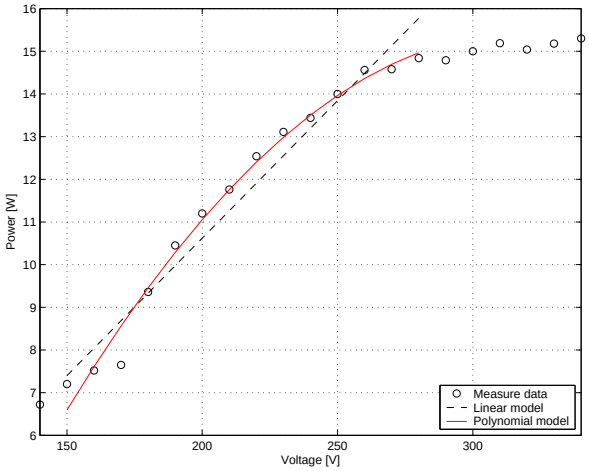

(l) Philips lamp (15 W, 1): Power vs. Voltage

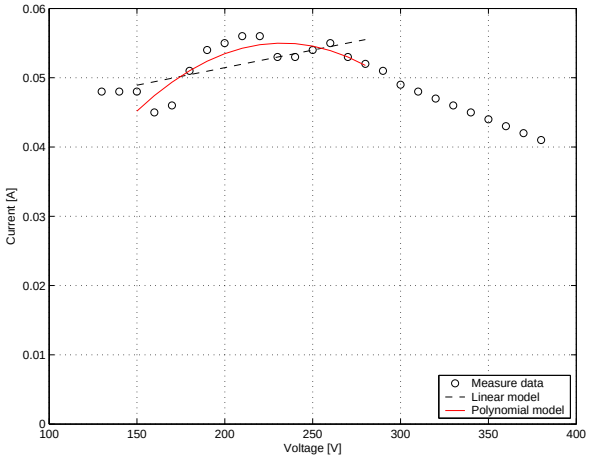

(m) Philips lamp (15 W, 2): Current vs. Voltage

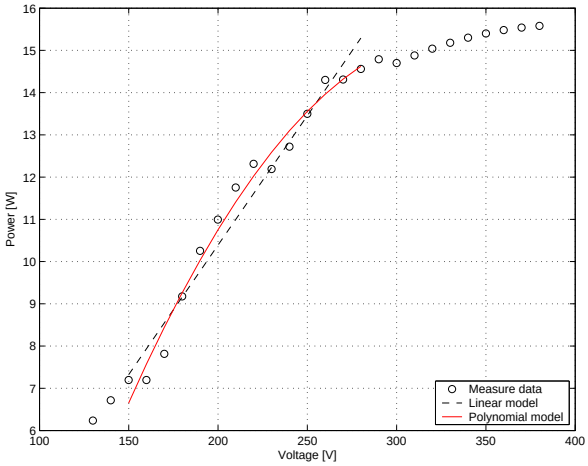

(n) Philips lamp (15 W, 2): Power vs. Voltage

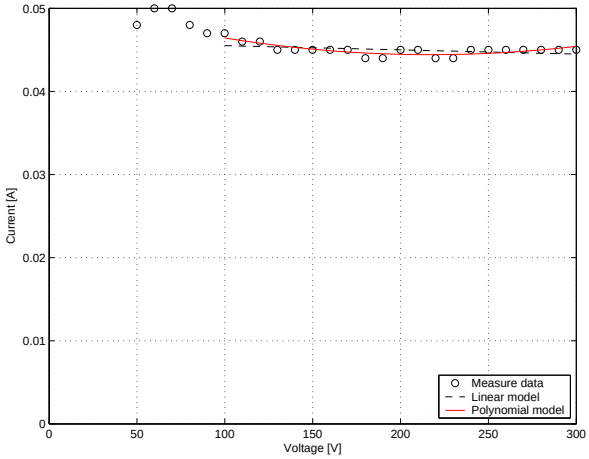

(o) Sylvania lamp: Current vs. Voltage

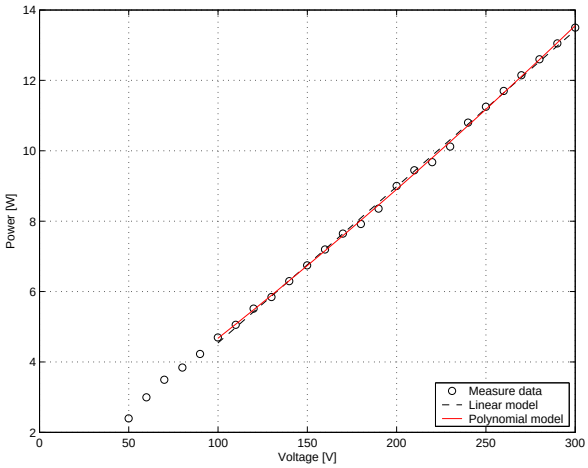

(p) Sylvania lamp: Power vs. Voltage

Figure 5.5: Characteristics of the compact fluorescent lamps.

Fluorescent Lamps

For the fluorescent lamps a lamp housing was gotten that could house two 120 cm T8 lamps, rated at 36 W each. This setup was tested with various ballasts.

Ballast (Philips)

The Philips Ballast is rated 72 W at 230 V. The ballast was tested between 150 V and 290 V. Below 150 V and above 290 V the ballast would not start. As Fig. 5.6 shows, the ballast has two operating regions. Between 150 V and 220 V the ballast draws constant current. Above 220 V it showed constant power behavior. So to model the load, the range must be split in two regions. Region one is the constant current region and Region two is the constant power region. The model parameters are then tabulated in Table 5.5.

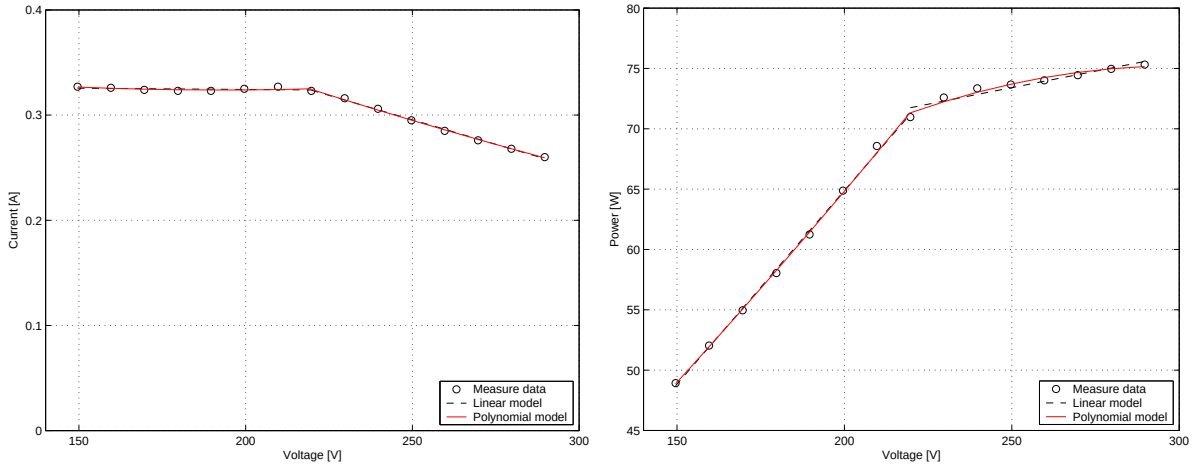

(a) Current vs. Voltage

(b) Power vs. Voltage

Figure 5.6: Characteristics of ballast (Philips).

Region 1	Y_{p2}	Y_{p1}	Y_{p0}	ε_Y	A_{p2}	A_{p1}	A_{p0}	ε_P
quadratic model:	$1.54 \cdot 10^{-6}$	$-5.94 \cdot 10^{-4}$	0.381	0.29	$2.26 \cdot 10^{-4}$	0.237	8.26	0.35
linear model:	0	$-2.38 \cdot 10^{-5}$	0.329	0.43	0	0.321	0.684	0.424
Region 2	Y_{p2}	Y_{p1}	Y_{p0}	ε_Y	A_{p2}	A_{p1}	A_{p0}	ε_P
quadratic model:	$1.13 \cdot 10^{-6}$	$-1.5 \cdot 10^{-3}$	0.601	0.29	$-6.07 \cdot 10^{-4}$	0.364	20.661	0.29
linear model:	0	$-9.29 \cdot 10^{-4}$	0.528	0.35	0	0.0548	59.71	0.40

Table 5.5: Model parameters for ballast (Philips).

From Fig. 5.6 and Table 5.5, the two regions of operation are shown. For region 1 the constant current relation is obvious. $Y_{p0} > Y_{p1} \cdot U$ by a factor of 60 and $Y_{p0} \approx A_{p1}$, so here a constant current model is suggested with a current of 0.325 A, the average current drawn in this region.

Region 2 is more complicated. It is not entirely constant power. If a constant power model is used and the power at 230 V is taken, or exactly 70.5 W, the error in the model will be 6.5% in the worst case. So there a constant power model should be assumed.

The load model is then, for the whole region of operation

Region 1, $150 - 220$ V, $R = U/0.325 \pm 1.2\%$
Region 2, $220 - 280$ V, $R = U^2/70.5 \pm 6.8\%$

Ballast (Tridonic)

The Tridonic ballast has rated power of 72 W at 230 V, given in their datasheets. The ballast was tested in the range of 130 V to 340 V. Below 130 V the current was 2 times higher the nominal. Between 130 V and 340 V the ballast shows a constant power relation, according to the datasheet the light output is kept constant on the interval of $200-270$ V, but no change was seen over the whole region, the ballast exceeded its specification. The lamp is guaranteed to work on dc as an emergency light. As showed in Fig. 5.7, the lamp is modelled for the whole region of operation and the model parameters are shown in Table 5.6.

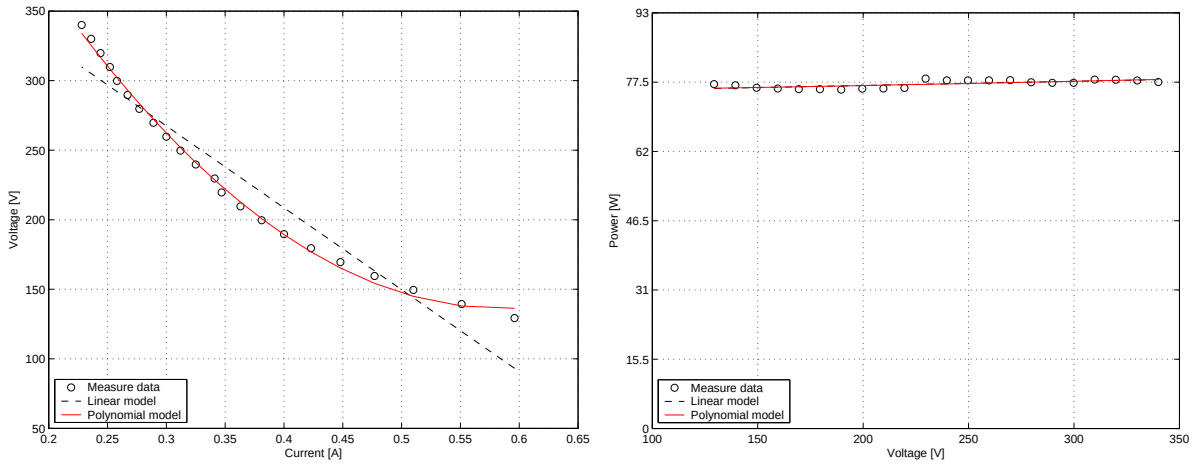

(a) Voltage vs. Current (b) Power vs. Voltage

Figure 5.7: Characteristics of ballast (Tridonic).

	R_{p2}	R_{p1}	R_{p0}	ε_R	A_{p2}	A_{p1}	A_{p0}	ε_P
linear model:	0	-588.7	444.1	6.98	0	$9.35 \cdot 10^{-3}$	74.892	0.69
quadratic model:	1553	-1817	667.7	1.49	$5.10 \cdot 10^{-6}$	$6.95 \cdot 10^{-3}$	75.15	0.69

Table 5.6: Model parameters for ballast (Tridonic).

Table 5.6 shows that the ballast is a constant power load. Since it is constant power there is no relation between the R_p model and the A_p model. It is though clear that the relation between the current and voltage is quadratic, since the linear model does not fit the data and $R_{p0} \neq 0$. Since the R_p model is quadratic, it suggests a constant power model which is confirmed by Fig. 5.7(b). The A_p model has almost the same A_{p0} coefficient for the linear and the quadratic model and the other two coefficients are very small.

From this the ballast is assumed to be a constant power load, with parameters

$$\boxed{R = U/75 \pm 0.7\ \%}$$

Dimmable Ballast (Tridonic)

This ballast has rated power of 70.4 W when supplied with dc, according to the datasheets, but should only consume about 0.25 A when it is in steady state, which gives the power rating of 55 W. The ballast was tested in the range of 110 V to 380 V. Below 110 V the

current was twice the nominal current. Between 110 V and 380 V the ballast shows a constant power behavior. According to the datasheet, the light output is kept constant but should only be about 70 % than in normal operation. The ballast is guaranteed to work on dc as an emergency light. This ballast is also dimmable, but according to the datasheet it is not possible when the ballast is supplied with dc. As showed in Fig. 5.8, the lamp is modelled for the whole region of operation and the model parameters are shown in Table 5.7.

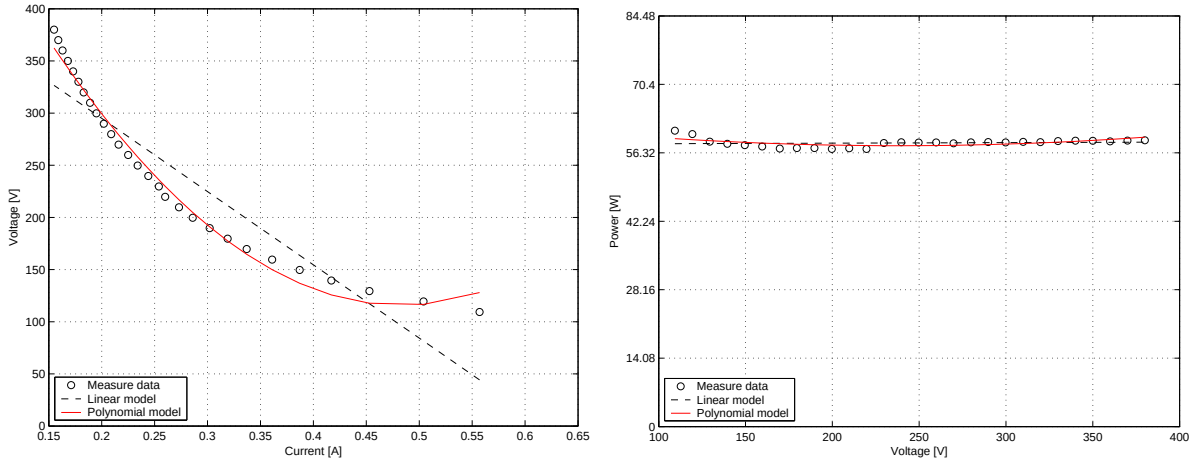

(a) Voltage vs. Current (b) Power vs. Voltage

Figure 5.8: Characteristics of dimmable ballast (Tridonic).

	R_{p2}	R_{p1}	R_{p0}	ε_R	A_{p2}	A_{p1}	A_{p0}	ε_P
quadratic model:	2288	-2212	650.4	3.85	$8.78 \cdot 10^{-5}$	-0.0419	62.76	0.99
linear model:	0	-702.3	435.4	12.2	0	$1.11 \cdot 10^{-3}$	58.1	0.94

Table 5.7: Model parameters for dimmable ballast (Tridonic).

As seen from Table 5.7, this ballast shows exactly the same behavior as the other Tridonic ballast. Again the measured power is a little higher than it is given by the specification. But still it is about 80% of the rated power. Table 5.7 shows that A_{p1} and A_{p2} are very small compared to A_{p0} and can be neglected. Then the ballast should be modelled as constant power load or as

$$\boxed{R = U/58.1 \pm 0.9\ \%}$$

Electronic Transformers for Low Voltage Halogen Lamps

For the low voltage halogen lamps, three lamps where gotten rated at 20 W each and 12 V. This setup was tested with two transformers.

Electronic Transformer (Co-Tech)

This transformer is rated 60 W. It was tested in the voltage range of 50 V to 300 V and showed exactly the same behavior as the other halogen lamps that had no electronics in front of them. It should then be modelled according to that, see Chapter 3. The results from the characterization are shown in Fig. 5.9 and the models are tabulated in Table 5.8.

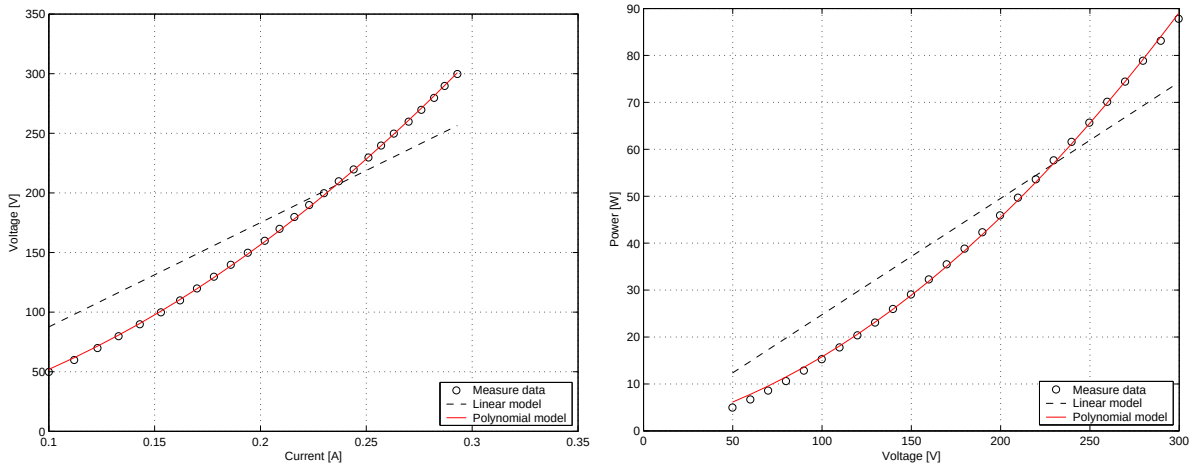

(a) Voltage vs. Current (b) Power vs. Voltage

Figure 5.9: Characteristics of electronic transformer (Co-Tech).

	R_{p2}	R_{p1}	R_{p0}	ε_R	A_{p2}	A_{p1}	A_{p0}	ε_P
quadratic model:	2625.7	257.2	0	0.88	-	-	-	0.88
linear model:	0	875.3	0	20.2	0	0.25	0	36.2

Table 5.8: Model parameters for electronic transformer (Co-Tech).

As seen from Table 5.8, the load is a variable resistor, and the power can be obtained from Eq. (3.3). The load can be modelled as a variable resistor as for the other halogen lamps, or as

$$\boxed{R = 2625.7 \cdot I + 257.2 \pm 0.9\ \%}$$

Electronic Transformer (Tridonic)

The Tridonic transformer is rated at 70 W, and is dimmable. It was tested in the voltage range of 100 V to 380 V. The transformer has a controller to control the light output. As shown in Fig. 5.10, the current decreases as the voltage decreases, when the supply voltage is between 100 V and 190 V. Here the light output from the lamp dimmed with decreasing voltage. Above 190 V, the power drawn by the load is constant, there is a variation of 10 W. A simple model for this load is not possible. Table 5.9 shows that it is possible to model the load over two regions. Region 1 is from 100 V to 190 V, and region 2 is above 190 V.

Region 1	Y_{p2}	Y_{p1}	Y_{p0}	ε_Y	A_{p2}	A_{p1}	A_{p0}	ε_P
quadratic model:	$-1.62 \cdot 10^{-6}$	$1.41 \cdot 10^{-3}$	0.0551	0.46	$7.32 \cdot 10^{-4}$	0.147	-4.07	0.42
linear model:	0	$9.46 \cdot 10^{-4}$	0.0872	0.73	0	0.358	-18.6	1.67
Region 2	Y_{p2}	Y_{p1}	Y_{p0}	ε_Y	A_{p2}	A_{p1}	A_{p0}	ε_P
quadratic model:	$2.86 \cdot 10^{-6}$	-0.00216	0.572	0.60	$2.66 \cdot 10^{-4}$	-0.096	59.7	0.65
linear model:	0	$-5.29 \cdot 10^{-4}$	0.349	3.86	0	0.0553	39.0	1.47

Table 5.9: Model parameters for electronic transformer (Tridonic).

As seen from Table 5.9 for region 1, the relation between voltage and current appears to be linear, and a linear model should be used. The power relation is also linear but has

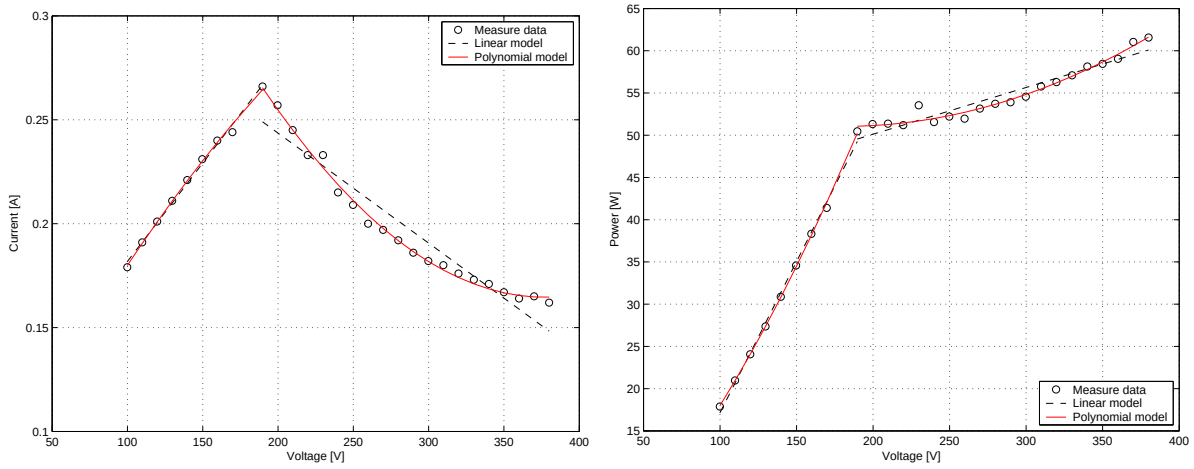

(a) Current vs. Voltage

(b) Power vs. Voltage

Figure 5.10: Characteristics of electronic transformer (Tridonic).

a negative constant power part, which suggests a controller. The model for this region should then be

$$\boxed{R = U/(9.46 \cdot 10^{-4} \cdot U + 0.0872) \pm 0.7\ \%}$$

In region 2, the relation between voltage and current appears to be quadratic, and $Y_{p0} \neq 0$, so a constant power model should be used, but the power is varying by 10 W at this level, so it will not be that accurate. The power measured at 230 V is 51.3 W which is about 10 W from what the quadratic model gives for A_{p0}. So in this region a constant power model is suggested, where

$$\boxed{R = U^2/51.3 \pm 20\ \%}$$

5.1.2 Electronics for General Purposes

Computers

A computer consumes different power at different stages of operation. The Bios of the computer will regulate the amount of power drawn by the various components of the computer, like the hard drive and CPU. The power is dependent on the amount of current needed to power each component. The size of the power supply sets the current size and how many components the computer system can have. This makes it hard to characterize a computer as load and predict how it would behave. The computers below were all tested when the computer was in idle operation, that is it was turned on but was not doing anything.

Power Supply (Chieftech)

According to measurements, the Chieftech power supply consumes about 40 W when supplied with 230 V but the rated power was 350 W. The power supply was tested between 200 V and 380 V. When the load was fed with voltages below 200 V the load did not turn on. Fig. 5.11 and Table 5.10 show the results from the characterization.

From the results shown in Fig. 5.11 and the parameters tabulated in Table 5.10 it would be reasonable to assume that the load is constant power, since $R_{p0} \neq 0$. From

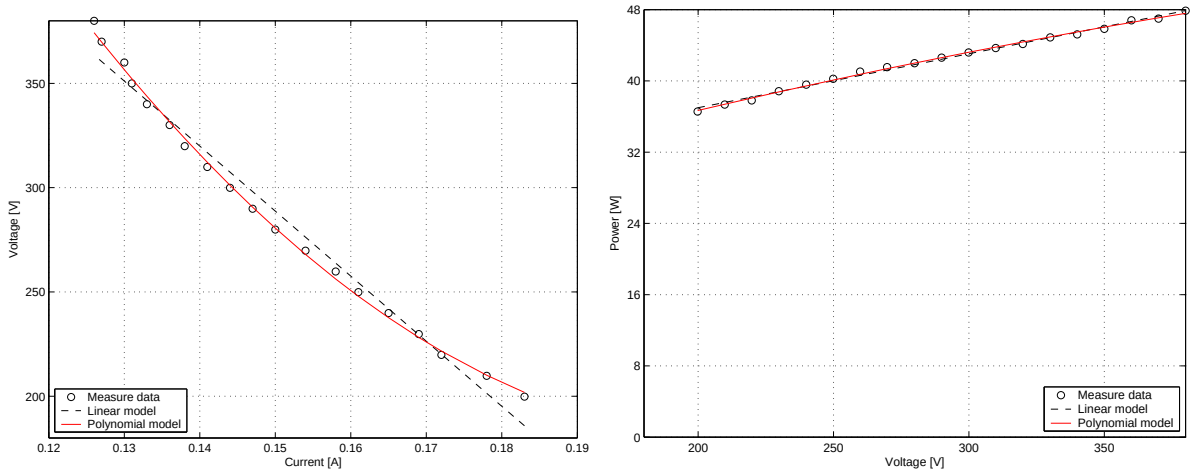

(a) Current vs. Voltage (b) Power vs. Voltage

Figure 5.11: Characteristics of power supply (Chieftech).

	R_{p2}	R_{p1}	R_{p0}	ε_R	A_{p2}	A_{p1}	A_{p0}	ε_P
quadratic model:	$2.66 \cdot 10^4$	$-1.12 \cdot 10^4$	1368	0.74	$-5.89 \cdot 10^{-5}$	0.095	20.1	0.35
linear model:	0	-3119	756.6	2.20	0	0.0605	24.9	0.49

Table 5.10: Model parameters for power supply (Chieftech).

Table 5.10 it is clear that $A_{p2} < A_{p1} < A_{p0}$ which verifies that the load is constant power. The model of the Chieftech power supply is obtained by using the power at 230 V, which will give an error of ± 20 % in the worst case. But when comparing a 10 W difference at a 350 W base the error would be mush less. So the model for the computer supplied with this power supply is

$$\boxed{R = U^2/40 \pm 20\ \%}$$

Power Supply (Dell)

According to measurements, the Dell power supply consumes about 43.5 W when supplied with 230 V, but the rated power was not specified on the nameplate. The power supply was tested between 170 V and 380 V. When the load was fed with voltages below 170 V, it did not work. Fig. 5.12 and Table 5.11 shows the results from the characterization.

	R_{p2}	R_{p1}	R_{p0}	ε_R	A_{p2}	A_{p1}	A_{p0}	ε_P
quadratic model:	9368	-4944	831.7	1.75	$2,22 \cdot 10^{-4}$	-0.113	58.3	1.20
linear model:	0	-1306	495.7	5.03	0	$3.90 \cdot 10^{-3}$	43.8	1.53

Table 5.11: Model parameters for power supply (Dell).

From the results shown in Fig. 5.12 and in Table 5.11, it would be reasonable to assume that the load is constant power, since $R_{p0} \neq 0$. From Table 5.11 it is clear that $A_{p2} < A_{p1} < A_{p0}$ which verifies that the load draws constant power, much more flat than the Chieftech power supply. The model of the Dell power supply is obtained by using the power at 230 V, which will give an error of ± 1.5 % for the whole region. The model is

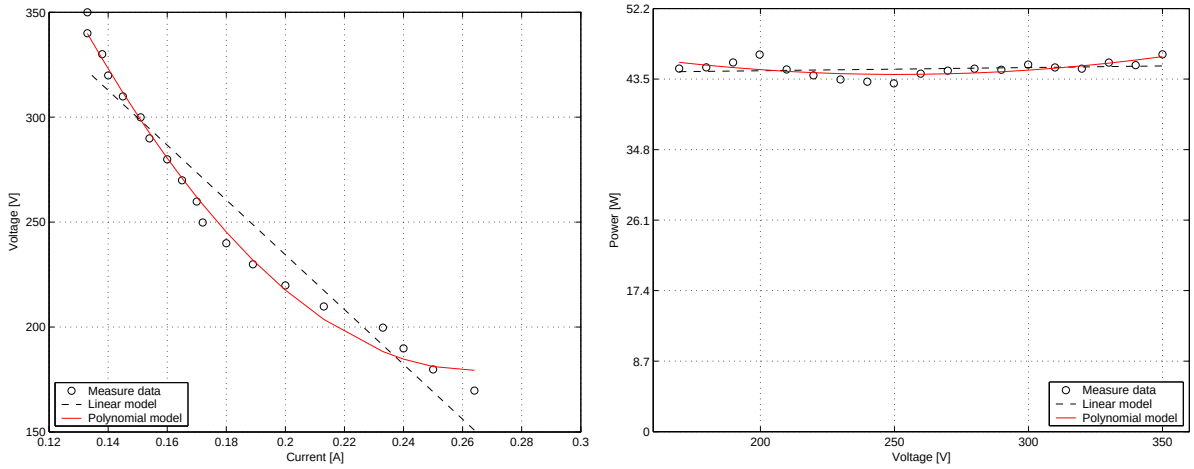

(a) Current vs. Voltage (b) Power vs. Voltage

Figure 5.12: Characteristics of power supply (Dell).

$$\boxed{R = U^2/43.5 \pm 1.5\ \%}$$

Power Supply (Macintosh)

According to measurements, the Macintosh power supply consumes about 43.7 W when supplied with 230 V but the rated power is 87 W, so the power supply is well matched to the computer. The power supply was tested between 150 V and 380 V. When the load was fed with voltages below 150 V, it did not work. Fig. 5.13 and Table 5.12 show the results from the characterization.

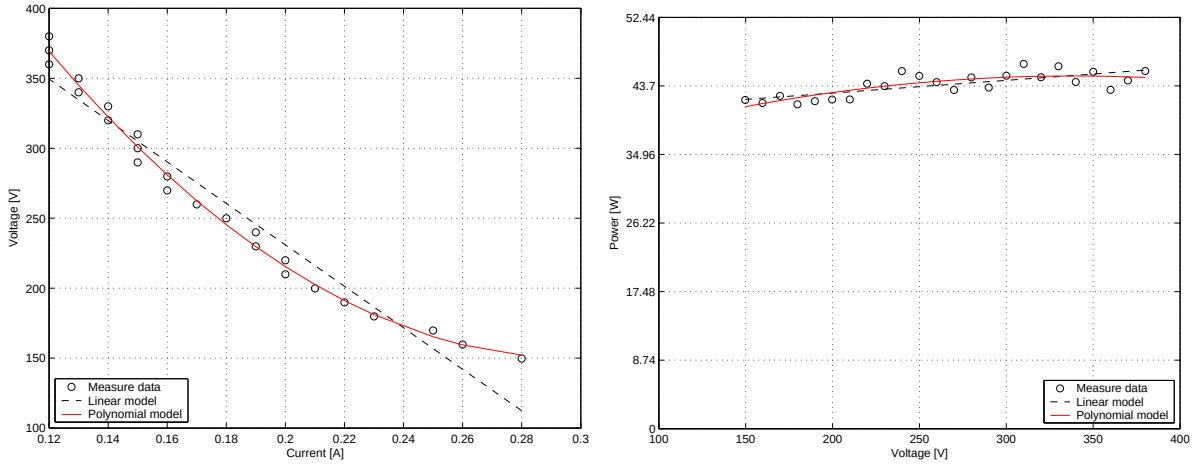

(a) Current vs. Voltage (b) Power vs. Voltage

Figure 5.13: Characteristics of power supply (Macintosh).

From the results shown in Fig. 5.13 and in Table 5.12 it can be assumed that the load is constant power, since $R_{p0} \neq 0$. From table 5.12 it is clear that $A_{p2} < A_{p1} < A_{p0}$ which verifies that the load is constant power. The model of the Macintosh power supply is obtained by using the power at rated voltage, which will give an error of ± 4 % in the worst case. The model is then

	R_{p2}	R_{p1}	R_{p0}	ε_R	A_{p2}	A_{p1}	A_{p0}	ε_P
quadratic model:	7070	-4185	769.7	1.76	$-1.11 \cdot 10^{-4}$	0.0742	32.4	1.77
linear model:	0	-1482	527.3	5.89	0	0.0162	39.6	1.94

Table 5.12: Model parameters for power supply (Macintosh).

$$\boxed{R = U^2/43.5 \pm 4\ \%}$$

Power Supply (Sirtech)

According to measurements, the Sirtech power supply consumes about 40 W when supplied with 230 V but the rated power is 235 W, The power supply was tested between 180 V and 380 V. When the load was fed with voltages below 180 V, it did not work. Fig. 5.14 and Table 5.13 show the results from the characterization.

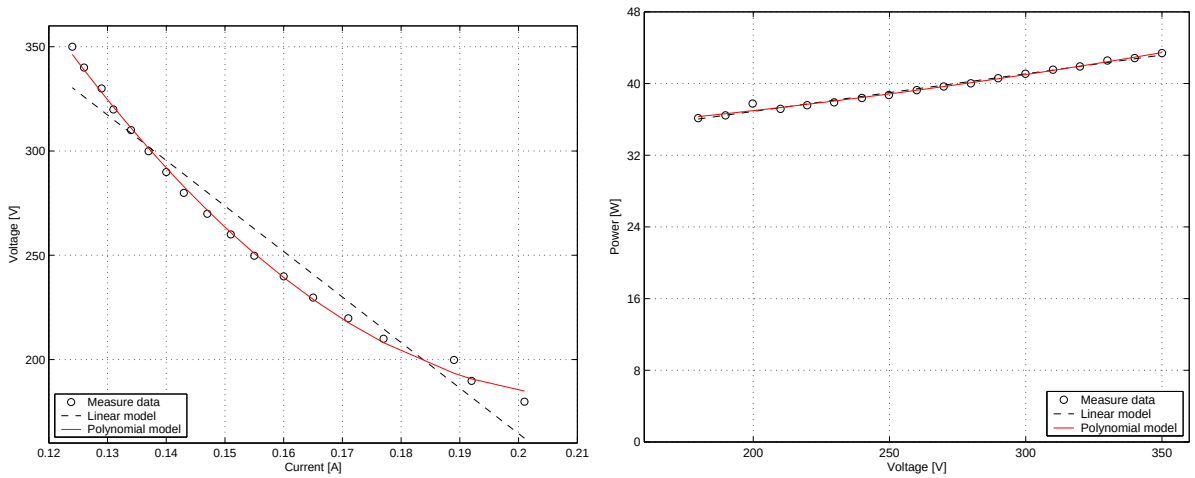

(a) Current vs. Voltage (b) Power vs. Voltage

Figure 5.14: Characteristics of power supply (Sirtech).

	R_{p2}	R_{p1}	R_{p0}	ε_R	A_{p2}	A_{p1}	A_{p0}	ε_P
quadratic model:	$2.13 \cdot 10^4$	-9028	1137.8	0.85	$5.92 \cdot 10^{-5}$	0.0106	32.5	0.34
linear model:	0	-2183	601.0	3.85	0	0.0419	28.5	0.44

Table 5.13: Model parameters for power supply (Sirtech).

From the results shown in Fig. 5.14 and in Table 5.13 it is reasonable to assume that the load is constant power, since $R_{p0} \neq 0$. Also $A_{p2} < A_{p1} < A_{p0}$, which verifies that the load is constant power. The model of the Sirtech power supply is obtained by using the power at rated voltage, which will give an error of ± 20 % in the worst case, as for the Chieftech power supply (these two power supplies where used to supply the same computer). The model is then

$$\boxed{R = U^2/37.9 \pm 20\ \%}$$

Other Electronic Devises

Chargers (Ericsson)

According to measurements the Ericsson chargers consumes between 6.7 W and 8 W when supplied with 230 V but the rated power is not given for any of the chargers. The chargers were tested between 100 V and 300 V, when the charger was charging a battery. When the voltage was below 100 V the load was drawing almost twice the current then at 230 V. Fig. 5.15 and Table 5.14 shows the results from the characterization.

	Model	R_{p2}	R_{p1}	R_{p0}	ε_R	A_{p2}	A_{p1}	A_{p0}	ε_P
Charger[1]	quadratic:	$1.48 \cdot 10^5$	$-1.75 \cdot 10^4$	626.7	2.34	$2.86 \cdot 10^{-6}$	$3.80 \cdot 10^{-3}$	5.83	0.91
	linear:	0	-5219	391.8	9.39	0	$4.95 \cdot 10^{-3}$	5.73	0.91
Charger[2]	quadratic:	$7.69 \cdot 10^4$	$-1.16 \cdot 10^4$	545.4	2.10	$-1.01 \cdot 10^{-5}$	$5.39 \cdot 10^{-3}$	7.24	2.04
	linear:	0	-3968	373.0	9.14	0	$0.36 \cdot 10^{-3}$	7.61	2.0
Charger[3]	quadratic:	$1.49 \cdot 10^5$	$-1.75 \cdot 10^4$	621.3	3.18	$2.32 \cdot 10^{-5}$	$-4.80 \cdot 10^{-3}$	6.58	0.97
	linear:	0	-5065	384.2	9.99	0	$4.48 \cdot 10^{-3}$	5.73	1.44

Table 5.14: Model parameters for chargers (Ericsson).

As seen from Table 5.14, it is clear that the chargers are a constant power load. However, the power is slightly varying, as for the computers, and the power base for the load is assumed equal to the power consumed at 230 V or 6.7 W, 6.9 W and 8.05 W. This will give an error of about 2 % to 8.0 %. The models are tabulated in Table 5.15

Load	Model $[R =]$	Error
Charger [1]	$U^2/6.7$	± 8.0 %
Charger [2]	$U^2/6.9$	± 4.3 %
Charger [3]	$U^2/8.05$	± 2.0 %

Table 5.15: Summary of model parameters for chargers (Ericsson).

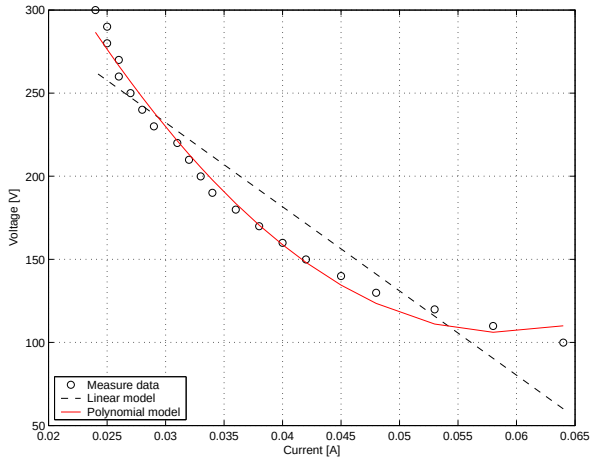

(a) Charger 1: Current vs. Voltage

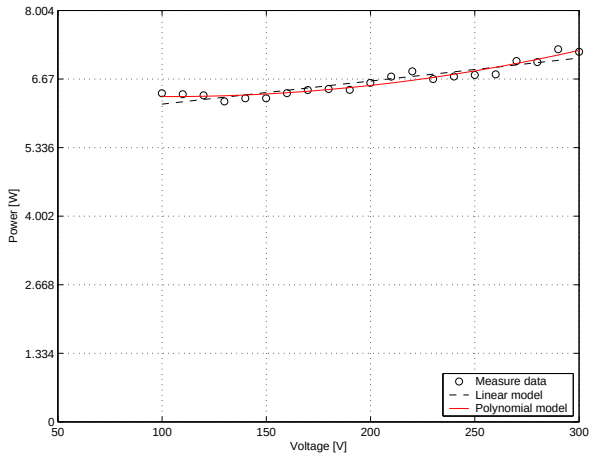

(b) Charger 1: Power vs. Voltage

[1]Model No. 4020036 BV, 1
[2]Model No. 4020036 BV, 2
[3]Model No. 4020037 BV

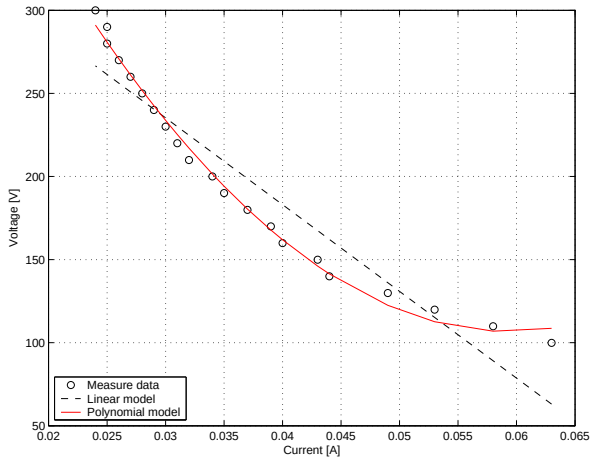

(c) Charger 2: Current vs. Voltage

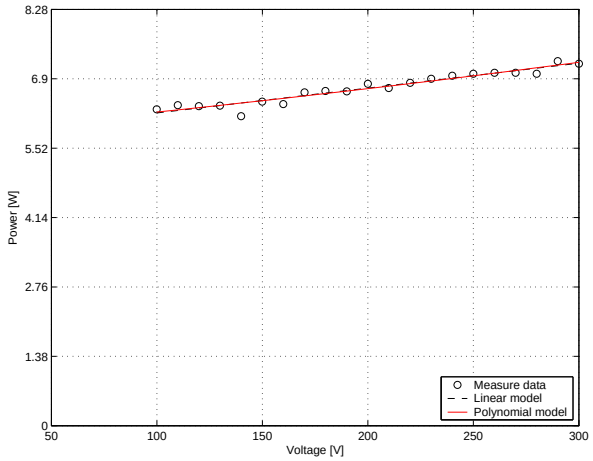

(d) Charger 2: Power vs. Voltage

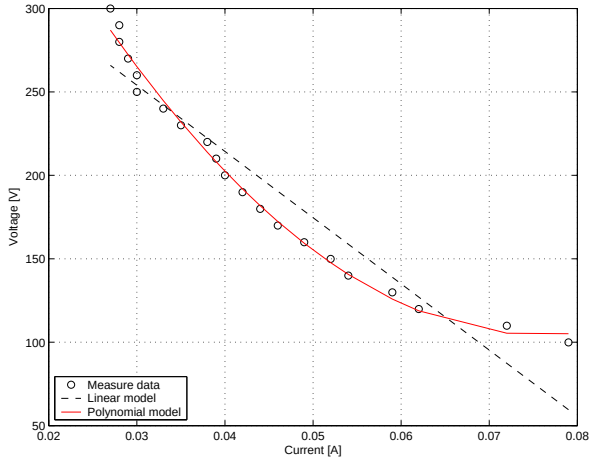

(e) Charger 3: Current vs. Voltage

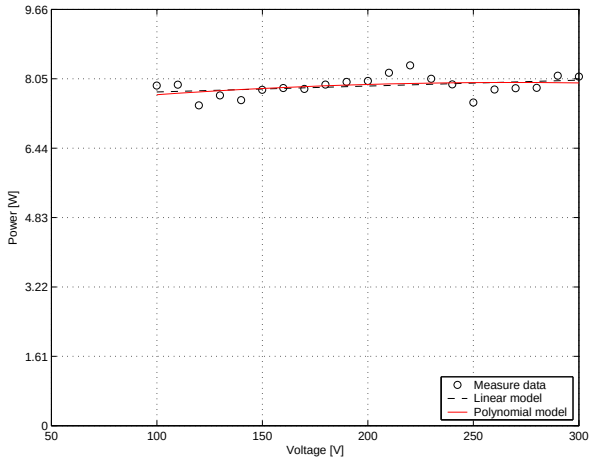

(f) Charger 3: Power vs. Voltage

Figure 5.15: Characteristics of chargers (Ericsson). 1 is Model No. 4020036 BV, 1; 2 is Model No. 4020036 BV, 2; and charger 3 is Model No. 4020037 BV.

IP Telephone (Grandstream)

According to measurements, the IP telephone consumes about 2.75 W when supplied with 230 V but the rated power is not given. The telephone was tested between 100 V and 380 V. When the voltage was below 100 V the load was drawing more than twice the current at 230 V. Fig. 5.16 and Table 5.16 shows the results from the characterization.

	R_{p2}	R_{p1}	R_{p0}	ε_R	A_{p2}	A_{p1}	A_{p0}	ε_P
quadratic model:	$1.57 \cdot 10^6$	$-6.80 \cdot 10^4$	838.4	6.37	$7.68 \cdot 10^{-6}$	$-6.68 \cdot 10^{-5}$	2.40	2.12
linear model:	0	$-1.79 \cdot 10^4$	478.4	14.9	0	$3.62 \cdot 10^{-3}$	2.01	2.48

Table 5.16: Model parameters for IP telephone (Grandstream).

As seen from Table 5.16 it is reasonable to assume that the telephone is a constant power load. As for the other general purpose electronic loads, the power base for the load is obtained from the power consumed at 230 V or 2.76 W. This will give an error of 24 %, which is quite large. However, the error is partly due to measurement error, since the current at this level is really low. The model for the IP telephone is assumed to be

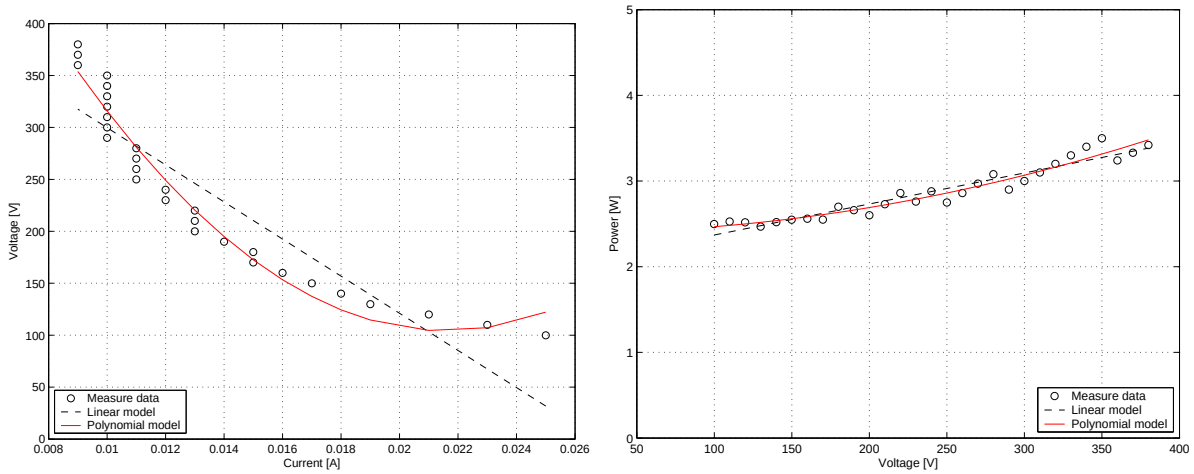

(a) Current vs. Voltage (b) Power vs. Voltage

Figure 5.16: Characteristics of IP telephone (Grandstream).

$$R = U^2/2.76 \pm 24\ \%$$

LCD Monitor (AOC)

According to measurements, the monitor consumes about 30 W when supplied with 230 V but the rated 32 W. The monitor was tested between 130 V and 330 V. When the voltage was below 130 V, the load current was about twice the nominal current. This monitor had perfect picture quality over the whole range. Fig. 5.17 and Table 5.17 show the results from the characterization.

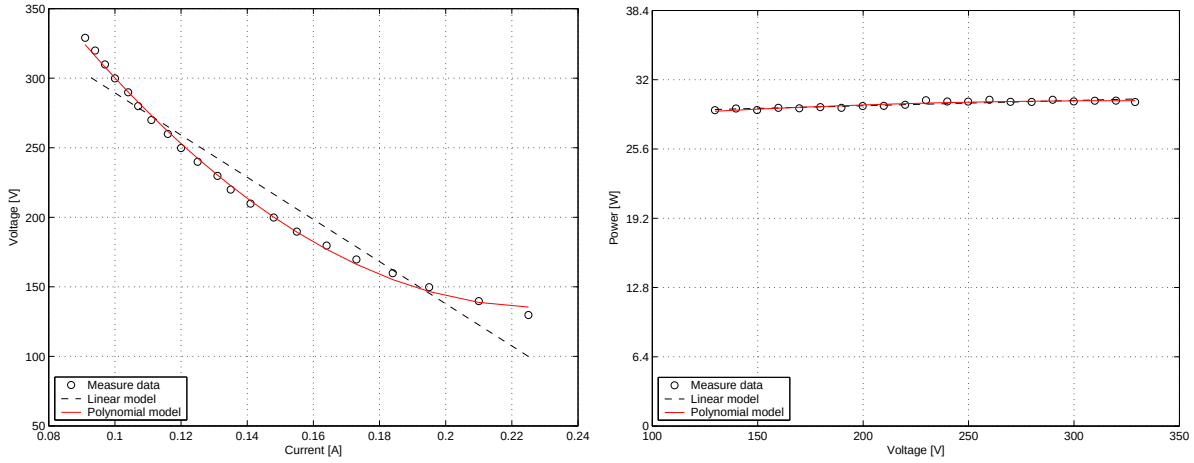

(a) Current vs. Voltage (b) Power vs. Voltage

Figure 5.17: Characteristics of LCD monitor (AOC).

As seen from Table 5.17 it is clear that the monitor is a constant power load. As for the other general purpose electronic loads the power base for the load is obtained from the power consumed at 230 V or 30 W. This will give an error of 1.3 %. The model for the LCD monitor is

$$R = U^2/30 \pm 1.2\ \%$$

	R_{p2}	R_{p1}	R_{p0}	ε_R	A_{p2}	A_{p1}	A_{p0}	ε_P
quadratic model:	9964.5	-4556.5	656.23	1.20	$-2.64 \cdot 10^{-5}$	0.0170	27.33	0.33
linear model:	0	-1516.2	441.03	6.08	0	0.00486	28.62	0.37

Table 5.17: Model parameters for LCD monitor (AOC).

Monitor (NCD)

According to measurements, the monitor consumes about 84 W when supplied with 230 V but the rated power is not given. The monitor was tested between 200 V and 350 V. When the voltage was below 200 V, the load did not start. The colors of the monitor were a bit off and shades were noticed all over. That is probably due to the fact that the field in the tube is somewhat controlled based on the ac input. Fig. 5.18 and Table 5.18 show the results from the characterization.

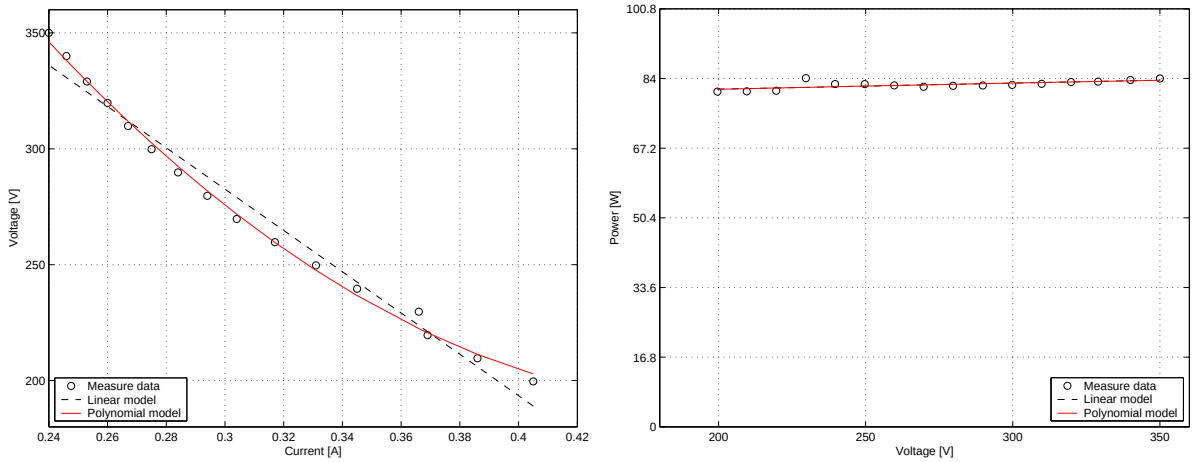

(a) Current vs. Voltage

(b) Power vs. Voltage

Figure 5.18: Characteristics of monitor (NCD).

	R_{p2}	R_{p1}	R_{p0}	ε_R	A_{p2}	A_{p1}	A_{p0}	ε_P
quadratic model:	2906	-2743	837.0	0.88	$-9.35 \cdot 10^{-6}$	$0.61 \cdot 10^{-3}$	77.9	0.60
linear model:	0	-891.2	550.0	2.28	0	$14.47 \cdot 10^{-3}$	78.5	0.60

Table 5.18: Model parameters for monitor (NCD).

As seen from Table 5.18, it is clear that the monitor is a constant power load. As for the other general purpose electronic loads the power base for the load is obtained from the power consumed at 230 V or 84 W, which will give an error of 3.8 %. The model for the monitor is

$$\boxed{R = U^2/84 \pm 3.8\ \%}$$

Satellite Receiver (Triasat)

According to measurements, the satellite receiver consumes about 16.6 W when supplied with 230 V but the rated power is not given. The satellite receiver was tested between

160 V and 300 V. When the voltage was below 160 V, the load did not start. It only worked when the plug of the receiver was connected in the "right" way, that is the load probably only has a half wave diode rectifier, and that is why higher voltages where not tested. Fig. 5.19 and Table 5.19 show the results from the characterization.

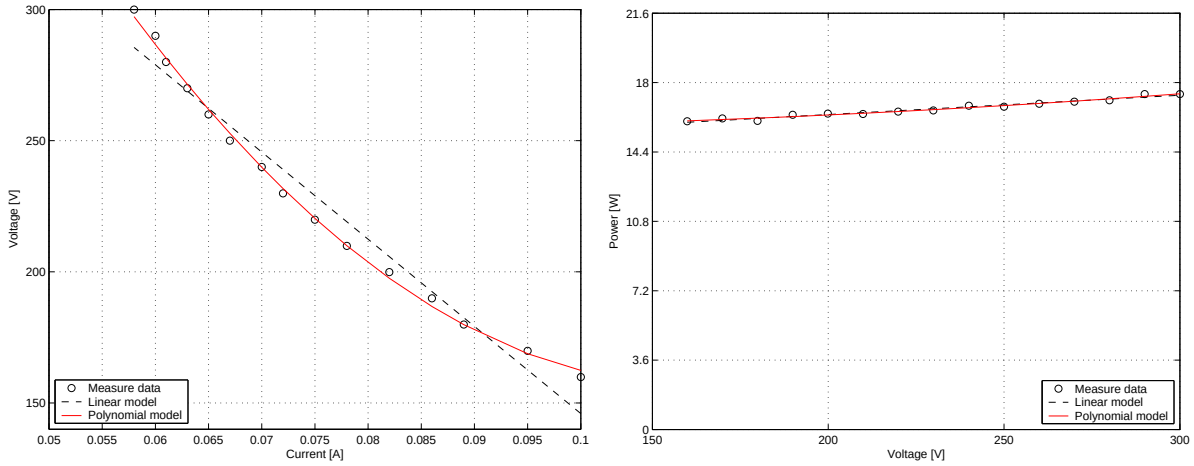

(a) Current vs. Voltage (b) Power vs. Voltage

Figure 5.19: Characteristics of satellite receiver (Triasat).

	R_{p2}	R_{p1}	R_{p0}	ε_R	A_{p2}	A_{p1}	A_{p0}	ε_P
quadratic model:	$5.24 \cdot 10^4$	$-1.15 \cdot 10^4$	787.7	0.75	$2.44 \cdot 10^{-5}$	$-0.22 \cdot 10^{-3}$	15.5	0.36
linear model:	0	-3324	478.4	3.16	0	0.0100	14.3	0.45

Table 5.19: Model parameters for satellite receiver (Triasat).

As seen from Table 5.19, it is clear that the monitor is a constant power load. The load was modelled based on the power consumed at 230 V or 16.6 W, giving an error of 4.8 %. The model for the satellite receiver is

$$\boxed{R = U^2/16.6 \pm 4.8\ \%}$$

5.1.3 Summary

The results of the characterization of the electronic loads are tabulated in Table 5.20 with the estimated error of the models.

Table 5.20 shows that all of the loads categorized for general use are constant power loads. The error is quite high for some of the loads, which can be partly explained by measurement errors, and partly because some of these loads are hard to characterize, for instance a computer supplied with a huge power supply will give a huge error.

Loads for lighting purposes are much more complicated. Generally the compact fluorescent lamps showed a constant current behavior, and that is also the proposed model. But the models are only valid over a certain range of voltage. Some lamps turned off at low voltage to protect them from breaking. But some of the lamps did not work very well at lower voltages and broke.

The fluorescent lamps did not show the same behavior as the compact ones, because they have more sophisticated control gear. For those loads, the model is somewhat more complicated, but can also be simpler, as for the Tridonic ballasts.

For the transformers for the low voltage halogen lamps it is hard to say what to expect. Simpler transformers probably have no control gear, only transform the voltage to the right level, and then the load acts as a lamp, i.e. Co-Tech transformer. The Tridonic transformer showed very different behavior and a simple model over the whole region is not possible, but a piecewise model is suggested.

Lighting

Compact Fluorescent Lamps	P_{rated} [W]	Range [V]	Model [$R =$]	Error [%]
Eurolight	9	100-300	$U/0.029$	7.5
Ikea	11	190-380	$U/0.038$	2.1
Osram	23	120-300	$U/0.067$	10
Philips (9 W)	9	120-300	$U/0.035$	1.2
Philips (9 W)	11	120-300	$U/0.041$	4.3
Philips (15 W, 1)	15	140-280	$U/0.057$	15
Philips (15 W, 2)	15	140-280	$U/0.057$	15
Sylvania	10	100-300	$U/0.046$	1.1
Fluorescent Lamps	P_{rated} [W]	Range [V]	Model [$R =$]	Error [%]
Ballast (Philips)	72	150-220	$U/0.325$	1.2
		220-280	$U^2/70.5$	6.8
Ballast (Tridonic)	72	130-340	$U^2/75$	0.7
Dimmable Ballast (Tridonic)	70.4	110-380	$U^2/58.1$	0.9
Electronic Transformers[1]	P_{rated} [W]	Range [V]	Model [$R =$]	Error [%]
Co-Tech	60	150-300	$2626 \cdot I + 257.2$	0.9
Tridonic	60	100-190	$U/(9.46 \cdot 10^{-4} \cdot U + 0.087)$	0.7
		190-380	$U^2/51.3$	20

Electronics for General Purposes

Computer Power Supplies	P_{rated} [W]	Range [V]	Model [$R =$]	Error [%]
Chieftech	350	200-380	$U^2/40$	20
Dell	unknown	170-380	$U^2/43.5$	1.5
Macintosh	87	150-380	$U^2/43.5$	4
Sirtech	235	180-380	$U^2/37.9$	20
Other Devices	P_{rated} [W]	Range [V]	Model [$R =$]	Error [%]
Charger[2]	unknown	100-300	$U^2/6.7$	8.0
Charger[3]	unknown	100-300	$U^2/6.9$	4.3
Charger[4]	unknown	100-300	$U^2/8.05$	2.0
IP Telephone (Grandstream)	unknown	100-380	$U^2/2.76$	24
LCD Monitor (AOC)	32	130-330	$U^2/30$	1.2
Monitor (NCD)	unknown	200-350	$U^2/84$	3.8
Satellite Receiver (Triasat)	unknown	200-350	$U^2/16.6$	4.8

Table 5.20: Model parameters for electronic loads and estimated error.

[1]Transformers for low voltage halogen lamps
[2]Ericsson, Model No. 4020036 BV, 1
[3]Ericsson, Model No. 4020036 BV, 2
[4]Ericsson, Model No. 4020037 BV

5.2 Frequency Spectrum Analysis

The models realized in the characterization of the electronic loads, see Section 5.1, are used as a base for the frequency spectrum analysis. Each load was supplied with 230 V dc. The calculated distortion factor obtained in the measurements is in turn compared to the distortion calculated for the models. As stated above, electronic loads are divided into two subcategories, general electronics and electronics used for lighting purposes.

5.2.1 Lighting

It was found out that these loads can, in steady state, be modelled as constant current, except for the ballasts and the electronic transformer[1] which could be modelled as constant power and as a variable resistor, respectively. The results from the measurements and simulations are listed in Table 5.21.

Compact Fluorescent Lamps

	Measurements				Simulations			
	Magnitude		Distortion Factor		Magnitude		Distortion Factor	
Load	Voltage [V]	Current [A]	Voltage [%]	Current [%]	Voltage [V]	Current [A]	Voltage [%]	Current [%]
Eurolight (9W)	227.78	0.040	3.40	3.38	227.78	0.039	3.40	3.38
Ikea (11W)	228.18	0.028	3.39	3.22	228.18	0.038	3.38	3.38
Osram (23W)	229.30	0.069	3.39	3.30	229.30	0.067	3.39	3.38
Philips (9W)	229.42	0.040	3.37	3.40	229.42	0.035	3.37	3.38
Philips (11W)	230.50	0.040	3.37	3.44	230.50	0.041	3.37	3.38
Philips (15W, 1)	229.51	0.059	3.43	3.51	229.51	0.057	3.38	3.38
Philips (15W, 2)	230.53	0.054	3.43	3.48	230.53	0.053	3.38	3.38
Sylvania (10W)	227.52	0.051	3.38	3.39	227.52	0.046	3.38	3.38

Ballasts used for Fluorescent Lamps

	Measurements				Simulations			
	Magnitude		Distortion Factor		Magnitude		Distortion Factor	
Load	Voltage [V]	Current [A]	Voltage [%]	Current [%]	Voltage [V]	Current [A]	Voltage [%]	Current [%]
Philips	226.47	0.315	3.39	3.39	226.47	0.311	3.39	3.38
Tridonic	226.30	0.352	3.38	3.39	226.30	0.331	3.38	3.39
Tridonic[2]	226.92	0.251	3.35	3.39	226.92	0.256	3.35	3.42

Electronic Transformers[3]

	Measurements				Simulations			
	Magnitude		Distortion Factor		Magnitude		Distortion Factor	
Load	Voltage [V]	Current [A]	Voltage [%]	Current [%]	Voltage [V]	Current [A]	Voltage [%]	Current [%]
Co-Tech	226.03	0.251	3.38	3.38	226.03	0.248	3.38	3.38
Tridonic	228.17	0.229	3.44	3.47	228.17	0.225	3.39	3.38

Table 5.21: Frequency spectrum analysis results from measurement and simulation of lighting electronics.

The results tabulated in Table 5.21 shows that the lighting electronic loads cause very little distortion. The frequency components of these loads were in most cases 40 kHz or well above and this is due to the controller inside the load. The controller in the loads have not been modelled and therefore the obtained distortion factor in the current is different compared to the measurements. The conclusion of the steady state analysis is that the electronic loads used for lighting can be modelled according to the suggested models.

[1] From Tridonic and Clas Ohlson

[2] Dimmable ballast

[3] Electric transformers for low voltage halogen lamps

5.2.2 Electronics for General Purposes

For general electronic loads, it was found that these loads could be modelled as constant power in steady state. The loads were further divided into subcategories, computers and other electronic devices. The results from the measurements and simulations are listed in Table 5.22.

Computer Power Supplies

	Measurements				Simulations			
	Magnitude		Distortion Factor		Magnitude		Distortion Factor	
Load	Voltage [V]	Current [A]	Voltage [%]	Current [%]	Voltage [V]	Current [A]	Voltage [%]	Current [%]
Chieftech	226.08	0.173	3.43	4.73	226.08	0.177	3.38	3.39
Dell	226.54	0.146	3.45	6.58	226.54	0.192	3.39	3.38
Macintosh	226.11	0.198	3.44	4.15	226.11	0.192	3.39	3.37
Sirtech	226.15	0.179	3.44	3.89	226.15	0.177	3.39	3.38

Other Electronics Devices

	Measurements				Simulations			
	Magnitude		Distortion Factor		Magnitude		Distortion Factor	
Load	Voltage [V]	Current [A]	Voltage [%]	Current [%]	Voltage [V]	Current [A]	Voltage [%]	Current [%]
Charger[4]	228.68	0.035	3.50	5.53	228.68	0.035	3.41	3.35
Charger[5]	228.63	0.029	3.41	3.76	228.63	0.029	3.36	3.41
Charger[6]	228.51	0.030	3.42	4.23	228.51	0.030	3.37	3.40
Ip Telephone (Grandstream)	228.17	0.012	3.43	4.92	228.17	0.012	3.38	3.38
LCD Monitor (AOC)	231.05	0.121	3.43	4.74	231.05	0.124	3.38	3.39
Monitor (NCD)	226.57	0.343	3.44	5.62	226.57	0.371	3.36	3.41
Satellite receiver (Triasat)	226.30	0.078	3.42	4.00	226.30	0.073	3.37	3.40

Table 5.22: Frequency spectrum analysis results from measurement and simulation of general electronics.

The result of the steady-state analysis shown in Table 5.22 indicates that the loads cause some distortion in the current and the difference in distortion factor ranges from 0.3 % to 2.2 % approximately. The frequency component that cause this is at 100 Hz and the magnitude of the component is about $2-3$ % of the dc value.

The 100 Hz component found in the measured current can also be found in the measured voltage but with much lower amplitude. The origin of this 100 Hz component found in the voltage is the dc source and more information about the dc source can be found in Appendix C. Due to the construction of the loads, the ripple in voltage is mirrored in the current via the smoothing capacitor connected directly after the diode rectifier, see Fig. 5.3. The ripple in the current is related to the voltage according to

$$i_c(t) = C\frac{\mathrm{d}u_c(t)}{\mathrm{d}t} \tag{5.1}$$

This indicates that frequency component in the current is not caused by the load but by the dc source. This phenomena was not modeled, so the distortion factor of the current from these models are very similar to the distortion factor in the voltage. The conclusion drawn for these loads is that they cause no distortion.

To avoid ripple in the currents in a dc system, it is important to have as stable dc voltage as possible and to achieve this a filter of high order, due to low magnitude of the 100 Hz component, has to be installed at the dc source.

[4]Ericsson, Model No. 4020037 BV
[5]Ericsson, Model No. 4020036 BV, 1
[6]Ericsson, Model No. 4020036 BV, 2

5.3 Transient Behavior

To determine the transient behavior of the loads, they where subjected to 10 voltage step of four different magnitudes (that is 40 steps in total), or as long as the load was still operating. The measurement setup is explained in more detail in Chapter 2. One a typical transient step was taken and analyzed further for each load. From the characterization it can be seen over which voltage interval the load was working, and sets the number of steps. For instance, if a computer experiences a voltage lower than 180 V, it shuts down and the model will not work.

To model the electronic loads, a simple circuit was constructed as Fig. 5.20 shows. It shows half a diode bridge rectifier that is usually found in these loads, then after the diodes a series RLC circuit is put in parallel to the load.

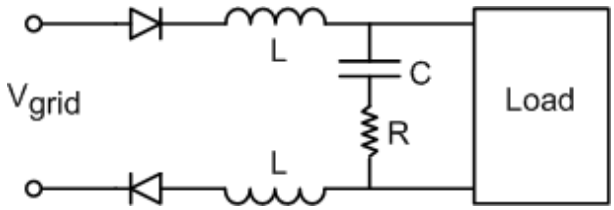

Figure 5.20: General circuit model for the electronic loads.

When the model shown in Fig. 5.20 is supplied with a fast voltage step, the diodes will block the current while the voltage over the capacitor is higher than the voltage at the terminals. The capacitors discharges through the load, and when the voltage of the capacitor reaches the voltage at the terminals, the diodes resume to conduct, and the load is again supplied from the terminals. In some cases, when the current returns it will show some oscillations. The oscillation can be modeled by properly sizing the inductor and capacitor and then R can be tuned to set the damping of the oscillation.

To estimate the size of the capacitance C, Eq. (5.1) was used. For each voltage step, the voltage difference before and after the step was taken as Δu, the time that the diodes were blocking was taken as Δt. The change in current Δi is the difference between the current before the step and the current while the diodes were blocking, that is zero. The capacitance C can be roughly estimated as

$$C \approx \frac{\Delta i \Delta t}{\Delta u} \tag{5.2}$$

For each load, the C should be constant for all steps, that is the discharge time is longer as the change in terminal voltage is bigger. This estimation was usually an underestimation but the C that was found to fit the measurement best was usually the next E12 value above this estimation. If not, it is probably due to that two or more capacitors are parallel connected.

5.3.1 Lighting

The transient behavior was different for each load category as was suspected from the load characterization.

Compact fluorescent lamps

The compact fluorescent lamps all showed constant current behavior. They all have a diode rectifier that blocks the current, but when the current starts flowing again, there is no oscillation so that the inductance in Fig. 5.20 can be assumed to be zero. The R and C were calculated and tabulated in Table 5.23

	R [Ω]	L [mH]	C [µF]
Eurolight	200	0	3.9
Ikea	300	0	2.7
Osram	300	0	4.7
Philips (9 W)	100	0	3.3
Philips (11 W)	100	0	3.3
Philips (15 W, 1 and 2)	100	0	12
Sylvania	200	0	4.7

Table 5.23: Model parameters for R, L and C in Fig. 5.20.

This construction is tested in EMTDC, where the models were subjected to a simulated step and to the step obtained from measurements. The results from that are shown in Figs. 5.21 to 5.28 where the measured transient is shown (denoted as "measured"), as well as the simulation results, both when the model is subjected to the simulated step (denoted as "modelled") and to the measured (denoted as "simulated").

Figure 5.21 shows the measurement result and the model result for the Eurolight lamp. The load only worked for three steps, according to the result from the characterization that at about 100 V the lamp behaves strangely. As can be seen, the model agrees with the measurements. There is a switching transient in the current at the beginning of the steps which is 3.0 p.u. for step 1, 11.3 p.u. for step 2 and 19.3 p.u. for step 3. This transient could be a result from a snubber on the input of the power supply or some other internal switching. This was not modelled.

The Ikea lamp worked for all four steps, although in steady-state it did not work below 190 V. As can be seen from Fig. 5.22, the model agrees with the measurements. There is a switching transient in the current at the beginning of the step which is ranging from 1.4 to 2.0 p.u. for all the steps. This transient is quite constant for all the steps and is not clear why that is.

The Osram lamp worked for all four steps. As can be seen from Fig. 5.23, the model agrees with the measurements except for the last step where the measured current is lower after the step. The measured current seems to flicker, but it is probable due to averaging since the current is osculating with a frequency of 50 kHz. There is no detectable switching transient from the measurement.

The Philips 9 W lamp worked for three steps, when the voltage was step down to lower than 0.5 p.u., the lamp turned off. As can be seen from Fig. 5.24, the model agrees with the measurements. There are some switching transients in the beginning of the step, which are ranging from 1.7 to 3 p.u. These transients are quite low and it is not clear why they are there.

The Philips 11 W lamp worked for three steps, when the voltage was step down, lower than 0.5 p.u., the lamp turned off. As can be seen from Fig. 5.25, the model agrees with the measurements. There are some switching transients in the beginning of the step, which are ranging from 1.7 to 3 p.u. These transients are quite low and it is not clear why they are there.

The Philips 15 W lamps worked for two steps, when the third step was applied, which is about 0.55 p.u., the lamp began to blink, which was also detectable in the current. This behavior is not considered and the lamp is simply said to turn off at this voltage. As can be seen from Fig. 5.26 and 5.27, the models agree with the measurements. There are some switching transients in the beginning of the step, which are about 1.7 p.u. for both steps. These transients are quite low and it is not clear why they are there.

The Sylvania lamp only worked for three steps, according to the result from the characterization that at about 100 W the lamp behaves strangely. As can be seen from Fig. 5.28 the model agrees with the measurements. There is a switching transient in the current at the beginning of the steps, which is 16 p.u. for step 1, 41 p.u. for step 2 and 61 p.u. for step 3. These transient is very high an it is unlikely that they are caused by the load only.

Eurolight

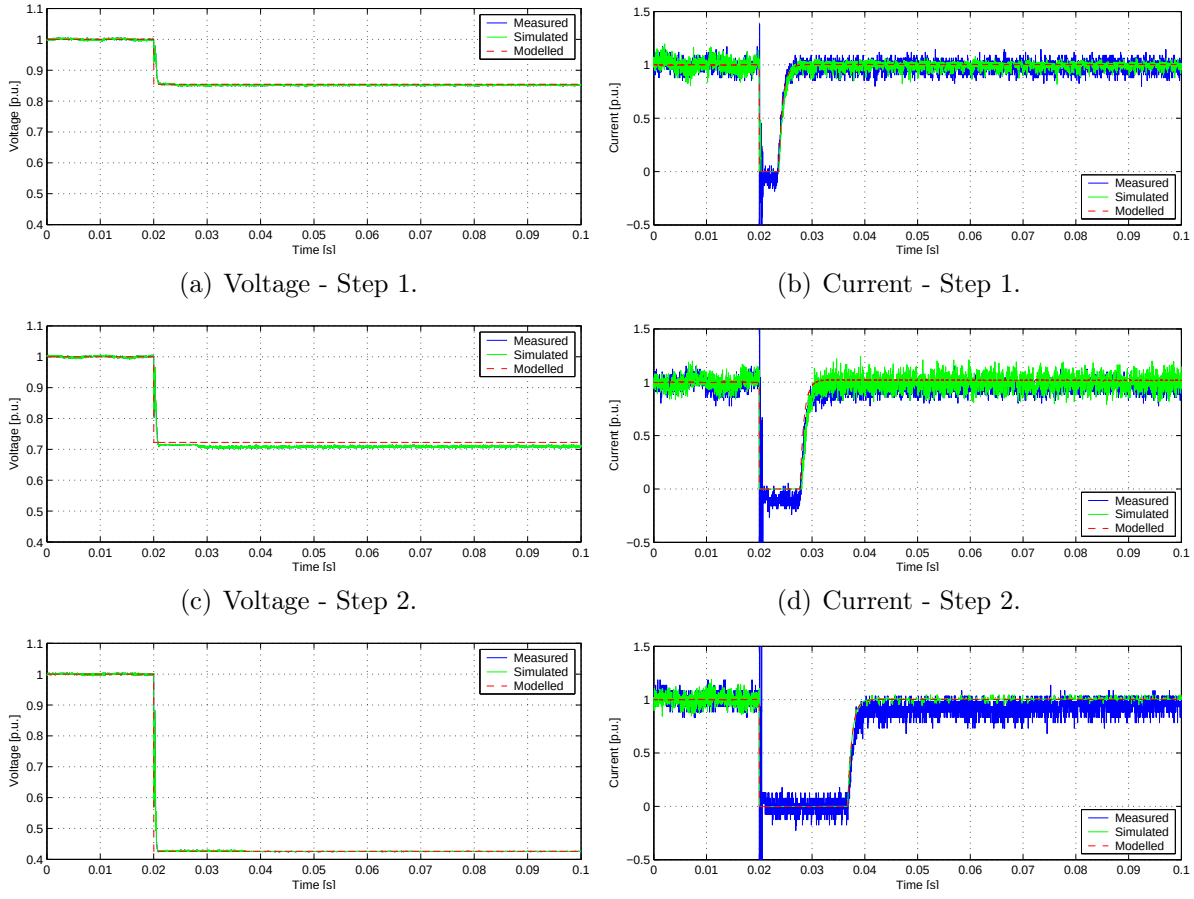

(a) Voltage - Step 1.

(b) Current - Step 1.

(c) Voltage - Step 2.

(d) Current - Step 2.

(e) Voltage - Step 3.

(f) Current - Step 3.

Figure 5.21: Transient behavior of compact fluorescent lamp (Eurolight).

Ikea

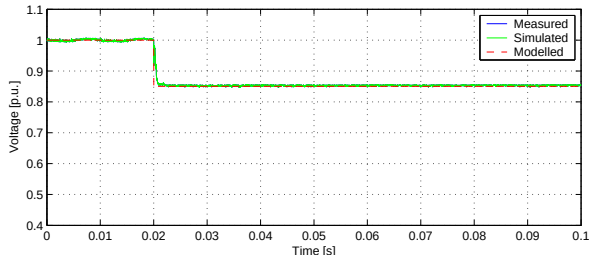

(a) Voltage - Step 1.

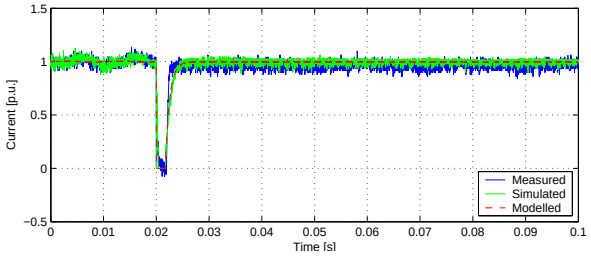

(b) Current - Step 1.

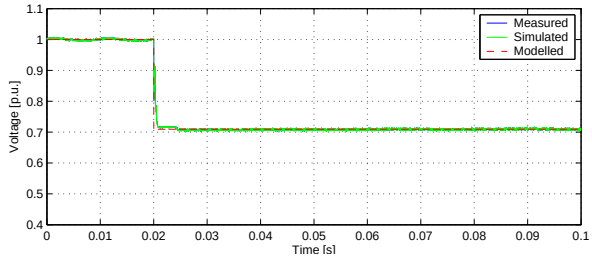

(c) Voltage - Step 2.

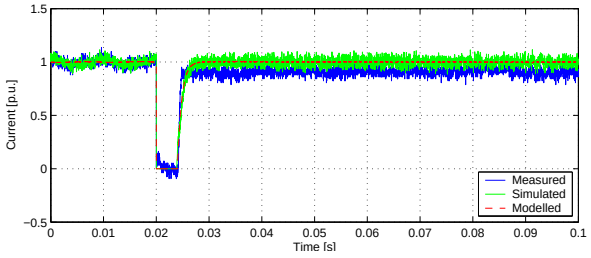

(d) Current - Step 2.

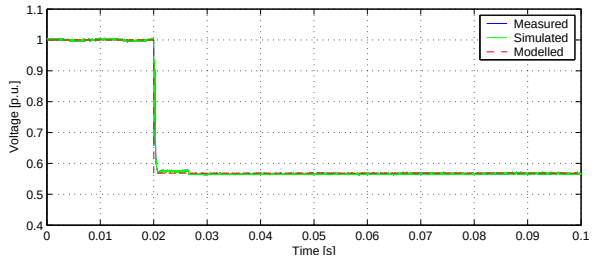

(e) Voltage - Step 3.

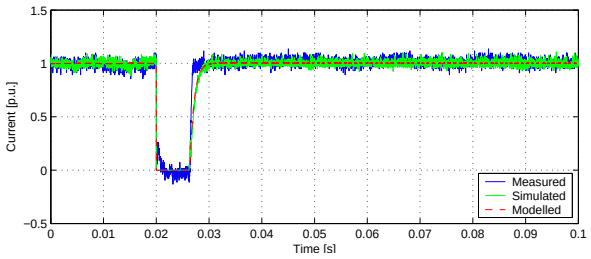

(f) Current - Step 3.

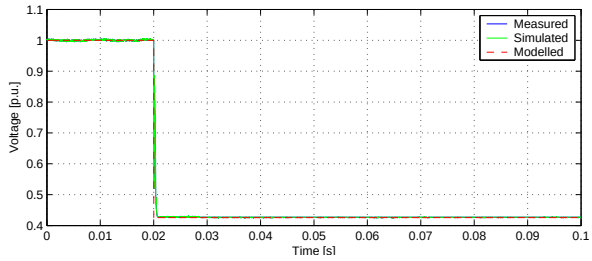

(g) Voltage - Step 4.

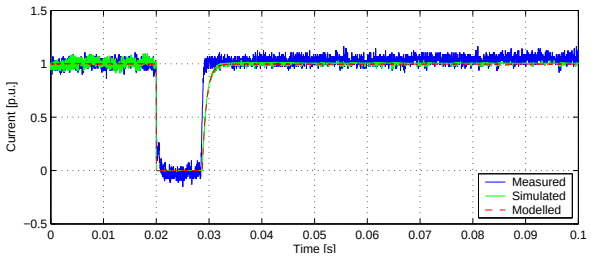

(h) Current - Step 4.

Figure 5.22: Transient behavior of compact fluorescent lamp (Ikea).

Osram

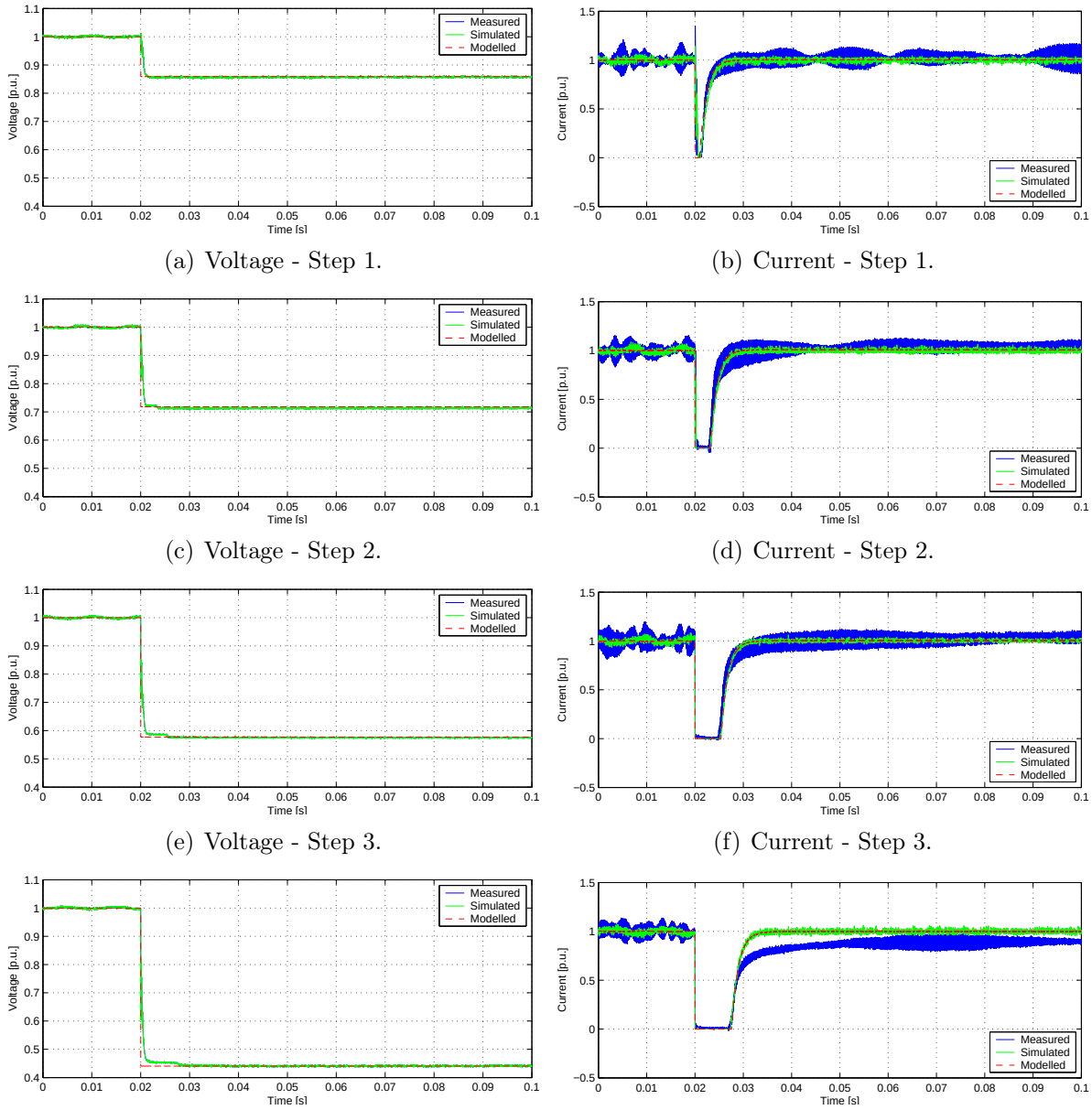

(a) Voltage - Step 1.

(b) Current - Step 1.

(c) Voltage - Step 2.

(d) Current - Step 2.

(e) Voltage - Step 3.

(f) Current - Step 3.

(g) Voltage - Step 4.

(h) Current - Step 4.

Figure 5.23: Transient behavior of compact fluorescent lamp (Osram).

Philips, 9W

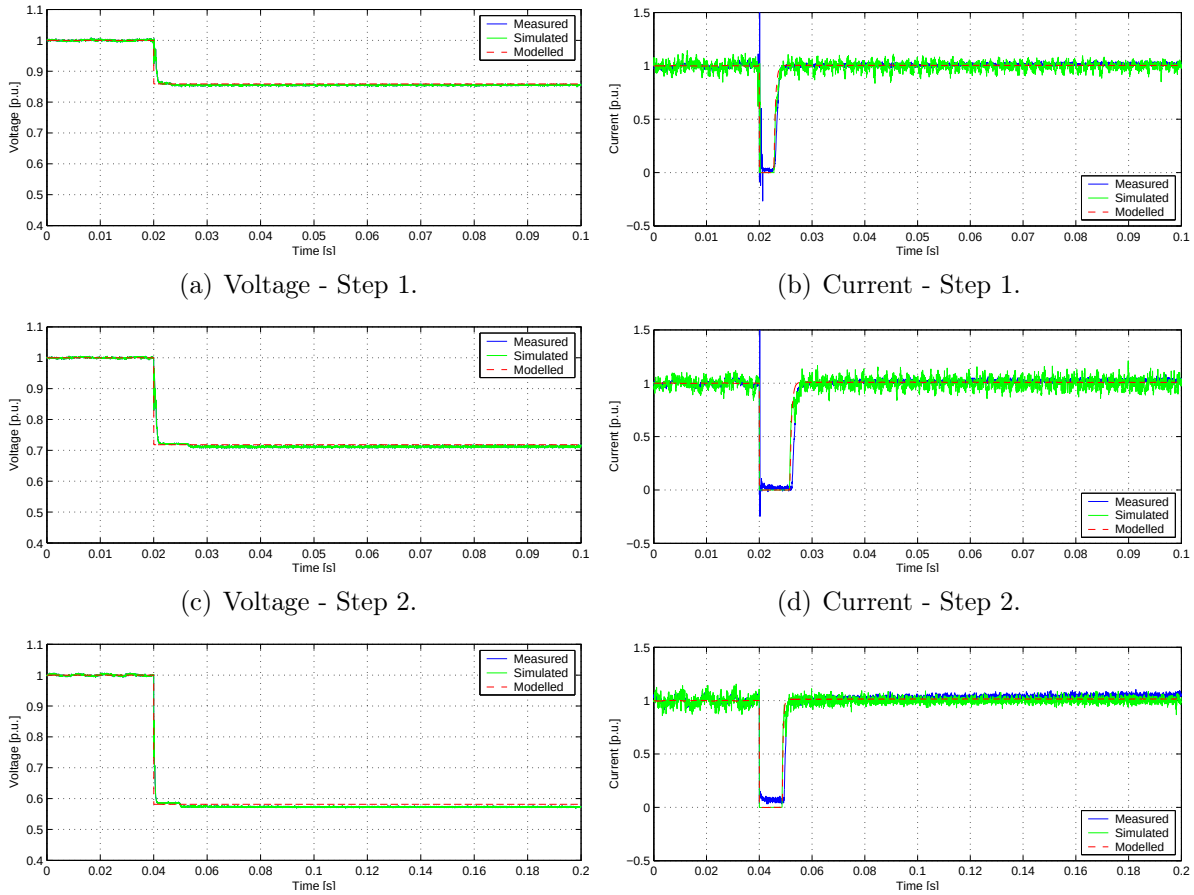

(a) Voltage - Step 1.

(b) Current - Step 1.

(c) Voltage - Step 2.

(d) Current - Step 2.

(e) Voltage - Step 3.

(f) Current - Step 3.

Figure 5.24: Transient behavior of compact fluorescent lamp (Philips, 9W).

Philips, 11W

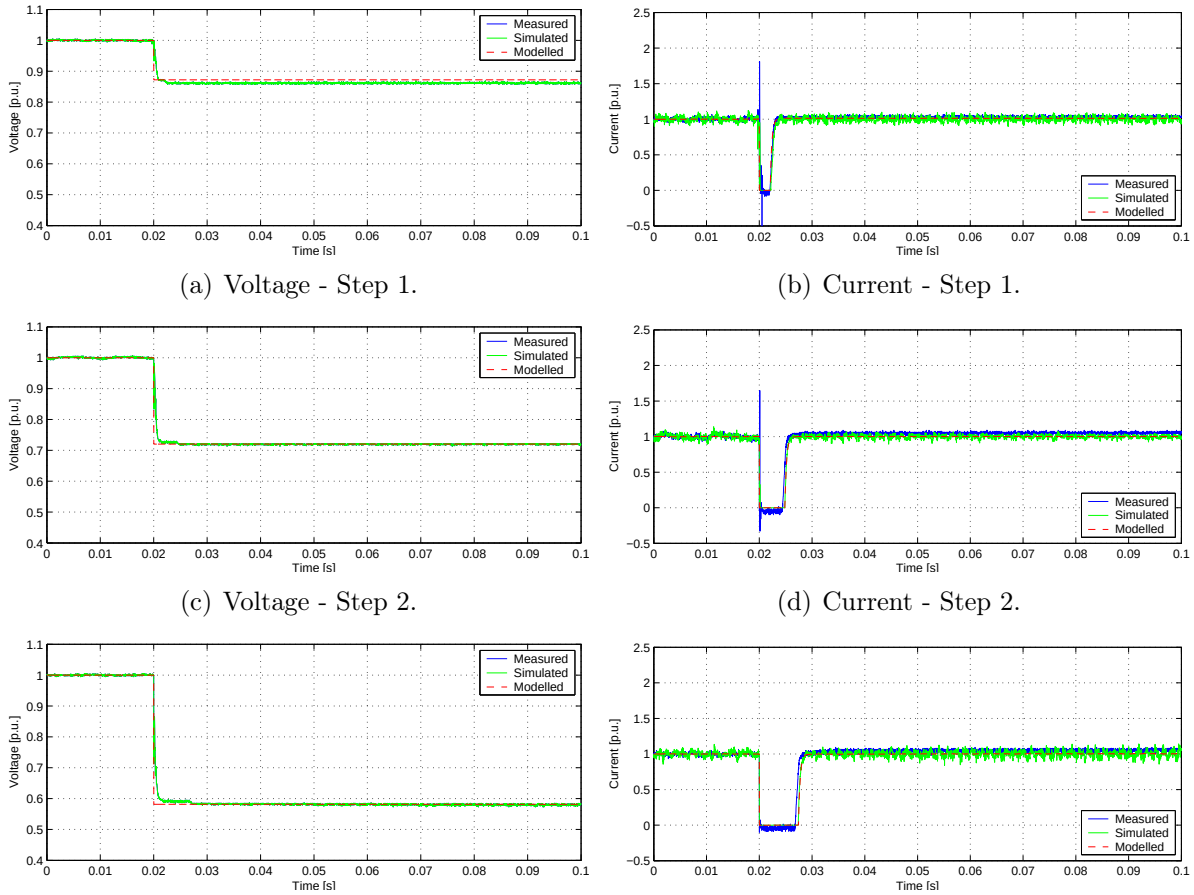

(a) Voltage - Step 1.

(b) Current - Step 1.

(c) Voltage - Step 2.

(d) Current - Step 2.

(e) Voltage - Step 3.

(f) Current - Step 3.

Figure 5.25: Transient behavior of compact fluorescent lamp (Philips, 11W).

Philips, 15W 1 and 2

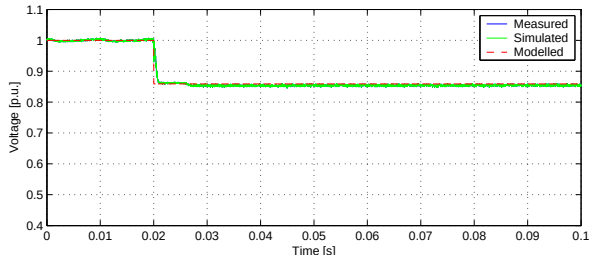

(a) Voltage - Step 1.

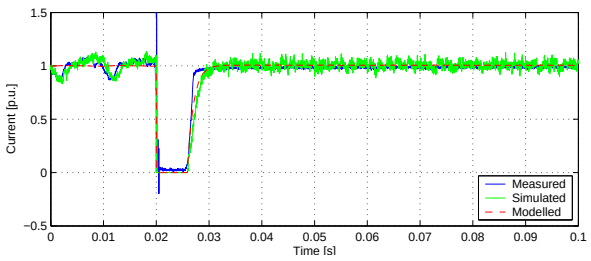

(b) Current - Step 1.

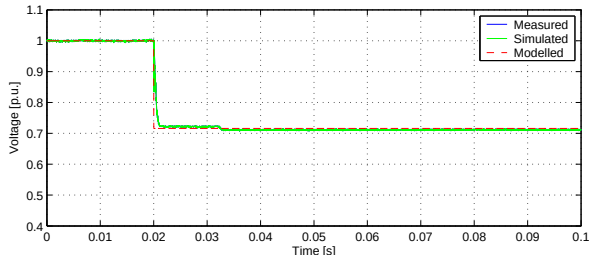

(c) Voltage - Step 2.

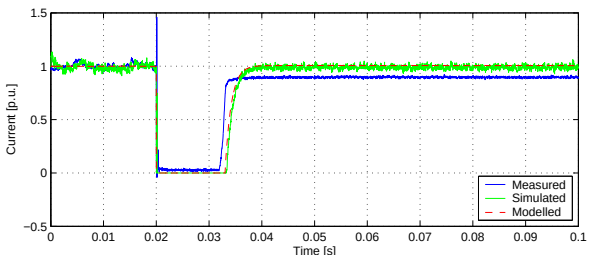

(d) Current - Step 2.

Figure 5.26: Transient behavior of compact fluorescent lamp (Philips, 15W 1).

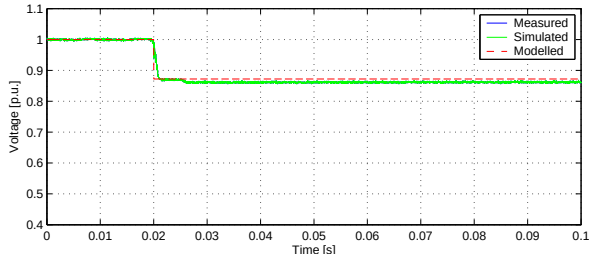

(a) Voltage - Step 1.

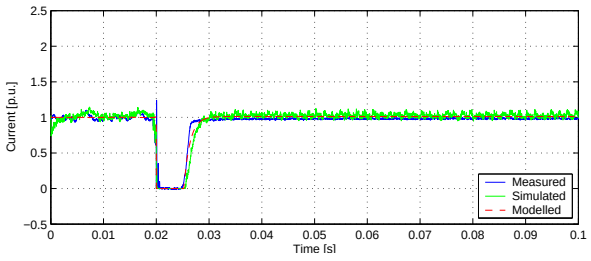

(b) Current - Step 1.

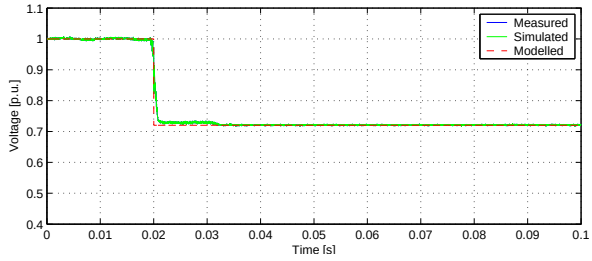

(c) Voltage - Step 2.

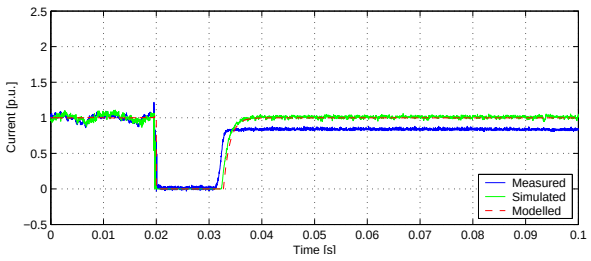

(d) Current - Step 2.

Figure 5.27: Transient behavior of compact fluorescent lamp (Philips, 15W 2).

Sylvania

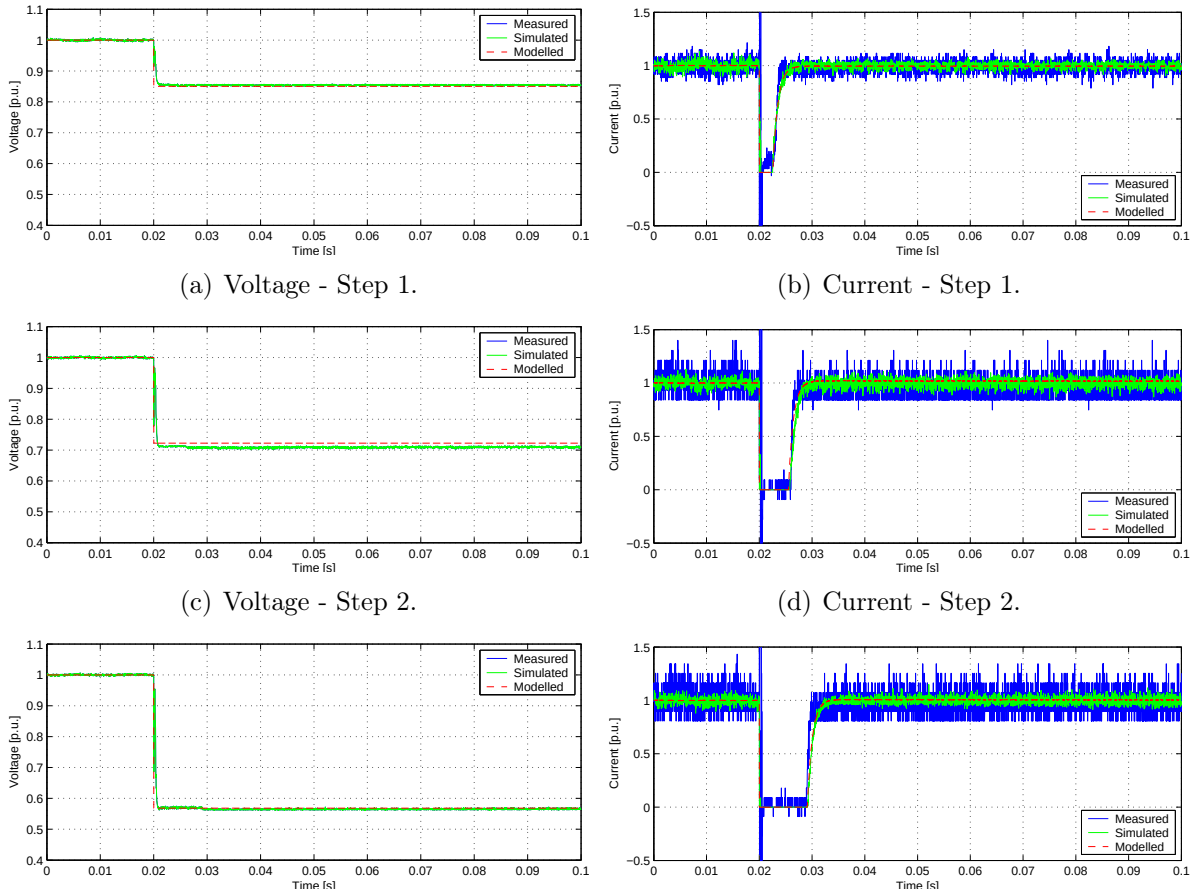

(a) Voltage - Step 1.

(b) Current - Step 1.

(c) Voltage - Step 2.

(d) Current - Step 2.

(e) Voltage - Step 3.

(f) Current - Step 3.

Figure 5.28: Transient behavior of compact fluorescent lamp (Sylvania).

The models all agree with the measurements when the load is supplied to these steps. For some lamps the current shapes did not follow the general rule for this kind of load and the lamp turned off at the lower voltages. It is then assumed that these lamps will not work properly at those levels, and generally it is around 100 V that the lamps did not work, or the fourth step. The Philips lamps were different though because they did not function at about 130 V.

Fluorescent Lamps

The ballasts for the fluorescent lamps are quite complicated and one general model is hard to derive. The construction of Fig. 5.20 was tested in EMTDC subjecting the model to a simulated step and a typical step obtained from measurements. If that was not possible, a model of the ballast as a second order system was tested as described below.

The Philips ballast was found to be of a constant current behavior, but the impedance of the lamp was found to decay exponentially as was found for the incandescent lamps. The lamp had a $\tau = 0.15$ s and it was quite constant for all the steps. In the beginning of the step, a fast switching transient was found, and it was tried to model that behavior with a snubber, where $C = 0.5$ µF and $R = 100$ Ω. this snubber did not show the

same behavior and it is probable not possible to model this ballast with such a simple model [21]. The results from the step are shown in Figs. 5.29.

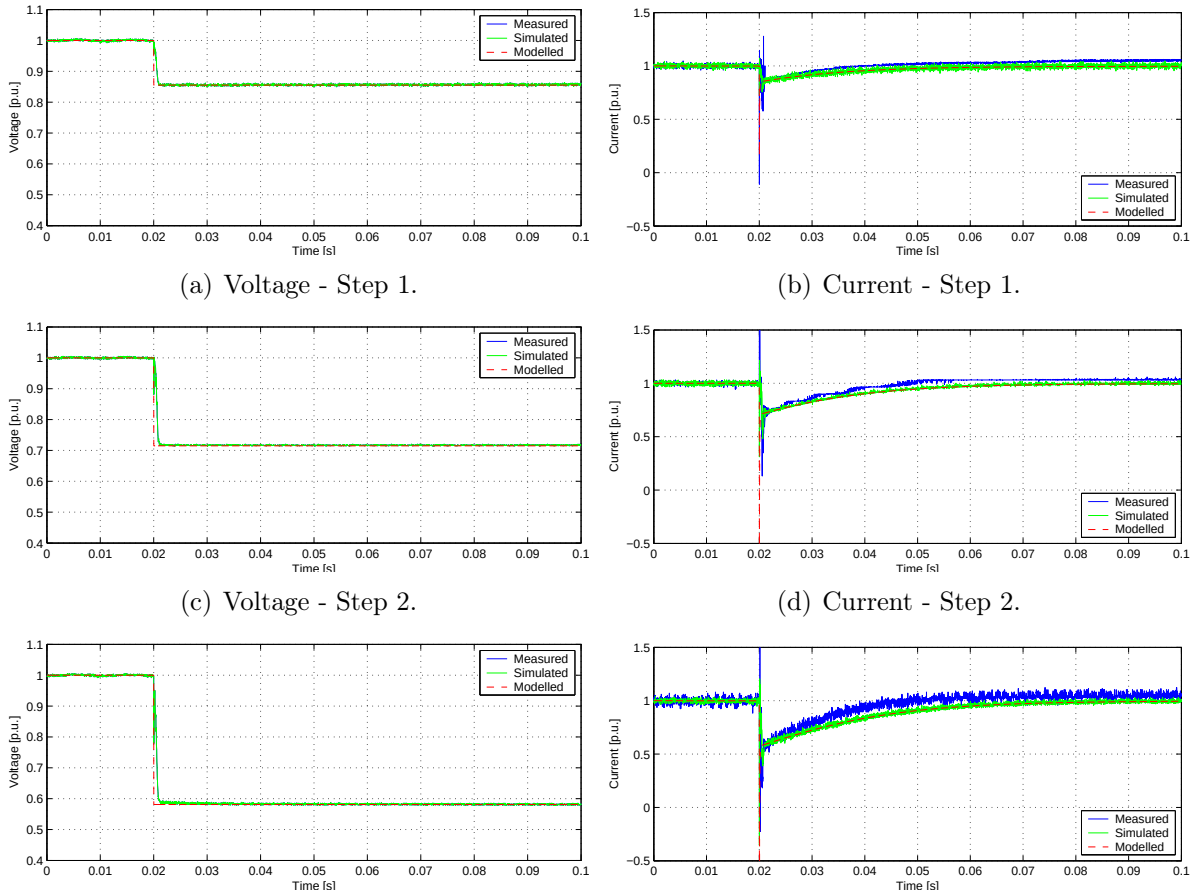

(a) Voltage - Step 1.

(b) Current - Step 1.

(c) Voltage - Step 2.

(d) Current - Step 2.

(e) Voltage - Step 3.

(f) Current - Step 3.

Figure 5.29: Transient behavior of ballast (Philips).

A model for the behavior of the Tridonic ballast is very complicated. The ballast showed a constant power behavior. When a sudden voltage change is made at the load terminals, the current oscillates quite a lot. It was tried to make a model of this oscillation with the RLC circuit parallel to the load, as showed in Fig. 5.20, but that was unsuccessful. This oscillation it probably due to internal controllers in the ballast and a such a simple model might be difficult to achieve [22].

To analyze the transients of the Tridonic ballasts further, an underdamped second order system was considered which has the following transfer function.

$$H(s) = \frac{\omega_n^2}{s^2 + 2\xi\omega_n s + \omega_n^2} \tag{5.3}$$

where ξ is defined as the damping ratio and ω_n is the natural frequency of the system. The inverse Laplace transform of the system can then be derived and the result is

$$h(t) = 1 - \frac{1}{\beta} e^{-\xi\omega_n t} \sin(\beta\omega_n t + \theta) \tag{5.4}$$

where $\beta = \sqrt{1-\xi^2}$ and $\theta = \tan^{-1}(\beta/\xi)$. In this response $\tau = 1/\xi\omega_n$ is the time constant of the exponentially damped sinusoid in seconds and $\beta\omega_n$ is the frequency of the damped sinusoid.

From the steps made on the ballast, the retained voltage after the step, u_{step}, was measured. It was noticed that, in p.u., the current after the step dropped by the same amount as the voltage, if the high current spike is neglected, and then stepped up to the new steady-state value. The difference in the current step was measured and denoted by i_{step}. The rise time T_r that is defined between 10% and 90% of i_{step} was also measured. The peak of the oscillation was measured and denoted by M_p and expressed in percentage of the steady state current after the step. The time where the peak occurred was also measured from the time when the step occurred and is denoted T_p. The settling time of the system was measured and it was defined as the time when the oscillation was less than $\pm 5\%$ of the steady-state current after the step. Finally, the frequency of the oscillation was measured and denoted by ω_{step}, which should be equal to the frequency of the damped sinusoid or $\beta\omega_n$. These quantities are indicated in Fig. 5.30.

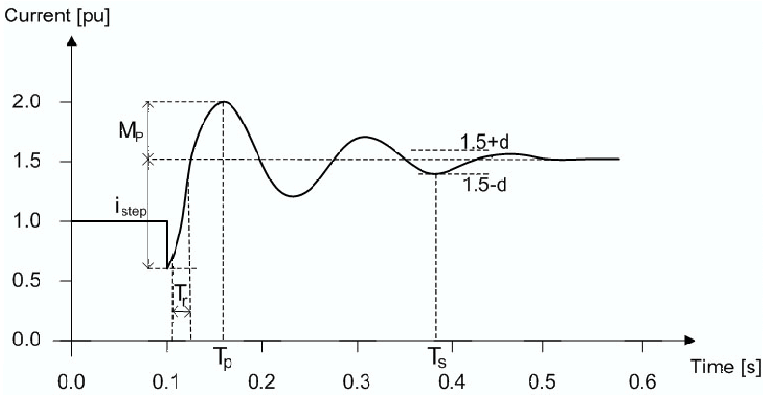

Figure 5.30: Typical transient behavior of Tridonic ballasts.

The settling time T_s will be directly proportional to the time constant τ for a standard underdamped second order system, or

$$T_s = \frac{k}{\xi\omega_n} \tag{5.5}$$

where k is defined by the percentage overshoot, M_p (see Fig. 5.30). In the case of 5% used here, $k = 3$. The following expression can be found from the system impulse response:

$$\beta\omega_n T_p = \omega_{step} T_p = \pi \tag{5.6}$$

This response of the system described by Eq. (5.4) is valid for step from zero to unity [23]. When making a step down in voltage, it results in a step up in current. As stated above, when the step in voltage occurs, at the time denoted by t_{step}, the current drops down as stated above and then steps up to the new steady-state with some oscillations. Before t_{step} the system is given by the steady-state model, or $i_{steady} = P/U$. The current after the step is $i_{steady,new} = P/u_{step}$, also obtained from the steady-state model in correspondence of the voltage after the step. The transient behavior is then defined as

$$i_{tr} = i_{steady,new} - \frac{i_{step}}{\beta} \mathrm{e}^{-\xi\omega_n(t-t_{step})} \sin(\beta\omega_n(t-t_{step}) + \theta) \quad \text{[pu]} \tag{5.7}$$

The measurement results for the constants are then presented in Table 5.24 for all steps and both transformers. It is clear from the table that as the step varies, the constants measured vary as well. The fourth step for the Tridonic ballast 1 is not included

because the measuring time of the step was not long enough to capture the step fully. It should also be noted that for Tridonic ballast 1, the steady-state current after the step is underestimated for step 3 and 4, which suggests that the steady-state model derived earlier is not valid at that low voltage. However, the ballast is not guaranteed to function properly at lower voltages than 154 V according to the manufacturer specification [24] and both those steps are lower than that voltage.

Ballast (Tridonic)

	Step 1	Step 2	Step 3	Step 4
u_{step} [pu]	0.861	0.719	0.582	-
i_{step} [pu]	1.02	1.11	1.30	-
T_r [ms]	4.8	7.1	10.3	-
T_p [ms]	17.0	27.2	32.9	-
M_p [%]	40.4	62.1	74.7	-
T_s [ms]	119.4	154.5	158.9	-
ω_{step} [rad/s]	151.5	123.0	108.9	-

Dimmable Ballast (Tridonic)

	Step 1	Step 2	Step 3	Step 4
u_{step} [pu]	0.862	0.721	0.579	0.454
i_{step} [pu]	1.02	1.11	1.30	1.66
T_r [ms]	9.8	14.2	18.3	23.8
T_p [ms]	28.9	36.1	45.1	61.4
M_p [%]	19.0	35.0	52.5	54.6
T_s [ms]	200.0	242.2	397.2	673.1
ω_{step} [rad/s]	92.6	76.9	63.6	48.9

Table 5.24: Transient behavior of ballasts (Tridonic).

To find the ω_n and ξ needed to describe the transient, the ξ was chosen so that it would give approximately the right overshoot. The overshoot of the system is very high and ξ was found with trial and error for both ballasts and was constant. Then the β is also known and from that and T_p, given in Table 5.24, ω_n can be calculated according to Eq. (5.6). The results that fitted best the curves are presented in Table 5.25.

From Table 5.25 it is clear that, as the voltage steps down, the natural frequency also steps down. The α presented in the table is found as $\omega_n = \alpha \cdot u_{step}$ and is found by employing the method of least squares to the data. This expression for the transient was tried in MATLAB and the results can be seen in Figs. 5.31 and 5.32.

Ballast (Tridonic)

	Step 1	Step 2	Step 3	Step 4
u_{step} [pu]	0.861	0.719	0.582	0.459
ω_n [rad/s]	184.9	115.8	95.6	80.2
ξ	0.08			
α	183.2			

Dimmable Ballast (Tridonic)				
	Step 1	Step 2	Step 3	Step 4
u_{step} [pu]	0.862	0.721	0.579	0.454
ω_n [rad/s]	109.2	87.5	70.0	51.4
ξ	0.1			
α	132.5			

Table 5.25: Parameters ξ and ω_n for Eq. (5.7).

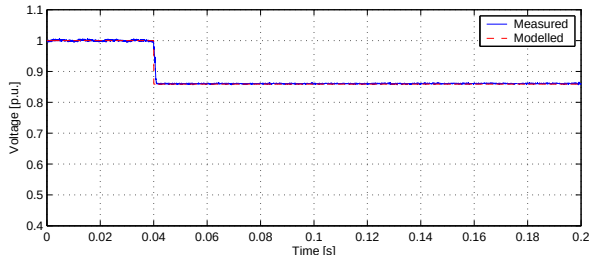

(a) Voltage - Step 1.

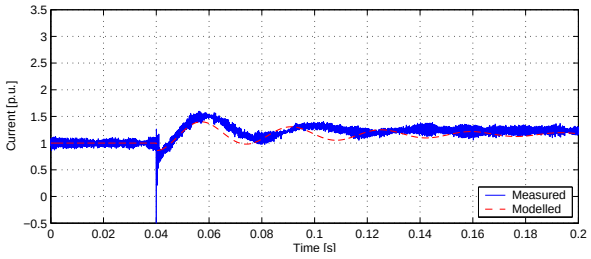

(b) Current - Step 1.

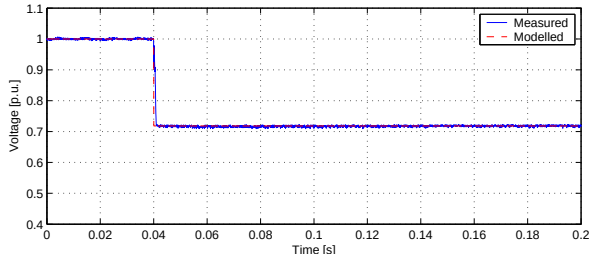

(c) Voltage - Step 2.

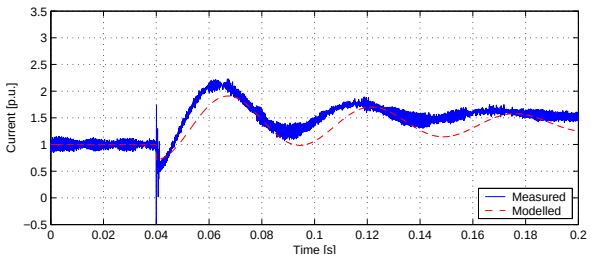

(d) Current - Step 2.

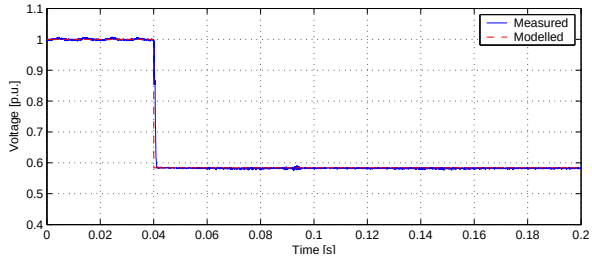

(e) Voltage - Step 3.

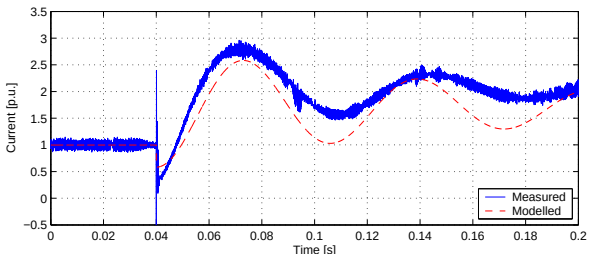

(f) Current - Step 3.

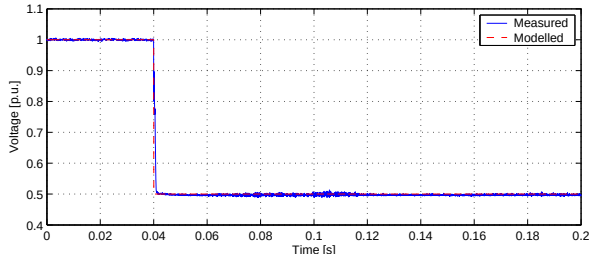

(g) Voltage - Step 4.

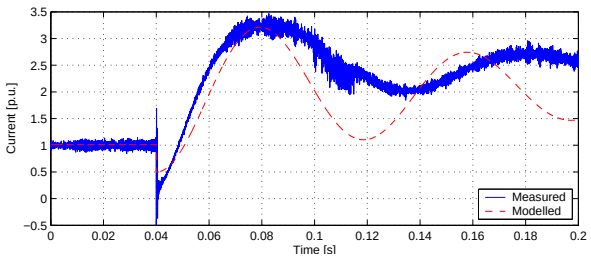

(h) Current - Step 4.

Figure 5.31: Transient behavior of ballast (Tridonic).

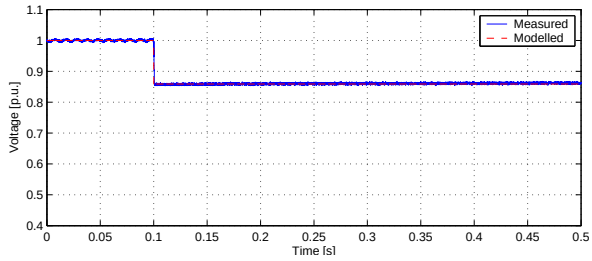

(a) Voltage - Step 1.

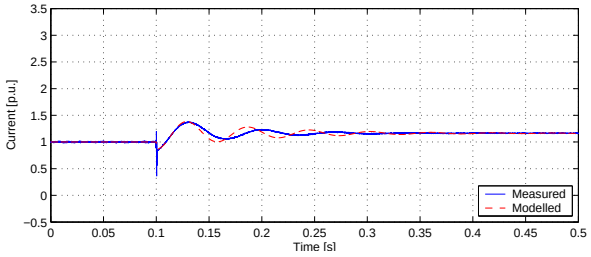

(b) Current - Step 1.

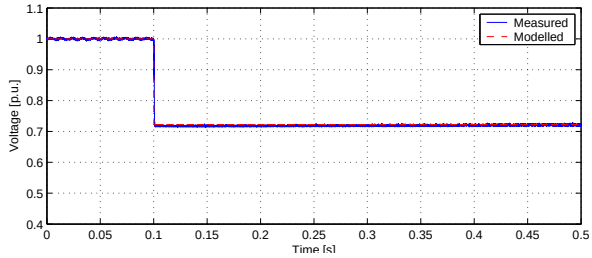

(c) Voltage - Step 2.

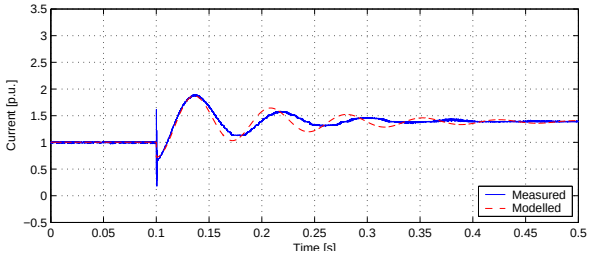

(d) Current - Step 2.

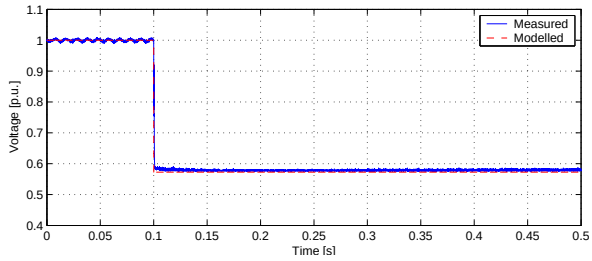

(e) Voltage - Step 3.

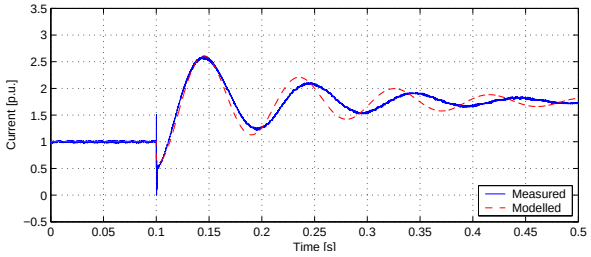

(f) Current - Step 3.

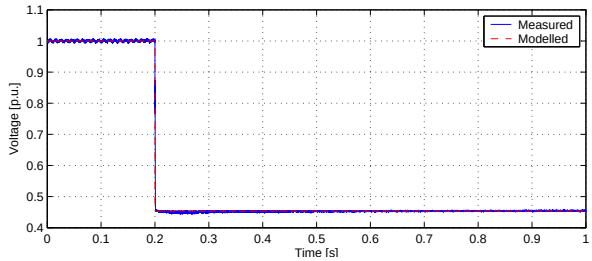

(g) Voltage - Step 4.

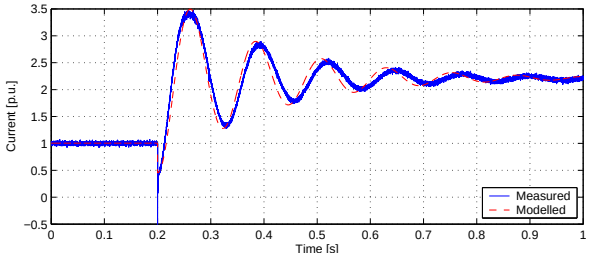

(h) Current - Step 4.

Figure 5.32: Transient behavior of dimmable ballast (Tridonic).

Electronic Transformers for Low Voltage Halogen Lamps

The transformer from Co-Tech was found to have a variable resistive behavior as a normal incandescent lamp, and the transient showed that it has a time constant of 0.01 s as can be seen in Fig. 5.33. The difference of this transformer from a normal incandescent lamp is that it has a switching transient in the beginning of the step. This transient is assumed to be caused by a snubber at the input to the transformer and it was found that $C = 0.25$ µF and $R = 100\ \Omega$ gave a similar behavior.

The transformer from Tridonic definitely has a complicated controller as it is dimmable. The model realized from the characterization is not valid for the transients as is showed in Fig. 5.34. A model for the transient behavior of this load has not yet been found.

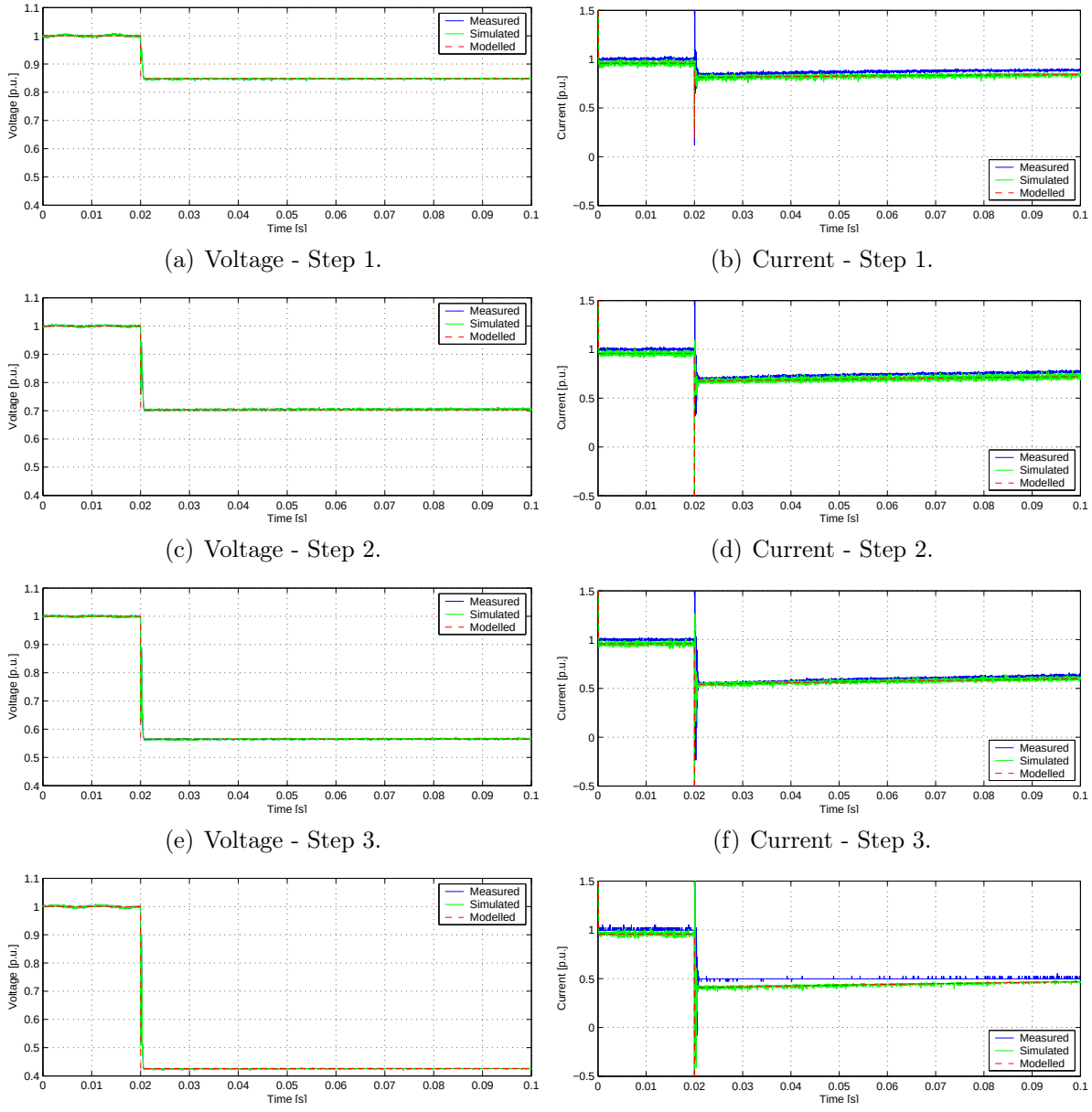

(a) Voltage - Step 1.

(b) Current - Step 1.

(c) Voltage - Step 2.

(d) Current - Step 2.

(e) Voltage - Step 3.

(f) Current - Step 3.

(g) Voltage - Step 4.

(h) Current - Step 4.

Figure 5.33: Transient behavior of electronic transformer (Co-Tech).

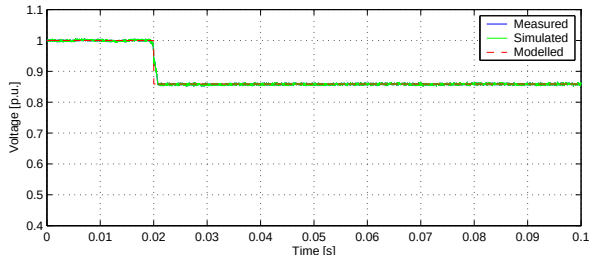

(a) Voltage - Step 1.

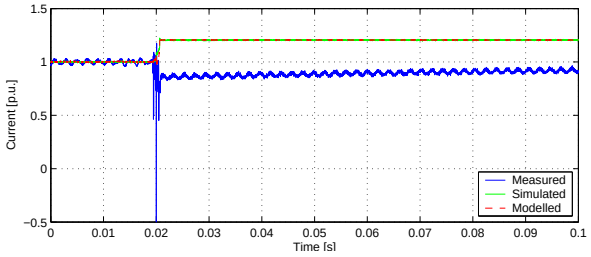

(b) Current - Step 1.

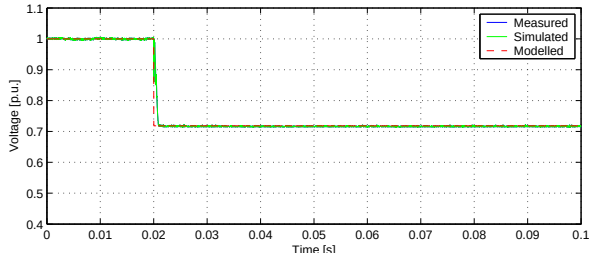

(c) Voltage - Step 2.

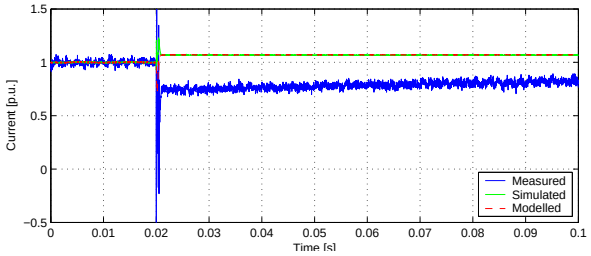

(d) Current - Step 2.

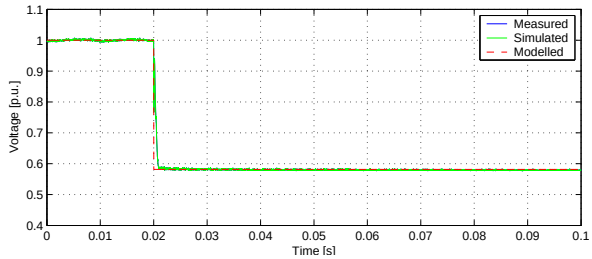

(e) Voltage - Step 3.

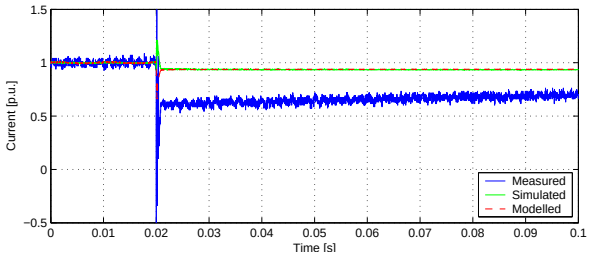

(f) Current - Step 3.

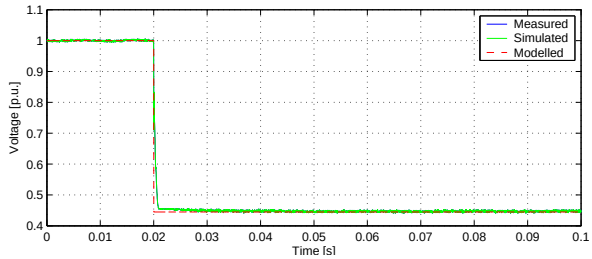

(g) Voltage - Step 4.

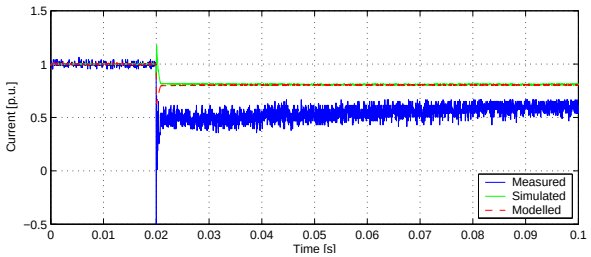

(h) Current - Step 4.

Figure 5.34: Transient behavior of electronic transformer (Tridonic).

5.3.2 Electronic Devices for General Purposes

All the loads that fall into this category are constant power loads and are constructed as in Fig. 5.3 and the model was realized as in Fig. 5.20. The parameters for the RLC circuit is tabulated in Table 5.26.

This construction is tested in EMTDC, and the results are shown in Figs. 5.35 to 5.45 where the measurement is shown (denoted as "measured") as well as the simulation results, both when the model is subjected to a simulated step (denoted as "modelled") and to a measured step (denoted as "simulated").

The loads with bigger L showed some oscillation when the load began to draw current from the grid and the simulation give the same amplitude but are more damped. As said before not all the loads where subjected to all steps because they shut down and restarted and then they need more power to start all the systems, for instance the computers.

Computer Power Supplies

	R [Ω]	L [mH]	C [µF]
Chieftech	7	25	350
Dell	10	1	230
Macintosh	10	0.1	200
Sirtech	10	25	350

Other Devices

	R [Ω]	L [mH]	C [µF]
Charger[1]	100	2	10
Charger[2]	100	2	10
Charger[3]	100	2	12
IP Telephone (Grandstream)	150	1	11
LCD Monitor (AOC)	100	1	70
Monitor (NCD)	1	0.2	300
Satellite Receiver (Triasat)	50	2	50

Table 5.26: Parameters R, L and C for model in Fig. 5.20.

The computers showed all a similar behavior. When the current comes back after the step, some show an oscillation and some do not. The Chieftech power supply only worked for one step. As can be seen from Fig. 5.35, the model agrees with the measurements. There is a switching transient in the current at the beginning of the step which is 2.2 p.u. This transient could be a result from a snubber on the input of the power supply or some other internal switching. This is not modelled.

The Dell power supply only worked for two steps. As can be seen from Fig. 5.36 the model agrees with the measurements. There are switching transients in the current at the beginning of the steps which are 2.4 p.u. for step one and 8.6 p.u. for step two.

Fig. 5.37 shows the results for the Macintosh PC. The load worked for three steps, and the model agrees with the measurements. There are switching transients in the current at the beginning of the steps which are 2.3 p.u. for step one, 7.1 p.u. for step two and 11.5 p.u. for step three.

[1]Ericsson, Model No. 4020036 BV, 1
[2]Ericsson, Model No. 4020036 BV, 2
[3]Ericsson, Model No. 4020037 BV

The PC with Sirtech power supply in Fig. 5.38 worked only for one step. The model agrees with the measurements. There is a switching transient in the current at the beginning of the step which is 2.3 p.u.

Power Supply (Chieftech)

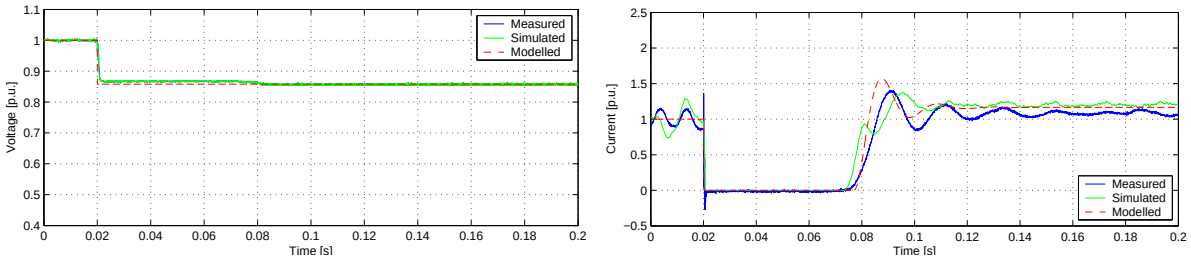

(a) Voltage - Step 1. (b) Current - Step 1.

Figure 5.35: Transient behavior of power supply (Chieftech).

Power Supply (Dell)

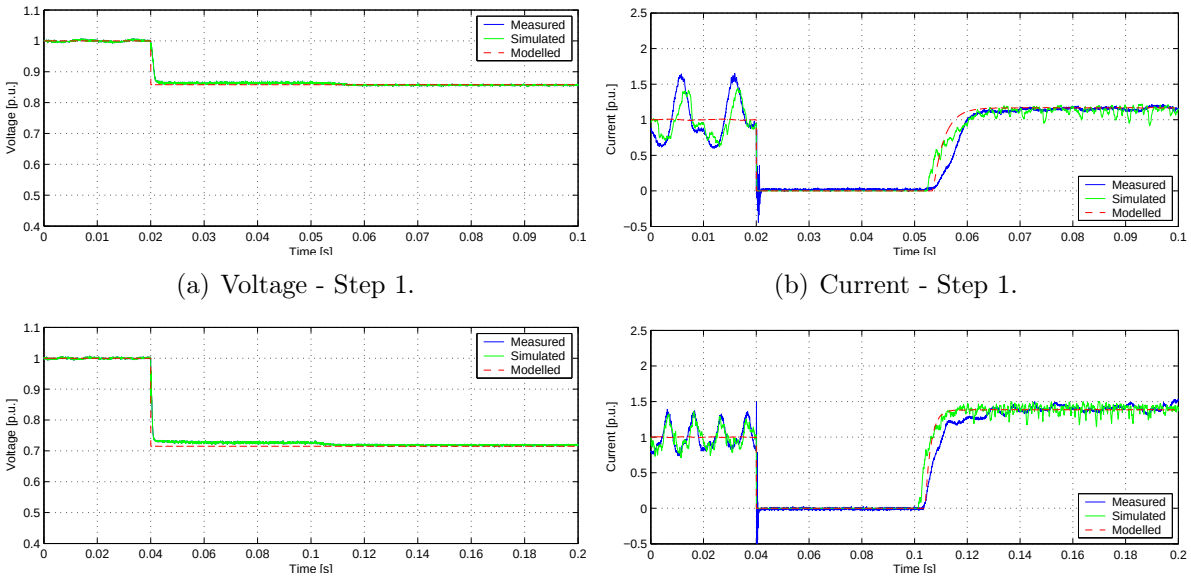

(a) Voltage - Step 1. (b) Current - Step 1.

(c) Voltage - Step 2. (d) Current - Step 2.

Figure 5.36: Transient behavior of power supply (Dell).

Power Supply (Macintosh)

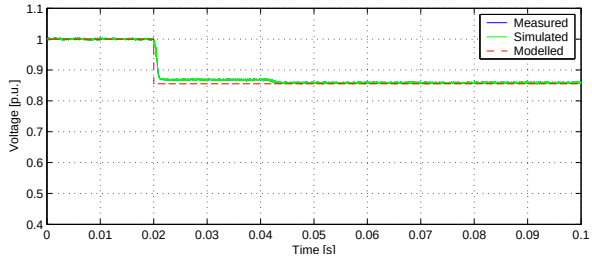

(a) Voltage - Step 1.

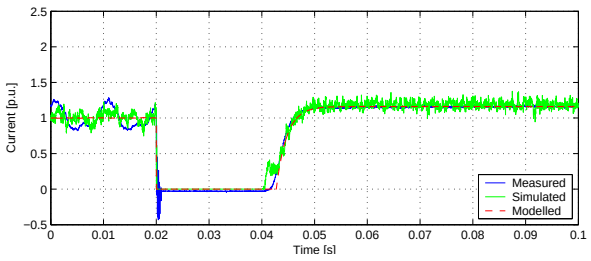

(b) Current - Step 1.

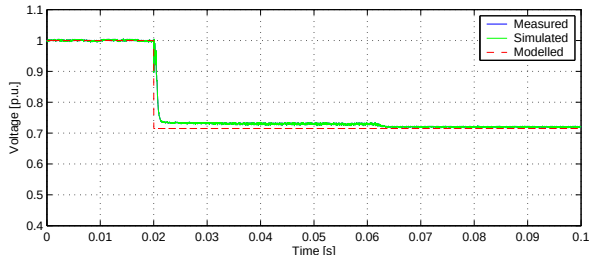

(c) Voltage - Step 2.

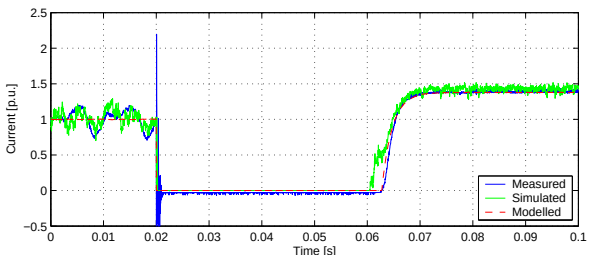

(d) Current - Step 2.

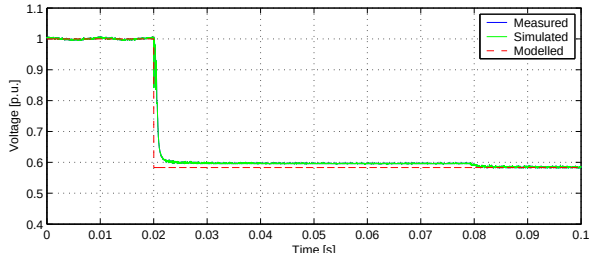

(e) Voltage - Step 3.

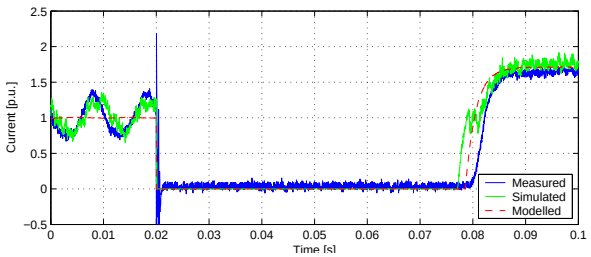

(f) Current - Step 3.

Figure 5.37: Transient behavior of power supply (Macintosh).

Power Supply (Sirtech)

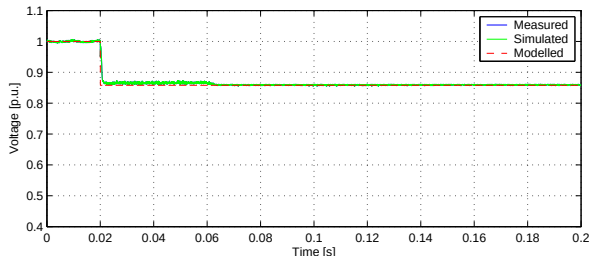

(a) Voltage - Step 1.

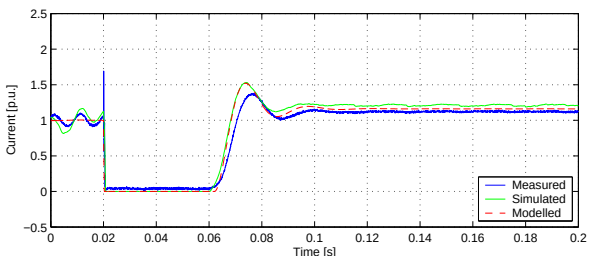

(b) Current - Step 1.

Figure 5.38: Transient behavior of power supply (Sirtech).

The other electronic devices also showed a similar behavior in general. The Ericsson chargers showed all the same behavior. They worked for all steps. As can be seen from Figs. 5.39 to 5.41, the model agrees with the measurements. In the last step for chargers 1 and 3 the load seems to be drawing less current than predicted, which might be due to measurement error, or the model acquired from the load characterization is not valid at this low voltage. It is also strange that there seems to be a switching transient for step one and two, and in some cases step three, but not three and four. This transient is neglected in the model.

Fig. 5.42 shows the measurement and model result for the IP telephone. The load only worked for all step. The model agrees with the measurements in average. However, this load was drawing next to no current when it was tested, so errors from the measurements will make up for errors in the model. The same strange transients can be seen in the beginning of the steps, as for the chargers above.

The LCD monitor worked for three steps, and it should actually work for the fourth step but since it was brand new that particular step was skipped, because of the load characteristics would make the load draw even higher current then in the previous steps. As can be seen from Fig. 5.43, the model agrees with the measurements in average. As for the other loads it has high transient in the beginning of the load that could be a result from a snubber. For step 1 the magnitude of the transient is 3.0 p.u. for step two it is 9.4 p.u. and for the third step it is 15.9 p.u.

The monitor only worked for three steps. As can be seen from Fig. 5.44, the model agrees with the measurements in average. In step one and step two the model follows the measurements very well. This is not the case for step 3, there the simulated step does not give the same high oscillating current as the measurement shows. But when the model is fed with the measured voltage the current shape (simulated) follow the measurement perfectly which confirms the validity of the model. There are some switching transients in the current at the beginning of the step. For step one it was not captured (it was too fast). For step two it was 6.0 p.u. and the same for step 3.

The satellite receiver only worked for two steps. As can be seen from Fig. 5.45 the model agrees with the measurements. There are switching transients in the current at the beginning of the steps. The peak value of these transient are 1.3 p.u. for step one and 5.6 p.u. for step two.

Charger (Ericsson, Model No. 4020036 BV, 1)

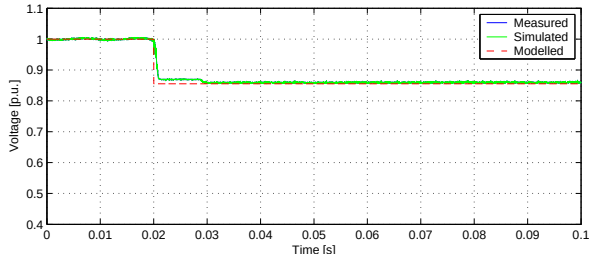

(a) Voltage - Step 1.

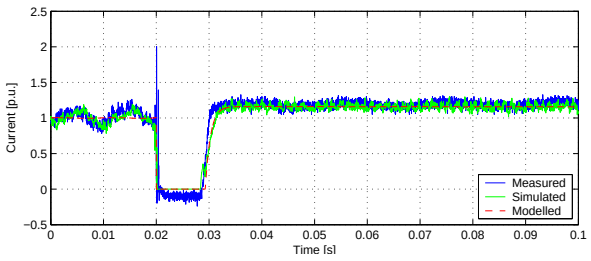

(b) Current - Step 1.

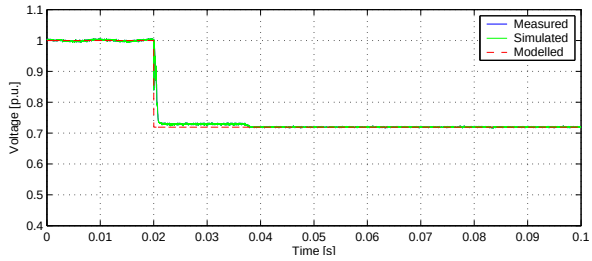

(c) Voltage - Step 2.

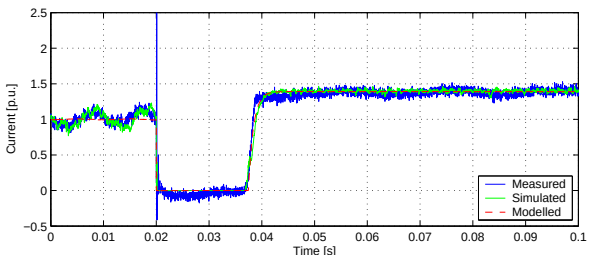

(d) Current - Step 2.

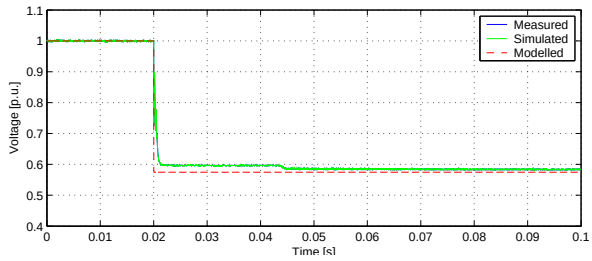

(e) Voltage - Step 3.

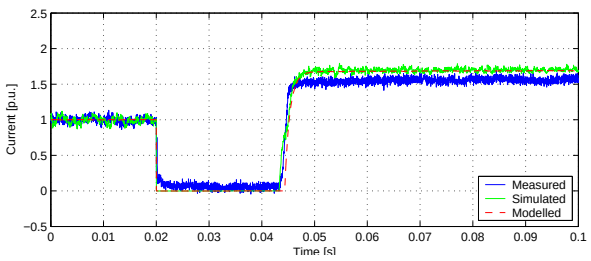

(f) Current - Step 3.

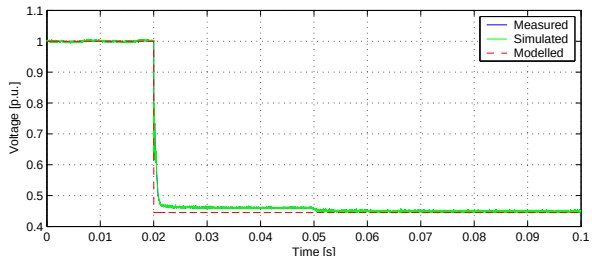

(g) Voltage - Step 4.

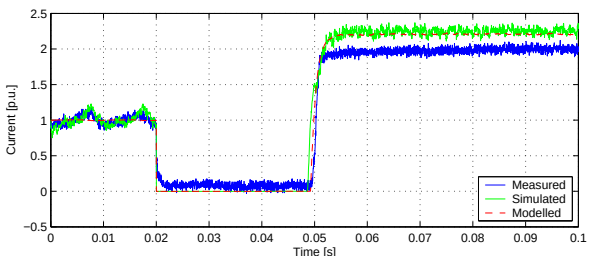

(h) Current - Step 4.

Figure 5.39: Transient behavior of charger (Ericsson, Model No. 4020036 BV, 1).

Charger (Ericsson, Model No. 4020036 BV, 2)

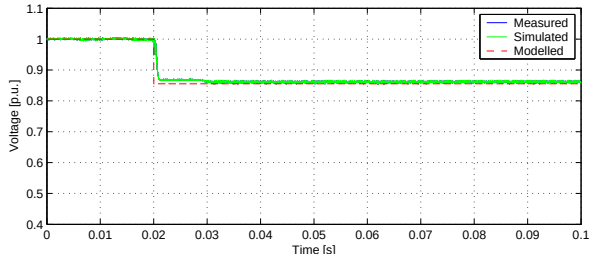

(a) Voltage - Step 1.

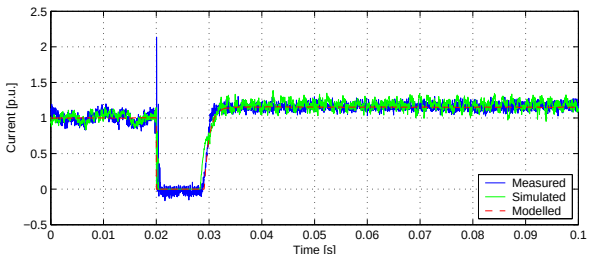

(b) Current - Step 1.

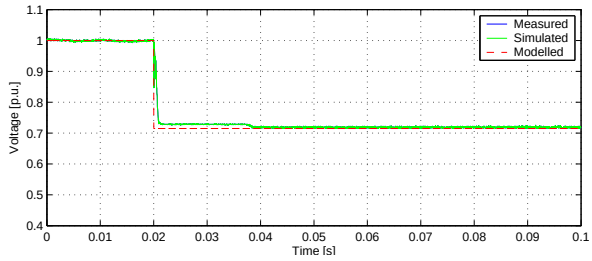

(c) Voltage - Step 2.

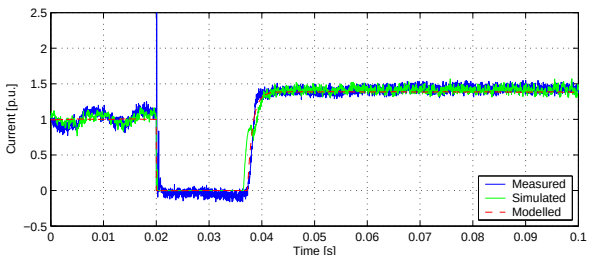

(d) Current - Step 2.

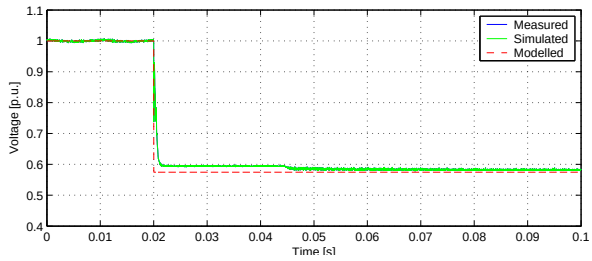

(e) Voltage - Step 3.

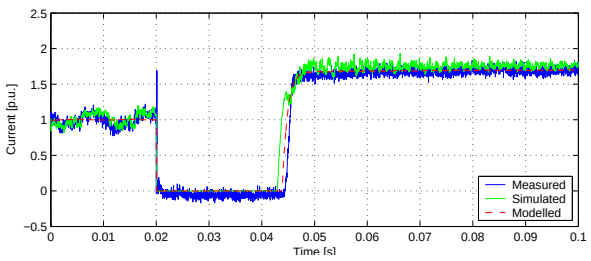

(f) Current - Step 3.

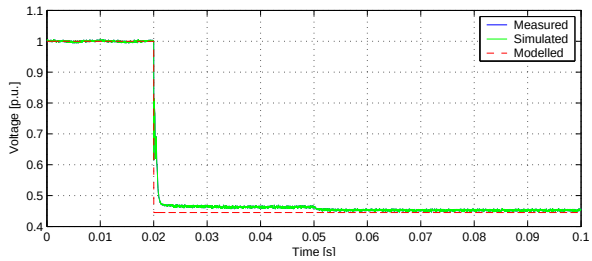

(g) Voltage - Step 4.

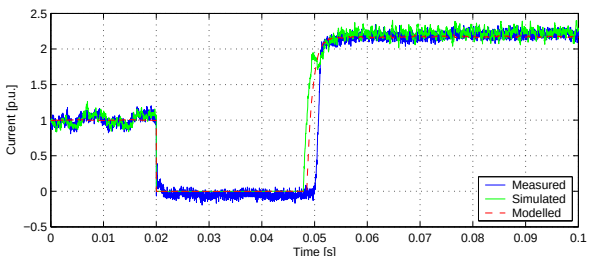

(h) Current - Step 4.

Figure 5.40: Transient behavior of charger (Ericsson, Model No. 4020036 BV, 2).

Charger (Ericsson, Model No. 4020037 BV)

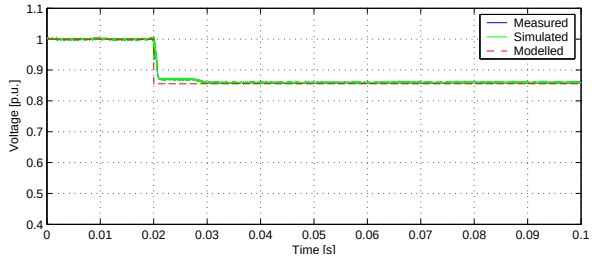

(a) Voltage - Step 1.

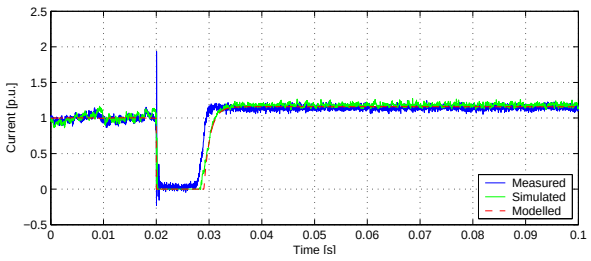

(b) Current - Step 1.

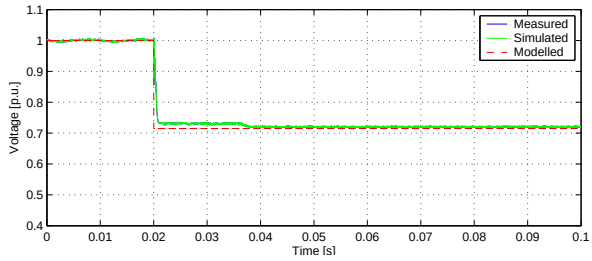

(c) Voltage - Step 2.

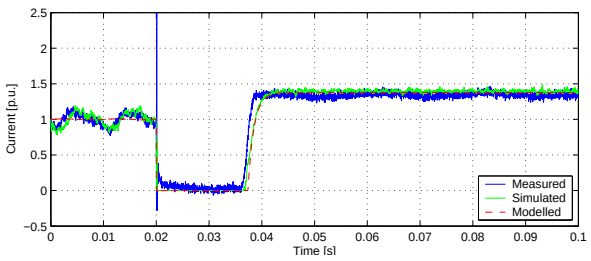

(d) Current - Step 2.

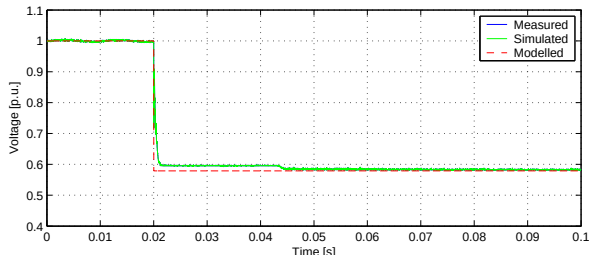

(e) Voltage - Step 3.

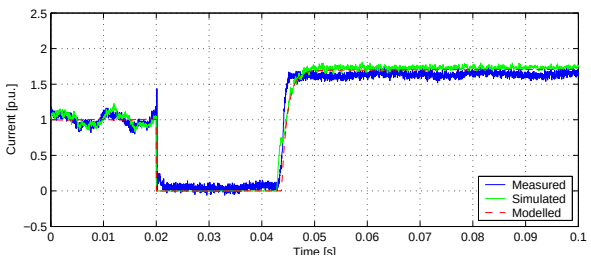

(f) Current - Step 3.

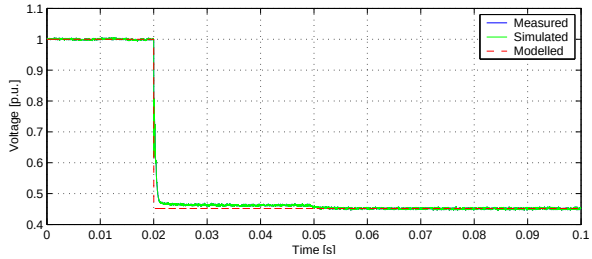

(g) Voltage - Step 4.

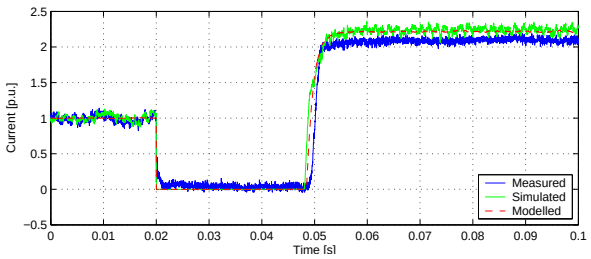

(h) Current - Step 4.

Figure 5.41: Transient behavior of charger (Ericsson, Model No. 4020037 BV).

IP Telephone (Grandstream)

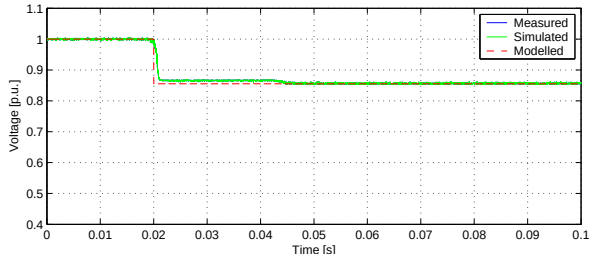

(a) Voltage - Step 1.

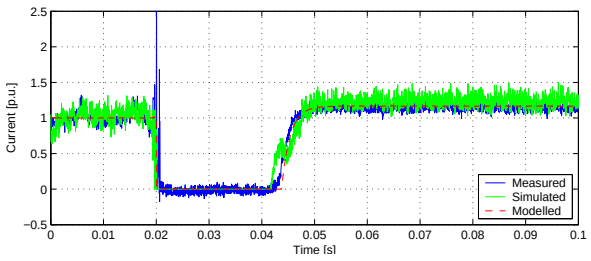

(b) Current - Step 1.

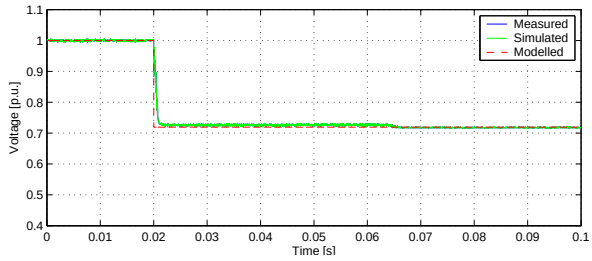

(c) Voltage - Step 2.

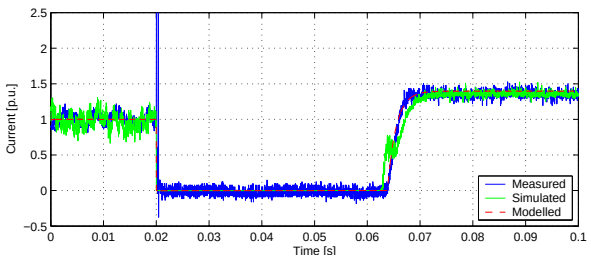

(d) Current - Step 2.

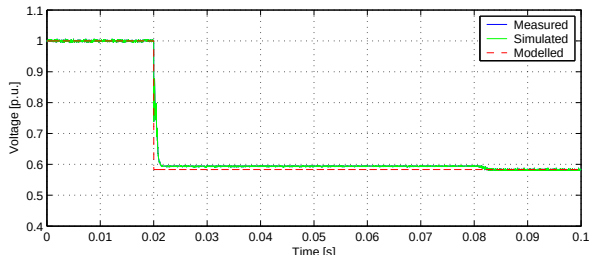

(e) Voltage - Step 3.

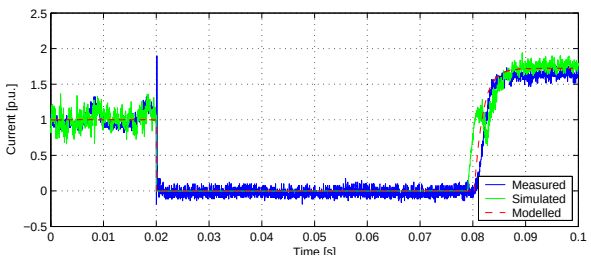

(f) Current - Step 3.

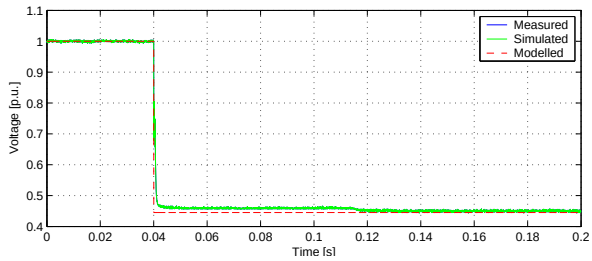

(g) Voltage - Step 4.

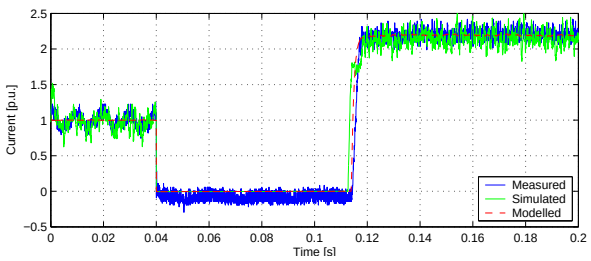

(h) Current - Step 4.

Figure 5.42: Transient behavior of IP telephone (Grandstream).

LCD Monitor (AOC)

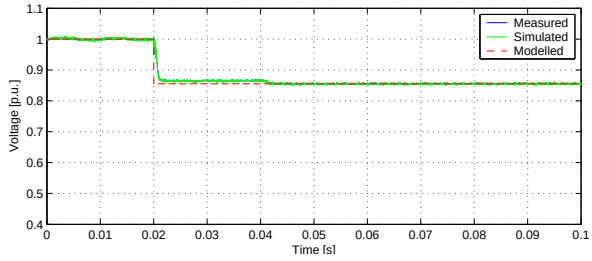

(a) Voltage - Step 1.

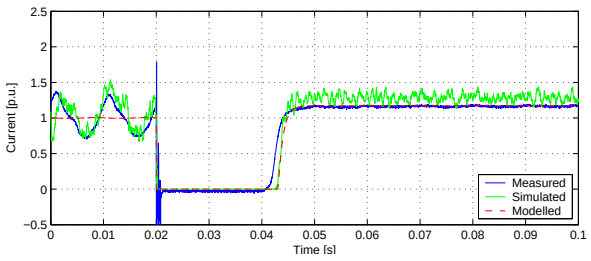

(b) Current - Step 1.

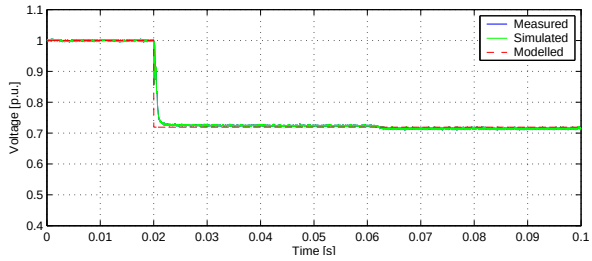

(c) Voltage - Step 2.

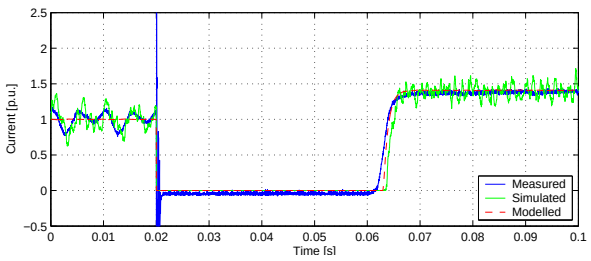

(d) Current - Step 2.

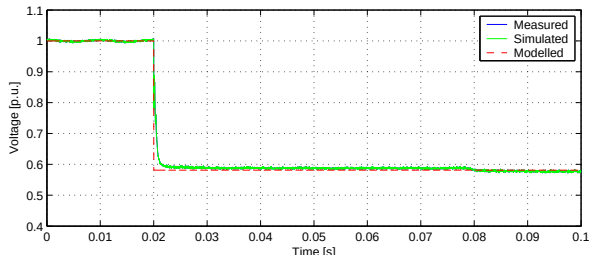

(e) Voltage - Step 3.

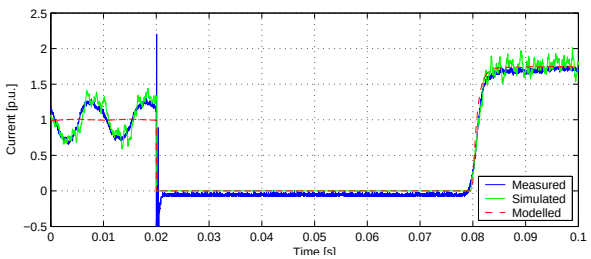

(f) Current - Step 3.

Figure 5.43: Transient behavior of LCD monitor (AOC).

Monitor (NCD)

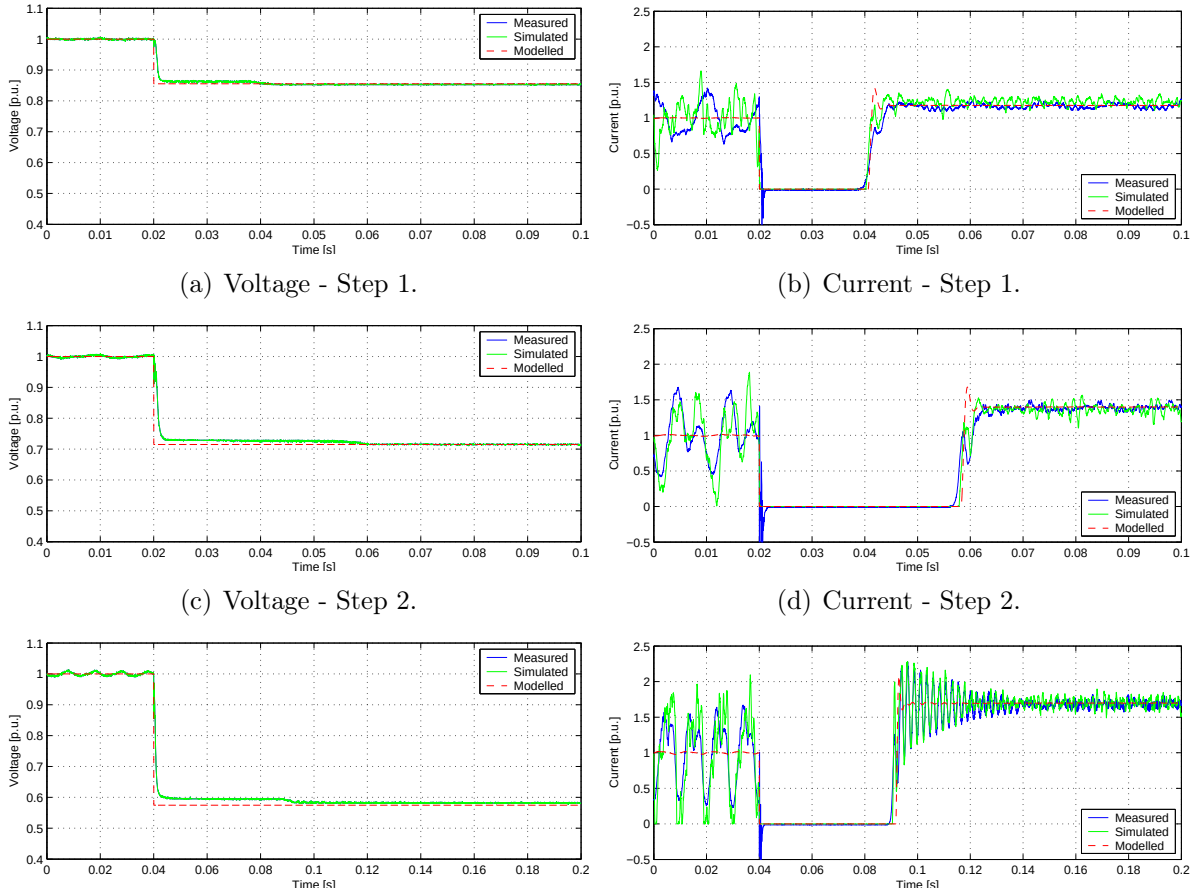

(a) Voltage - Step 1.

(b) Current - Step 1.

(c) Voltage - Step 2.

(d) Current - Step 2.

(e) Voltage - Step 3.

(f) Current - Step 3.

Figure 5.44: Transient behavior of monitor (NCD).

Satellite receiver (Triasat)

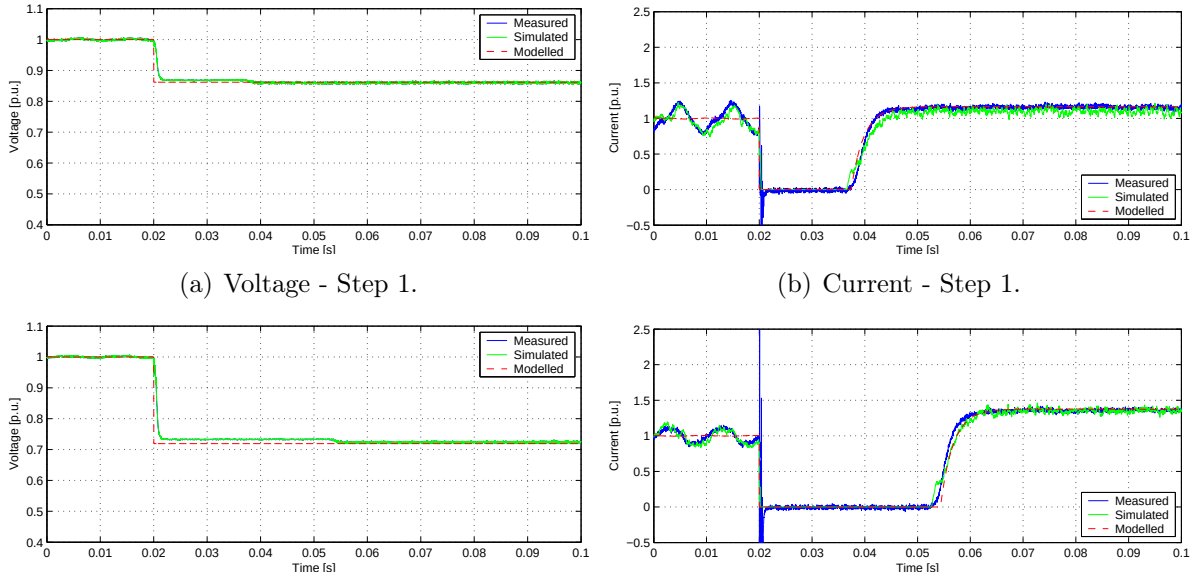

(a) Voltage - Step 1.

(b) Current - Step 1.

(c) Voltage - Step 2.

(d) Current - Step 2.

Figure 5.45: Transient behavior of the satellite receiver (Triasat).

5.4 Summary

The electronic loads were divided into two groups: loads used for lighting and loads used for general purposes. A general model that could describe the behavior of the loads was constructed and built in EMTDC. The construction of the load is shown in Fig. 5.20. It consists of two diodes in parallel to a RLC circuit that is in parallel to the load model obtained from the characterization.

The load is said to be constant current, constant resistance or constant power depending on how the voltage varied with current, or power varied with the voltage obtained from load characterization. One load could not be characterized: this is the low voltage halogen lamp transformer from Tridonic, see Section 5.1. The results of the characterization model can be seen in Tables 5.27 and 5.28.

From Table 5.27 it is clear that compact fluorescent lamps show a constant current behavior and fluorescent lamps are constant current or constant power, depending on the load that is used. For the transformers for low voltage halogen lamp, one showed a resistive behavior as discussed in Chapter 3 and the other did not show any relation two constant power, current or resistance, which is probably due to internal controllers in the device.

Table 5.28 show that electronic loads used for general purposes show a constant power relation, in some cases it was hard to characterize the load due to that it had many operating levels, for instance computers.

In steady-state the loads did not cause any distortion. The constant power loads showed a 100 Hz distortion in the current, but the same frequency component could be found in the voltage source used and is then mirrored in the current. If the source would be totally free of this 100 Hz component then the current would be as well.

Compact Fluorescent Lamps

	P_{rated} [W]	Range [V]	Model [R =]	Error [%]	Parameters
Eurolight	9	100-300	$U/0.029$	7.5	$R = 200\ \Omega$ $L = 0$ mH $C = 3.5$ µF
Ikea	11	190-380	$U/0.038$	2.1	$R = 300\ \Omega$ $L = 0$ mH $C = 2.7$ µF
Osram	23	120-300	$U/0.067$	10	$R = 300\ \Omega$ $L = 0$ mH $C = 4.7$ µF
Philips (9 W)	9	120-300	$U/0.035$	1.2	$R = 100\ \Omega$ $L = 0$ mH $C = 3.3$ µF
Philips (11 W)	11	120-300	$U/0.041$	4.3	$R = 100\ \Omega$ $L = 0$ mH $C = 3.3$ µF
Philips (15W, 1 and 2)	15	140-280	$U/0.057$	15	$R = 100\ \Omega$ $L = 0$ mH $C = 12$ µF
Sylvania	10	100-300	$U/0.046$	1.1	$R = 200\ \Omega$ $L = 0$ mH $C = 4.7$ µF

Ballasts for Fluorescent Lamps

	P_{rated} [W]	Range [V]	Model [R =]	Error [%]	Parameters
Philips	72	150-220 220-280	$U/0.325$ $U^2/70.5$	1.2 6.8	$\tau = 0.15$ s $R = 100\ \Omega$ $C = 0.5$ µF
Tridonic	72	130-340	$U^2/75$	0.7	$\xi = 0.08$ $\alpha = 183.2$
Tridonic (Dimmable)	70.4	110-380	$U^2/58.1$	0.9	$\xi = 0.1$ $\alpha = 132.5$

Electronic Transformers for Low Voltage Halogen Lamps

	P_{rated} [W]	Range [V]	Model [R =]	Error [%]	Parameters
Co-Tech	60	150-300	$2626 * I + 257.2$	0.9	$\tau = 0.01$ s
Tridonic	60	100-190 190-380	$U/(9.46 * 10^{-4} * U + 0.087)$ $U^2/51.3$	0.7 20	- -

Table 5.27: Model parameters for electronic loads used for lighting.

When the loads were subjected to sudden voltage steps, most of them showed a behavior that can be explained by the general model described in Section 5.3. The capacitor C in the circuit was chosen in the size so when the step was made the diodes block the current as the voltage over the capacitor is higher than the voltage at the terminals of the load. When the diodes start to conduct again the current might oscillate. That oscillation can be tuned with an inductor L in the circuit, and the damping with R. The parameters for R, L and C are then tabulated in Table 5.27 and 5.28.

For the Tridonic ballasts this was not possible. These ballasts were considered as a second order system and the current was said to step according to Eq. (5.7), where $\omega_n = \alpha u_{step,pu}$ and ξ is constant. The value of ξ and α are tabulated in Table 5.27.

For electronic loads used for lighting the rated power is given, but it is not necessarily the power used in nominal conditions when supplied with dc, as can be seen from Table 5.27. The rated power of electronic loads for general purposes was never given, except for the LCD. Instead the maximum power or current is given that the load can handle and has usually nothing to do with the nominal power consumption.

Computer Power Supplies

	P_{rated} [W]	Range [V]	Model [R =]	Error [%]	Parameters
Chieftech	350	200-380	$U^2/40$	20	$R = 7\ \Omega$ $L = 25$ mH $C = 350$ µF
Dell	?	170-380	$U^2/43.5$	1.5	$R = 10\ \Omega$ $L = 1$ mH $C = 230$ µF
Macintosh	87	150-380	$U^2/43.5$	4	$R = 10\ \Omega$ $L = 0.1$ mH $C = 230$ µF
Sirtech	235	180-380	$U^2/37.9$	20	$R = 10\ \Omega$ $L = 25$ mH $C = 350$ µF

Other Devices

	P_{rated} [W]	Range [V]	Model [R =]	Error [%]	Parameters
Charger[2]	unknown	100-300	$U^2/6.7$	8.0	$R = 100\ \Omega$ $L = 2$ mH $C = 10$ µF
Charger[3]	unknown	100-300	$U^2/6.9$	4.3	$R = 100\ \Omega$ $L = 2$ mH $C = 10$ µF
Charger[4]	unknown	100-300	$U^2/8.05$	2.0	$R = 100\ \Omega$ $L = 2$ mH $C = 10$ µF
IP Telephone (Grandstream)	unknown	100-380	$U^2/2.76$	24	$R = 150\ \Omega$ $L = 1$ mH $C = 11$ µF
LCD Monitor (AOC)	32	130-330	$U^2/30$	1.2	$R = 100\ \Omega$ $L = 1$ mH $C = 70$ µF
Monitor (NCD)	unknown	200-350	$U^2/84$	3.8	$R = 1\ \Omega$ $L = 0.2$ mH $C = 300$ µF
Satellite Receiver (Triasat)	unknown	200-350	$U^2/16.6$	4.8	$R = 50\ \Omega$ $L = 2$ mH $C = 50$ µF

Table 5.28: Model parameters for electronic loads for general purposes.

[2]Ericsson, Model No. 4020036 BV, 1
[3]Ericsson, Model No. 4020036 BV, 2
[4]Ericsson, Model No. 4020037 BV

Chapter 6

Sensitivity to Voltage Disturbances

This chapter will cover the issue of sensitivity to voltage disturbances of the loads tested in this thesis. The response of the loads to a voltage dip in ac and dc of the same magnitude and duration, was analyzed.

6.1 Measurement Setup

When a fault occurs at some point in the power system, the loads connected to the same bus, called point-of-common coupling (PCC), experience a drop in voltage until the fault is cleared. This phenomenon is called a voltage dip.

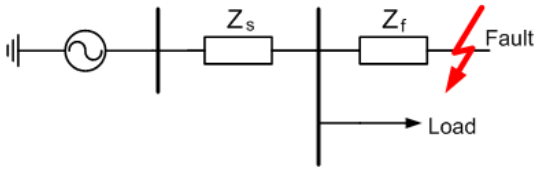

Figure 6.1: Simplified network model for voltage dip calculations.

The magnitude of the retained voltage depends on the impedance between the source and the PCC, as well as the fault impedance, see Fig 6.1, and is given by [25]

$$U_{PCC} = E\frac{Z_F}{Z_F + Z_S} \tag{6.1}$$

where E is the pre-fault voltage, Z_F the fault impedance and Z_S the source impedance.

If the ratio between resistance and reactance is different between the impedances Z_F and Z_S, the phase of the voltage at PCC will change at the instant of the fault, which is called phase-angle jump and calculated as [25]

$$\phi = arctan(\frac{X_F}{R_F}) - arctan(\frac{X_F + X_S}{R_F + R_S}) \tag{6.2}$$

In order to investigate the load behavior when a voltage dip occurs, the power system model at the Department of Electric Power Engineering at Chalmers University, shown in Appendix F, was utilized. The model consists of six sections with specified parameters, $X_s = 0.644\ \Omega$ and $R_s = 0.05\ \Omega$. This is a scaled model of an existing transmission line in Sweden.

The fault is generated by short circuiting the model at any of the six sections by closing a contactor connecting the model to ground through a short-circuit impedance of 2 Ω. In this thesis the fault location was at section 1. The model was also loaded with a 9 kW industrial fan in order to have the model loaded all the time, for safety reasons. The magnitude of the retained voltage as seen by the load was varied by connecting the loads to different sections of the model and thereby changing the impedance between the load and the PCC. The four last sections were used in order to match the magnitudes with that obtained from the voltage reduction circuit, see Appendix D. The magnitudes at the different points of connections are obtained using Eq. (6.1) and tabulated in Table 6.1 given in p.u. values together with the measured retained voltage at each section, with no load connected to that point.

Location	6	5	4	3
Calculated	0.874	0.753	0.643	0.548
Measured	0.862	0.728	0.580	0.450

Table 6.1: Magnitude of the retained voltage, in p.u., at different points of connection along the network model, when applying a fault in Section 1.

The small difference seen in the table is due to the algorithm calculating the RMS voltages. It always gives the minimum voltage that can be in the transient region of the dip, which is suggested in IEEE standard 1159-1995 [26].

The different point of connections will result in different phase-angle jumps at the corresponding connection points, obtained by Eq. (6.2) and listed in Table 6.2.

Location	6	5	4	3
Calculated	-4.2	-9.7	-17.3	-27.7

Table 6.2: Phase-angle jumps, in degrees, in different points of connection.

The duration of the voltage dip is controlled by a timer that keeps the switch closed for specified time. The control of the switch was done by a trigger device, which is shown in Fig. 6.2.

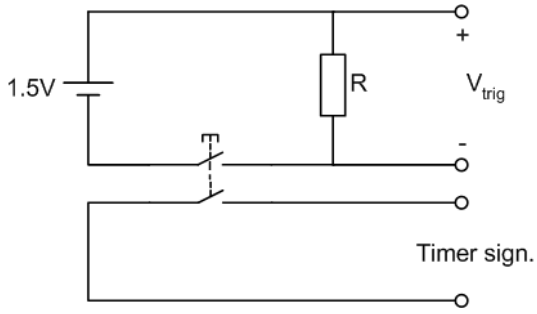

Figure 6.2: Device for controlling the short circuit switch and the triggering of the oscilloscope.

The device consists of a push-button, that closes the contactor, creating the short circuit in the network model and at the same time sending a trigger signal, formed by the voltage drop over the 10 kΩ resistor, to the oscilloscope. The triggering of the oscilloscope

is about 50 ms faster then the closing of the contactor due to long cables. The duration of the voltage dips was set to 300 ms in order to capture the load behavior when the voltage dip occurs. This duration varied with some milliseconds because of the mechanical structure of the contactor.

The network model was used to test the sensitivity of loads to voltage dips on ac. When measuring the sensitivity in dc, the voltage reduction circuit used for the transient measurements and explained in Appendix D, with small adjustments, was used. The manual switch reducing the voltage was replaced by the contactor of the network model, which was controlled by the same timer as for the ac tests. A voltage dip in dc is defined here as a step down in voltage, followed by a step up to the previous value after a certain duration, similarly to the plot of the RMS value of the ac voltage during the dip. The voltage reduction circuit was modified in order to make also a step up, not just a step down as for the transient measurements. The steps were done starting from 230 V dc and from 325 V dc. For the dc measurements with magnitudes of 325 V the voltage reduction circuit had to be reconfigured. The retained voltage level was chosen to be about 230 V for these tests, due to convenience of redesigning the voltage reduction circuit. One extra zener diode was needed. This zener diode was connected between the first and second diode after the fuse, see Fig. D.1 in Appendix D.

6.2 Results

As described earlier, a selection of loads were subjected to voltage dips of various magnitudes both in ac and dc, and their behavior was compared. The duration of the dip was kept at 300 ms, or there about, for all tests. The retained voltage of the steps made is listed in Table 6.3 with the corresponding section in the network model for the ac dip and the step made in dc, as described above. From the table it is clear that the steps made in ac match the steps in dc when the voltage was 230 V. The dip at location 5, step 2 for 230 V dc and the step made at 325 V dc are comparable.

230 V ac		230 V dc		325 V dc	
Location	V [pu]	Step	V [pu]	Step	V [pu]
6	0.862	1	0.862	1	0.710
5	0.728	2	0.721	-	-
4	0.580	3	0.574	-	-
3	0.450	4	0.435	-	-

Table 6.3: Voltage steps made for sensitivity analysis.

The loads that were tested are listed in Table 6.4 with the voltage level at which they shut down and what happened when the voltage returned back to the nominal level, referred to the location in ac and voltage step in dc. This is only for ac dips and dc dips form 230 V.

Table 6.4 shows that resistive loads and rotating loads are not very sensitive to voltage dips, which was expected and therefore only two loads from each group were tested. The electronic loads were a lot more sensitive. Almost all the compact fluorescent lamps shut down and restarted when the dip was severe enough and at the same level for ac and dc. In general, though, the lamps performed better under dc.

This is also the case for the ballast for fluorescent lamps. They performed better under dc than ac. This might be due to the fact that the ballasts tested are guaranteed to work

[1]Transformers for low voltage halogen lamps

Resistive Loads

Heaters	ac	Comments	dc	Comments
Kettle (Elram)	-	-	-	-
Kettle (Sollingmüller)	-	-	-	-
Lighting	**ac**	**Comments**	**dc**	**Comments**
Lamp (60W, 1)	-	-	-	-
Lamp (60W, 2)	-	-	-	-

Rotating Loads

Universal Motors	ac	Comments	dc	Comments
Vacuum (Electrolux)	-	-	-	-
Vacuum (LG)	-	-	-	-

Electronic Loads

Compact Fluorescent Lamps	ac	Comments	dc	Comments
Eurolight	-	-	-	-
Osram	Loc. 3	Restart	-	-
Philips (9W)	Loc. 3	Restart	Step 4	Restart
Philips (11W)	Loc. 3	Restart	Step 4	Restart
Philips (15W, 1)	Loc. 3	Restart	Step 4	Restart
Philips (15W, 2)	Loc. 3	Restart	Step 4	Restart
Sylvania	-	-	-	-
Ballasts for Fluorescent Lamps	**ac**	**Comments**	**dc**	**Comments**
Philips	Loc. 4	Shut off	Step 4	Restart
Tridonic	-	-	-	-
Dimmable Tridonic	Loc. 4	Restart	-	-
Electronic Transformers[1]	**ac**	**Comments**	**dc**	**Comments**
Co-tech	-	-	-	-
Tridonic	-	-	-	-
Computer Power Supplies	**ac**	**Comments**	**dc**	**Comments**
Chieftech	Loc. 4	Restart	Step. 2	Restart
Macintosh	-	-	-	-
Sirtech	Loc. 4	Restart	Step 2	Restart
Other Devices	**ac**	**Comments**	**dc**	**Comments**
IP Telephone (Grandstream)	-	-	-	-
Monitor (NCD)	-	-	-	-
Satellite Receiver (Triasat)	Loc. 3	Restart	Step 3	Restart

Table 6.4: Loads tested for sensitivity.

on dc as emergency lighting. The computers were more sensitive to voltage dips in dc than in ac. That is most likely because the computers are equipped with a full bridge rectifier and then the input voltage is 325 V dc when supplied with 230 V ac. This is also the case for the satellite receiver.

The light from all the lamps flickered when the dip was made, which shows that lamps are sensitive to voltage variations and are source of flicker, specially the compact fluorescent lamps. The Tridonic ballasts did not flicker that much. This is due to the fact that they are constant power loads, and then the light should not flicker. When the third and fourth step in dc and dips at location 4 and 3 in ac were made, for the Tridonic ballasts, the current and voltage had a high frequency oscillation when the voltage returned to the nominal value.

As stated earlier, a test was made, when the voltage was set to be 325 V dc, which matched a step made both in ac and dc, presented in Table 6.4. The results from that are presented in Figs. 6.3 to 6.23 where the ac RMS voltage and current are used as a base. The comparison of the nominal voltage for each measurement are presented in Table 6.5. There are small differences in voltage levels because in ac the loads were supplied with a real system and some voltage drops are then due to loading of the system. The voltage reduction circuit is not a realistic system and the voltage drop due to loading was eliminated by increasing the source voltage, up to 15 V.

[1]Transformers for low voltage halogen lamps

Resistive Loads

Heaters	230 V ac		230 V dc		325 V dc	
	Voltage [V]	Current [A]	Voltage [p.u.]	Current [p.u.]	Voltage [p.u.]	Current [p.u.]
Kettle (Elram)	219.25	8.25	1.05	1.05	1.46	1.37
Kettle (Sollingmüller)	219.29	8.37	1.05	1.05	1.45	1.43
Lighting	**230 V ac**		**230 V dc**		**325 V dc**	
	Voltage [V]	Current [A]	Voltage [p.u.]	Current [p.u.]	Voltage [p.u.]	Current [p.u.]
Lamp (60W, 1)	221.94	0.24	1.02	1.01	1.44	1.19
Lamp (60W, 2)	221.95	0.24	1.03	1.02	1.44	1.20

Rotating Loads

Universal Motors	230 V ac		230 V dc		325 V dc	
	Voltage [V]	Current [A]	Voltage [p.u.]	Current [p.u.]	Voltage [p.u.]	Current [p.u.]
Vacuum (Electrolux)	219.20	5.14	1.04	0.90	1.46	1.23
Vacuum (LG)	219.44	5.17	1.05	0.91	1.45	1.28

Electronic Loads

Compact Fluorescent Lamps	230 V ac		230 V dc		325 V dc	
	Voltage [V]	Current [A]	Voltage [p.u.]	Current [p.u.]	Voltage [p.u.]	Current [p.u.]
Eurolight	223.96	0.06	1.02	0.49	1.42	0.42
Osram	223.77	0.08	1.01	0.49	1.41	0.46
Philips (9W)	223.64	0.13	1.03	0.54	1.44	0.38
Philips (11W)	221.49	0.07	1.01	0.53	1.42	0.40
Philips (15W, 1)	223.81	0.08	1.03	0.43	1.43	0.32
Philips (15W, 2)	222.77	0.13	1.02	0.41	1.43	0.36
Sylvania	223.41	0.13	1.02	0.54	1.42	0.42
Ballasts for Fluorescent Lamps	**230 V ac**		**230 V dc**		**325 V dc**	
	Voltage [V]	Current [A]	Voltage [p.u.]	Current [p.u.]	Voltage [p.u.]	Current [p.u.]
Tridonic	223.82	0.35	1.02	0.97	1.42	0.77
Dimmable Tridonic	223.77	0.37	1.02	1.01	1.42	0.58
Electronic Transformers[1]	**230 V ac**		**230 V dc**		**325 V dc**	
	Voltage [V]	Current [A]	Voltage [p.u.]	Current [p.u.]	Voltage [p.u.]	Current [p.u.]
Co-Tech	223.20	0.24	1.02	1.03	1.42	1.43
Tridonic	223.47	0.27	1.02	0.84	1.42	0.81
Computer Power Supplies	**230 V ac**		**230 V dc**		**325 V dc**	
	Voltage [V]	Current [A]	Voltage [p.u.]	Current [p.u.]	Voltage [p.u.]	Current [p.u.]
Chieftech	223.24	0.27	1.03	0.63	1.42	0.45
Macintosh	223.38	0.35	1.03	0.55	1.43	0.39
Sirtech	223.04	0.24	1.02	0.77	1.42	0.52
Other Devices	**230 V ac**		**230 V dc**		**325 V dc**	
	Voltage [V]	Current [A]	Voltage [p.u.]	Current [p.u.]	Voltage [p.u.]	Current [p.u.]
IP Telephone (Grandstream)	224.07	0.03	1.03	0.43	1.42	0.46
Satellite Receiver (Triasat)	224.02	0.14	1.01	0.53	1.41	0.66

Table 6.5: Voltage and current drawn by the loads compared to ac base.

As can be seen from the figures and Table 6.4, the resistive loads are not sensitive to voltage dips. This is also the case for the rotating loads. But as the voltage returns the current steps up to a high level. As the dip is more severe the current steps up more, this high current might be high enough to trip protection devices in the system.

Table 6.5 shows that most of the loads are drawing more current when supplied with dc than with ac. This is due to many reasons. For incandescent lamps it is due to the fact that they are variable resistors as described in Chapter 3. For the rotating loads it is probably due to saturation.

It was stated earlier in Chapter 5 that compact fluorescent lamps are constant current loads. This is only true up to 300 V. That explains the difference in the current drawn at 230 V dc and 325 V dc which gives a hint of a constant power load, as for most other electronic loads. The resistive loads and rotating loads showed a behavior during the ac and dc dips, which could be readily explained on the basis of their transient models. The kettles behave as constant resistances, so the current follows the voltage in Figs. 6.3 and 6.4. The lamps in Figs. 6.5 and 6.6 show the characteristic exponential trend for the current and the same for the rotating loads in Figs. 6.8 and 6.7 due to the mechanical time constant.

At the beginning of the voltage dip, most of the electronic loads had a current spike. That might be due to some capacitive circuit at the input of the load. As the voltage returned, the spike was much higher and usually lasted for a longer time. For the computers this spike was 40 p.u. and higher than in ac. This current spike is due to the capacitor, which has discharged during the dip and now draws a high current, and is dependent on the difference of the voltage before and after the step. In ac, the voltage might return on the zero crossing that will then result in no current spike, or at the voltage peak, which

will then theoretically be as high as the current spike that can be seen when the load is supplied with dc.

It should be noted that the computers restarted when they were supplied with 230 V dc and a dip was made. But they continued operating when they were supplied with 325 V dc and the same drop in voltage was applied. This indicates that the computers are peak invariant, but most of the other loads tested in this thesis are RMS invariant.

Resistive Loads

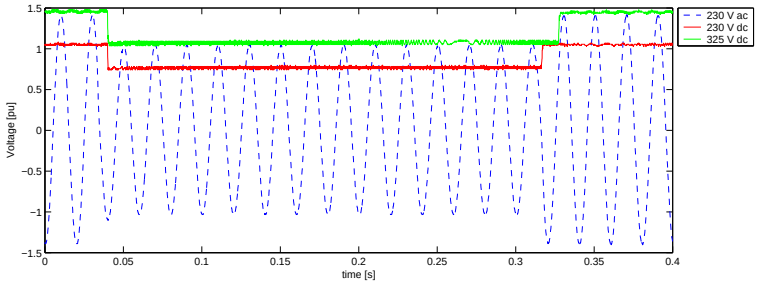

(a) Voltage

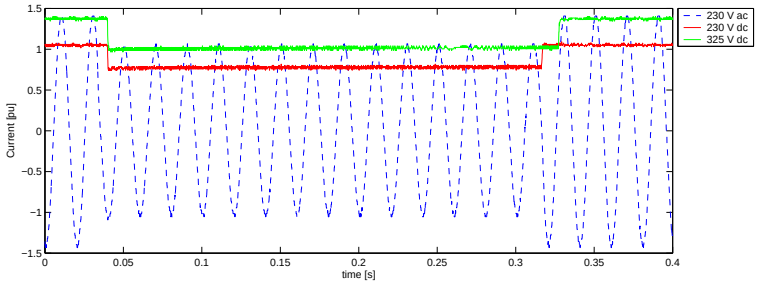

(b) Current

Figure 6.3: Dip response of kettle (Elram).

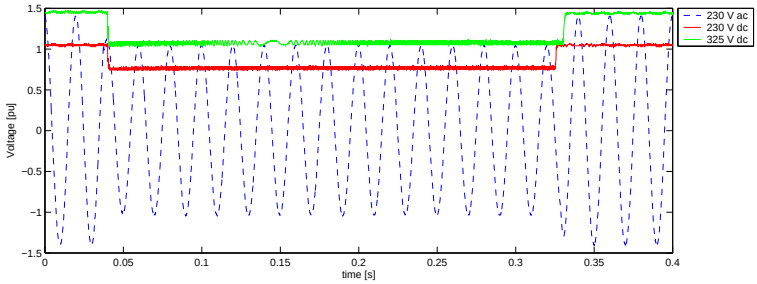

(a) Voltage

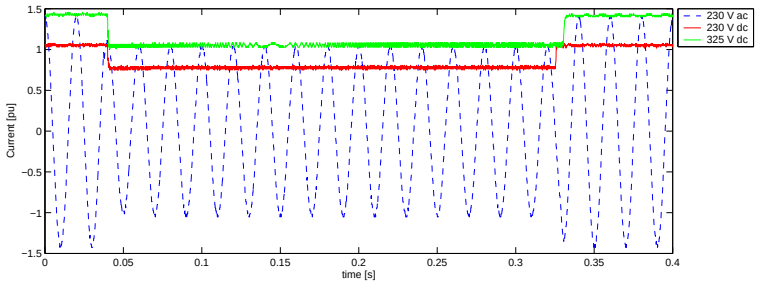

(b) Current

Figure 6.4: Dip response of kettle (Sollingmüller).

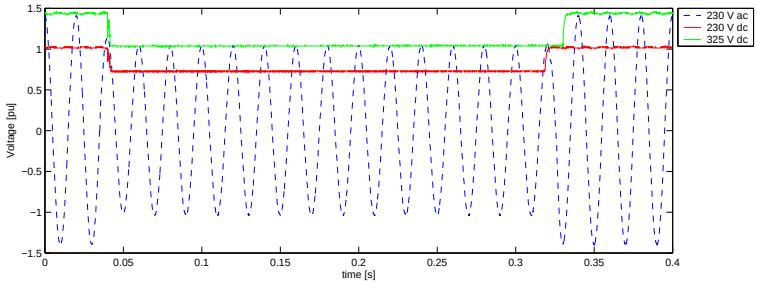

(a) Voltage

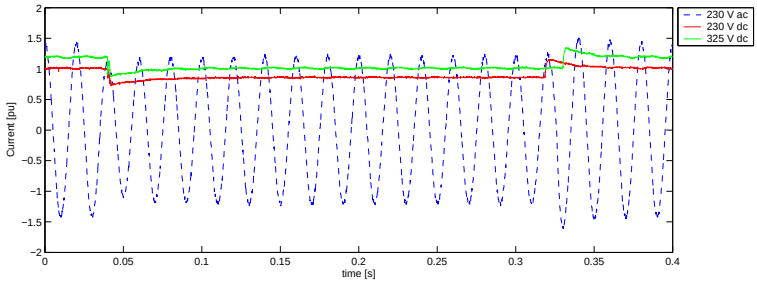

(b) Current

Figure 6.5: Dip response of incandescent lamp (60 W, 1).

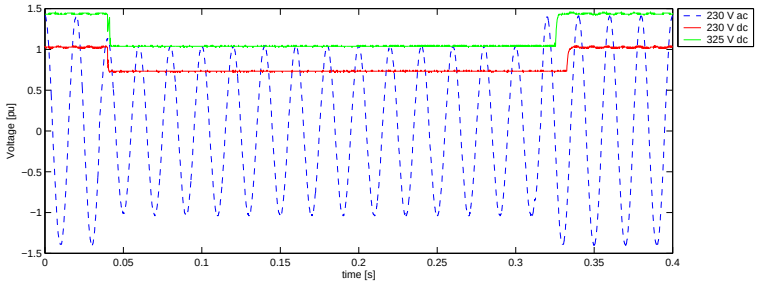

(a) Voltage

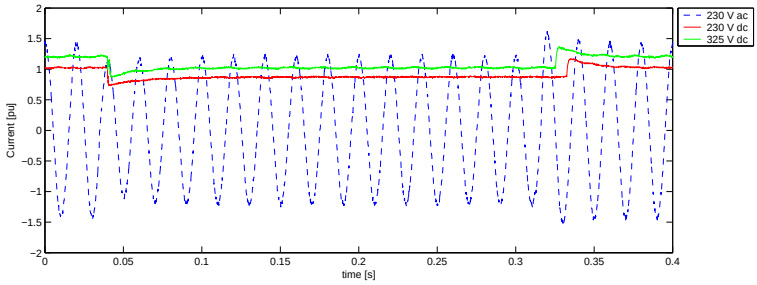

(b) Current

Figure 6.6: Dip response of incandescent lamp (60 W, 2).

Rotating Loads

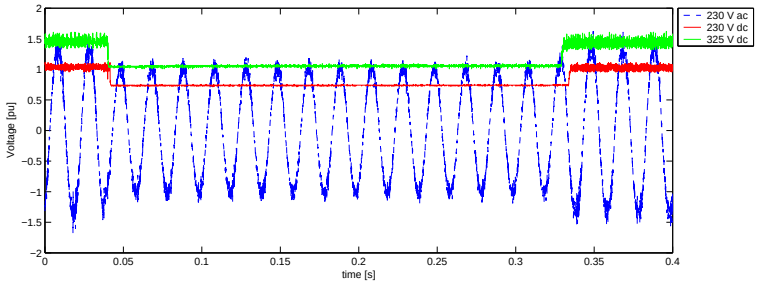

(a) Voltage

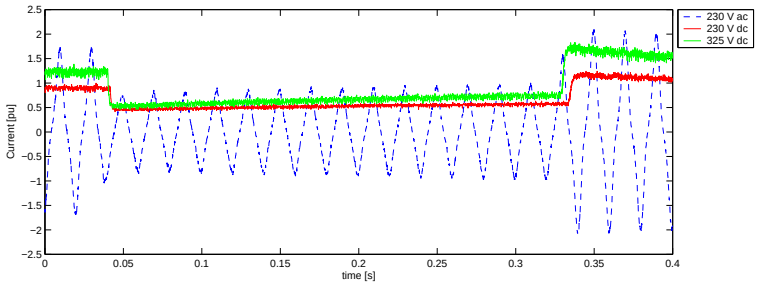

(b) Current

Figure 6.7: Dip response of vacuum cleaner (Electrolux).

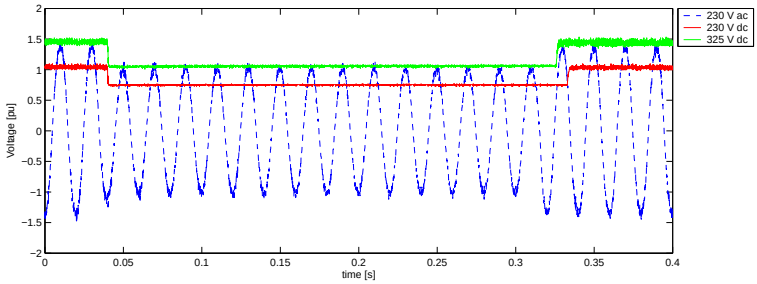

(a) Voltage

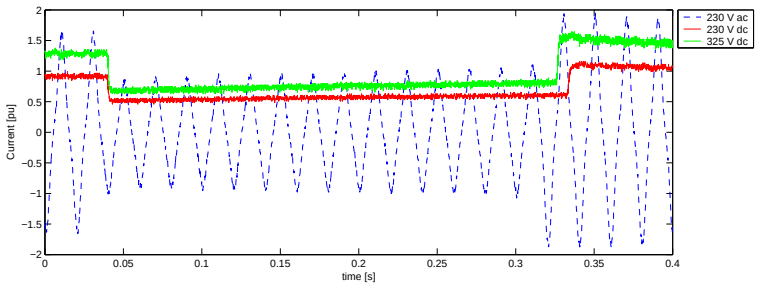

(b) Current

Figure 6.8: Dip response of a vacuum cleaner (LG).

Electronic Loads

Compact Fluorescent Lamps

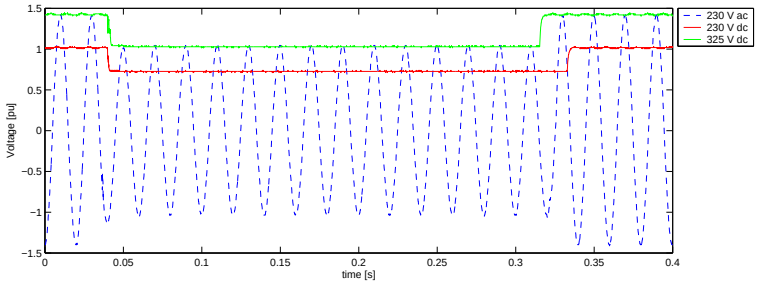

(a) Voltage

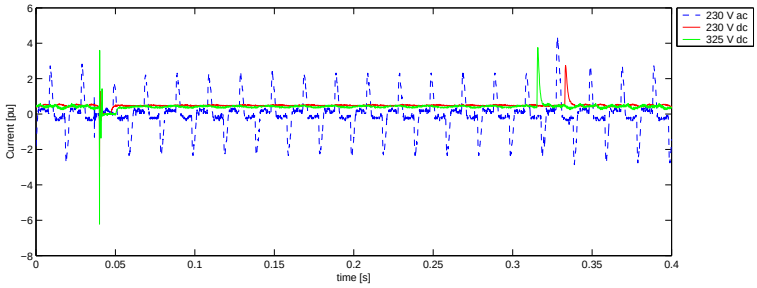

(b) Current

Figure 6.9: Dip response of compact fluorescent lamp (Eurolight).

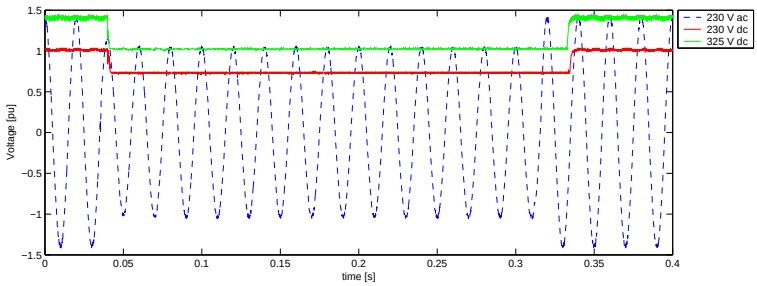

(a) Voltage

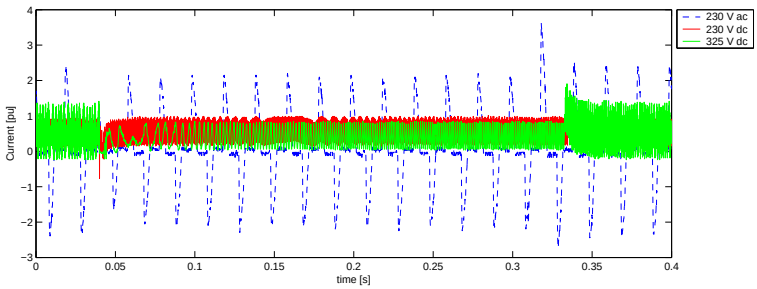

(b) Current

Figure 6.10: Dip response of compact fluorescent lamp (Osram).

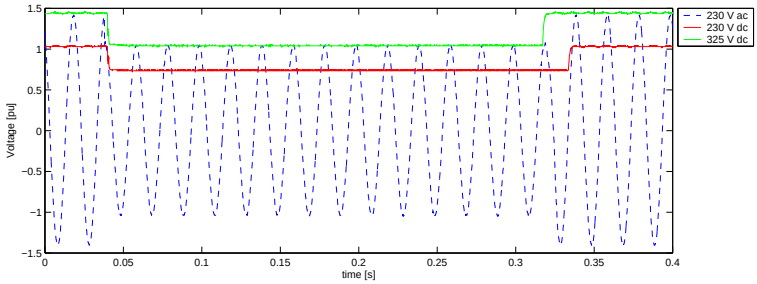

(a) Voltage

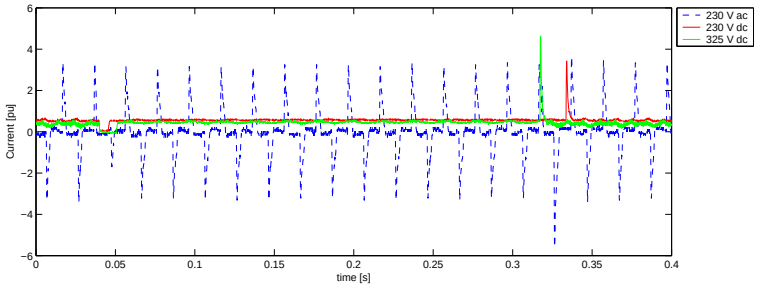

(b) Current

Figure 6.11: Dip response of compact fluorescent lamp (Philips 9W).

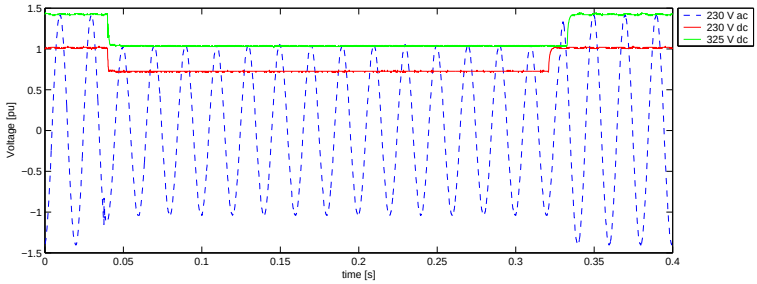

(a) Voltage

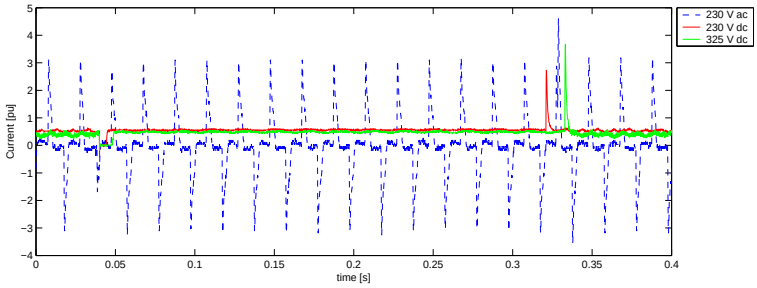

(b) Current

Figure 6.12: Dip response of compact fluorescent lamp (Philips 11W).

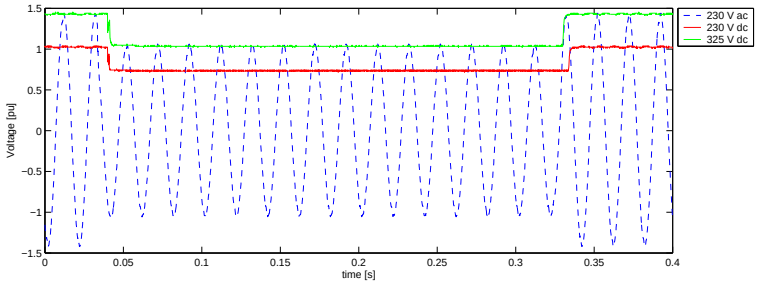

(a) Voltage

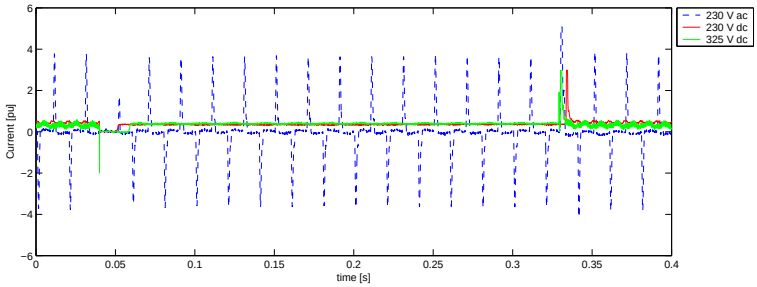

(b) Current

Figure 6.13: Dip response of compact fluorescent lamp (Philips 15W, 1).

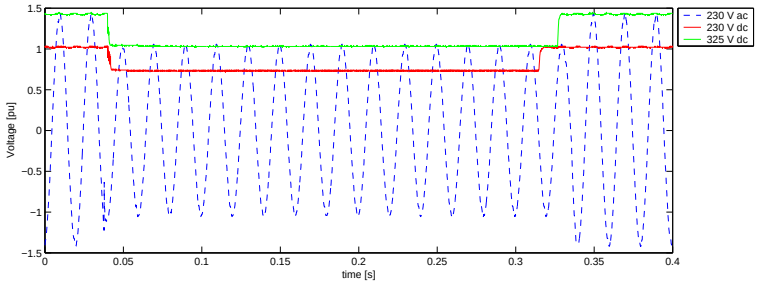

(a) Voltage

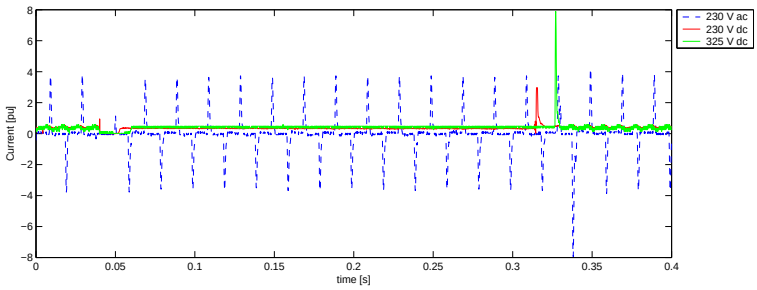

(b) Current

Figure 6.14: Dip response of compact fluorescent lamp (Philips 15W, 2).

Ballasts for Fluorescent Lamps

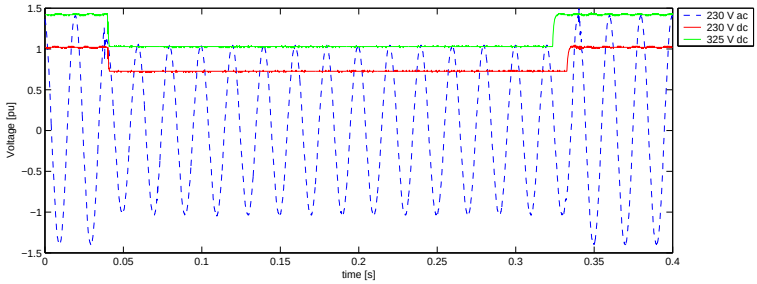

(a) Voltage

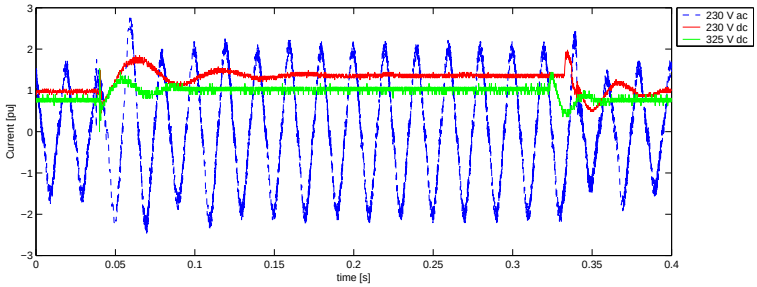

(b) Current

Figure 6.15: Dip response of ballast (Tridonic).

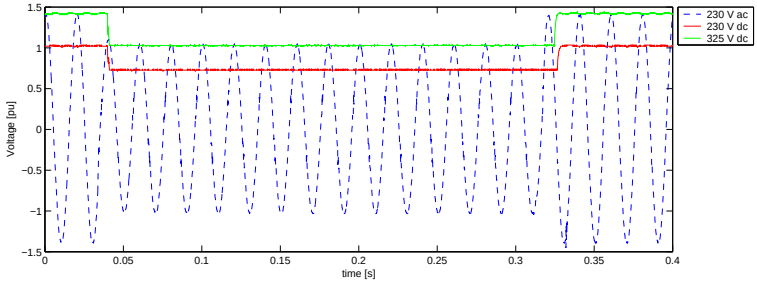

(a) Voltage

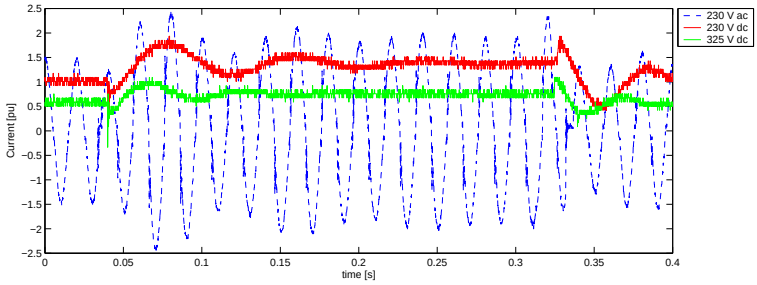

(b) Current

Figure 6.16: Dip response of dimmable ballast (Tridonic).

Electronic Transformers for Low Voltage Halogen Lamps

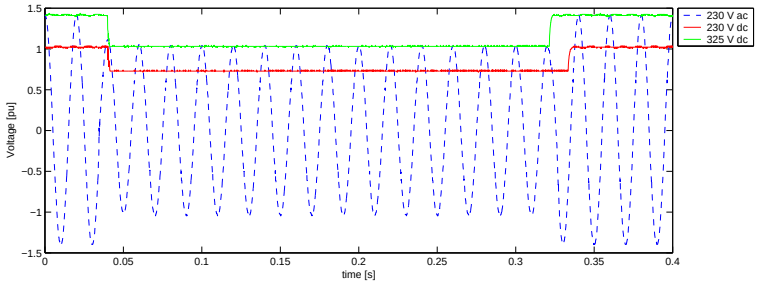

(a) Voltage

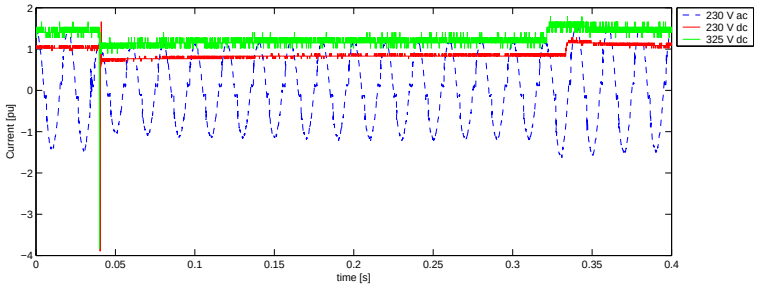

(b) Current

Figure 6.17: Dip response of electronic transformer (Co-Tech).

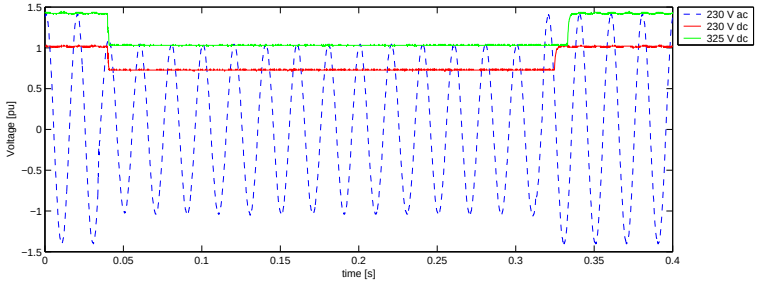

(a) Voltage

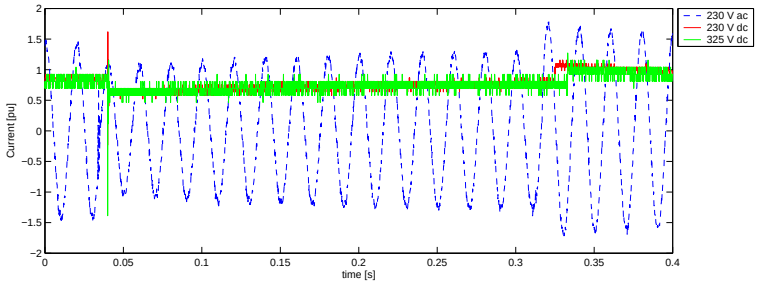

(b) Current

Figure 6.18: Dip response of electronic transformer (Tridonic).

Computers

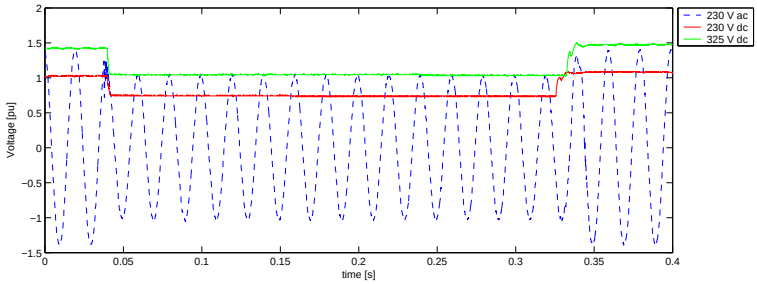

(a) Voltage

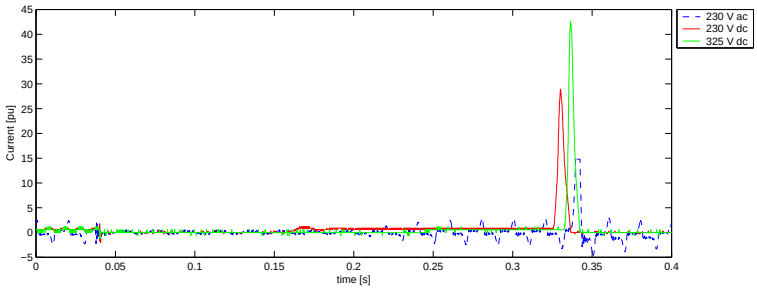

(b) Current

Figure 6.19: Dip response of power supply (Chieftech).

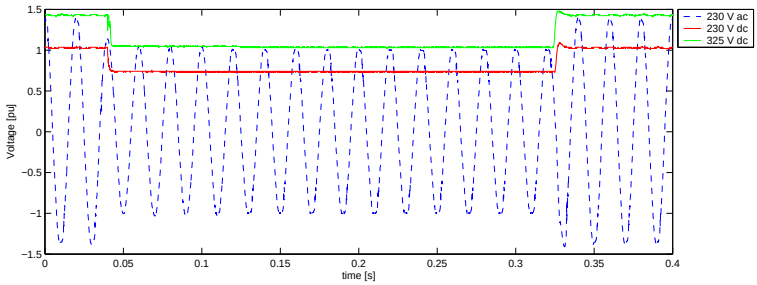

(a) Voltage

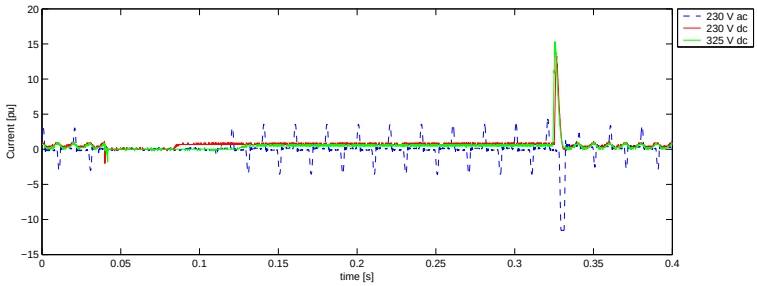

(b) Current

Figure 6.20: Dip response of power supply (Macintosh).

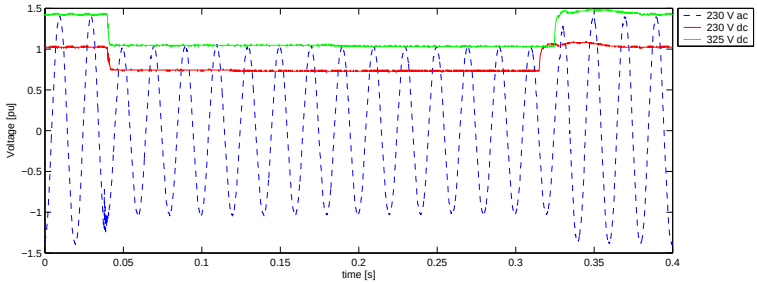

(a) Voltage

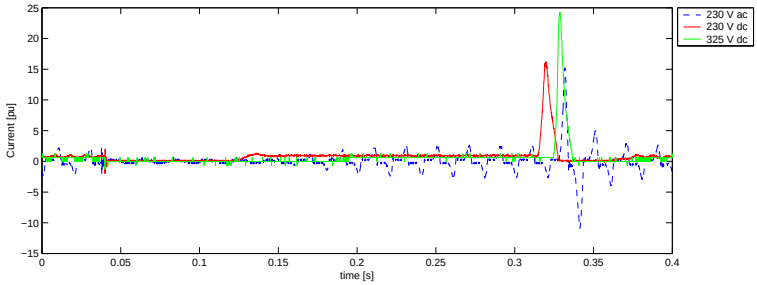

(b) Current

Figure 6.21: Dip response of power supply (Sirtech).

Other Devices

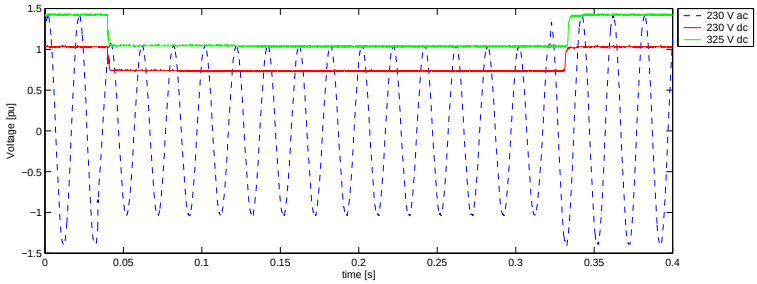

(a) Voltage

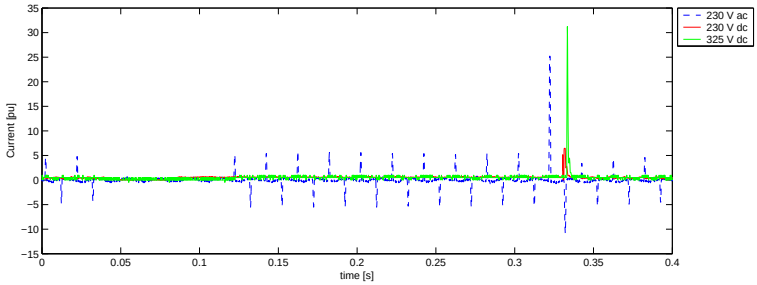

(b) Current

Figure 6.22: Dip response of IP telephone (Grandstream).

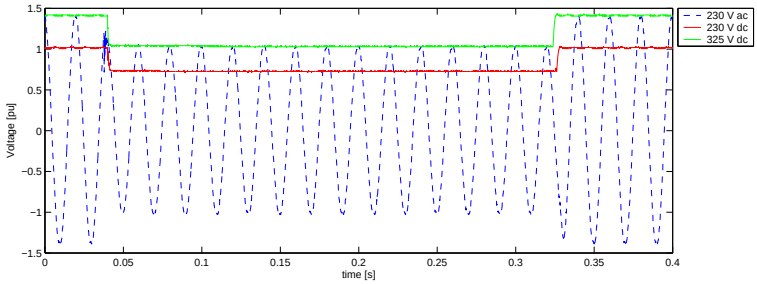

(a) Voltage

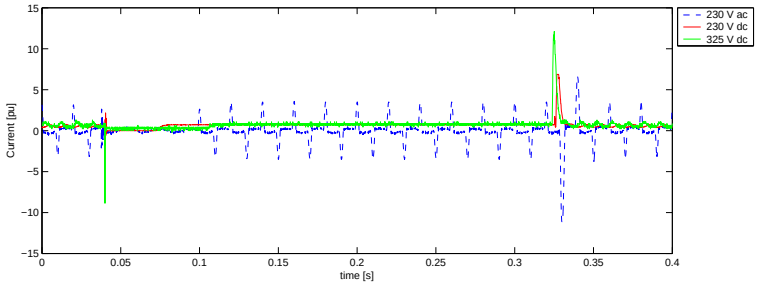

(b) Current

Figure 6.23: Dip response of satellite receiver (Triasat).

6.2.1 Simulations

For the computers and the constant power loads, a simulation in EMTDC of the dip done in the lab was made to test the response for the computers and other devices. These were those loads where the high current spike was recorded. This was done both when the load was fed with 230 V dc and 325 V dc. The response of the other loads to the dips could readily be explained based on the transient models developed, so only the loads showing the high current spikes were simulated.

The results from this can be seen in Figs. 6.24 to 6.33. The measurement is shown (indicated as "measured") as well as the simulation results, both when the model is subjected to a simulated step ("modelled") and a measured step ("simulated").

It is clear that the model that was derived in Chapter 5 is adequate for the current transient when the voltage returns. The magnitude is in general a little lower than measured, but that might be due to the sampling time of the data.

When the Chieftech power supply and Sirtech power supply were supplied with 230 V dc it was stated earlier that they restarted as the dip was made. That can be seen clearly by the post event voltage that is higher than the pre event voltage. This is due to the fact that the voltage reduction circuit has a rather high impedance compared to the load and shows that the device is quite sensitive to the dips made. This is not the case in the simulation where an ideal source is used. In general the voltage is a bit higher when the diodes are blocking the current.

Computers

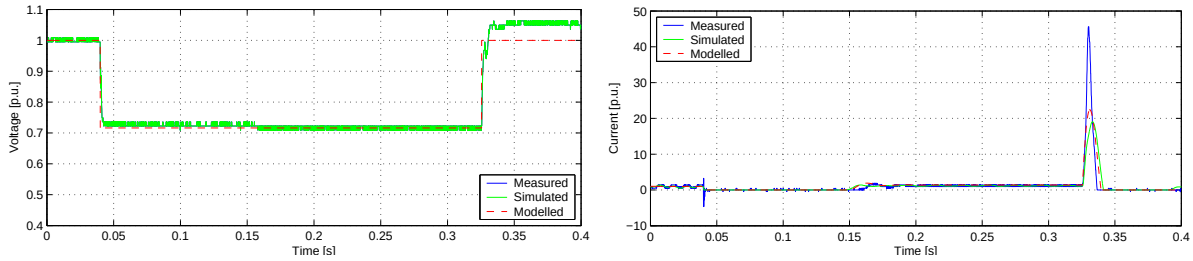

(a) Voltage (b) Current

Figure 6.24: Dip response of power supply (Chieftech) supplied with 230 V dc.

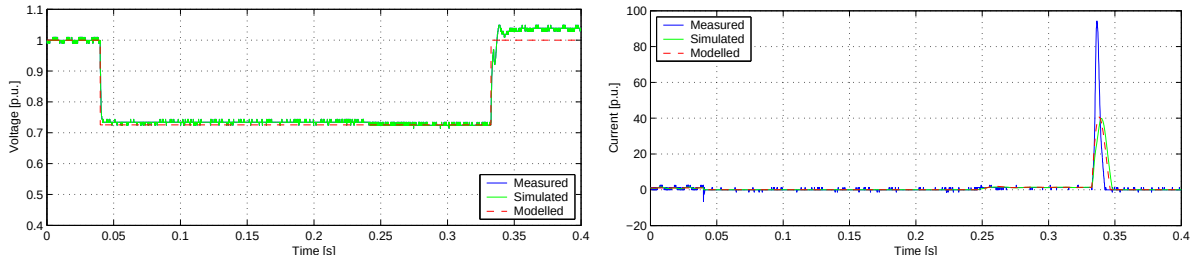

(a) Voltage (b) Current

Figure 6.25: Dip response of power supply (Chieftech) supplied with 325 V dc.

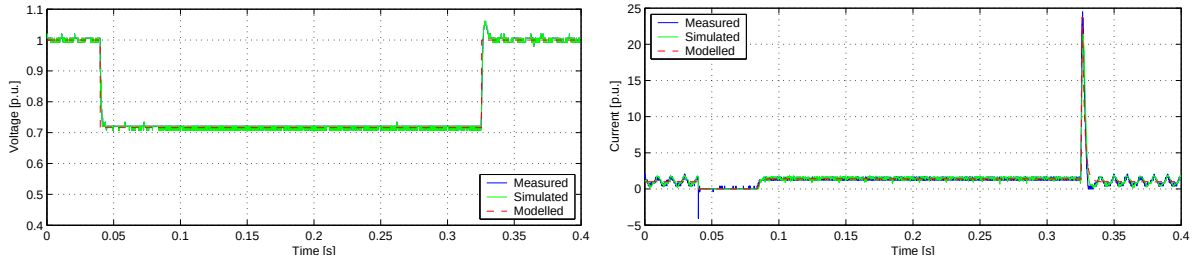

(a) Voltage (b) Current

Figure 6.26: Dip response of power supply (Macintosh) supplied with 230 V dc.

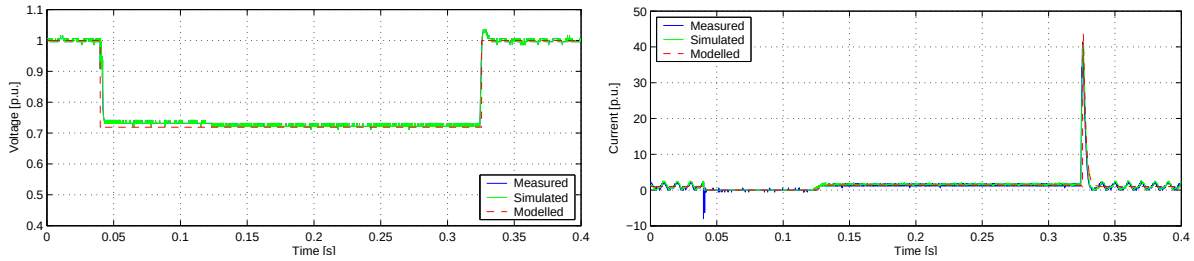

(a) Voltage (b) Current

Figure 6.27: Dip response of power supply (Macintosh) supplied with 325 V dc.

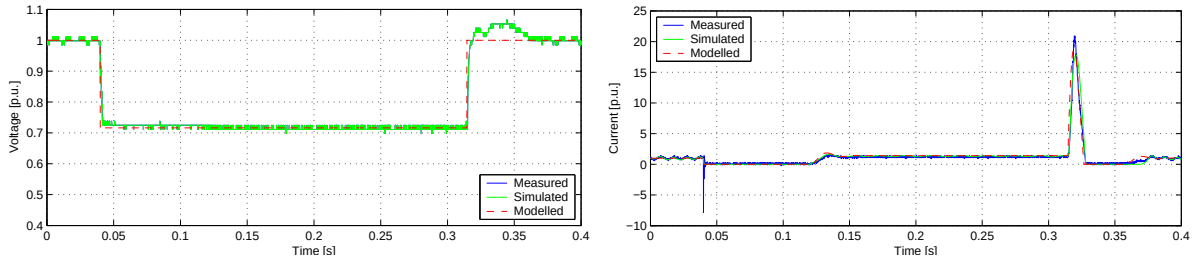

(a) Voltage (b) Current

Figure 6.28: Dip response of power supply (Sirtech) supplied with 230 V dc.

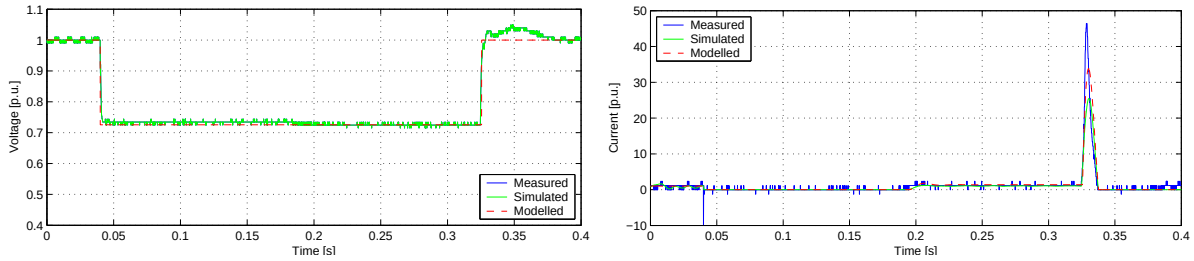

(a) Voltage (b) Current

Figure 6.29: Dip response of power supply (Sirtech) supplied with 325 V dc.

Other Devices

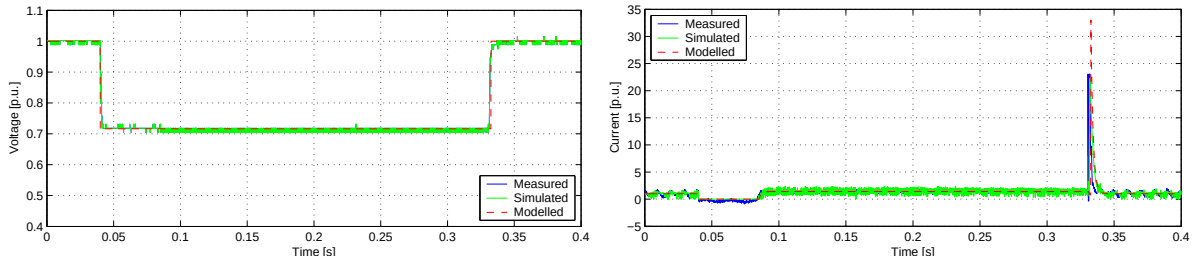

(a) Voltage (b) Current

Figure 6.30: Dip response of IP telephone (Grandstream) supplied with 230 V dc.

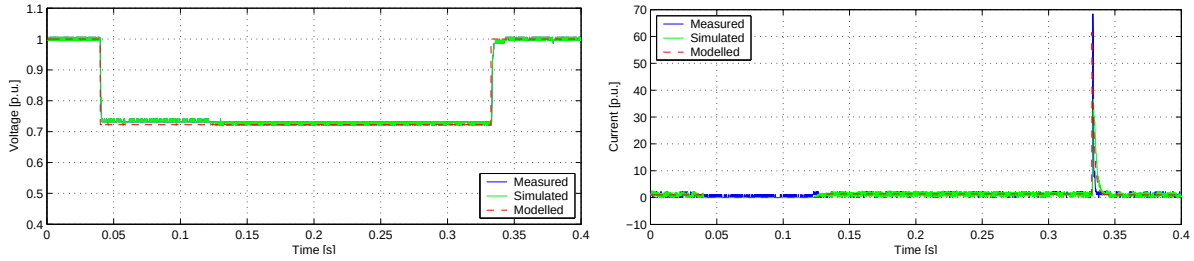

(a) Voltage (b) Current

Figure 6.31: Dip response of IP telephone (Grandstream) supplied with 325 V dc.

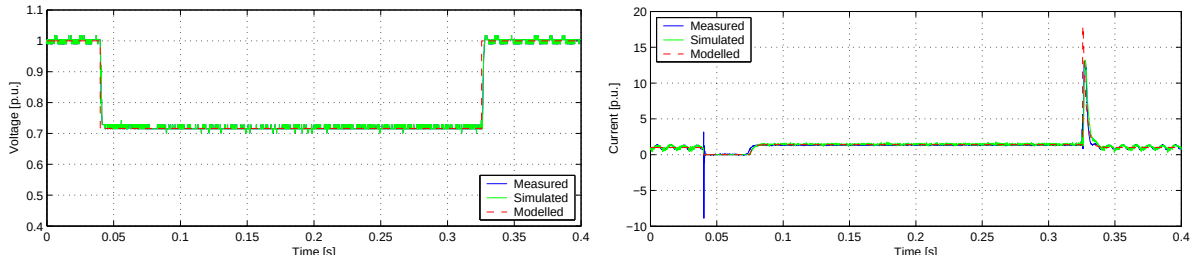

(a) Voltage (b) Current

Figure 6.32: Dip response of satellite receiver (Triasat) supplied with 230 V dc.

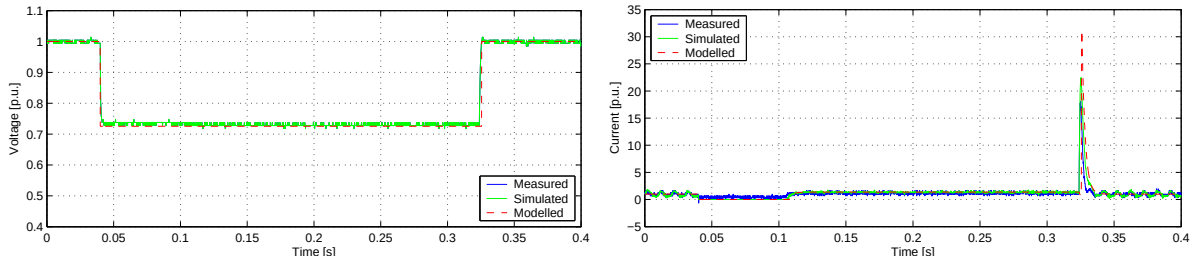

(a) Voltage (b) Current

Figure 6.33: Dip response of satellite receiver (Triasat) supplied with 325 V dc.

6.3 Summary

A selection of loads tested in this thesis was taken and they were subjected to a voltage dip in both ac and dc, which lasted for 300 ms. It was found that resistive loads are not sensitive to such a dip, but if it is a lamp for instance the light will flicker and the flicker is noticeable and can be annoying.

Rotating load were also found to be nonsensitive to dips, at least not the universal motors that were tested. When the voltage recovered from the dip, the current was higher than before the dip, and then slowly settled. This is due to the inertia of the motor.

Electronic loads are very sensitive to voltage dips as can be seen from Table 6.4. The level where the loads stopped working is dependent on what kind of rectifier it has on its input. The electronic loads that are used for lighting where found to be RMS invariant. That is, when the load was loaded with dc voltage that is equal to the RMS ac voltage, the loads stopped working approximately the same level.

When the voltage recovered after the dip, a very noticeable spike in the current of several p.u. was recorded for most of the electronic loads, This is due to recharging of the smoothing capacitor after the diode rectifier. To see if this phenomenon was correctly represented in the transient model, the dip was modelled in EMTDC and the model was found to show the same behavior. In ac this spike was usually measured lower than in dc. That is because of the natural characteristics of ac, an absolute maximum will be gotten when the highest difference between the voltage before and after the diode rectifier is gotten. Theoretically the spike in ac should be as high as the spike in dc. Since such a smoothing capacitor is not needed in dc it could be removed and then the current spike will be eliminated. Another option to reduce the current spike when the voltage recovers is to connect a relay, closed during normal, in parallel with a PTC resistor. The relay should be set to open when the voltage increases above a certain level, which means that the PTC resistor is connected. The operation principle of a PTC resistor is that initially the resistance is large and as the temperature increases the resistance decreases and results in that the current spike is reduced.

Chapter 7

Conclusions

In this thesis, steady-state and dynamic behavior of common loads for domestic use was investigated when the loads were supplied with dc. A mathematical model of the load behavior was developed and implemented in EMTDC and compared to measurements. These models can then be used for steady-state and transient analysis of larger dc distribution networks.

In total 81 loads were tested on ac to see whether they would work on dc. Of the loads tested it was found that 64 functioned on dc and were categorized in three categories. These categories are resistive, rotating and electronic loads. Each category was then further sub categorized because of different behavior and usage.

Resistive loads all worked on dc and were divided into two categories: Heaters and loads used for lighting.

The heaters were found to be constant resistive and followed Ohm's law. The loads used for lighting were found to have a strong temperature dependency on the current and were modelled as variable resistors. In steady state it was found that these loads caused absolutely no disturbance towards the grid either in ac or dc. When the loads were subjected to a fast voltage reduction it was found, for the heaters, the current dropped in direct proportion to the retained voltage according to Ohm's law. Since the resistance of the lamps is current dependent, the current did not drop in proportion to the voltage. Furthermore, the resistance of the lamps does not change instantaneously but decays exponentially towards the new steady-state value with a time constant that was found to be logarithmically dependent on the rated power of the lamp.

Rotating loads were divided into two categories: Universal motors and motors that showed resistive behavior. Not all rotating loads for domestic use can be supplied with dc. Only universal motors work properly on both ac and dc. Other motors, for instance single phase induction motors, asynchronous and synchronous motors require rotating field, sinusoidal current, to operate.

Universal motors were modelled as controllable current sources as described in Chapter 4. In steady state it was found that these motors caused very little distortion. A dynamic model of such a motor was difficult to realize since only voltage and current are known. A mathematical model was derived from the measurement result but the parameters were different for each motor, because they do not have the same mechanical structure.

Electronic loads were divided into two main sub categories. That is loads for lighting and loads for general purposes.

Several lamp types fall into the lighting category. First, compact fluorescent lamps

that were found to be constant current loads, but in limited range. Second, ballasts for fluorescent lamps that were found to have both constant current and constant power characteristics, depending on the manufacturer and range. Finally electronic transformers for low voltage halogen lamps. No general model has been found for this load type due to controllers that are found in these devices, but they were modelled separately as described in Chapter 5. The compact fluorescent lamp with a magnetic choke obviously did not function on dc.

Electronic loads for general purposes were found to have constant power behavior. Not all general purpose electronic loads can be used on dc because some of them have a transformer with an iron core in the input stage.

In steady-state the it was found that all loads had low distortion factor, which is advantageous compared to ac. A frequency component of 100 Hz was found in the current for all loads. However, this frequency component was found to have its origin from the voltage supplying the loads.

For the transient analysis, dynamic models were developed consisting of resistors, inductors, capacitors, the diode rectifier and the load characteristic model for each load, described more thoroughly in Chapter 5. The sizes of the passive components were chosen so the models would fit the measurements. This general dynamic model did not work for the ballasts, due complex circuit structures. However, if they were analyzed as second order systems, a simple mathematical expression for the behavior was obtained, as described in Chapter 5.

A selection of the loads tested in this thesis were subjected in various voltage dips in ac and dc in order to investigate their sensitivity. It was found that the resistive and rotating loads were not sensitive to voltage dips. The electronic loads were found to be sensitive to voltage dips, some more then others as described in Chapter 6, for both ac and dc of 230 V. When the loads were supplied with 325 V dc most of them showed no improvement with respect to sensitivity. Loads with a full bridge diode rectifier became less sensitive because they are constructed to have a nominal dc link voltage of this level. When the voltage recovered after the dip, a noticeable current spike was measured and modelled. To reduce this spike the smoothing capacitor, after the diode rectifier, should be removed. The spike was also found in the ac current measurements but had lower peak compared to dc. This can be explained by the natural characteristics of ac, see Chapter 6.

In general if the load does not require a rotation field, or a sinusoidal current, it will function properly on dc. In steady state the loads supplied with dc were found to cause less disturbances to the grid compared to ac, especially the electronic loads. Furthermore no improvement in sensitivity was achieved. Most of the load worked when supplied with 325 V dc but most of them are constructed to operate on 230 V ac RMS.

In order to decide the voltage level to be used, long term tests should be carried out. Further work is required to model the dynamic behavior of the loads, especially rotating and electronic loads. More sensitivity analysis should be carried out in ac and dc to determine if something can be gained by changing distribution system to dc. For instance, the effect of removing the smoothing capacitor in the electronic loads should be evaluated.

References

[1] (2004, Nov.) Direct current, encyclopædia britannica 2004. [Online]. Available: http://search.eb.com/eb/article?tocId=9030595

[2] L. M. Faulkenberry and W. Coffer, *Electrical Power Distribution and Transmission.* Prentice Hall, 1996.

[3] N. Mohan, T. M. UnderLand, and W. P. Robbins, *Power Electronics, converters, Applications and Design*, 3rd ed. Jogn Wiley & Sons, Inc, 2003.

[4] A. Sannino, G. Postiglione, and M. Bollen, "Feasibility of a dc network for commercial facilities," in *IEEE Transactions on Industry Applications*, no. 5, 2003.

[5] D. Nilsson and A. Sannino, "Load modelling for steady-state and transient analysis of low-voltage dc systems," in *Conference Record of the 2004 Industry Applications Conference*, vol. 2. IEEE, Oct. 2004, pp. 774– 780.

[6] G. Postiglione, "Dc distribution system for home and office," Chalmers University of Technology, Master Thesis TR-20R, Oct. 2001.

[7] (2004, Nov.) Lecroy digital oscilloscopes and oscilloscope accessories. [Online]. Available: http://www.lecroy.com

[8] (2004, Nov.) Fluke electronics. [Online]. Available: http://www.fluke.com

[9] *IEEE Recommended Practices and Requirements for Harmonic Control in Electrical Power Systems*, IEEE Std.519-1992, IEEE, 1992.

[10] *IEEE Recommended Practice for Electronic Power Subsystems: Parameter Definitions, Test conditions , and Test Methods*, IEEE Std.1515-2000, IEEE, 2000.

[11] K. Lindén and I. Segerqvist, "Modelling of load devices and studying load/system characteristics," Department of Electrical Power Systems, School of Electrical and Computer Engineering, Chalmers University, Licentiate Thesis TR-131L, Aug. 1992.

[12] B. Porat, *A Course in Digital Signal Processing.* John Wiley & Sons, INC, 1997.

[13] (2004, Nov.) Bimetal thermostat and temperature control. [Online]. Available: http://www.thermodisc.com

[14] S. T. Henderson and A. M. Marsden, *Lamps and Lighting*, 2nd ed. Edward Arnold, 1972.

[15] (2004, June) Franklin electric corporate information. [Online]. Available: http://www.franklin-electric.com/aid/vol20no4.html

[16] P. C. Cen, *Principles of electric macheines and power electronics*, 2nd ed. John Wiley & Sons, 1996.

[17] R. N. Ebben, J. R. Brauer, Z. J. Cenders, and N. A. Demerdash, "Prediction of performance characteristics of a universal motor using parametric finite element analysis," in *Electric Machines and Drives, 1999. International Conference IEMD '99.* IEEE, 1999, pp. 192–194.

[18] N. Mohan, *Electric Drives an intergrative approach.* MNPERE, 2003.

[19] Z. Ping, J. Brauer, S. Stanton, Z. Cendes, and R. Ebben, "Dynamic modeling of universal motors," in *Electric Machines and Drives, 1999. International Conference IEMD '99.* IEEE, May 1999, pp. 419–421.

[20] (2004, Nov.) Osram - see the world in a new light. [Online]. Available: http://www.osram.com/products/general/fluorescent/index.html

[21] L. Nerone, "Analysis and design of a self-oscillating class e ballast for compact fluorescent lamps," *IEEE Transactions on Industrial Electronics*, vol. 48, no. 1.

[22] G. Marent and S. Zudrell-Koch, "Novel electronic ballast with integrated digital power factor controller," in *Industry Applications Conference, 2003. 38th IAS Annual Meeting.* IEEE, Oct. 2003, pp. 791–798.

[23] C. L. Philips, *Feedback Control Systems*, 4th ed. Prentice Hall International, Inc., 2000.

[24] (2004, Nov.) Tridonic acto gmbh & co kg. [Online]. Available: http://www.tridonic.com/produkt/trafos_uk.asp

[25] M. H. J. Bollen, *Understanding power quality problems - voltage sags and interruptons.* IEEE Press, 2000.

[26] *IEEE Recommended Practice for Monitoring Electric Power Quality*, IEEE Std.1159-1995, IEEE, 1995.

[27] D. Kincaid and W. Cheney, *Numberical Analysis: Mathematics of Scientific Computing*, 3rd ed. Brooks/Cole, 2002.

Appendix A

Per Unit Calculations

A method of solving power system problem has been developed to make the calculations of a system with several voltage levels easier. The method is called the per unit system and the calculations are done with percentages of the base voltage [2]. This is applicable for both current, power and impedances. Their definitions are

$$U_{pu} = \frac{U}{U_{base}} \tag{A.1}$$

$$I_{pu} = \frac{I}{I_{base}} \tag{A.2}$$

where U is the voltage, U_{base} is the base voltage, I is the current and I_{base} is the base current. Ohms law is still valid, by combining Eq. (A.1) and (A.2) results in

$$V_{pu} = I_{pu} \cdot Z_{pu} \tag{A.3}$$

and the by applying the definition of power, Eq. (A.1) and (A.2) can be written as

$$S_{pu} = V_{pu} \cdot I_{pu} \tag{A.4}$$

The equations specified above were utilized throughout the thesis.

Appendix B

The Method of Least Squares

The method of least squares is often used to derive a relation between variables of different magnitude. In this report it is used to see if it possible to find a simple relation between voltage and current, and so forth. A brief description of the method is given here below.

Let (x_i, y_i) be points in a plane with $x_i \in [a, b]$ and $f_1, \ldots, f_n$ be real functions on this interval. It is desired to find a function of the type

$$f(x) = c_1 f_1(x) + c_2 f_2(x) +, \ldots, + c_m f_m(x) \tag{B.1}$$

with the coefficients $c_1, \ldots c_n$ that minimize the square sum

$$\sum_{i=1}^{n} (y_i - f(x_i))^2 \tag{B.2}$$

which can be done by linear algebra. If $b_i = f(x_i)$ is set to represent some of the coefficients $c_1, \ldots c_m$, then the column vectors, $y^T = [y_1, \ldots, y_n]$, $b^T = [b_1, \ldots, b_n]$ and $c^T = [c_1, \ldots, c_m]$ and the matrix

$$A = \begin{bmatrix} f_1(x_1) & f_2(x_1) & \cdots & f_n(x_1) \\ f_1(x_2) & f_2(x_2) & \ldots & f_n(x_2) \\ \vdots & \vdots & \ddots & \vdots \\ f_1(x_m) & f_2(x_m) & \cdots & f_n(x_m) \end{bmatrix} \tag{B.3}$$

are defined. Then $Ac = B$ and in the end c is chosen so that

$$\sum_{i=1}^{n} (y_i - b_i)^2 = ||y - b||^2 = ||y - Ac||^2 \tag{B.4}$$

is minimized, where $||\quad||$ is the Euclidean norm. A vector of the type $b = Ac$ spans the column space of the matrix A and then it is possible to write

$$b = a_1 A_1 +, \ldots, + a_n A_n \tag{B.5}$$

where A_j is column vector number j. Then the problem is to find that vector in the column space that is closest to y. The vector b is closest to y if and only if $(y - b)$ is orthogonal to all the vectors in the column space. That can be described as a dot product.

$$A_j \cdot (y - b) = 0, \qquad j = 1, \ldots n \tag{B.6}$$

In matrix format

$$A^T (y - b) = 0 \tag{B.7}$$

By substituting $b = Ac$, c can be determined by $A^T(y - Ac) = 0$, which is the same as $(A^T A)c = A^T y$ [27].

Example

As an example, if a linear relation is to be derived between two sets of variables x_i and y_i. Then $f_1(x) = 1$ and $f_2(x) = x$, this will give an equation $f(x) = c_1 * 1 + c_2 * x$. To realize this, A is defined as

$$A = \begin{bmatrix} 1 & x_1 \\ 1 & x_2 \\ \vdots & \vdots \\ 1 & x_m \end{bmatrix} \tag{B.8}$$

and

$$y = \begin{bmatrix} y_1 \\ y_2 \\ \vdots \\ y_m \end{bmatrix} \tag{B.9}$$

Then constants c_1 and c_2 are obtained from

$$(A^T A)c = A^T y \tag{B.10}$$

If for some reason the line is assumed to cross through zero, then $f_1(x) = 0$, and then $c_1 = 0$.

Appendix C

Source

In order to get as good results as possible when the load measurements are conducted it is important to know how clean the sources are of disturbances. Any disturbance that originates in the source will affect the measurements results and may even give false results. The sources that was used for the measurements are of two kinds, ac and dc. The ac source was the network used for the laboratory measurements at the department and the dc was supplied from a dc machine where we could vary the voltage from 30 V to 440 V and with a rated current of 16 A, and we have 10 A fuses as protection.

Ac source

To see how clean the ac source was, the no load voltage was measured for 1 s, which will give a frequency resolution of 1 Hz, at a level of 230 V RMS. The ac source is expected to be very clean, since it is separated from the office grid of the department and then any external disturbances will not be visible in the measurements. The results are shown in Fig. C.1.

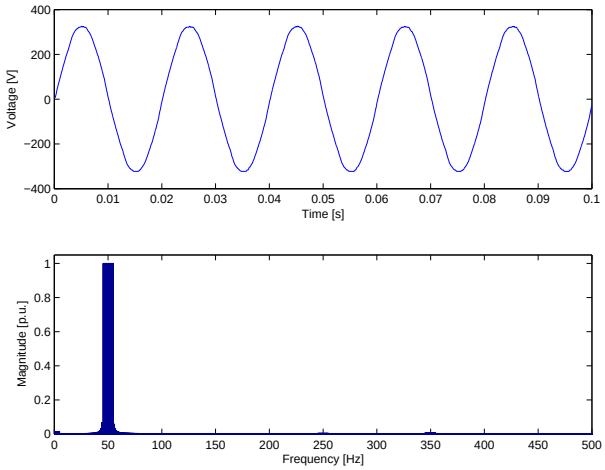

Figure C.1: Upper plot: measured phase voltage. Lower plot: voltage frequency spectrum.

The harmonic distortion of the measurements was then calculated. It shows that the source is quite clean with harmonic distortion of only 1.16 %. This value is below the error of the probes, ±2 %, used for these measurement. Therefore it is assumed that the ac source is free of disturbances, which is indicated in the Fig. C.1.

Dc source

The analysis of the dc source was done for 1 s and at a voltage level of 230 V in three types of configurations, no shunt capacitor, one shunt capacitor and with two shunt capacitors connected to the output of the source. The objective to have these capacitors is to reduce the ripple in the dc voltage. The disturbance of the source with no, one or two shunt capacitors was very low, see Fig. C.2. The measurements obtained from the dc source were run through an average filter, with 50 samples interval. This will give a result with no frequency components above 1 kHz, see Section 2.

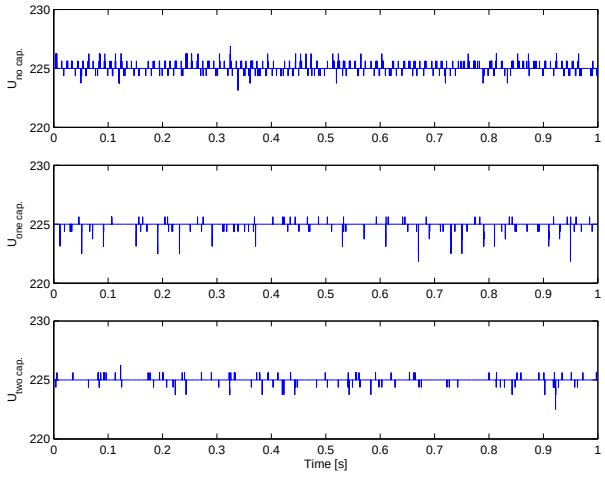

Figure C.2: Upper plot: dc voltage with no capacitor connected, middle plot: one capacitor; Lower: two capacitors connected

There are no high frequency disturbances detectable and there was a error factor of ±2 % of the measured values which was constant through the measurements, due to the inaccuracy of the probes, see Chapter 2. The distortion factors of the dc source with the three different configurations was measured and the result is shown in Table C.1.

Number of capacitors	Distortion factor
0	0.12
1	0.09
2	0.07

Table C.1: Distortion factor calculated for the different connections.

It is observed that the disturbance is decreased with the number of capacitors connected to the source, see Table C.1. The magnitude of this frequency component is more noticeable when the dc source is analyzed the ac coupling on the oscilloscope. To detect some frequency components in dc, the same measurements with the three configurations was done with ac coupling on the oscilloscope, seen in Fig. C.3.

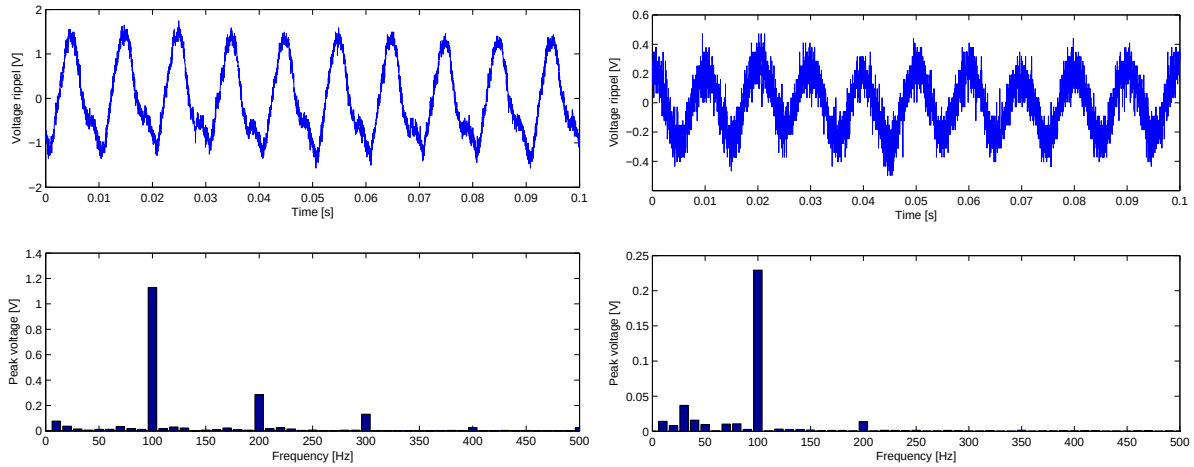

(a) With no capacitor

(b) With one capacitor

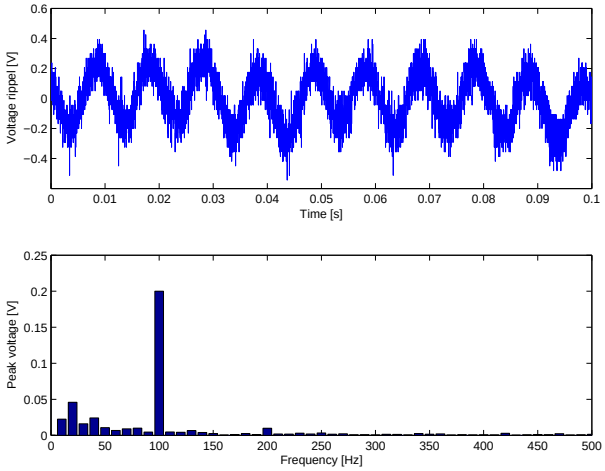

(c) With two capacitor

Figure C.3: Results from the dc measurements with ac coupling.

From Fig. C.3 it is observed that the oscillations in the dc voltage have a dominating frequency of 100 Hz and this magnitude is decreasing as the number of shunt capacitors are increased. The magnitude of the voltage ripple obtained from the setup with no capacitor connected was approximately 1.15 V, for the setup with one capacitor about 0.23 V and for two capacitor the magnitude was around 0.20 V. The amount of capacitors connected will reduce the peak to peak ripple of the 100 Hz frequency component the voltage, but not get rid of it.

Appendix D

Circuit to make a Fast Voltage Step in dc

To determine the transient behavior of the loads, it was decided to subject them to fast voltage reduction. To do that a circuit was designed and built to step down the voltage. The device is shown in Fig. D.1 and consists of one transistor, a resistor, six 33 V zener diodes, two RC filters, a capacitor (over the collector and emitter to protect the transistor from overvoltages), a variable resistor (to prevent overheating the transistor) and two switches, one to select the number of diodes and one that turns the step circuit on. The value of the variable resistor depends on the load current, see Appendix E.

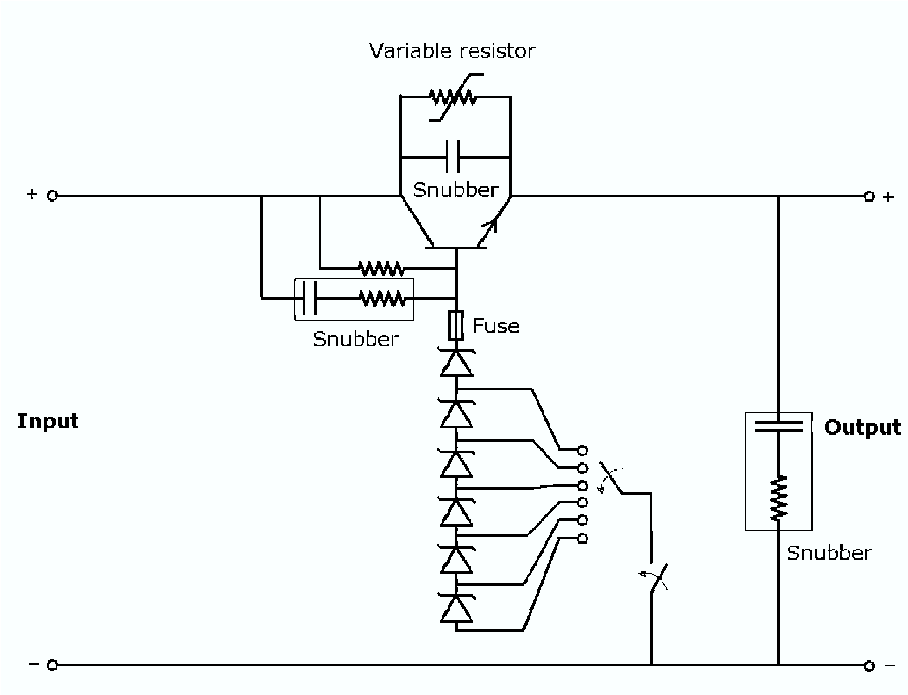

Figure D.1: Schematic diagram of the voltage step circuit.

When the latter switch is open, the load is supplied with nominal voltage. When it is closed, the load is supplied with a reduced voltage whose magnitude is determined by the zener diodes. When all diodes are connected, the voltage is 198 V over the load, when five are connected the voltage is 165 V over the load, etc.

To be sure that the transistor is able to handle breaking the voltage very fast, a

protection circuit was connected in parallel over the collector and emitter. First a fast capacitor, to handle the overvoltages caused when the valves of the transistor switch on, is connected. Fig. D.2 shows two examples of how the snubber works, one example of we loaded the circuit with 0.5 A and then with 1 A where the upper plots are without the capacitor and the lower ones are with capacitor in Figs. D.2(a) and D.2(b), respectively.

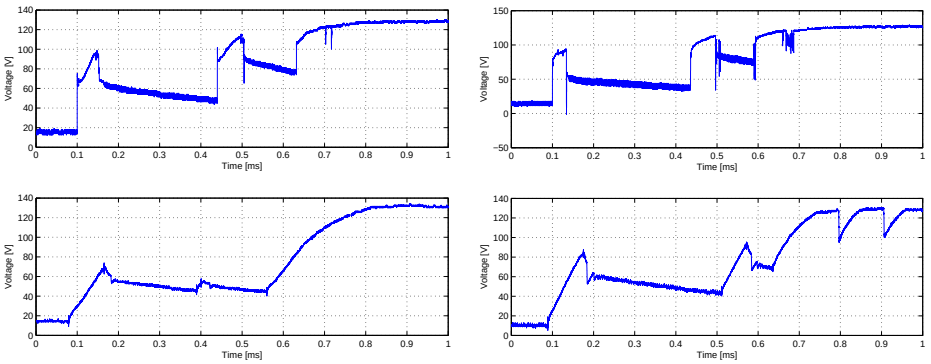

(a) 0.5 A load (b) 1 A load

Figure D.2: Voltage measured over the collector and emitter for two different loads, where the upper plots are without a snubber capacitor and the lower are with a snubber.

To protect the transistor from overheating, a variable resistor was then also connected in parallel over the collector and emitter. The resistivity of the resistor was chosen so that when the voltage step is made about 80% of the current would go through the resistor and about 20% through the transistor. When the load is supplied with nominal voltage, the transistor provides a low impedance path for the current and then hardly no current should go through the variable resistor.

Tests were done on this voltage divider to confirm the design and see how it may effect the measurements on the transients. This was done by putting the current probe of the oscilloscope (Chapter 2) before the voltage reduction circuit and the voltage probe was put after the circuit. Each step was done ten times to get a better statistical result for the transients. The average step is listed in Table D.1. A voltage meter and a current meter were also put at the input and it recorded that the voltage was constant at 230 V and the current was 38 mA during no load and stepped up when the voltage stepped down.

No. Diodes	Before step [V]	After step [V]	percentage
1	228.1	199.7	87.5 %
2	228.3	172.8	75.7 %
3	228.1	141.4	61.9 %
4	226.4	106.6	47.1 %
5	226.3	73.5	32.4 %

Table D.1: Measured voltage output from the voltage reduction circuit.

The last step was skipped because it was not used in any of the tests on the loads. Then the transients of this voltage stepping circuit was analyzed further for each step using MATLAB.

Step 1

In this step the voltage was stepped down to about 200 V. Figs. D.3(a) and D.3(b) shows how the voltage and current transient typically behaves when the step is made. Table D.2 shows the characteristic of the transient, which is impulsive in this case, as with all other cases.

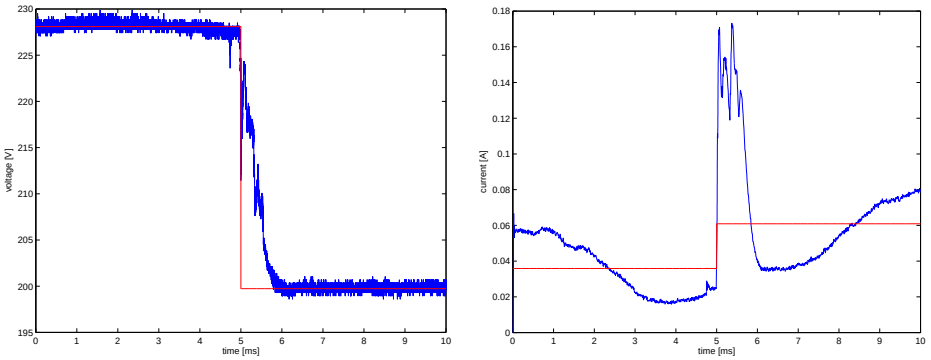

(a) Step 1 - voltage (b) Step 1 - current

Figure D.3: Typical transients of step 1.

Transients	Voltage	Current
peak	24.6 V	0.112 A
rise time	0.08 ms	0.19 ms
time to half	0.25 ms	0.33 ms

Table D.2: Typical transient behavior of step 1.

Table D.2 shows that the voltage has a very short rise time and then decays to the final value in about 0.25 ms. The peak value is almost the difference in the voltage before the step and after the step, see table D.1. The current transient is a bit slower both in the rise time and time to half. In this step, the transient caused is not that high compared with the other steps and probably it is related to the remaining magnitude of the step (lower retained voltage gives higher current transients). The oscillation that can be seen in the current is due to the fact that when the tests were made no capacitors was connected to the source because it caused a much higher transient in the current on the output side when they where connected. Although the input on the circuit is oscillating much, the output hardly has any oscillations when a load is connected to it.

Step 2

In this step, the voltage was brought down to 173 V. Fig. D.4 shows the typical shape of the transient and Table D.3 shows it characteristics. The transient behaves like it was described in Step 1.

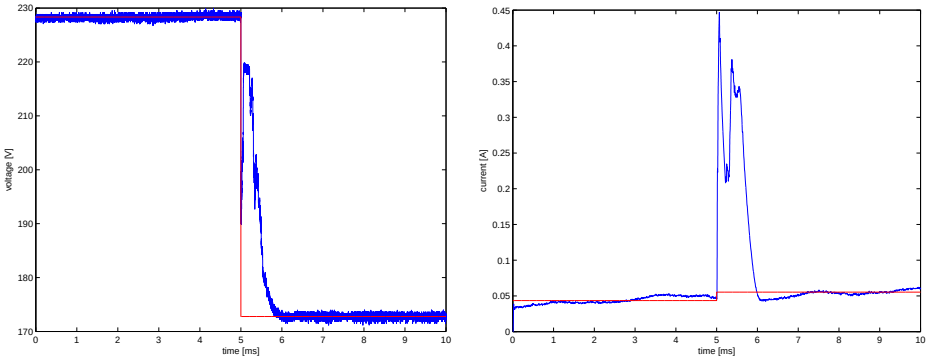

(a) Step 2 - voltage (b) Step 2 - current

Figure D.4: Typical transients of step 2.

Transients	Voltage	Current
peak	47.0 V	0.392 A
rise time	0.06 ms	0.04 ms
time to half	0.23 ms	0.34 ms

Table D.3: Typical transient behavior of step 2.

Step 3

In this step, the voltage was brought down to 142 V. Fig. D.5 shows the typical shape of the transient and Table D.4 shows it characteristics. The transient behaves like it was described in Step 1.

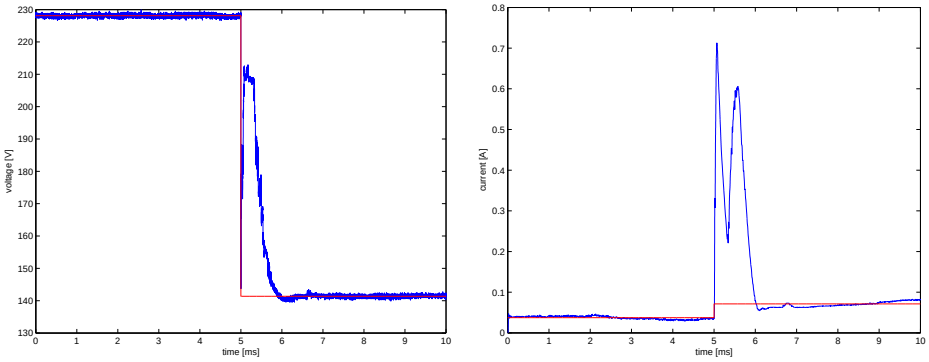

(a) Step 3 - voltage (b) Step 3 - current

Figure D.5: Typical transients of step 3.

Transients	Voltage	Current
peak	71.5 V	0.641 A
rise time	0.07 ms	0.04 ms
time to half	0.23 ms	0.37 ms

Table D.4: Typical transient behavior of step 3.

Step 4

In this step, the voltage was brought down to 107 V. Fig. D.6 shows the typical shape of the transient and Table D.5 shows it characteristics. The transient behaves like it was described in Step 1.

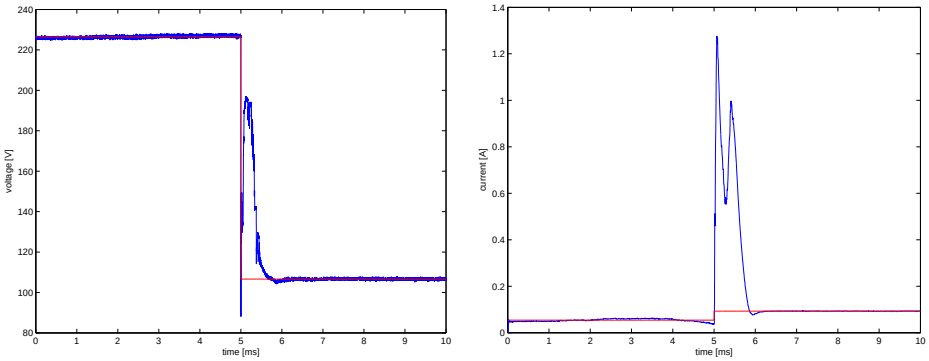

(a) Step 4 - voltage (b) Step 4 - current

Figure D.6: Typical transients of step 4.

Transients	Voltage	Current
peak	90.2 V	1.182 A
rise time	0.08 ms	0.04 ms
time to half	0.18 ms	0.29 ms

Table D.5: Typical transient behavior of step 4.

Step 5

In this step, the voltage was brought down to 73 V. Fig. D.7 shows the typical shape of the transient and Table D.6 shows it characteristics. The transient behaves like it was described in Step 1.

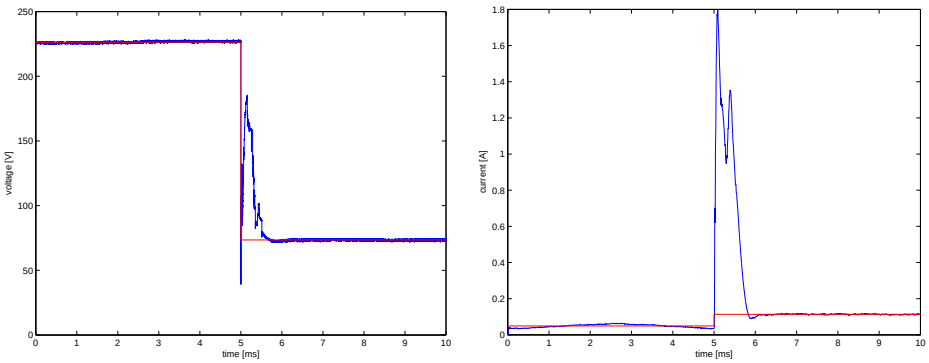

(a) Step 5 - voltage (b) Step 5 - current

Figure D.7: Typical transients of step 5.

Transients	Voltage	Current
peak	111.9 V	1.68 A
rise time	0.05 ms	0.05 ms
time to half	0.25 ms	0.25 ms

Table D.6: Typical transient behavior of step 5.

Here the current transient is more than 1 A and will probable not be used on the load tests.

Summary

The transients in the voltage reduction circuit is probably due to the switching in of the capacitors when the voltage step is made. The peak value of the voltage is proportional to how big the voltage step is as well in the current. The rise time of the voltage was the same in all cases or less than 0.1 ms and the decay time as well, normally about 0.25 ms. The same can be said for the current, the rise time is about the same or usually about 0.05 ms but the time to half is a little bit longer or for $0.3 - 0.4$ ms.

These transients are all very fast and not that high in amplitude. If the two large capacitors are put in parallel to the dc source, see Appendix C. The current transient are much larger, so the transient tests on the loads will be tested without those capacitors to minimize the effect from the source.

Appendix E

Lookup Table for the Variable Resistor

	Step 1		Step 2		Step 3		Step 4	
Current	ΔU	R	ΔU	R	ΔU	R	ΔU	R
0.00	30.00	*N/A*	60.00	*N/A*	90.00	*N/A*	120.00	*N/A*
0.05	30.00	5000.00	60.00	5769.23	90.00	5769.23	120.00	6000.00
0.10	30.00	2500.00	60.00	2884.62	90.00	2884.62	120.00	3000.00
0.15	30.00	1666.67	60.00	1923.08	90.00	1923.08	120.00	2000.00
0.20	30.00	1250.00	60.00	1442.31	90.00	1442.31	120.00	1500.00
0.25	30.00	1000.00	60.00	1153.85	90.00	1153.85	120.00	1200.00
0.30	30.00	833.33	60.00	961.54	90.00	961.54	120.00	1000.00
0.35	30.00	714.29	60.00	824.18	90.00	824.18	120.00	857.14
0.40	30.00	625.00	60.00	721.15	90.00	721.15	120.00	750.00
0.45	30.00	555.56	60.00	641.03	90.00	641.03	120.00	666.67
0.50	30.00	500.00	60.00	576.92	90.00	576.92	120.00	600.00
0.55	30.00	454.55	60.00	524.48	90.00	524.48	120.00	545.45
0.60	30.00	416.67	60.00	480.77	90.00	480.77	120.00	500.00
0.65	30.00	384.62	60.00	443.79	90.00	443.79	120.00	461.54
0.70	30.00	357.14	60.00	412.09	90.00	412.09	120.00	428.57
0.75	30.00	333.33	60.00	384.62	90.00	384.62	120.00	400.00
0.80	30.00	312.50	60.00	360.58	90.00	360.58	120.00	375.00
0.85	30.00	294.12	60.00	339.37	90.00	339.37	120.00	352.94
0.90	30.00	277.78	60.00	320.51	90.00	320.51	120.00	333.33
0.95	30.00	263.16	60.00	303.64	90.00	303.64	120.00	315.79
1.00	30.00	250.00	60.00	288.46	90.00	288.46	120.00	300.00
1.05	30.00	238.10	60.00	274.73	90.00	274.73	120.00	285.71
1.10	30.00	227.27	60.00	262.24	90.00	262.24	120.00	272.73
1.15	30.00	217.39	60.00	250.84	90.00	250.84	120.00	260.87
1.20	30.00	208.33	60.00	240.38	90.00	240.38	120.00	250.00
1.25	30.00	200.00	60.00	230.77	90.00	230.77	120.00	240.00
1.30	30.00	192.31	60.00	221.89	90.00	221.89	120.00	230.77
1.35	30.00	185.19	60.00	213.68	90.00	213.68	120.00	222.22
1.40	30.00	178.57	60.00	206.04	90.00	206.04	120.00	214.29
1.45	30.00	172.41	60.00	198.94	90.00	198.94	120.00	206.90
1.50	30.00	166.67	60.00	192.31	90.00	192.31	120.00	200.00

	Step 1		Step 2		Step 3		Step 4	
Current	ΔU	R	ΔU	R	ΔU	R	ΔU	R
1.55	30.00	161.29	60.00	186.10	90.00	186.10	120.00	193.55
1.60	30.00	156.25	60.00	180.29	90.00	180.29	120.00	187.50
1.65	30.00	151.52	60.00	174.83	90.00	174.83	120.00	181.82
1.70	30.00	147.06	60.00	169.68	90.00	169.68	120.00	176.47
1.75	30.00	142.86	60.00	164.84	90.00	164.84	120.00	171.43
1.80	30.00	138.89	60.00	160.26	90.00	160.26	120.00	166.67
1.85	30.00	135.14	60.00	155.93	90.00	155.93	120.00	162.16
1.90	30.00	131.58	60.00	151.82	90.00	151.82	120.00	157.89
1.95	30.00	128.21	60.00	147.93	90.00	147.93	120.00	153.85
2.00	30.00	125.00	60.00	144.23	90.00	144.23	120.00	150.00
2.05	30.00	121.95	60.00	140.71	90.00	140.71	120.00	146.34
2.10	30.00	119.05	60.00	137.36	90.00	137.36	120.00	142.86
2.15	30.00	116.28	60.00	134.17	90.00	134.17	120.00	139.53
2.20	30.00	113.64	60.00	131.12	90.00	131.12	120.00	136.36
2.25	30.00	111.11	60.00	128.21	90.00	128.21	120.00	133.33
2.30	30.00	108.70	60.00	125.42	90.00	125.42	120.00	130.43
2.35	30.00	106.38	60.00	122.75	90.00	122.75	120.00	127.66
2.40	30.00	104.17	60.00	120.19	90.00	120.19	120.00	125.00
2.45	30.00	102.04	60.00	117.74	90.00	117.74	120.00	122.45
2.50	30.00	100.00	60.00	115.38	90.00	115.38	120.00	120.00
2.55	30.00	98.04	60.00	113.12	90.00	113.12	120.00	117.65
2.60	30.00	96.15	60.00	110.95	90.00	110.95	120.00	115.38
2.65	30.00	94.34	60.00	108.85	90.00	108.85	120.00	113.21
2.70	30.00	92.59	60.00	106.84	90.00	106.84	120.00	111.11
2.75	30.00	90.91	60.00	104.90	90.00	104.90	120.00	109.09
2.80	30.00	89.29	60.00	103.02	90.00	103.02	120.00	107.14
2.85	30.00	87.72	60.00	101.21	90.00	101.21	120.00	105.26
2.90	30.00	86.21	60.00	99.47	90.00	99.47	120.00	103.45
2.95	30.00	84.75	60.00	97.78	90.00	97.78	120.00	101.69
3.00	30.00	83.33	60.00	96.15	90.00	96.15	120.00	100.00
3.05	30.00	81.97	60.00	94.58	90.00	94.58	120.00	98.36
3.10	30.00	80.65	60.00	93.05	90.00	93.05	120.00	96.77
3.15	30.00	79.37	60.00	91.58	90.00	91.58	120.00	95.24
3.20	30.00	78.13	60.00	90.14	90.00	90.14	120.00	93.75
3.25	30.00	76.92	60.00	88.76	90.00	88.76	120.00	92.31
3.30	30.00	75.76	60.00	87.41	90.00	87.41	120.00	90.91
3.35	30.00	74.63	60.00	86.11	90.00	86.11	120.00	89.55
3.40	30.00	73.53	60.00	84.84	90.00	84.84	120.00	88.24
3.45	30.00	72.46	60.00	83.61	90.00	83.61	120.00	86.96
3.50	30.00	71.43	60.00	82.42	90.00	82.42	120.00	85.71
3.55	30.00	70.42	60.00	81.26	90.00	81.26	120.00	84.51
3.60	30.00	69.44	60.00	80.13	90.00	80.13	120.00	83.33
3.65	30.00	68.49	60.00	79.03	90.00	79.03	120.00	82.19
3.70	30.00	67.57	60.00	77.96	90.00	77.96	120.00	81.08
3.75	30.00	66.67	60.00	76.92	90.00	76.92	120.00	80.00

	Step 1		Step 2		Step 3		Step 4	
Current	ΔU	R	ΔU	R	ΔU	R	ΔU	R
3.80	30.00	65.79	60.00	75.91	90.00	75.91	120.00	78.95
3.85	30.00	64.94	60.00	74.93	90.00	74.93	120.00	77.92
3.90	30.00	64.10	60.00	73.96	90.00	73.96	120.00	76.92
3.95	30.00	63.29	60.00	73.03	90.00	73.03	120.00	75.95
4.00	30.00	62.50	60.00	72.12	90.00	72.12	120.00	75.00
4.05	30.00	61.73	60.00	71.23	90.00	71.23	120.00	74.07
4.10	30.00	60.98	60.00	70.36	90.00	70.36	120.00	73.17
4.15	30.00	60.24	60.00	69.51	90.00	69.51	120.00	72.29
4.20	30.00	59.52	60.00	68.68	90.00	68.68	120.00	71.43
4.25	30.00	58.82	60.00	67.87	90.00	67.87	120.00	70.59
4.30	30.00	58.14	60.00	67.08	90.00	67.08	120.00	69.77
4.35	30.00	57.47	60.00	66.31	90.00	66.31	120.00	68.97
4.40	30.00	56.82	60.00	65.56	90.00	65.56	120.00	68.18
4.45	30.00	56.18	60.00	64.82	90.00	64.82	120.00	67.42
4.50	30.00	55.56	60.00	64.10	90.00	64.10	120.00	66.67
4.55	30.00	54.95	60.00	63.40	90.00	63.40	120.00	65.93
4.60	30.00	54.35	60.00	62.71	90.00	62.71	120.00	65.22
4.65	30.00	53.76	60.00	62.03	90.00	62.03	120.00	64.52
4.70	30.00	53.19	60.00	61.37	90.00	61.37	120.00	63.83
4.75	30.00	52.63	60.00	60.73	90.00	60.73	120.00	63.16
4.80	30.00	52.08	60.00	60.10	90.00	60.10	120.00	62.50
4.85	30.00	51.55	60.00	59.48	90.00	59.48	120.00	61.86
4.90	30.00	51.02	60.00	58.87	90.00	58.87	120.00	61.22
4.95	30.00	50.51	60.00	58.28	90.00	58.28	120.00	60.61
5.00	30.00	50.00	60.00	57.69	90.00	57.69	120.00	60.00
5.05	30.00	49.50	60.00	57.12	90.00	57.12	120.00	59.41
5.10	30.00	49.02	60.00	56.56	90.00	56.56	120.00	58.82
5.15	30.00	48.54	60.00	56.01	90.00	56.01	120.00	58.25
5.20	30.00	48.08	60.00	55.47	90.00	55.47	120.00	57.69
5.25	30.00	47.62	60.00	54.95	90.00	54.95	120.00	57.14
5.30	30.00	47.17	60.00	54.43	90.00	54.43	120.00	56.60
5.35	30.00	46.73	60.00	53.92	90.00	53.92	120.00	56.07
5.40	30.00	46.30	60.00	53.42	90.00	53.42	120.00	55.56
5.45	30.00	45.87	60.00	52.93	90.00	52.93	120.00	55.05
5.50	30.00	45.45	60.00	52.45	90.00	52.45	120.00	54.55
5.55	30.00	45.05	60.00	51.98	90.00	51.98	120.00	54.05
5.60	30.00	44.64	60.00	51.51	90.00	51.51	120.00	53.57
5.65	30.00	44.25	60.00	51.06	90.00	51.06	120.00	53.10
5.70	30.00	43.86	60.00	50.61	90.00	50.61	120.00	52.63
5.75	30.00	43.48	60.00	50.17	90.00	50.17	120.00	52.17
5.80	30.00	43.10	60.00	49.73	90.00	49.73	120.00	51.72
5.85	30.00	42.74	60.00	49.31	90.00	49.31	120.00	51.28
5.90	30.00	42.37	60.00	48.89	90.00	48.89	120.00	50.85
5.95	30.00	42.02	60.00	48.48	90.00	48.48	120.00	50.42
6.00	30.00	41.67	60.00	48.08	90.00	48.08	120.00	50.00

	Step 1		Step 2		Step 3		Step 4	
Current	ΔU	R	ΔU	R	ΔU	R	ΔU	R
6.05	30.00	41.32	60.00	47.68	90.00	47.68	120.00	49.59
6.10	30.00	40.98	60.00	47.29	90.00	47.29	120.00	49.18
6.15	30.00	40.65	60.00	46.90	90.00	46.90	120.00	48.78
6.20	30.00	40.32	60.00	46.53	90.00	46.53	120.00	48.39
6.25	30.00	40.00	60.00	46.15	90.00	46.15	120.00	48.00
6.30	30.00	39.68	60.00	45.79	90.00	45.79	120.00	47.62
6.35	30.00	39.37	60.00	45.43	90.00	45.43	120.00	47.24
6.40	30.00	39.06	60.00	45.07	90.00	45.07	120.00	46.88
6.45	30.00	38.76	60.00	44.72	90.00	44.72	120.00	46.51
6.50	30.00	38.46	60.00	44.38	90.00	44.38	120.00	46.15
6.55	30.00	38.17	60.00	44.04	90.00	44.04	120.00	45.80
6.60	30.00	37.88	60.00	43.71	90.00	43.71	120.00	45.45
6.65	30.00	37.59	60.00	43.38	90.00	43.38	120.00	45.11
6.70	30.00	37.31	60.00	43.05	90.00	43.05	120.00	44.78
6.75	30.00	37.04	60.00	42.74	90.00	42.74	120.00	44.44
6.80	30.00	36.76	60.00	42.42	90.00	42.42	120.00	44.12
6.85	30.00	36.50	60.00	42.11	90.00	42.11	120.00	43.80
6.90	30.00	36.23	60.00	41.81	90.00	41.81	120.00	43.48
6.95	30.00	35.97	60.00	41.51	90.00	41.51	120.00	43.17
7.00	30.00	35.71	60.00	41.21	90.00	41.21	120.00	42.86
7.05	30.00	35.46	60.00	40.92	90.00	40.92	120.00	42.55
7.10	30.00	35.21	60.00	40.63	90.00	40.63	120.00	42.25
7.15	30.00	34.97	60.00	40.34	90.00	40.34	120.00	41.96
7.20	30.00	34.72	60.00	40.06	90.00	40.06	120.00	41.67
7.25	30.00	34.48	60.00	39.79	90.00	39.79	120.00	41.38
7.30	30.00	34.25	60.00	39.52	90.00	39.52	120.00	41.10
7.35	30.00	34.01	60.00	39.25	90.00	39.25	120.00	40.82
7.40	30.00	33.78	60.00	38.98	90.00	38.98	120.00	40.54
7.45	30.00	33.56	60.00	38.72	90.00	38.72	120.00	40.27
7.50	30.00	33.33	60.00	38.46	90.00	38.46	120.00	40.00
7.55	30.00	33.11	60.00	38.21	90.00	38.21	120.00	39.74
7.60	30.00	32.89	60.00	37.96	90.00	37.96	120.00	39.47
7.65	30.00	32.68	60.00	37.71	90.00	37.71	120.00	39.22
7.70	30.00	32.47	60.00	37.46	90.00	37.46	120.00	38.96
7.75	30.00	32.26	60.00	37.22	90.00	37.22	120.00	38.71
7.80	30.00	32.05	60.00	36.98	90.00	36.98	120.00	38.46
7.85	30.00	31.85	60.00	36.75	90.00	36.75	120.00	38.22
7.90	30.00	31.65	60.00	36.51	90.00	36.51	120.00	37.97
7.95	30.00	31.45	60.00	36.28	90.00	36.28	120.00	37.74
8.00	30.00	31.25	60.00	36.06	90.00	36.06	120.00	37.50
8.05	30.00	31.06	60.00	35.83	90.00	35.83	120.00	37.27
8.10	30.00	30.86	60.00	35.61	90.00	35.61	120.00	37.04
8.15	30.00	30.67	60.00	35.39	90.00	35.39	120.00	36.81
8.20	30.00	30.49	60.00	35.18	90.00	35.18	120.00	36.59
8.25	30.00	30.30	60.00	34.97	90.00	34.97	120.00	36.36

	Step 1		Step 2		Step 3		Step 4	
Current	ΔU	R	ΔU	R	ΔU	R	ΔU	R
8.30	30.00	30.12	60.00	34.75	90.00	34.75	120.00	36.14
8.35	30.00	29.94	60.00	34.55	90.00	34.55	120.00	35.93
8.40	30.00	29.76	60.00	34.34	90.00	34.34	120.00	35.71
8.45	30.00	29.59	60.00	34.14	90.00	34.14	120.00	35.50
8.50	30.00	29.41	60.00	33.94	90.00	33.94	120.00	35.29
8.55	30.00	29.24	60.00	33.74	90.00	33.74	120.00	35.09
8.60	30.00	29.07	60.00	33.54	90.00	33.54	120.00	34.88
8.65	30.00	28.90	60.00	33.35	90.00	33.35	120.00	34.68
8.70	30.00	28.74	60.00	33.16	90.00	33.16	120.00	34.48
8.75	30.00	28.57	60.00	32.97	90.00	32.97	120.00	34.29
8.80	30.00	28.41	60.00	32.78	90.00	32.78	120.00	34.09
8.85	30.00	28.25	60.00	32.59	90.00	32.59	120.00	33.90
8.90	30.00	28.09	60.00	32.41	90.00	32.41	120.00	33.71
8.95	30.00	27.93	60.00	32.23	90.00	32.23	120.00	33.52
9.00	30.00	27.78	60.00	32.05	90.00	32.05	120.00	33.33
9.05	30.00	27.62	60.00	31.87	90.00	31.87	120.00	33.15
9.10	30.00	27.47	60.00	31.70	90.00	31.70	120.00	32.97
9.15	30.00	27.32	60.00	31.53	90.00	31.53	120.00	32.79
9.20	30.00	27.17	60.00	31.35	90.00	31.35	120.00	32.61
9.25	30.00	27.03	60.00	31.19	90.00	31.19	120.00	32.43
9.30	30.00	26.88	60.00	31.02	90.00	31.02	120.00	32.26
9.35	30.00	26.74	60.00	30.85	90.00	30.85	120.00	32.09
9.40	30.00	26.60	60.00	30.69	90.00	30.69	120.00	31.91
9.45	30.00	26.46	60.00	30.53	90.00	30.53	120.00	31.75
9.50	30.00	26.32	60.00	30.36	90.00	30.36	120.00	31.58
9.55	30.00	26.18	60.00	30.21	90.00	30.21	120.00	31.41
9.60	30.00	26.04	60.00	30.05	90.00	30.05	120.00	31.25
9.65	30.00	25.91	60.00	29.89	90.00	29.89	120.00	31.09
9.70	30.00	25.77	60.00	29.74	90.00	29.74	120.00	30.93
9.75	30.00	25.64	60.00	29.59	90.00	29.59	120.00	30.77
9.80	30.00	25.51	60.00	29.43	90.00	29.43	120.00	30.61
9.85	30.00	25.38	60.00	29.29	90.00	29.29	120.00	30.46
9.90	30.00	25.25	60.00	29.14	90.00	29.14	120.00	30.30
9.95	30.00	25.13	60.00	28.99	90.00	28.99	120.00	30.15
10.00	30.00	25.00	60.00	28.85	90.00	28.85	120.00	30.00

Table E.1: Lookup table for the resistance connected in parallel over the voltage stepper.

Appendix F

Network Model

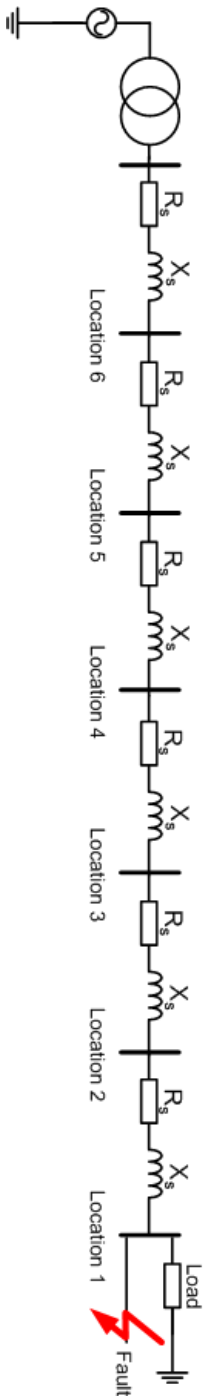

Figure F.1: Network model used for sensitivity measurements.

Appendix G

Transient Results for Heaters

From Fig. G.1, the Philips coffee machine behaves as a constant resistance load, the current drops by approximately the same amount as the voltage. The model agrees to the measurement quite well. The difference in current is about 5 % in the worst case (Step 4) which is quite acceptable, since the model is said to have an inaccuracy of about 2 % and the measurement equipment have the same inaccuracy.

The curling brush (Fig. G.2) behaves as a constant resistance load, the current drops by approximately the same amount as the voltage. The measured current is extremely noisy, although it was tried to filter the noise as much as possible. This huge noise is mostly due to the fact of the amount of current that the load draws is very little, and the rated power consumption is about 11 W. The models are though following the average current. The model describes the curling iron quite well.

The kettle in Fig. G.3 behaves as a constant resistive load, the current drops by approximately the same amount as the voltage. In the first step it is strange that the voltage and the current are not constant after the step. That might be due to measurement failure, but it is more likely because of the extensive use of this kettle, and its age. This is not as visible in the other steps probably because of the larger scale and some differences between the model and the measurements are present. In general the model agrees with the measurements quite well.

For the kettle in Fig. G.4, the sandwich makers in Fig. G.6, and the stove in Fig. G.7, the behavior is again as a constant resistance, the current drops by approximately the same amount as the voltage. The model agrees well with the measurements, both in voltage and current.

Also the sandwich maker in Fig. G.5 behaves as a constant resistance load but some difference between measurements and model can be noticed. However, the error between the measurements and the model is about 5 % in the worst case, which is quite acceptable since the model is said to have an error of 5.66 %.

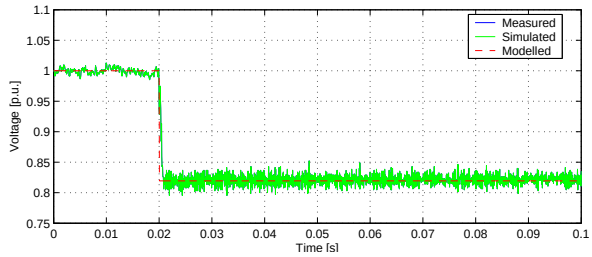

(a) Voltage - Step 1.

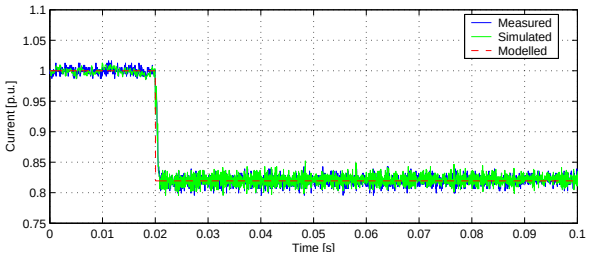

(b) Current - Step 1.

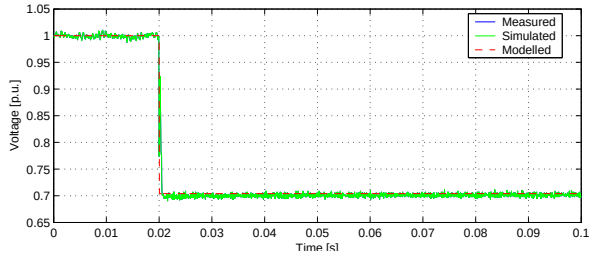

(c) Voltage - Step 2.

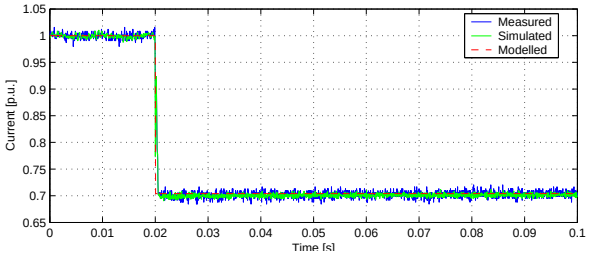

(d) Current - Step 2.

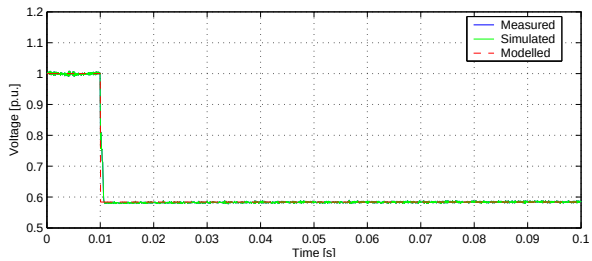

(e) Voltage - Step 3.

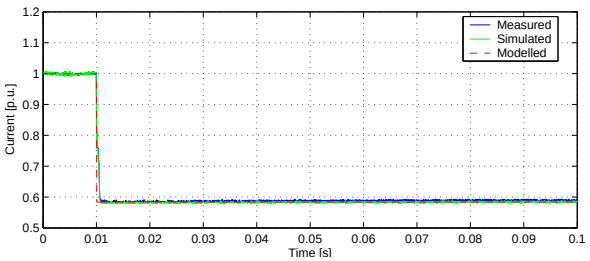

(f) Current - Step 3.

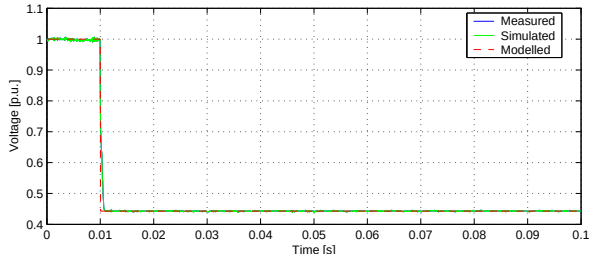

(g) Voltage - Step 4.

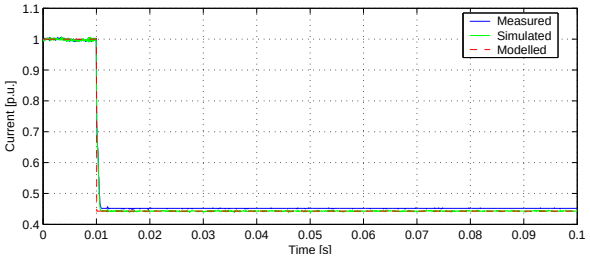

(h) Current - Step 4.

Figure G.1: Transient behavior of coffee machine (Philips.)

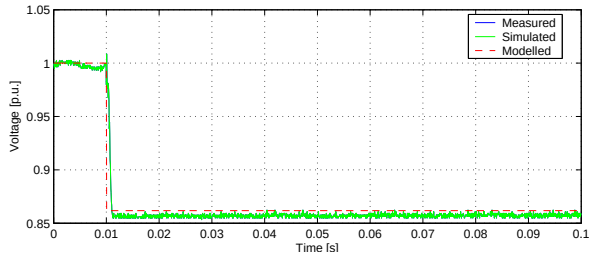

(a) Voltage - Step 1.

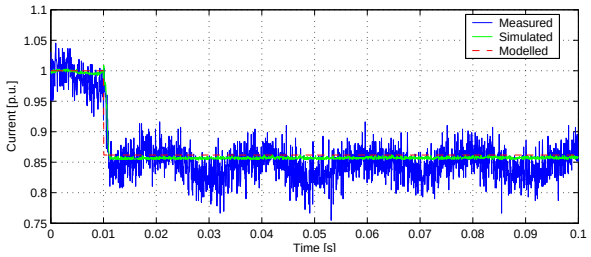

(b) Current - Step 1.

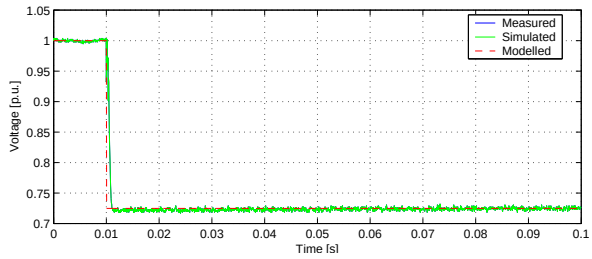

(c) Voltage - Step 2.

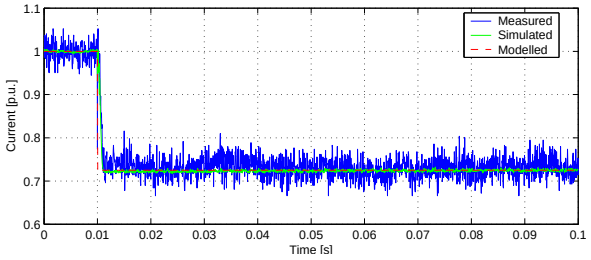

(d) Current - Step 2.

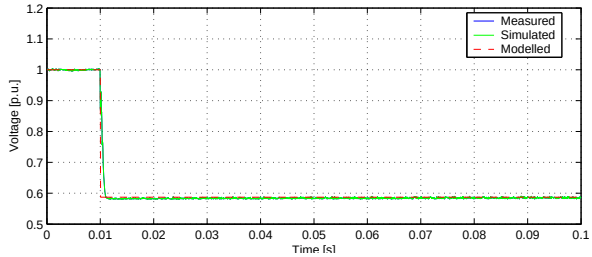

(e) Voltage - Step 3.

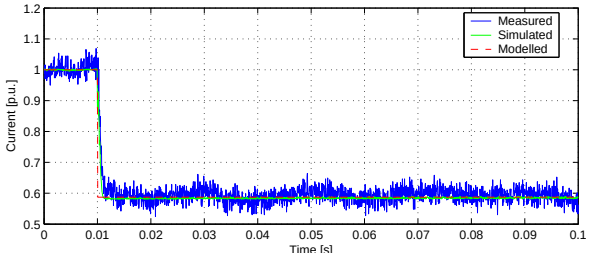

(f) Current - Step 3.

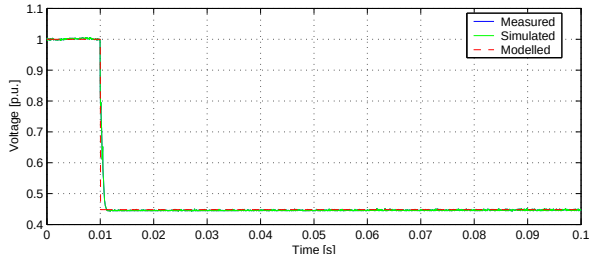

(g) Voltage - Step 4.

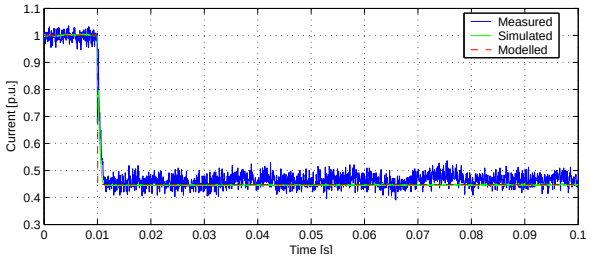

(h) Current - Step 4.

Figure G.2: Transient behavior of curling brush (XL Concept).

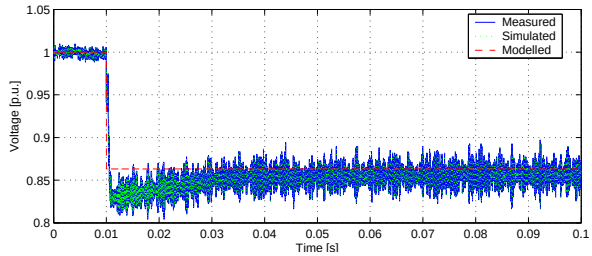

(a) Voltage - Step 1.

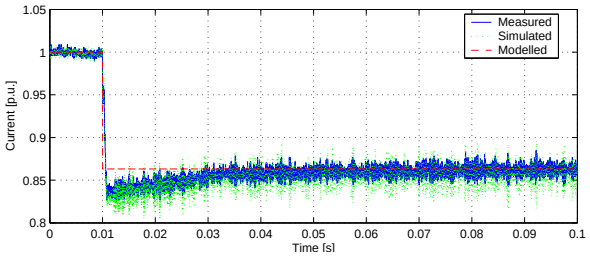

(b) Current - Step 1.

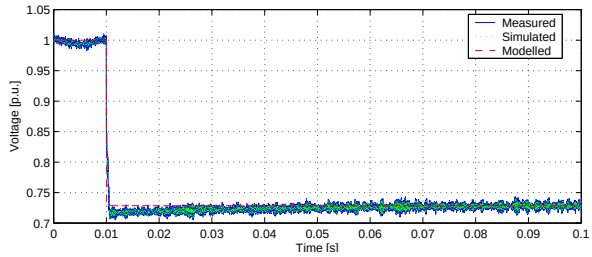

(c) Voltage - Step 2.

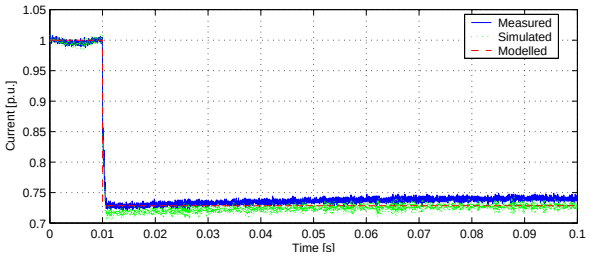

(d) Current - Step 2.

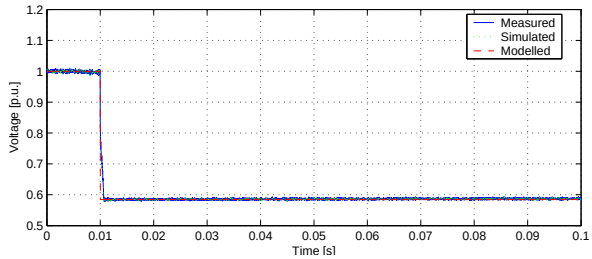

(e) Voltage - Step 3.

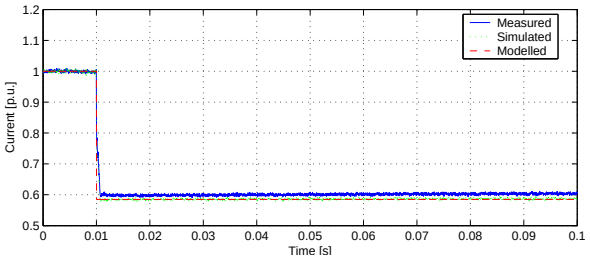

(f) Current - Step 3.

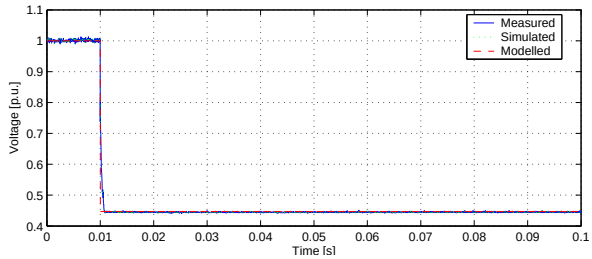

(g) Voltage - Step 4.

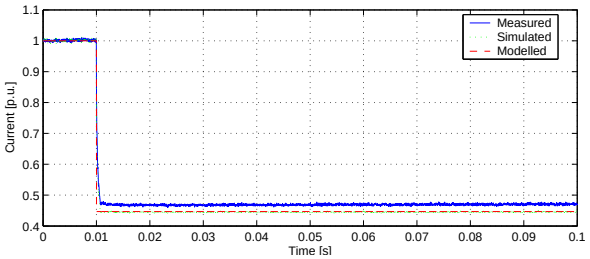

(h) Current - Step 4.

Figure G.3: Transient behavior of kettle (Elram).

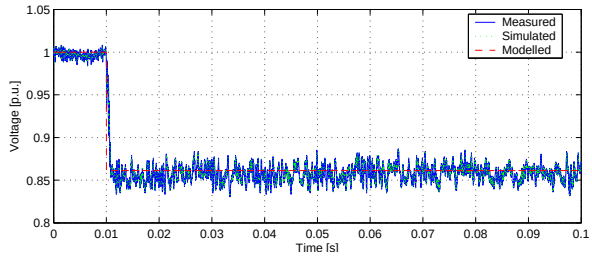

(a) Voltage - Step 1.

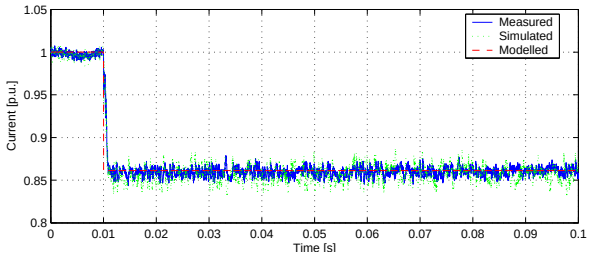

(b) Current - Step 1.

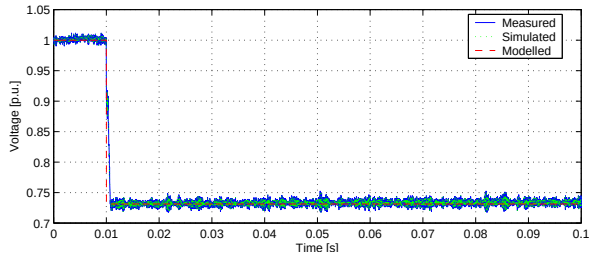

(c) Voltage - Step 2.

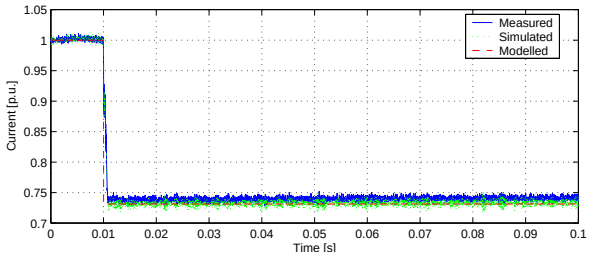

(d) Current - Step 2.

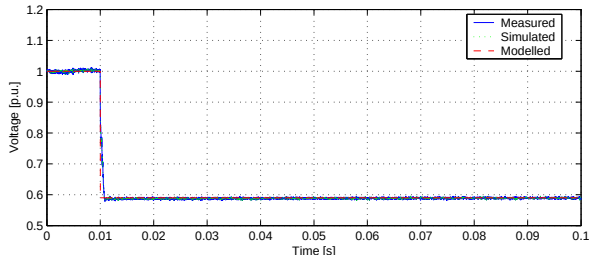

(e) Voltage - Step 3.

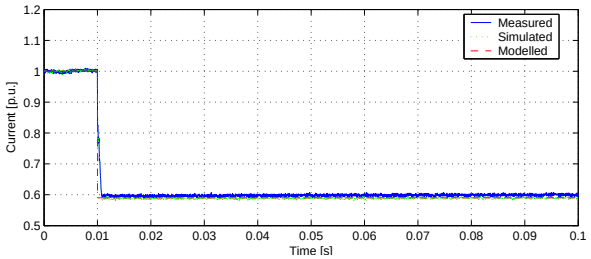

(f) Current - Step 3.

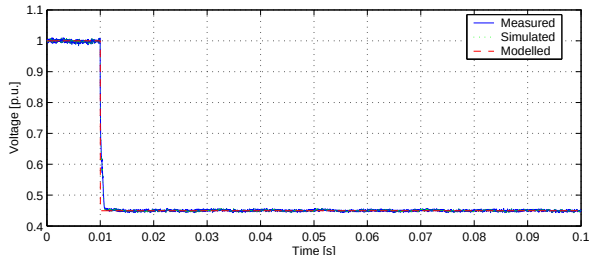

(g) Voltage - Step 4.

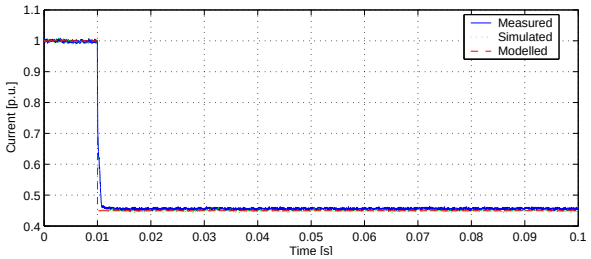

(h) Current - Step 4.

Figure G.4: Transient behavior of kettle (Sollingmüller).

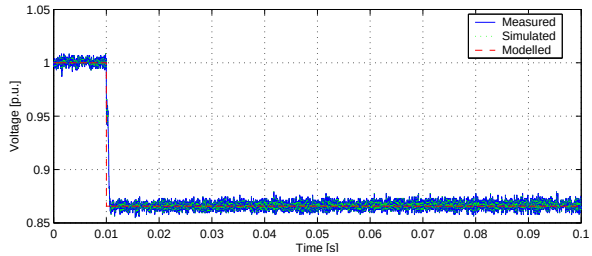

(a) Voltage - Step 1.

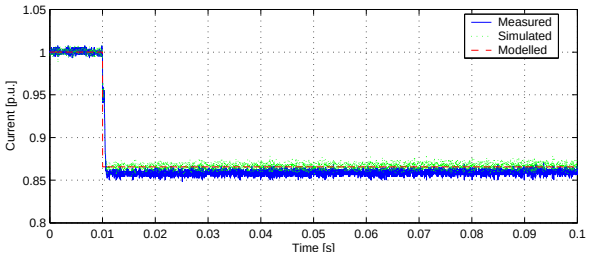

(b) Current - Step 1.

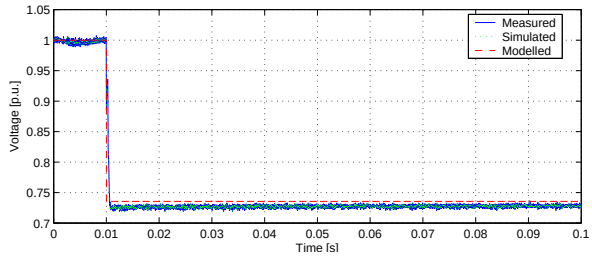

(c) Voltage - Step 2.

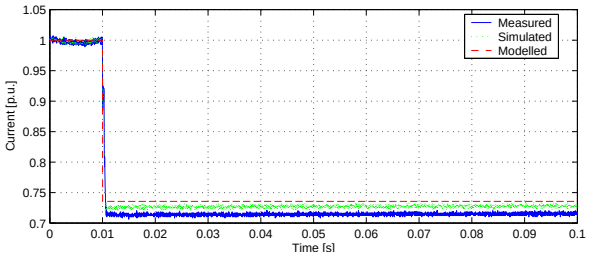

(d) Current - Step 2.

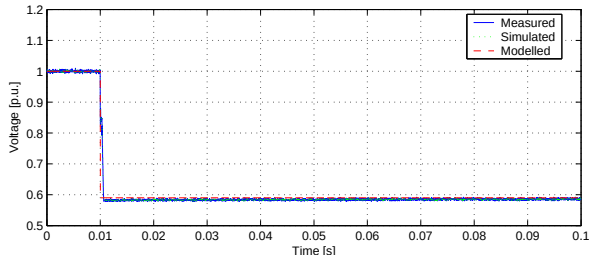

(e) Voltage - Step 3.

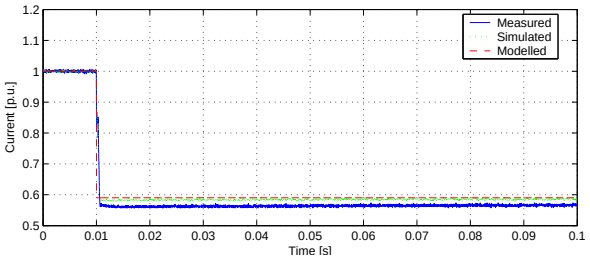

(f) Current - Step 3.

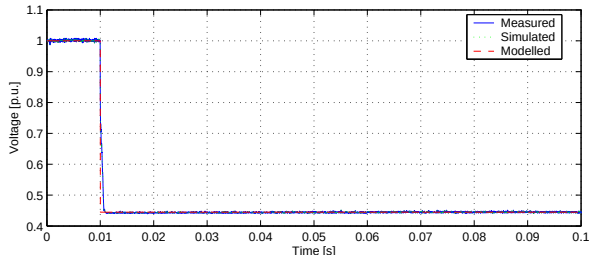

(g) Voltage - Step 4.

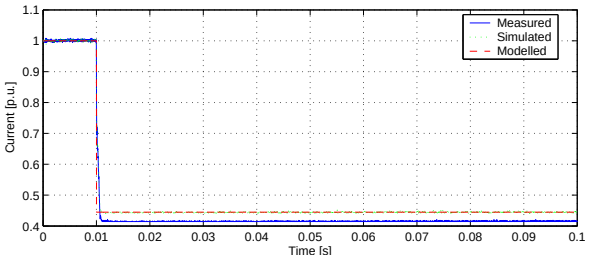

(h) Current - Step 4.

Figure G.5: Transient behavior of sandwich maker (Mirabelle).

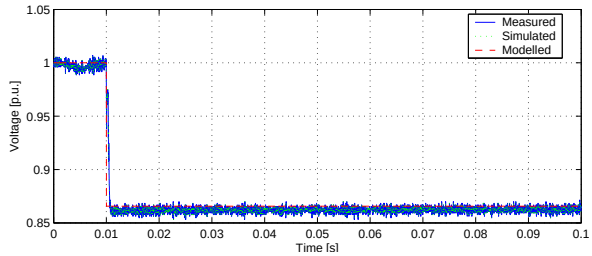

(a) Voltage - Step 1.

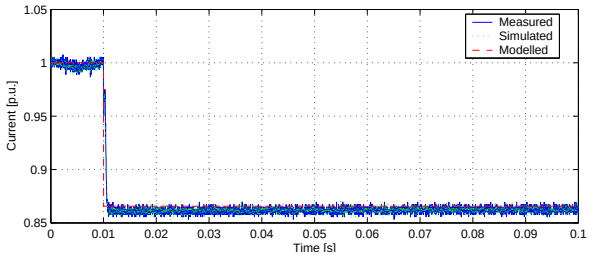

(b) Current - Step 1.

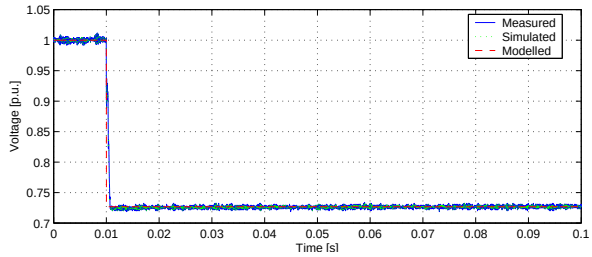

(c) Voltage - Step 2.

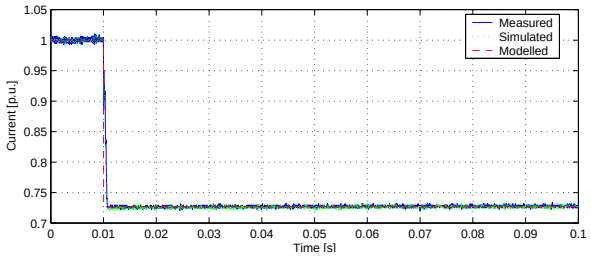

(d) Current - Step 2.

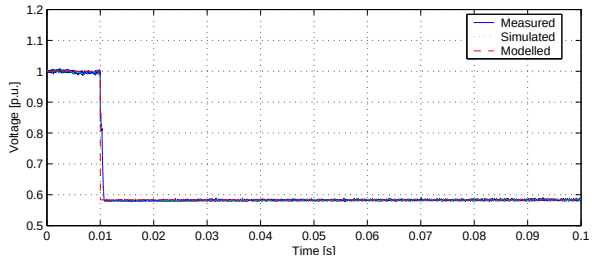

(e) Voltage - Step 3.

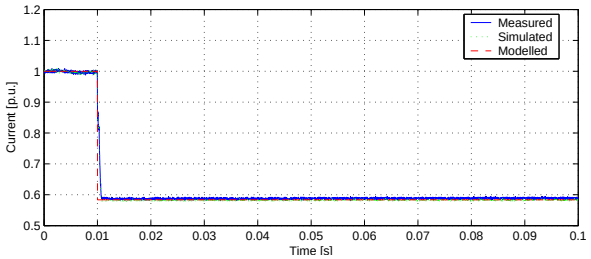

(f) Current - Step 3.

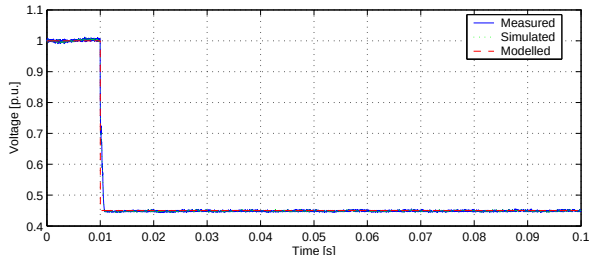

(g) Voltage - Step 4.

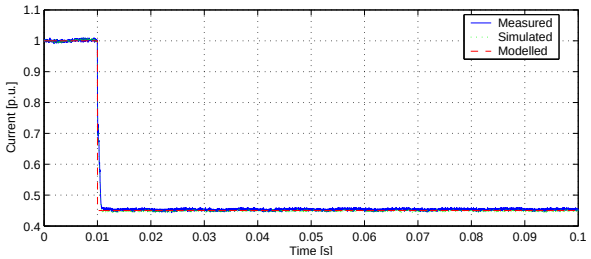

(h) Current - Step 4.

Figure G.6: Transient behavior of sandwich maker (AFK).

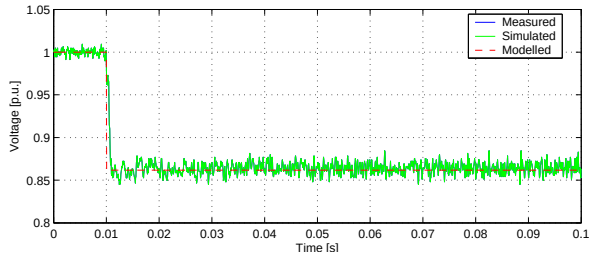

(a) Voltage - Step 1.

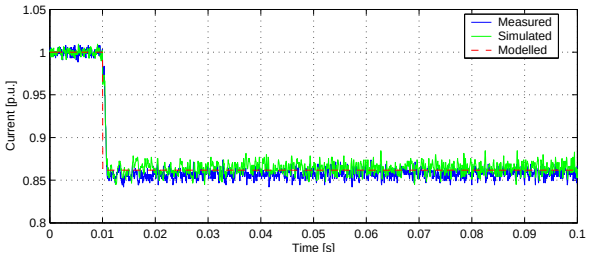

(b) Current - Step 1.

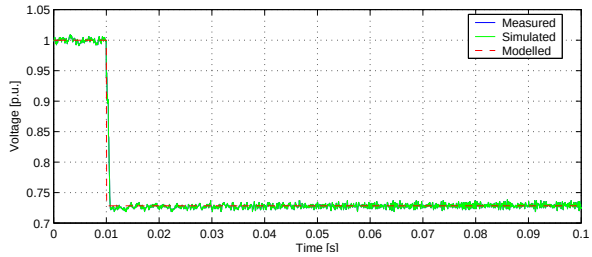

(c) Voltage - Step 2.

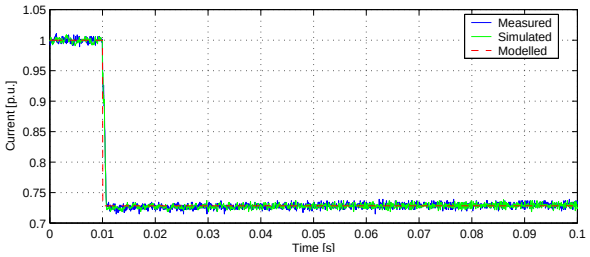

(d) Current - Step 2.

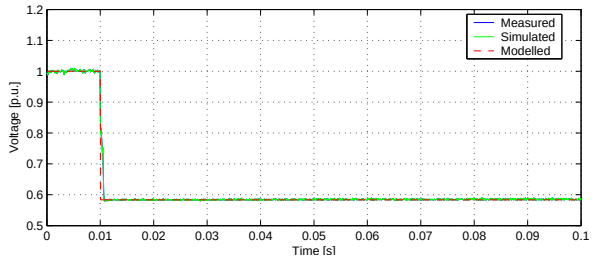

(e) Voltage - Step 3.

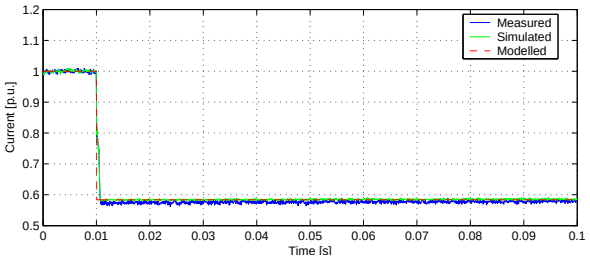

(f) Current - Step 3.

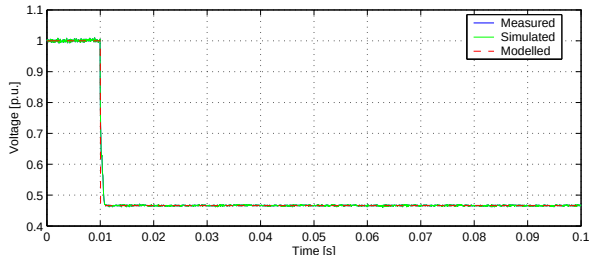

(g) Voltage - Step 4.

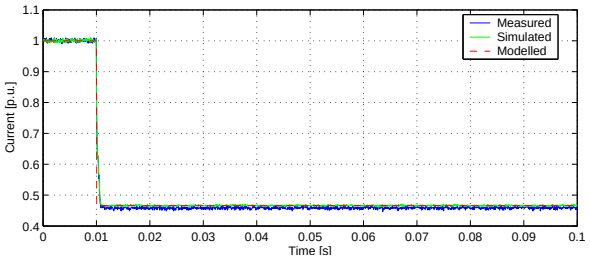

(h) Current - Step 4.

Figure G.7: Transient behavior of stove (Siemens).

Appendix H

Lamp Characteristics and Transient Results

Characteristics

The following plots shows the characteristics of the lamps tested. Due to the amount of lamps, most of them are shown in this appendix.

25 W Incandescent Lamps

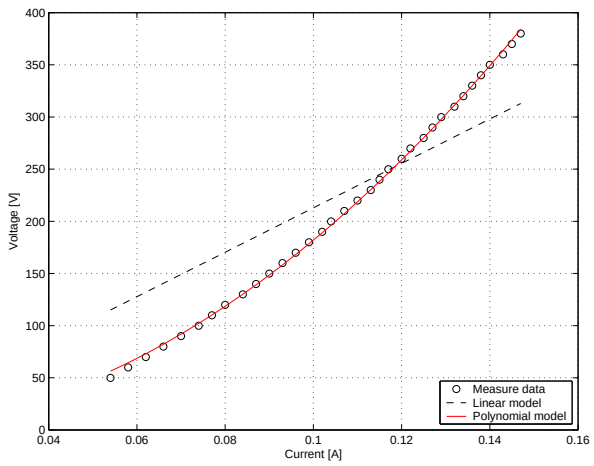

(a) Lamp 2: Voltage vs. Current.

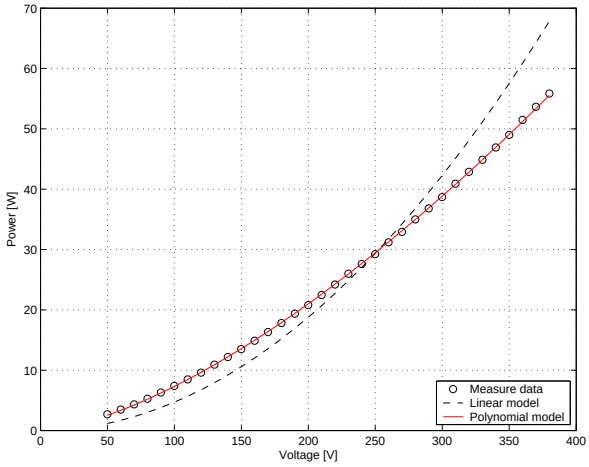

(b) Lamp 2: Power vs. Voltage.

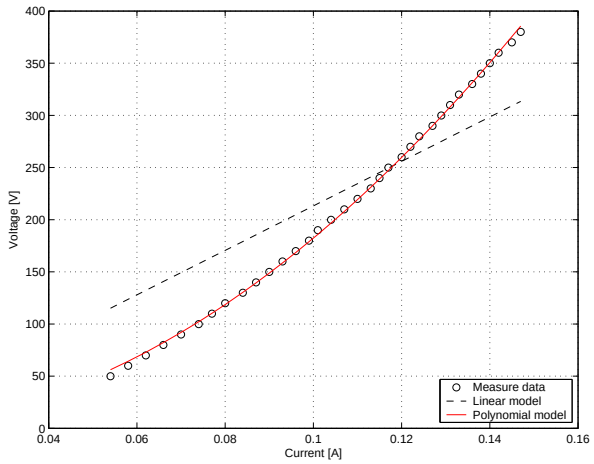

(c) Lamp 3: Voltage vs. Current.

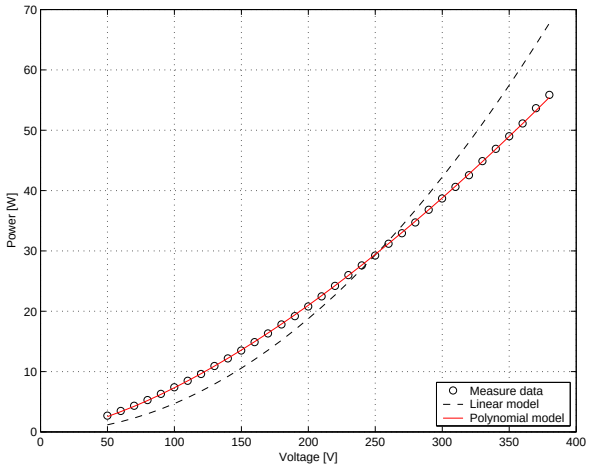

(d) Lamp 3: Power vs. Voltage.

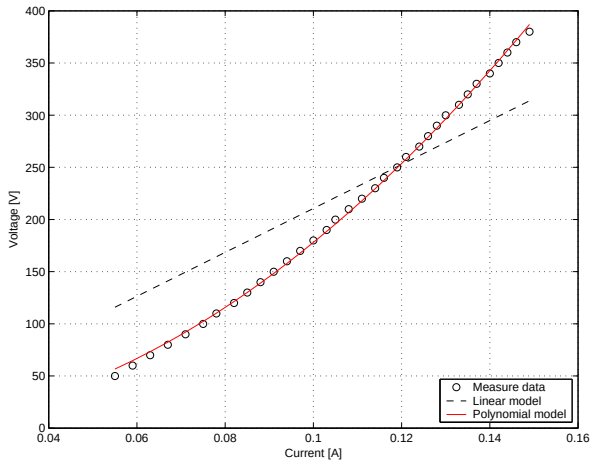

(e) Lamp 4: Voltage vs. Current.

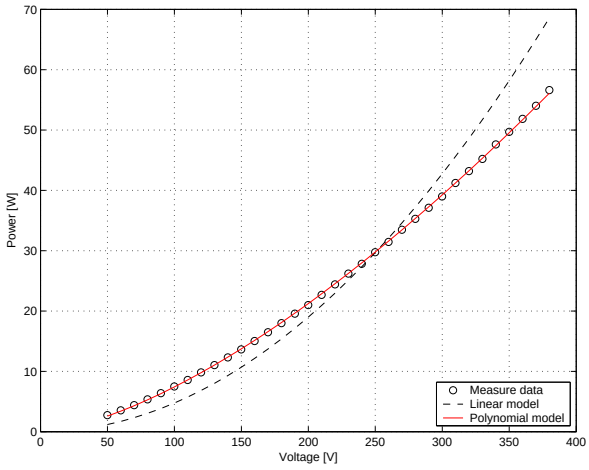

(f) Lamp 4: Power vs. Voltage.

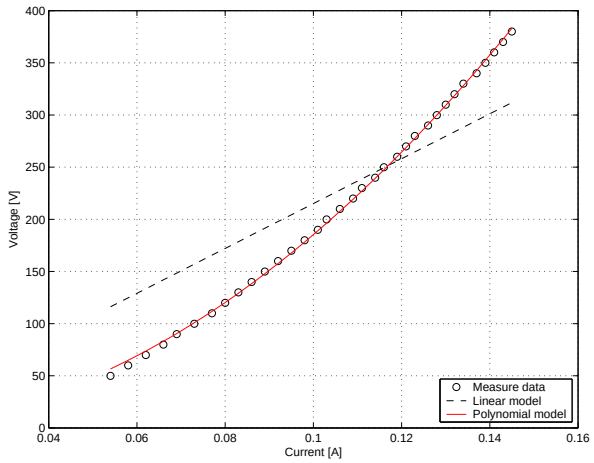

(g) Lamp 5: Voltage vs. Current.

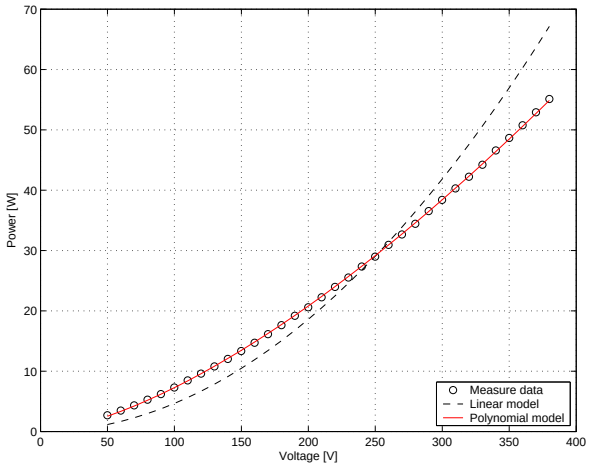

(h) Lamp 5: Power vs. Voltage.

Figure H.1: Characteristics of 25 W incandescent lamps.

40 W Incandescent Lamps

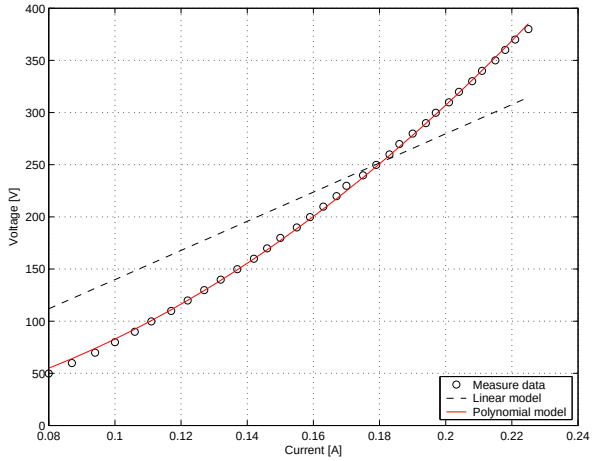

(a) Lamp 2: Voltage vs. Current.

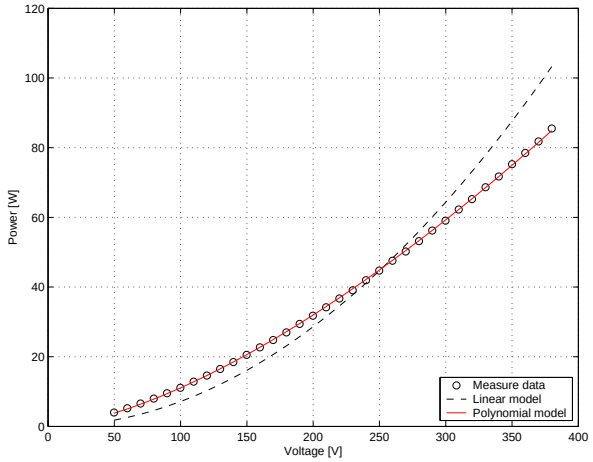

(b) Lamp 2: Power vs. Voltage.

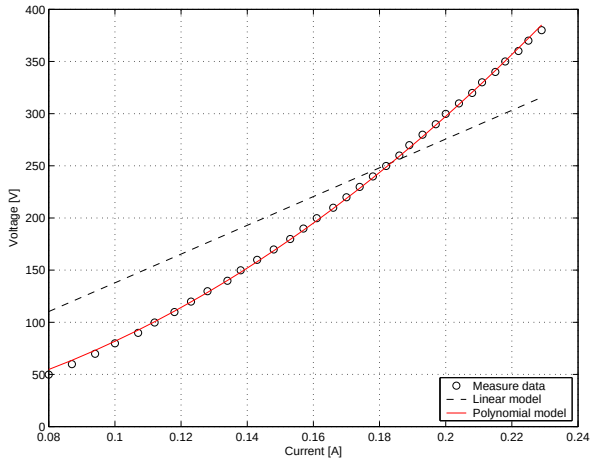

(c) Lamp 3: Voltage vs. Current.

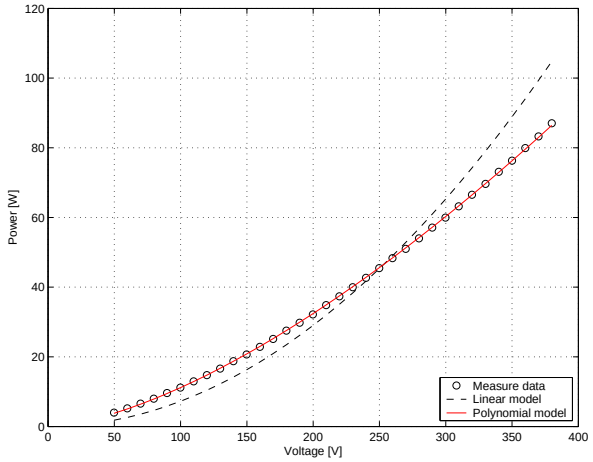

(d) Lamp 3: Power vs. Voltage.

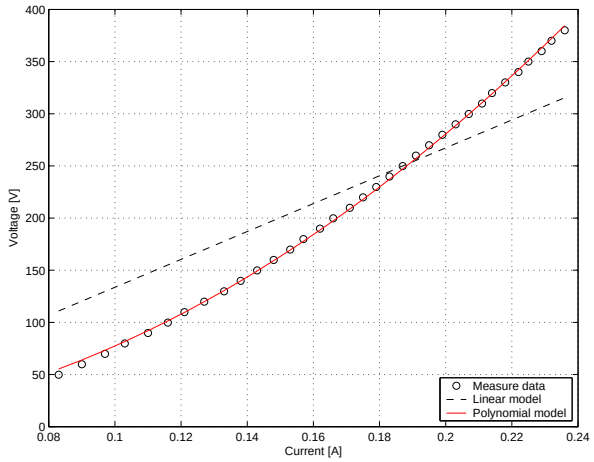

(e) Lamp 4: Voltage vs. Current.

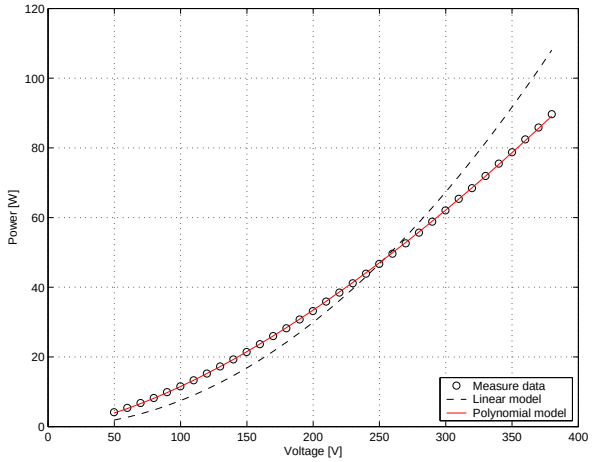

(f) Lamp 4: Power vs. Voltage.

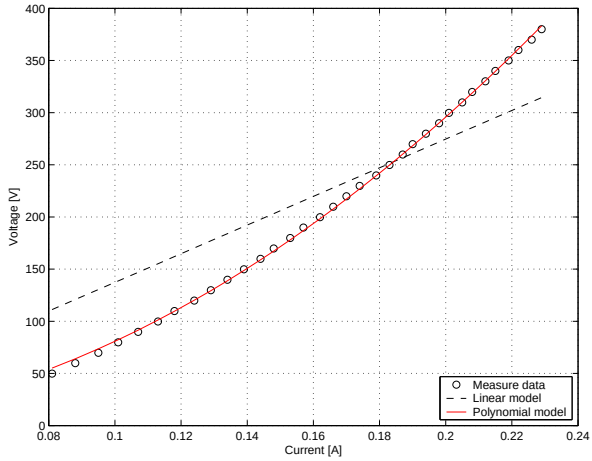

(g) Lamp 5: Voltage vs. Current.

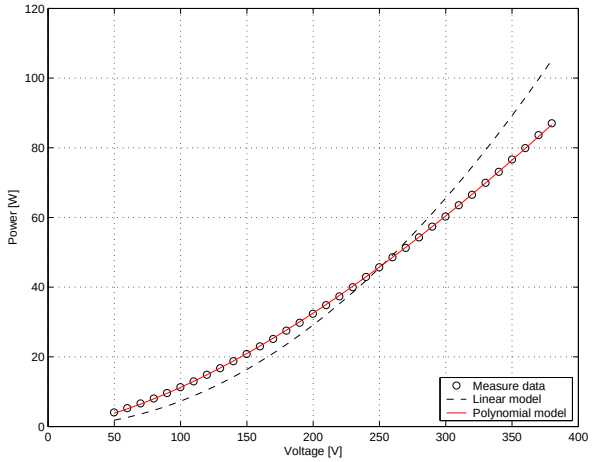

(h) Lamp 5: Power vs. Voltage.

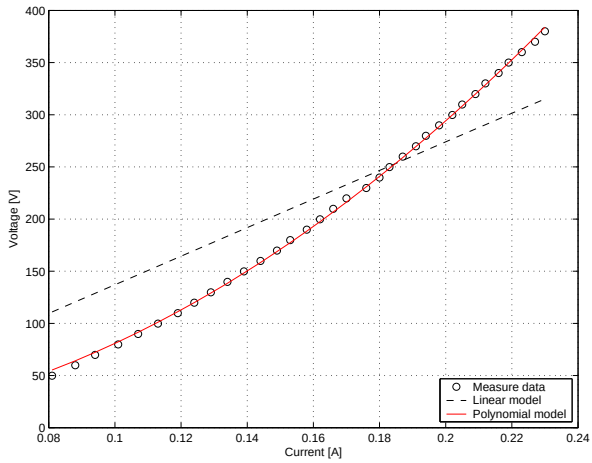

(i) Lamp 6: Voltage vs. Current.

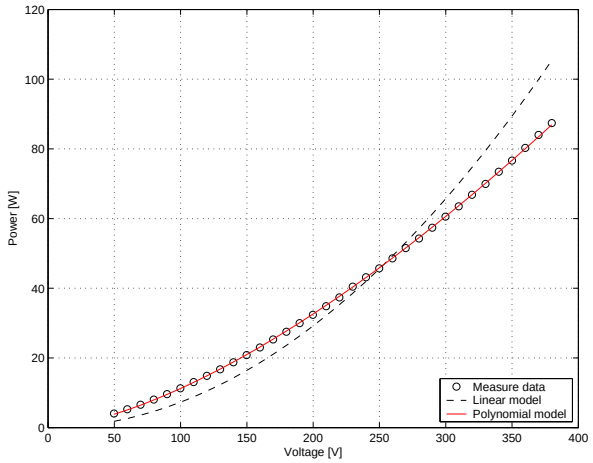

(j) Lamp 6: Power vs. Voltage.

Figure H.2: Characteristics of 40 W incandescent lamps.

60 W Incandescent Lamps

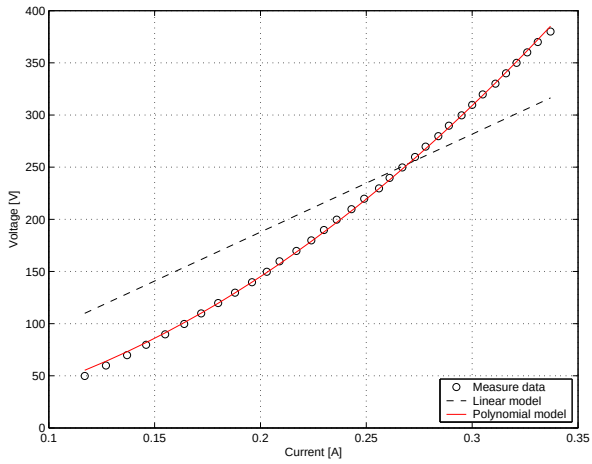

(a) Lamp 2: Voltage vs. Current.

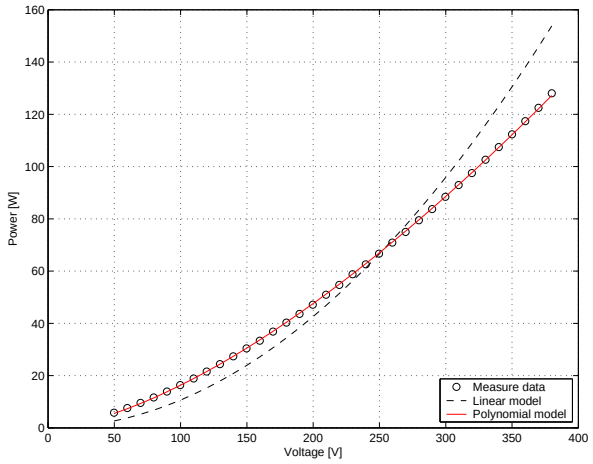

(b) Lamp 2: Power vs. Voltage.

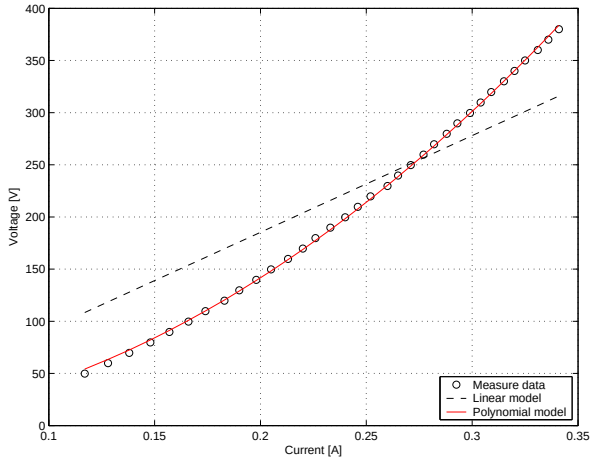

(c) Lamp 3: Voltage vs. Current.

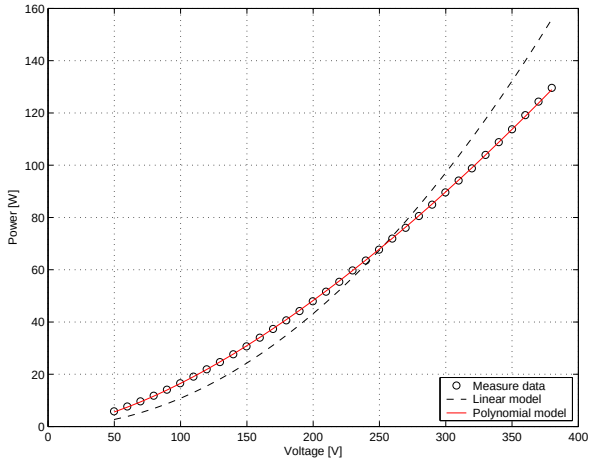

(d) Lamp 3: Power vs. Voltage.

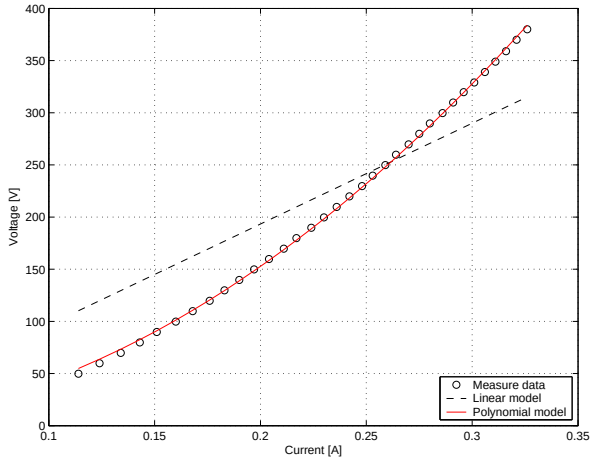

(e) Lamp 4: Voltage vs. Current.

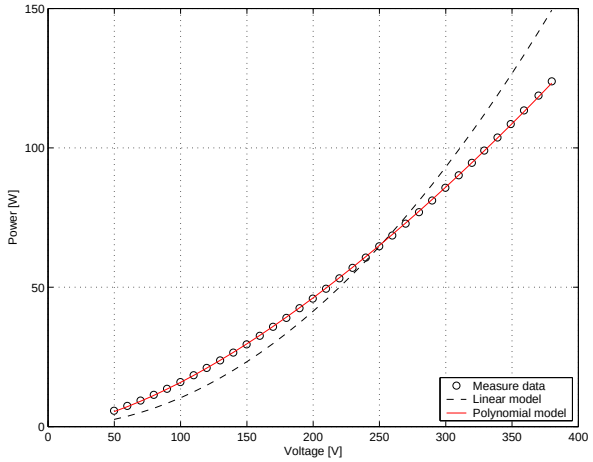

(f) Lamp 4: Power vs. Voltage.

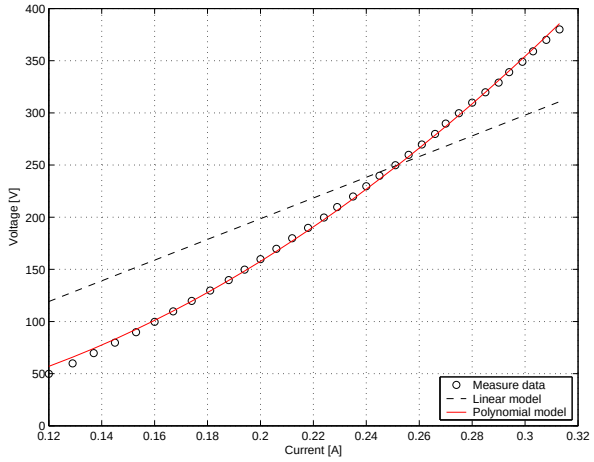

(g) Lamp 5: Voltage vs. Current.

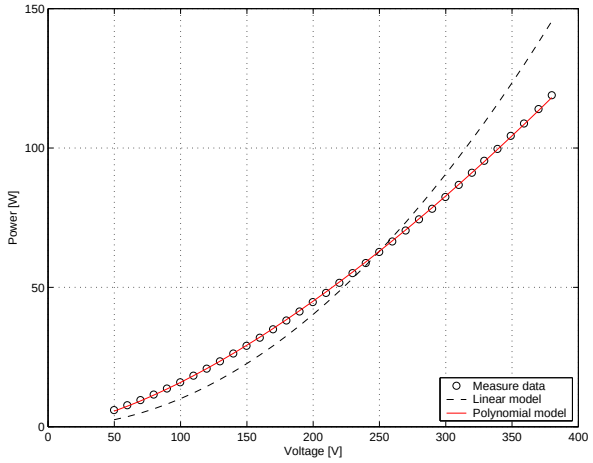

(h) Lamp 5: Power vs. Voltage.

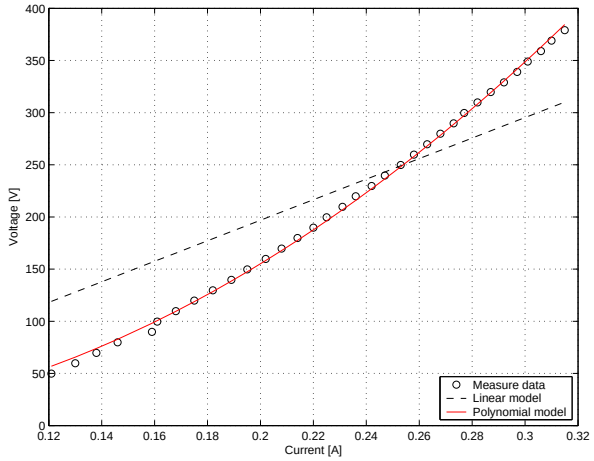

(i) Lamp 6: Voltage vs. Current.

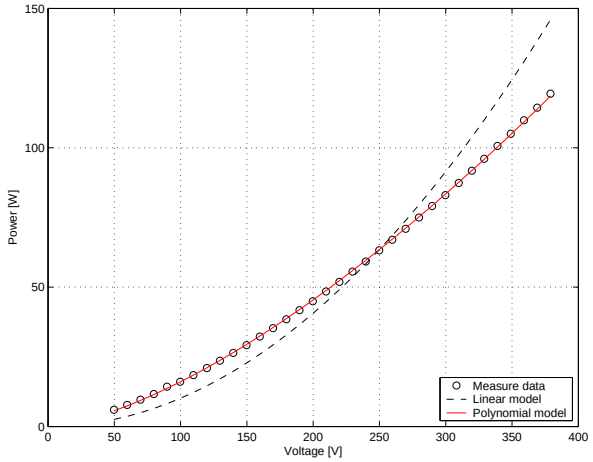

(j) Lamp 6: Power vs. Voltage.

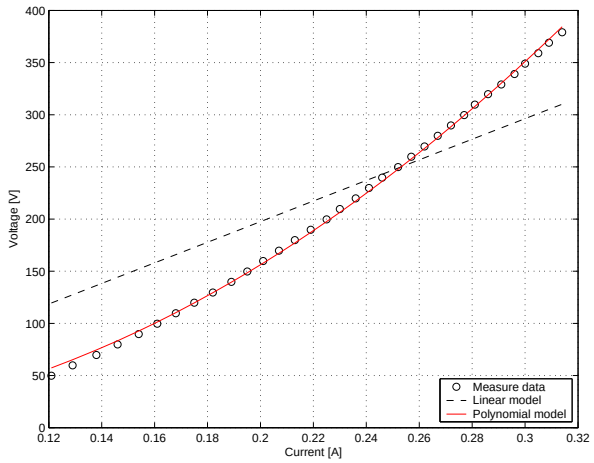

(k) Lamp 7: Voltage vs. Current.

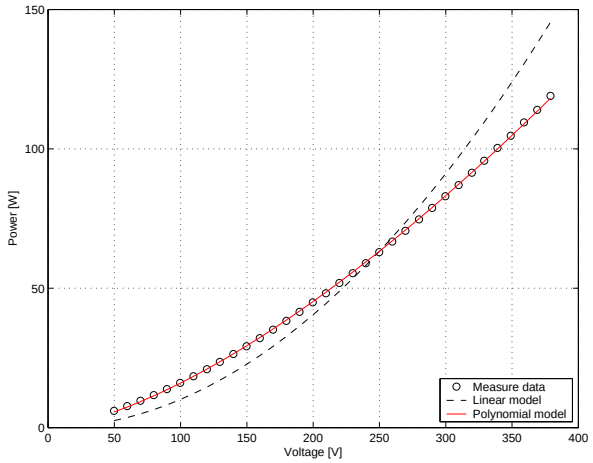

(l) Lamp 7: Power vs. Voltage.

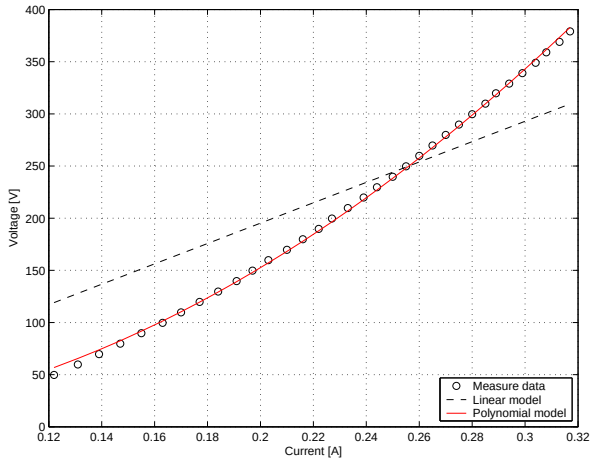

(m) Lamp 8: Voltage vs. Current.

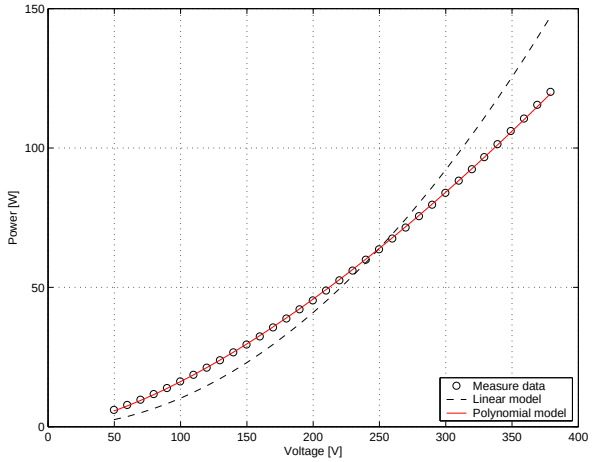

(n) Lamp 8: Power vs. Voltage.

Figure H.3: Characteristics of 60 W incandescent lamps.

75 W Incandescent Lamps

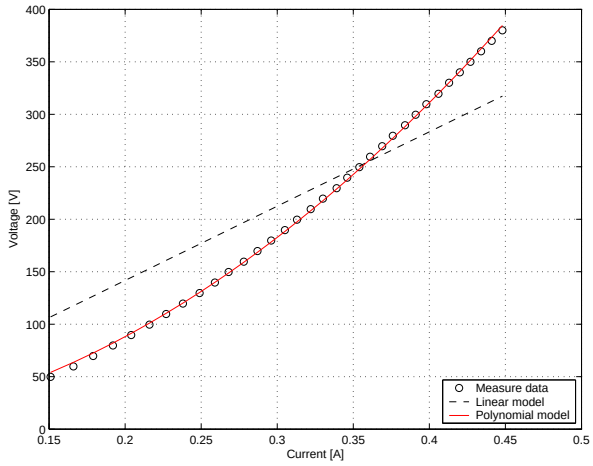

(a) Lamp 2: Voltage vs. Current.

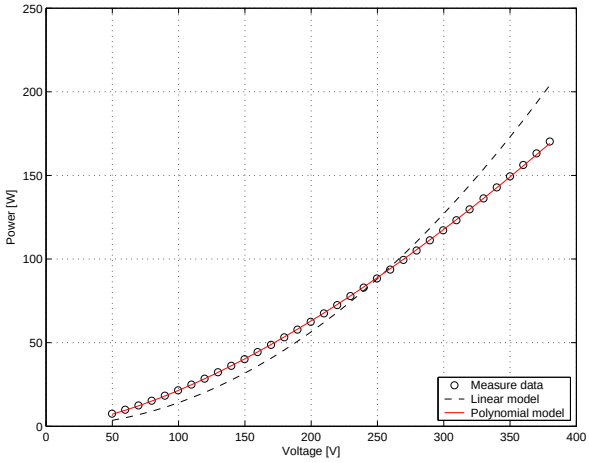

(b) Lamp 2: Power vs. Voltage.

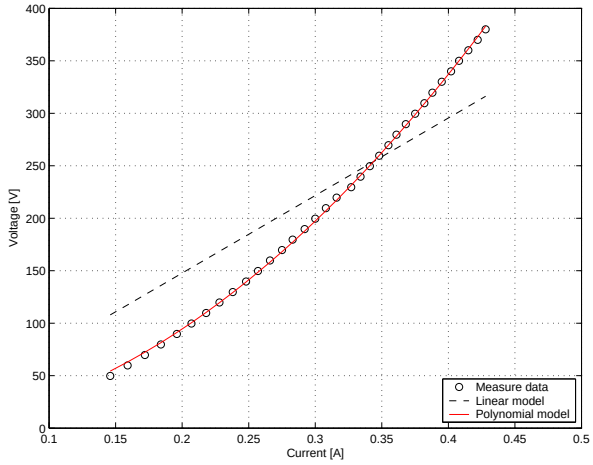

(c) Lamp 3: Voltage vs. Current.

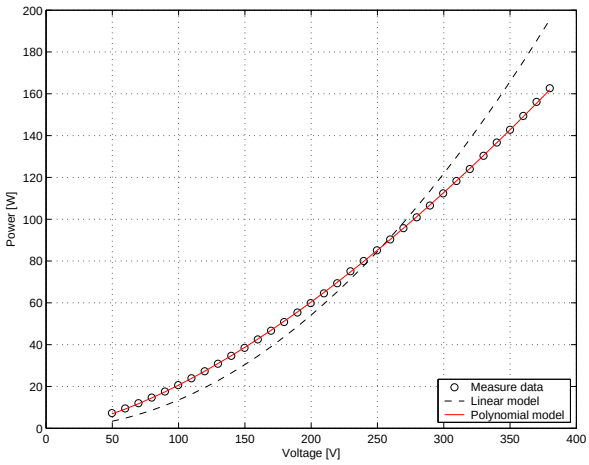

(d) Lamp 3: Power vs. Voltage.

Figure H.4: Characteristics of 75 W incandescent lamps.

100 W Incandescent Lamps

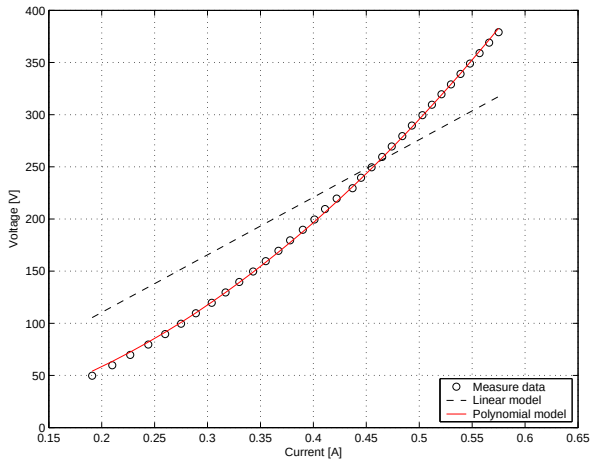

(a) Lamp 2: Voltage vs. Current.

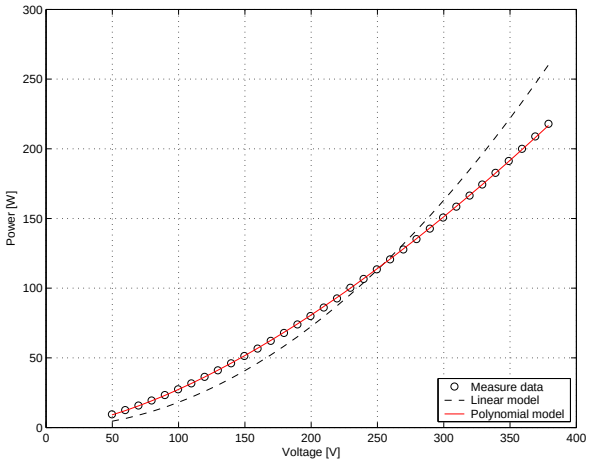

(b) Lamp 2: Power vs. Voltage.

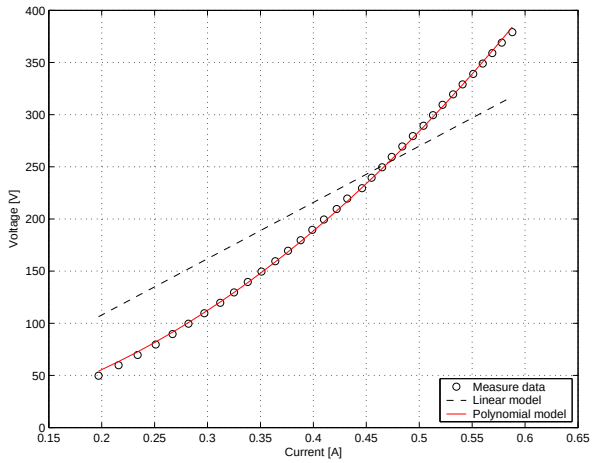

(c) Lamp 3: Voltage vs. Current.

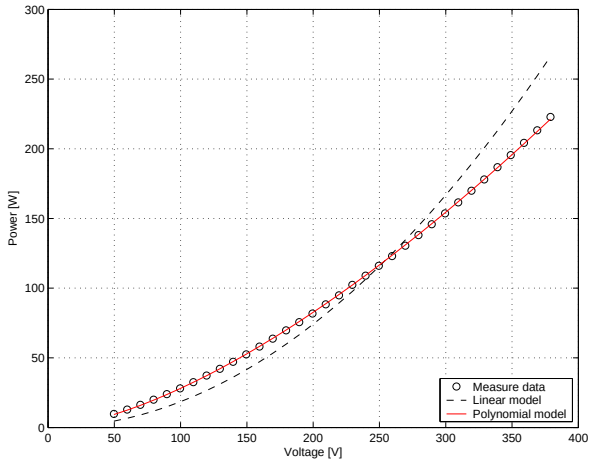

(d) Lamp 3: Power vs. Voltage.

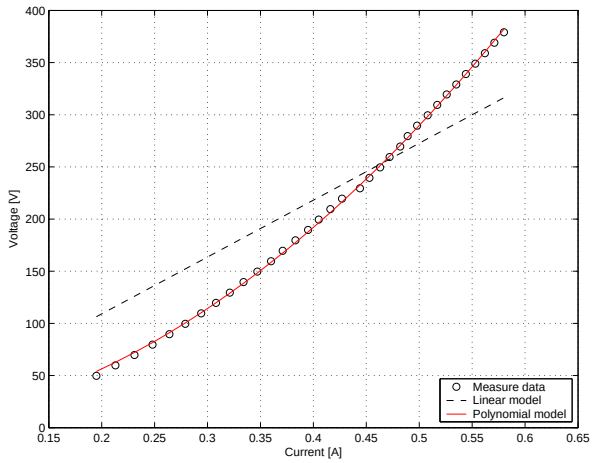

(e) Lamp 4: Voltage vs. Current.

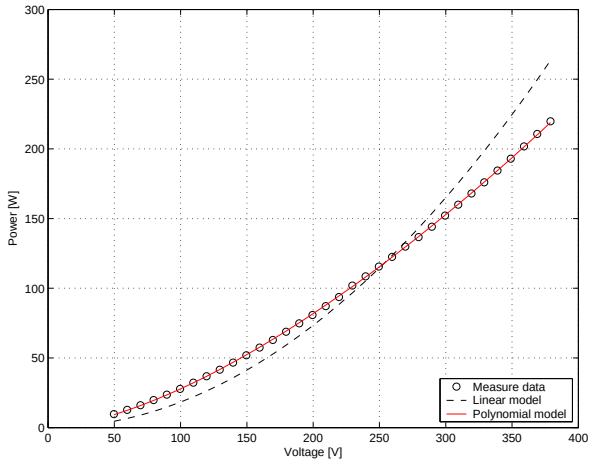

(f) Lamp 4: Power vs. Voltage.

Figure H.5: Characteristics of 100 W incandescent lamps.

Transients

The following figures presents the results obtained in the transient analysis of the lamps tested in this thesis, where the measurement is shown (measured) as well as the simulation results, both when the model is subjected to the analytical step (modelled) and a typical step obtained from measurements (simulated).

25 W Incandescent Lamp 2

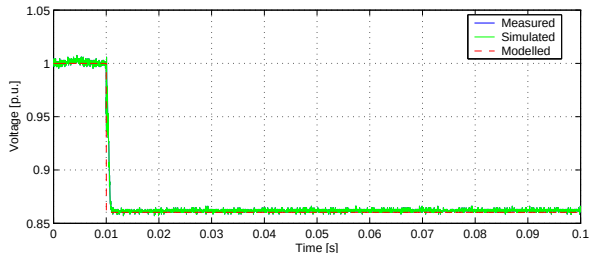

(a) Voltage - Step 1.

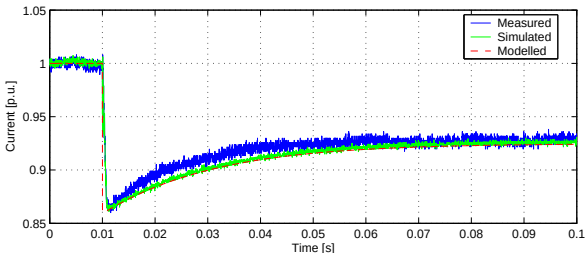

(b) Current - Step 1.

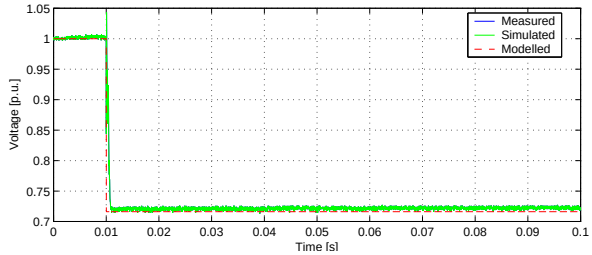

(c) Voltage - Step 2.

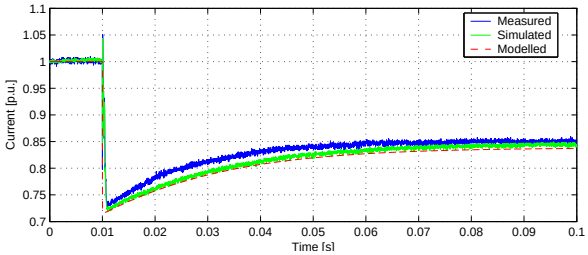

(d) Current - Step 2.

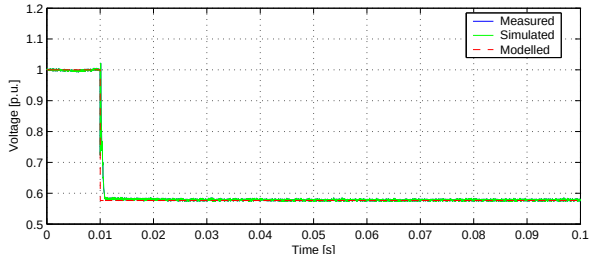

(e) Voltage - Step 3.

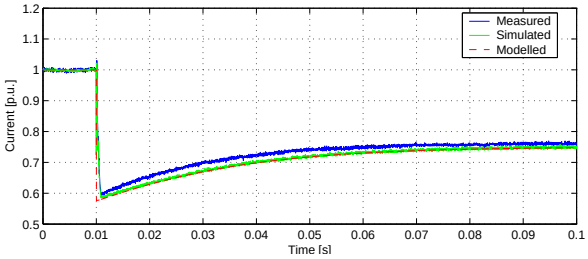

(f) Current - Step 3.

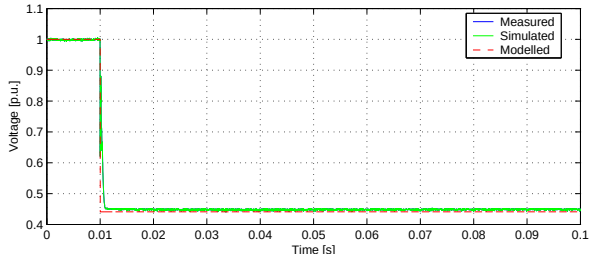

(g) Voltage - Step 4.

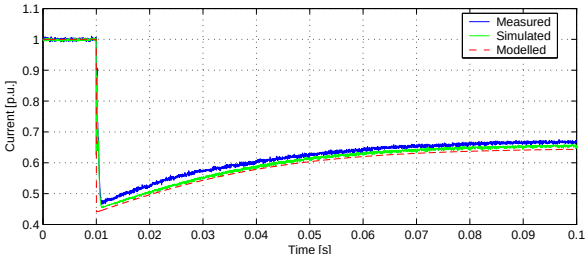

(h) Current - Step 4.

Figure H.6: Transient behavior of 25 W incandescent lamp 2.

25 W Incandescent Lamp 3

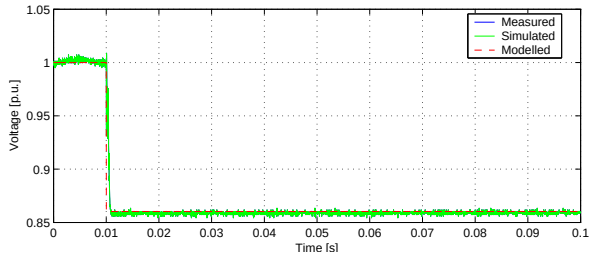

(a) Voltage - Step 1.

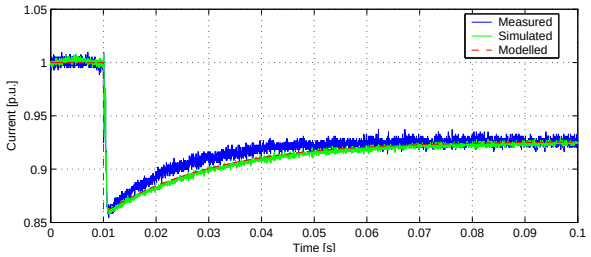

(b) Current - Step 1.

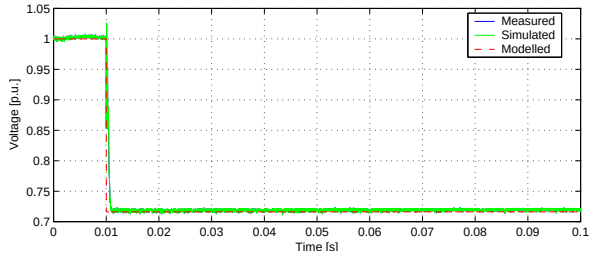

(c) Voltage - Step 2.

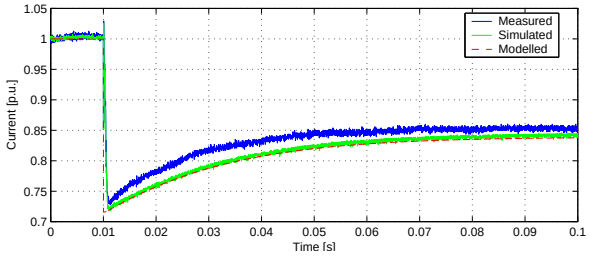

(d) Current - Step 2.

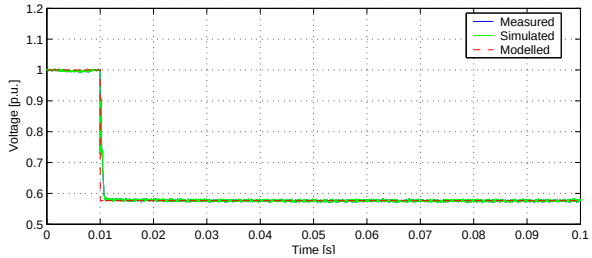

(e) Voltage - Step 3.

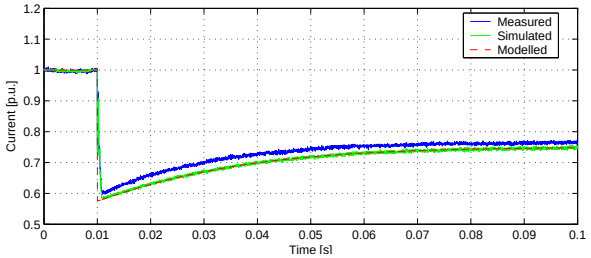

(f) Current - Step 3.

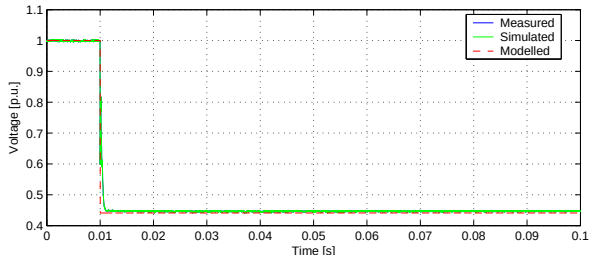

(g) Voltage - Step 4.

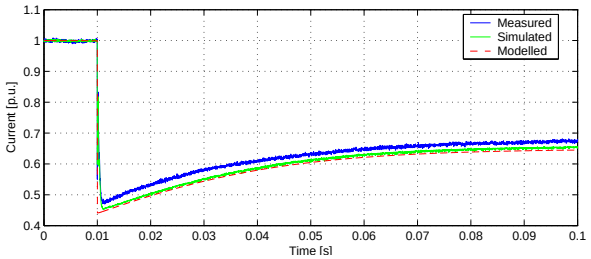

(h) Current - Step 4.

Figure H.7: Transient behavior of 25 W incandescent lamp 3.

25 W Incandescent Lamp 4

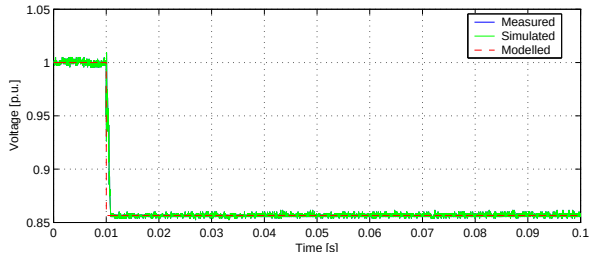

(a) Voltage - Step 1.

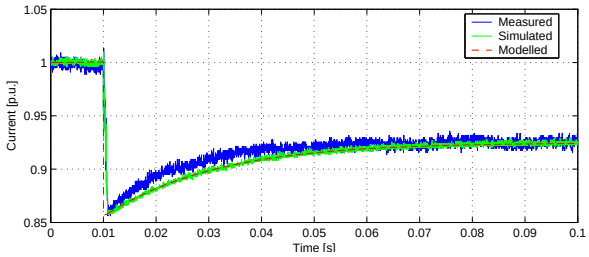

(b) Current - Step 1.

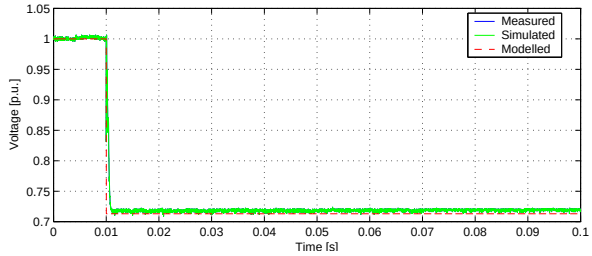

(c) Voltage - Step 2.

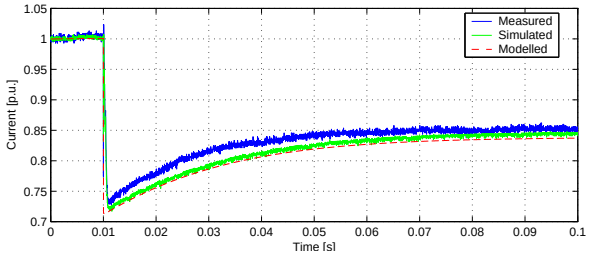

(d) Current - Step 2.

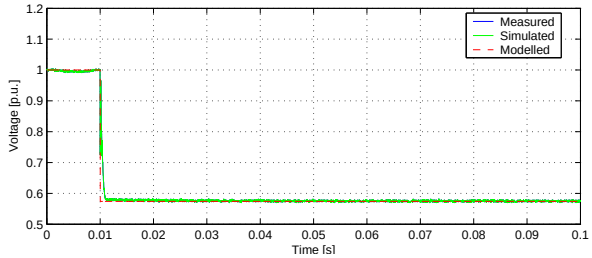

(e) Voltage - Step 3.

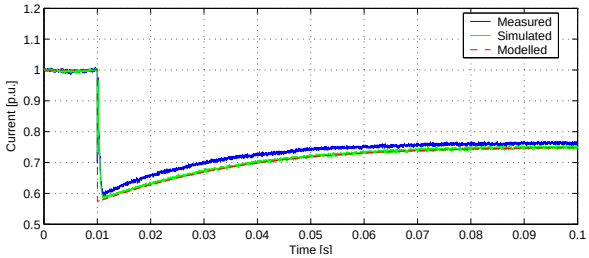

(f) Current - Step 3.

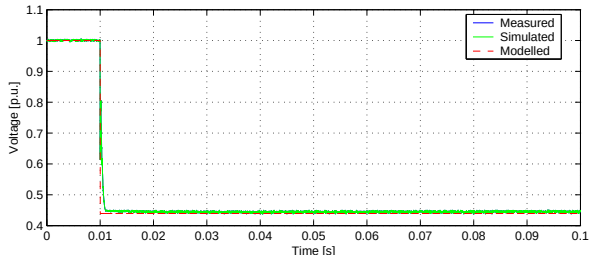

(g) Voltage - Step 4.

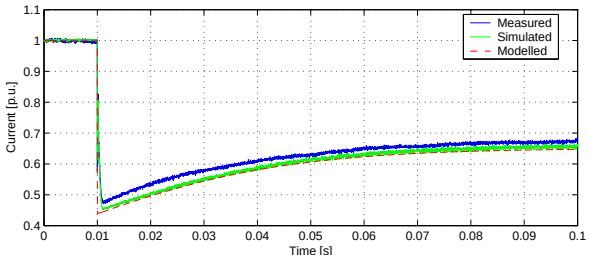

(h) Current - Step 4.

Figure H.8: Transient behavior of 25 W incandescent lamp 4.

25 W Incandescent Lamp 5

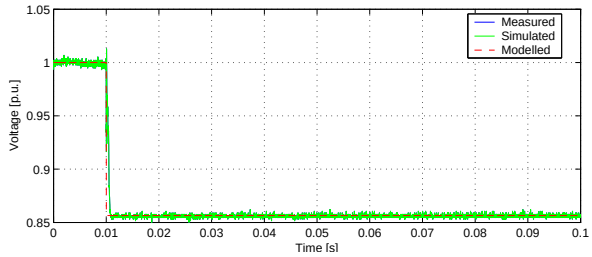

(a) Voltage - Step 1.

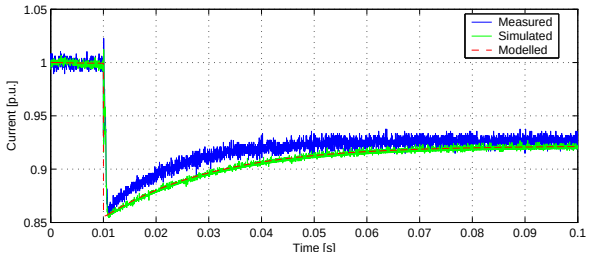

(b) Current - Step 1.

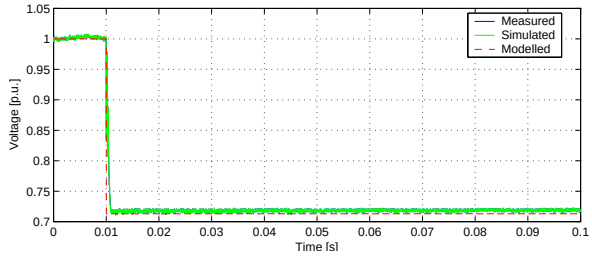

(c) Voltage - Step 2.

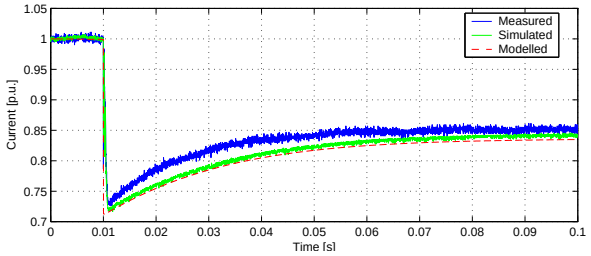

(d) Current - Step 2.

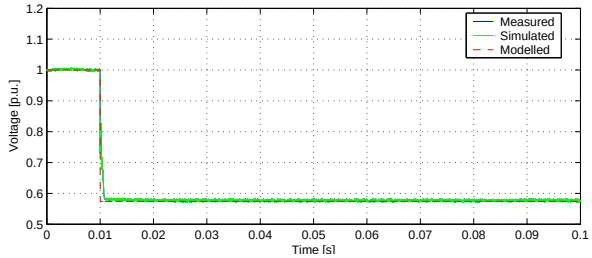

(e) Voltage - Step 3.

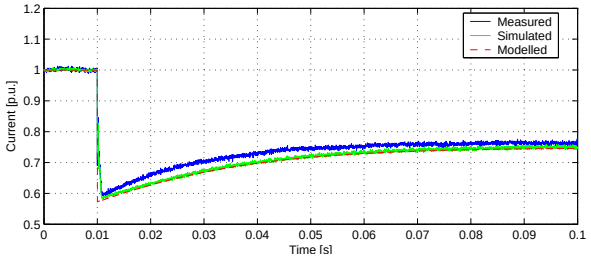

(f) Current - Step 3.

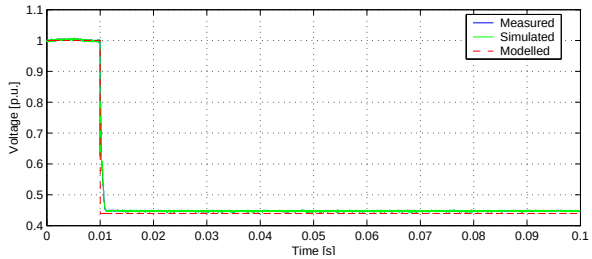

(g) Voltage - Step 4.

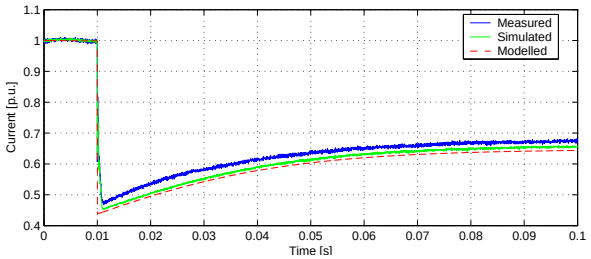

(h) Current - Step 4.

Figure H.9: Transient behavior of 25 W incandescent lamp 5.

40 W Incandescent Lamp 2

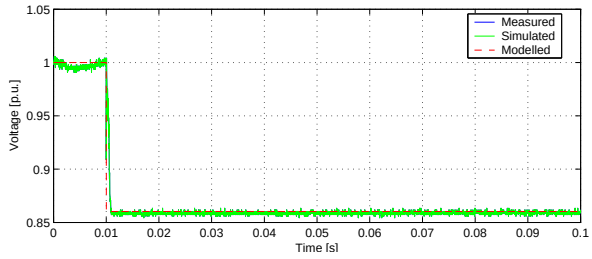

(a) Voltage - Step 1.

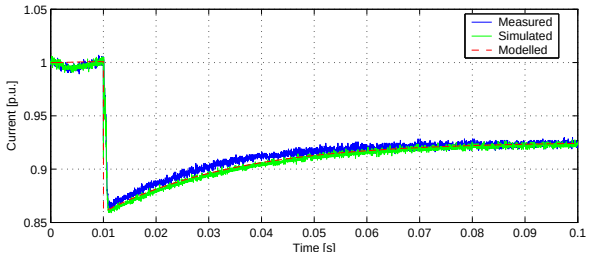

(b) Current - Step 1.

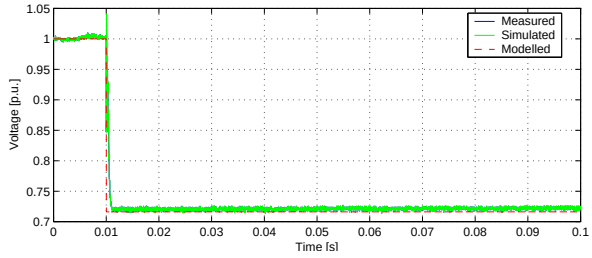

(c) Voltage - Step 2.

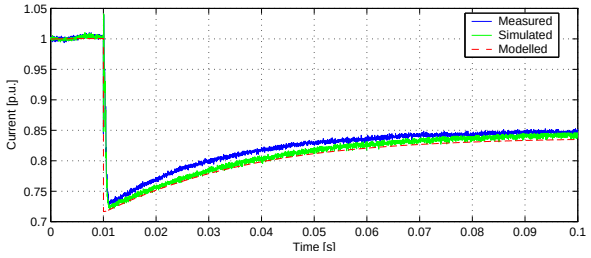

(d) Current - Step 2.

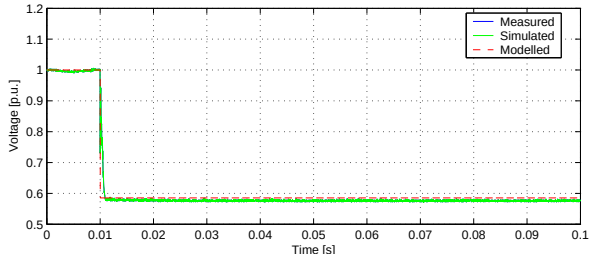

(e) Voltage - Step 3.

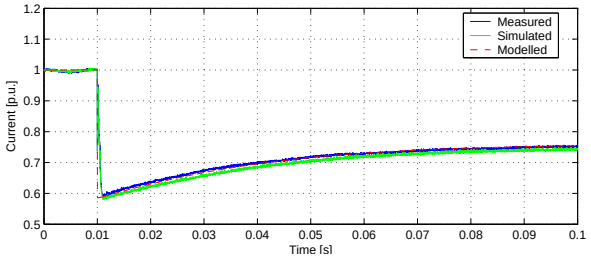

(f) Current - Step 3.

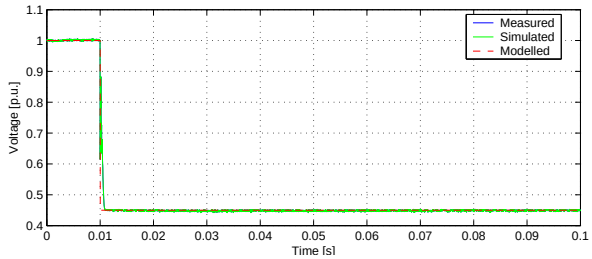

(g) Voltage - Step 4.

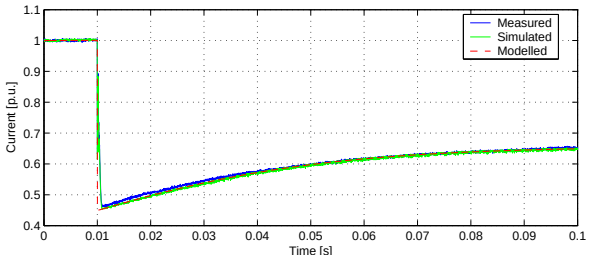

(h) Current - Step 4.

Figure H.10: Transient behavior of 40 W incandescent lamp 2.

40 W Incandescent Lamp 3

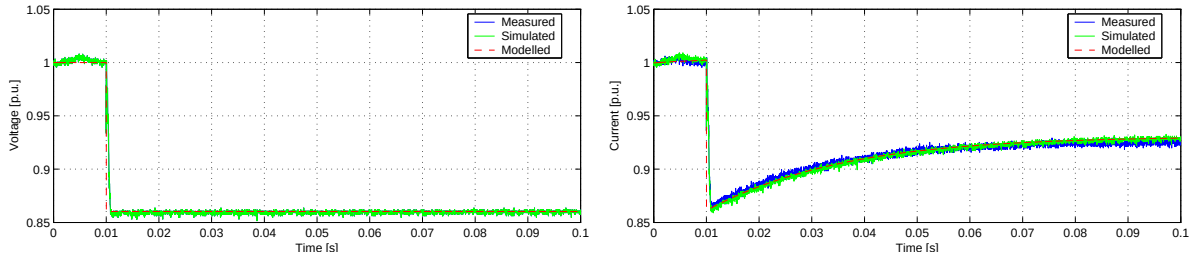

(a) Voltage - Step 1.

(b) Current - Step 1.

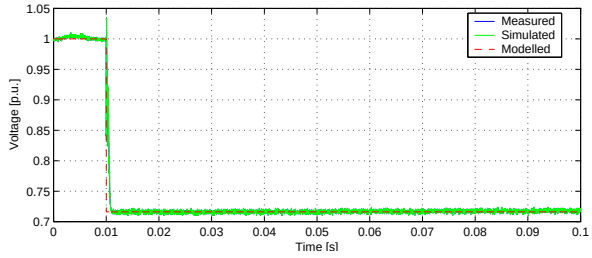

(c) Voltage - Step 2.

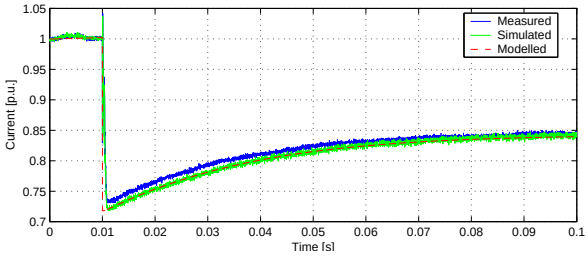

(d) Current - Step 2.

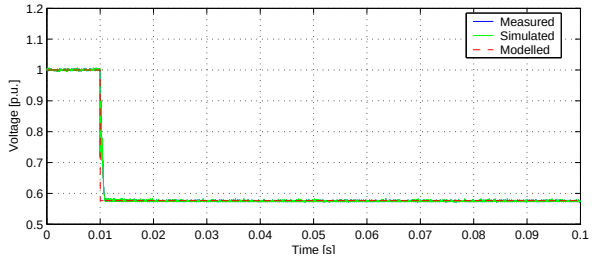

(e) Voltage - Step 3.

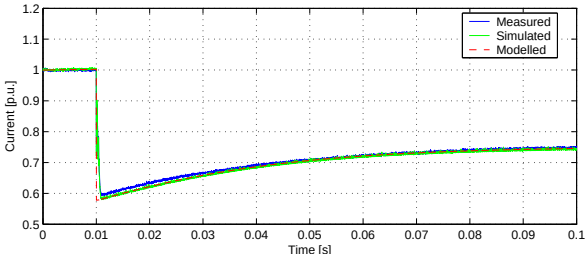

(f) Current - Step 3.

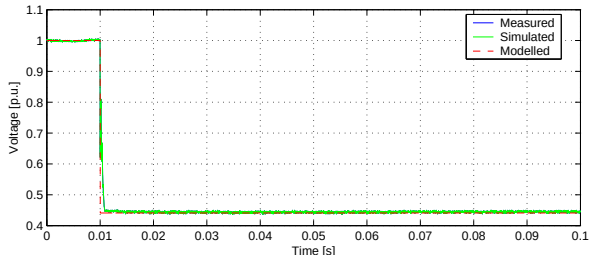

(g) Voltage - Step 4.

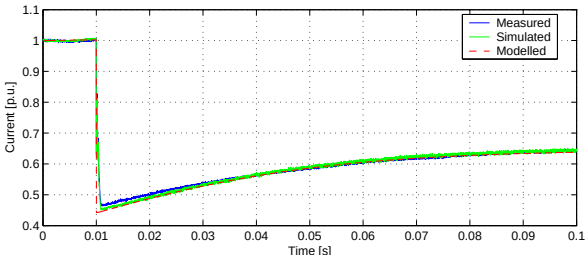

(h) Current - Step 4.

Figure H.11: Transient behavior of 40 W incandescent lamp 3.

40 W Incandescent Lamp 4

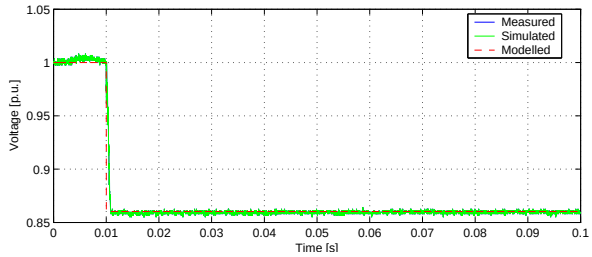

(a) Voltage - Step 1.

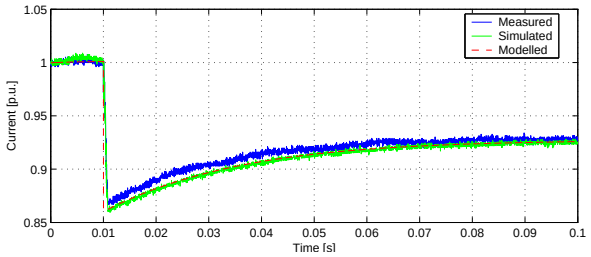

(b) Current - Step 1.

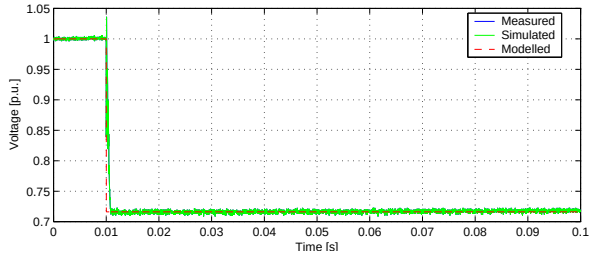

(c) Voltage - Step 2.

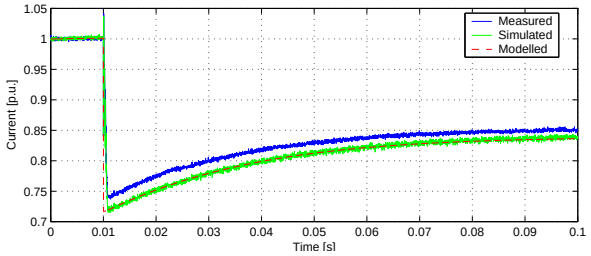

(d) Current - Step 2.

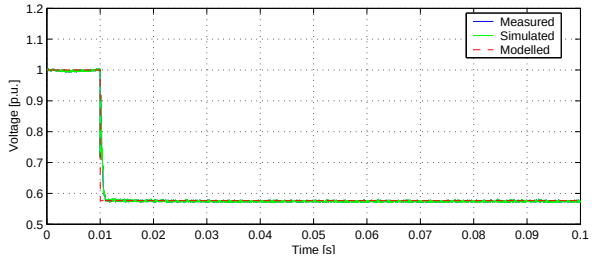

(e) Voltage - Step 3.

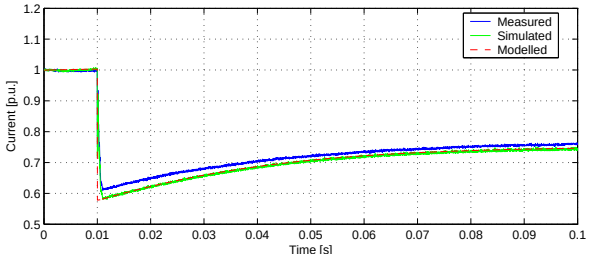

(f) Current - Step 3.

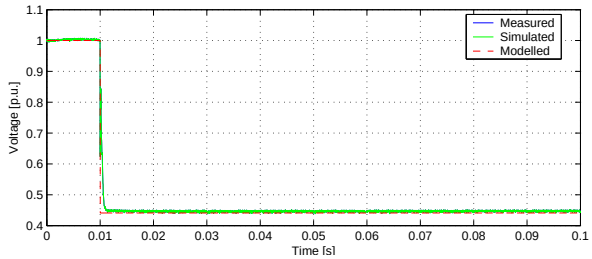

(g) Voltage - Step 4.

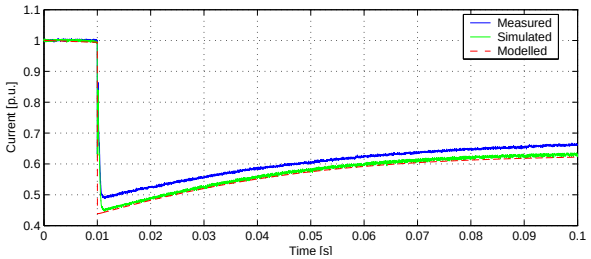

(h) Current - Step 4.

Figure H.12: Transient behavior of 40 W incandescent lamp 4.

40 W Incandescent Lamp 5

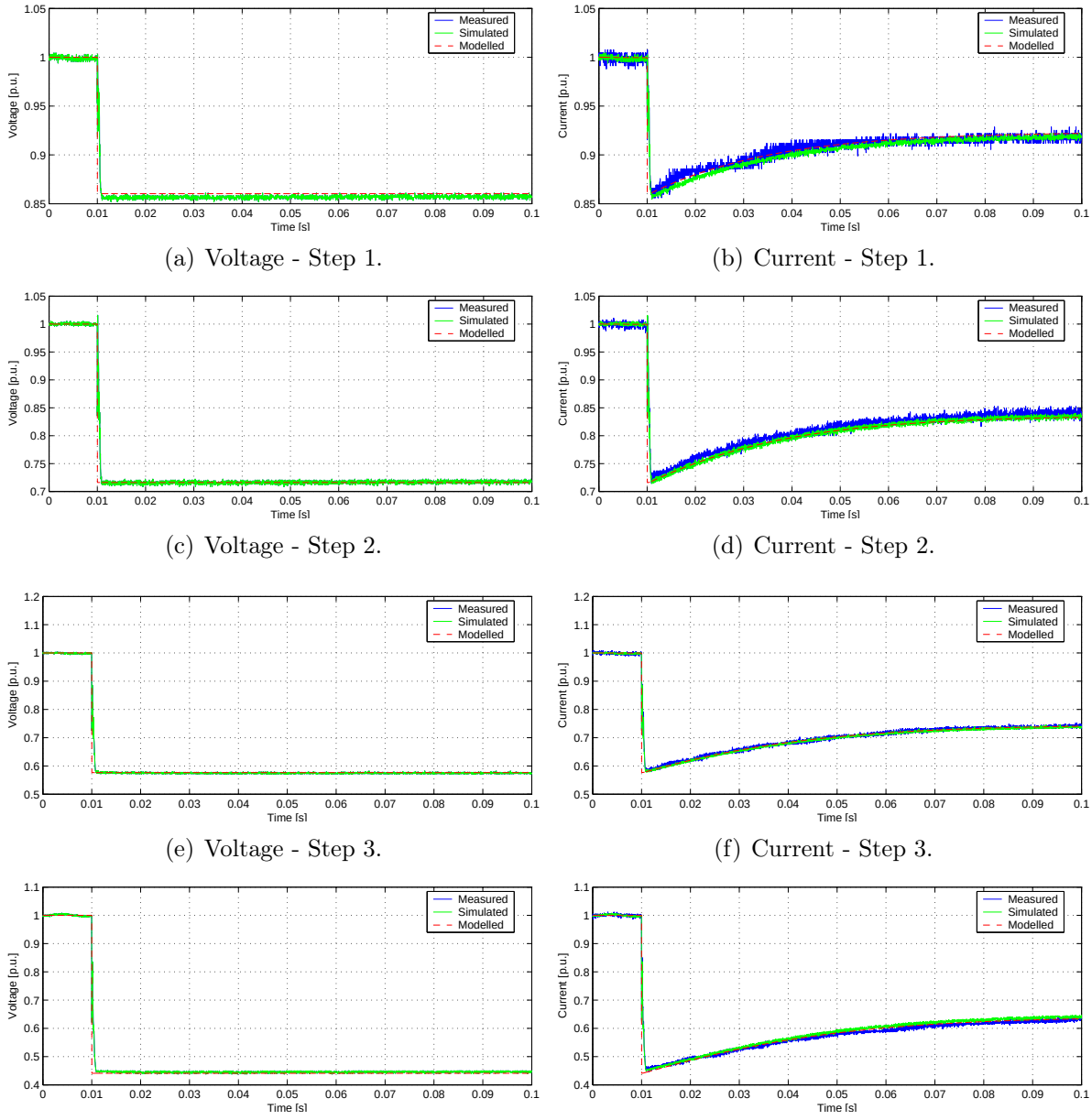

(a) Voltage - Step 1.

(b) Current - Step 1.

(c) Voltage - Step 2.

(d) Current - Step 2.

(e) Voltage - Step 3.

(f) Current - Step 3.

(g) Voltage - Step 4.

(h) Current - Step 4.

Figure H.13: Transient behavior of 40 W incandescent lamp 5.

40 W Incandescent Lamp 6

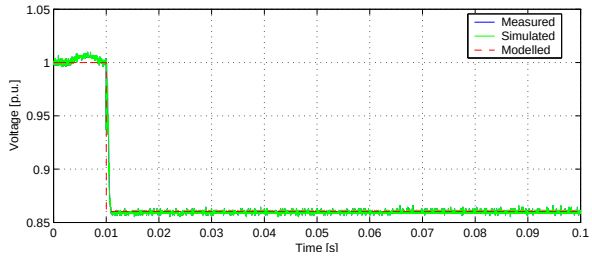

(a) Voltage - Step 1.

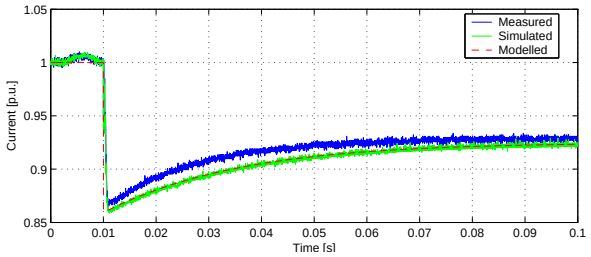

(b) Current - Step 1.

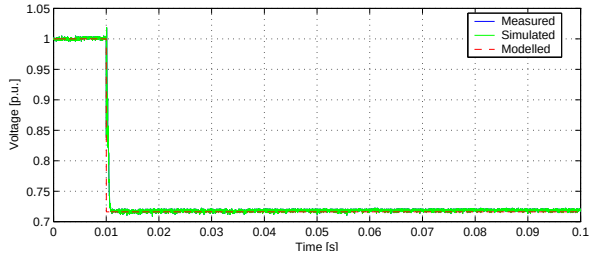

(c) Voltage - Step 2.

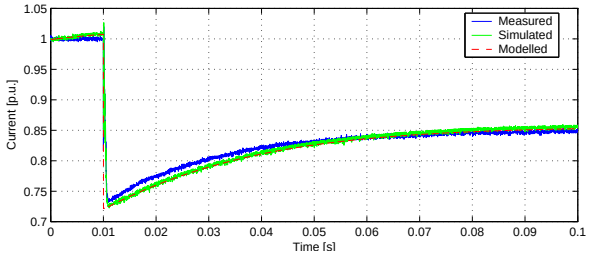

(d) Current - Step 2.

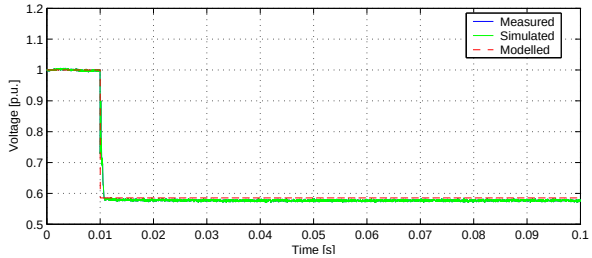

(e) Voltage - Step 3.

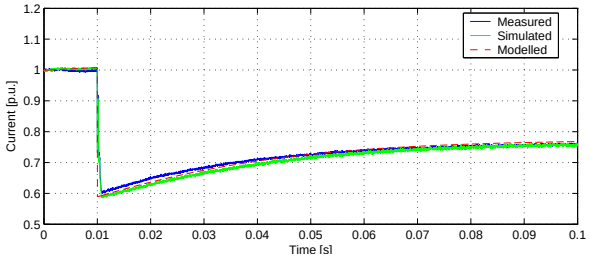

(f) Current - Step 3.

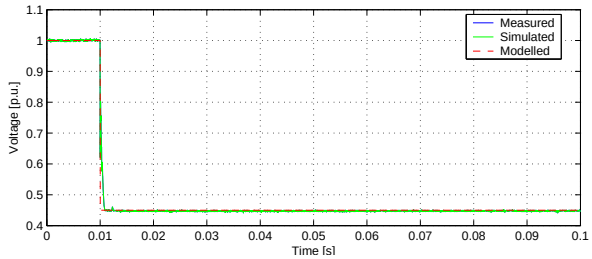

(g) Voltage - Step 4.

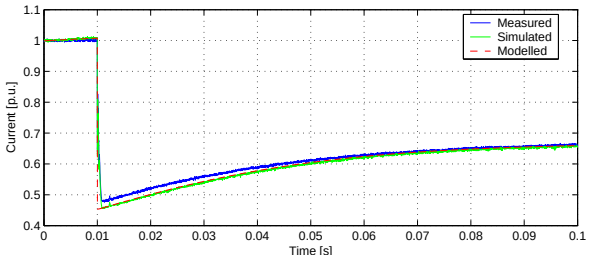

(h) Current - Step 4.

Figure H.14: Transient behavior of 40 W incandescent lamp 6.

60 W Incandescent Lamp 2

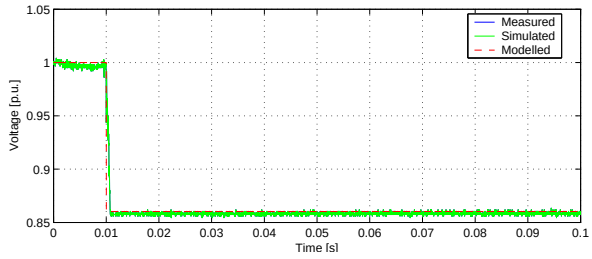

(a) Voltage - Step 1.

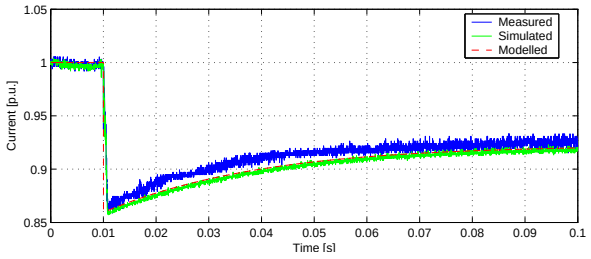

(b) Current - Step 1.

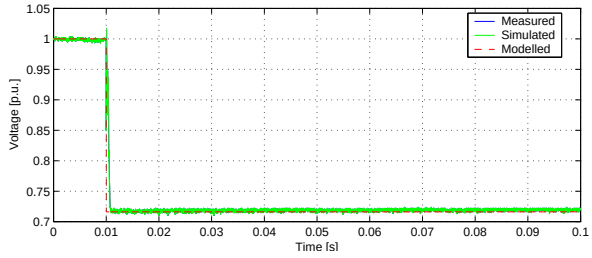

(c) Voltage - Step 2.

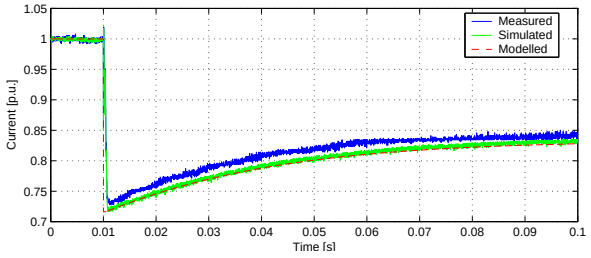

(d) Current - Step 2.

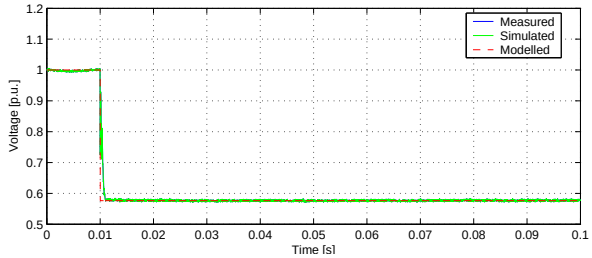

(e) Voltage - Step 3.

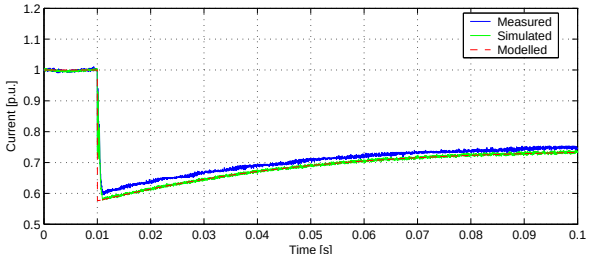

(f) Current - Step 3.

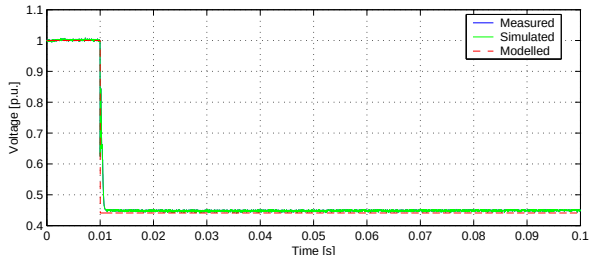

(g) Voltage - Step 4.

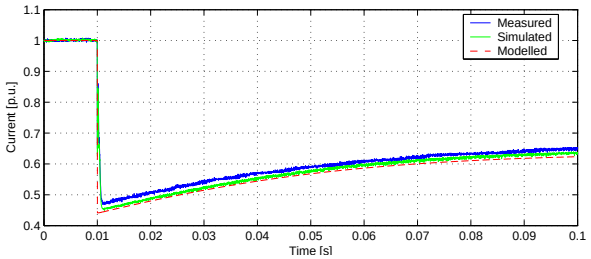

(h) Current - Step 4.

Figure H.15: Transient behavior of 60 W incandescent lamp 2.

60 W Incandescent Lamp 3

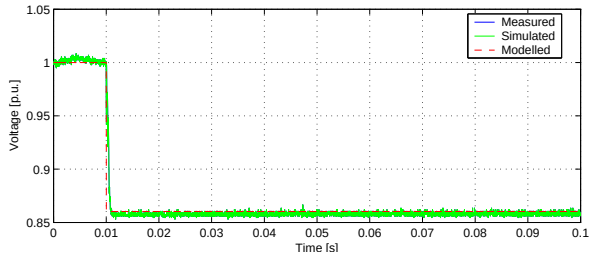

(a) Voltage - Step 1.

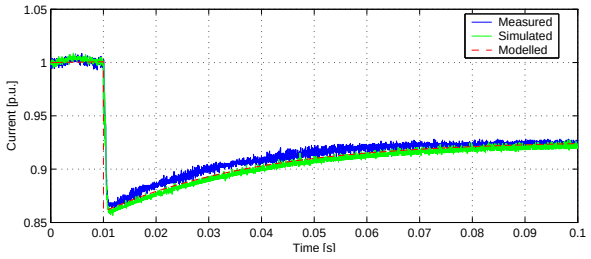

(b) Current - Step 1.

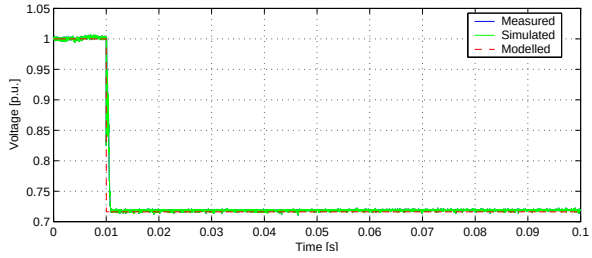

(c) Voltage - Step 2.

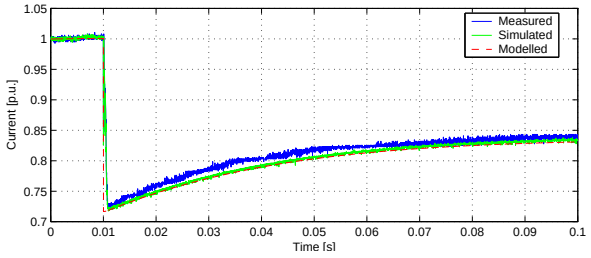

(d) Current - Step 2.

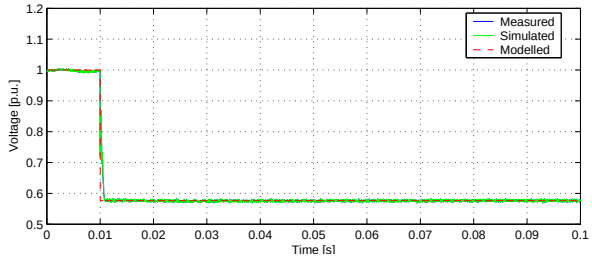

(e) Voltage - Step 3.

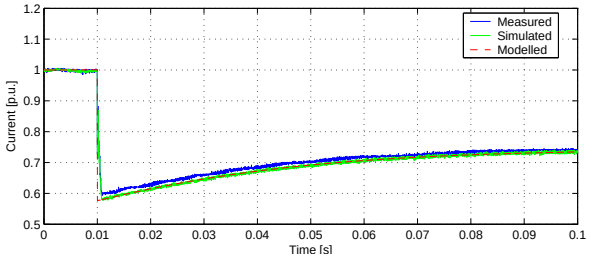

(f) Current - Step 3.

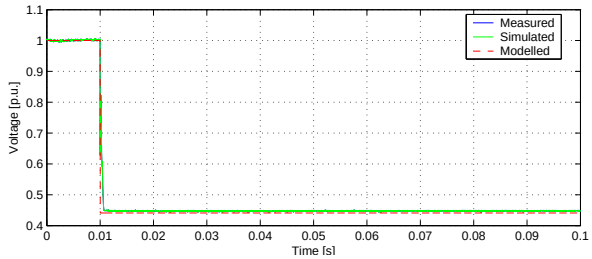

(g) Voltage - Step 4.

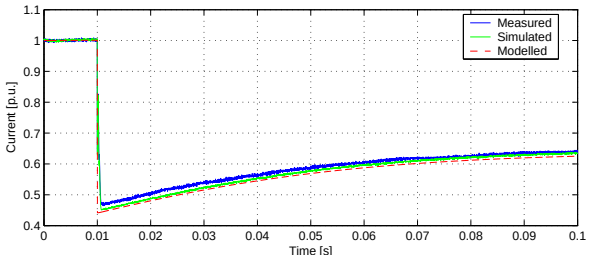

(h) Current - Step 4.

Figure H.16: Transient behavior of 60 W incandescent lamp 3.

60 W Incandescent Lamp 4

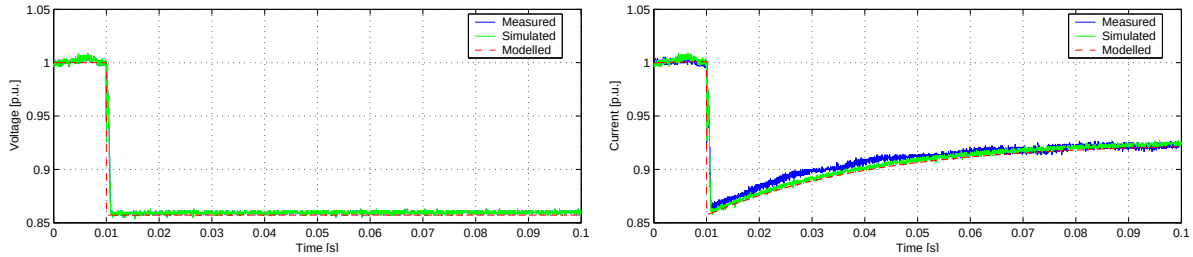

(a) Voltage - Step 1.

(b) Current - Step 1.

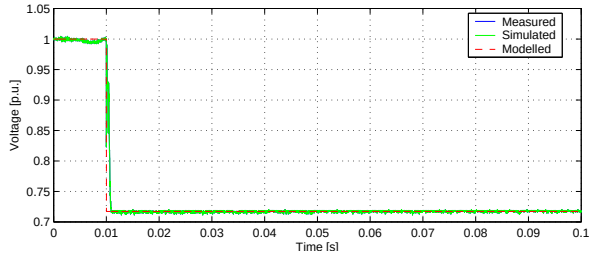

(c) Voltage - Step 2.

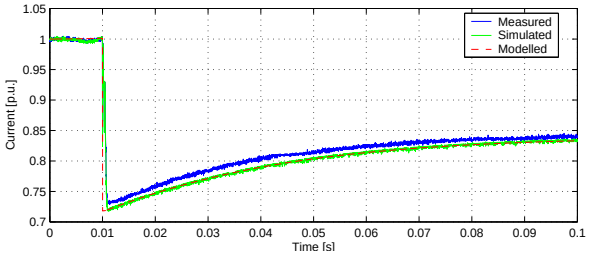

(d) Current - Step 2.

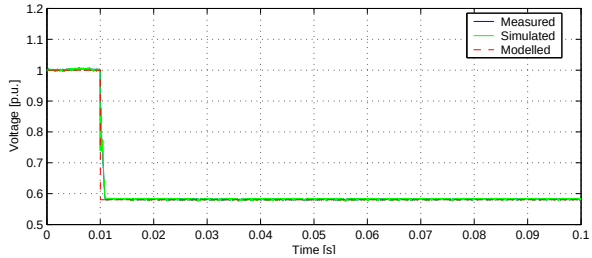

(e) Voltage - Step 3.

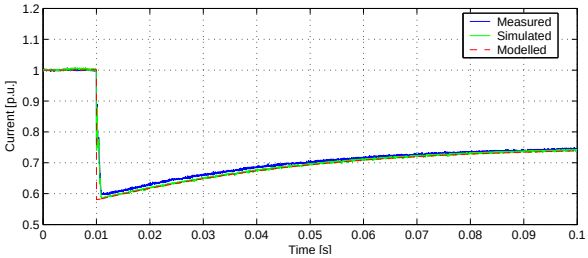

(f) Current - Step 3.

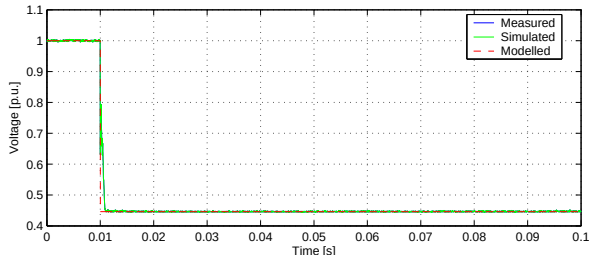

(g) Voltage - Step 4.

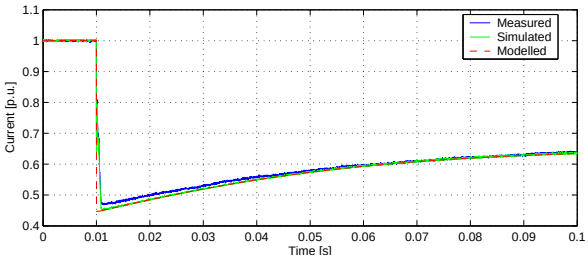

(h) Current - Step 4.

Figure H.17: Transient behavior of 60 W incandescent lamp 4.

60 W Incandescent Lamp 5

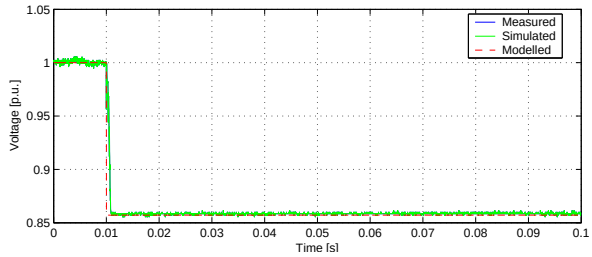

(a) Voltage - Step 1.

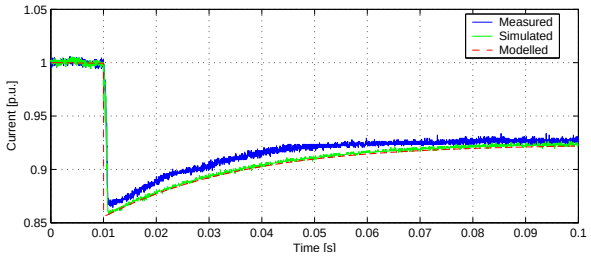

(b) Current - Step 1.

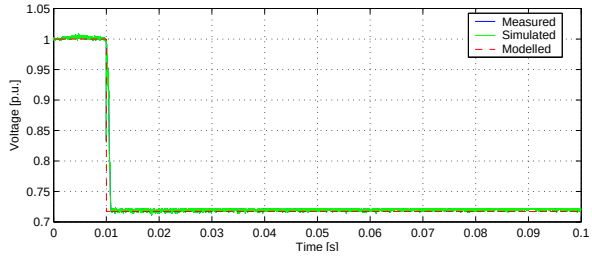

(c) Voltage - Step 2.

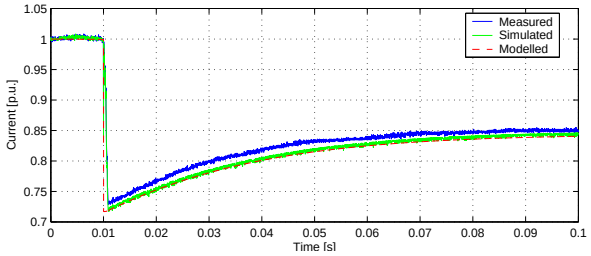

(d) Current - Step 2.

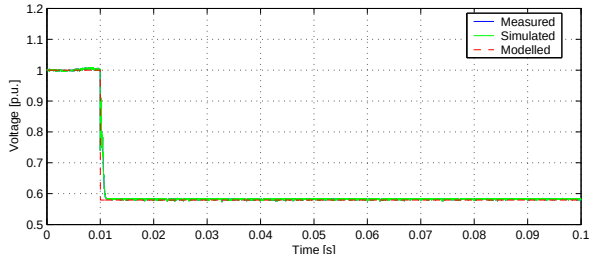

(e) Voltage - Step 3.

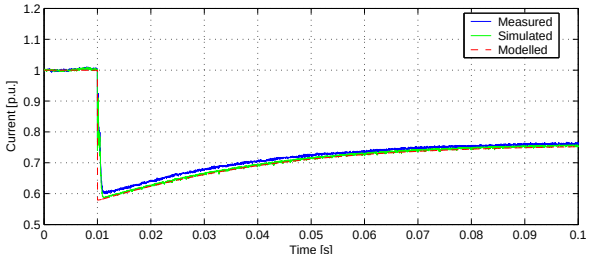

(f) Current - Step 3.

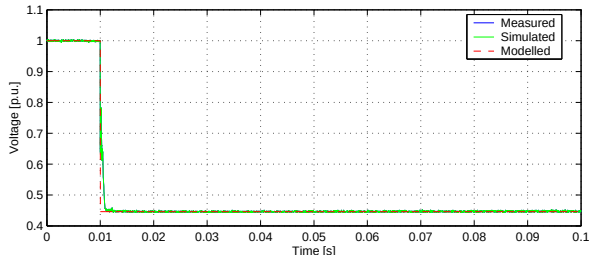

(g) Voltage - Step 4.

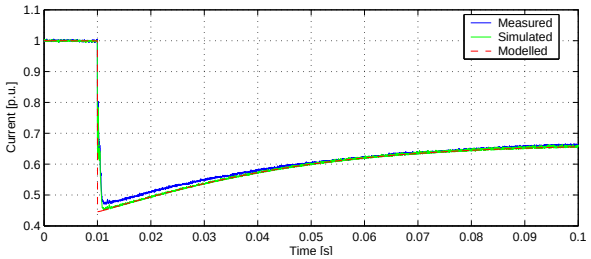

(h) Current - Step 4.

Figure H.18: Transient behavior of 60 W incandescent lamp 5.

60 W Incandescent Lamp 6

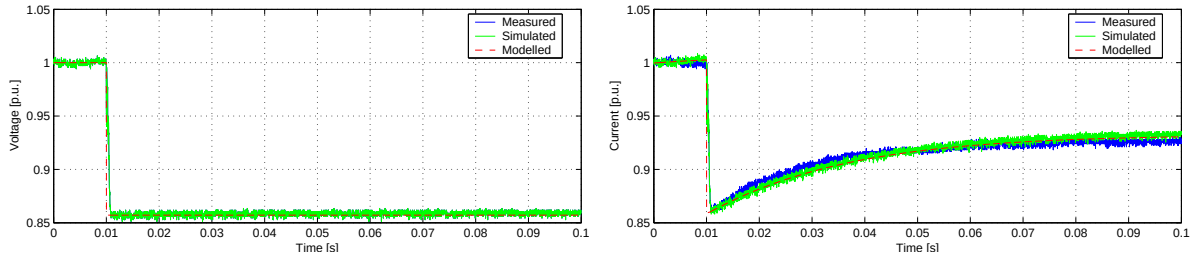

(a) Voltage - Step 1.

(b) Current - Step 1.

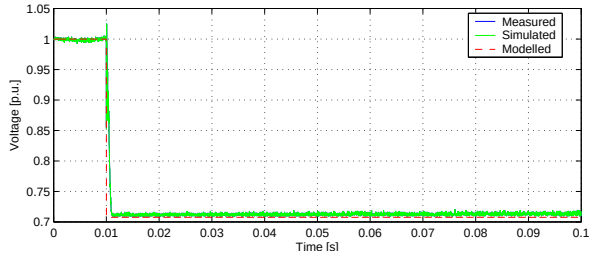

(c) Voltage - Step 2.

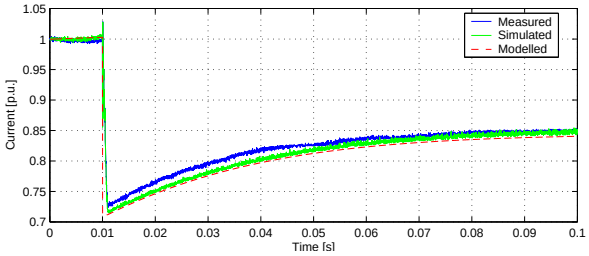

(d) Current - Step 2.

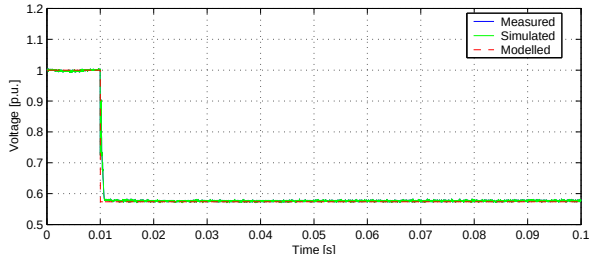

(e) Voltage - Step 3.

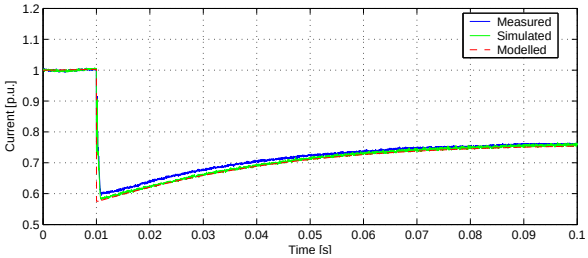

(f) Current - Step 3.

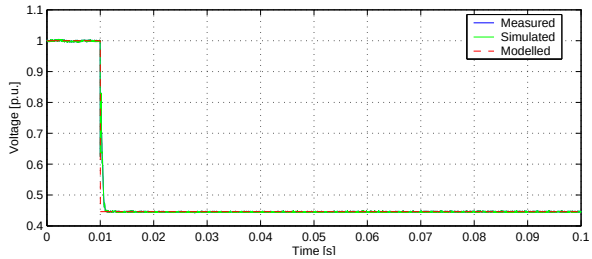

(g) Voltage - Step 4.

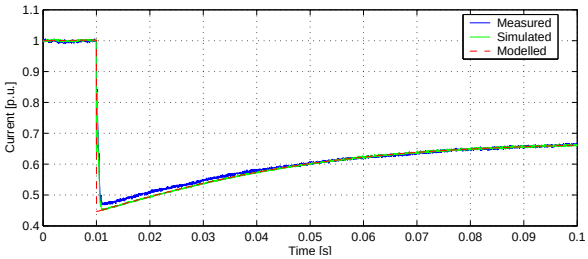

(h) Current - Step 4.

Figure H.19: Transient behavior of 60 W incandescent lamp 6.

60 W Incandescent Lamp 7

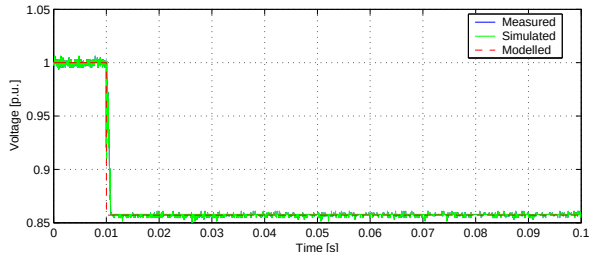

(a) Voltage - Step 1.

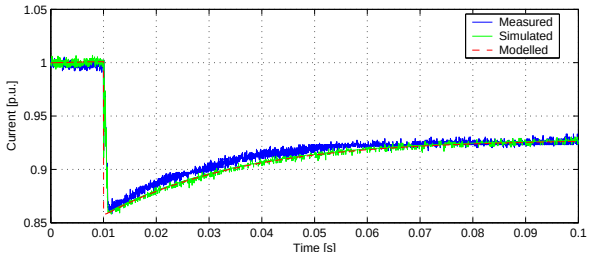

(b) Current - Step 1.

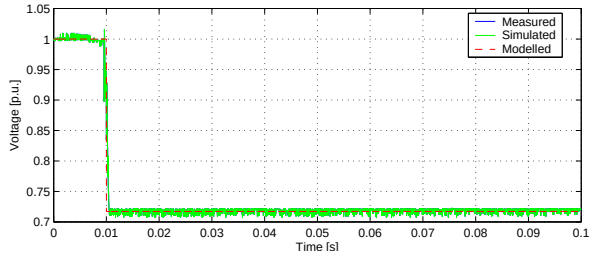

(c) Voltage - Step 2.

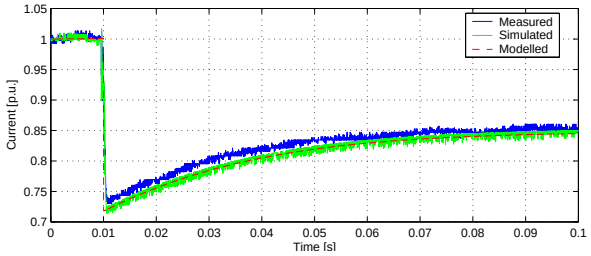

(d) Current - Step 2.

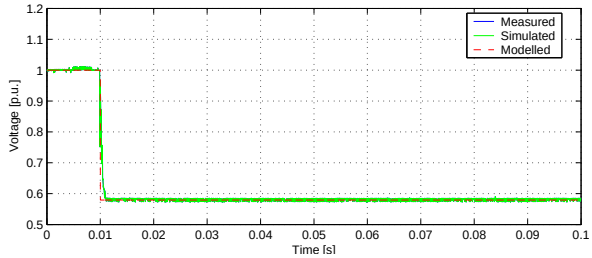

(e) Voltage - Step 3.

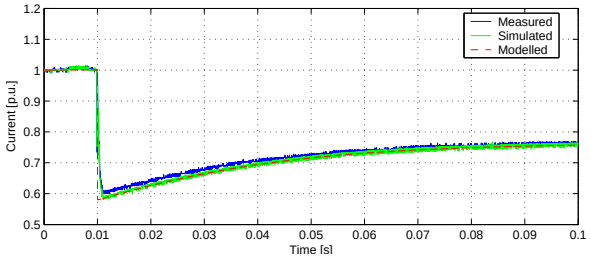

(f) Current - Step 3.

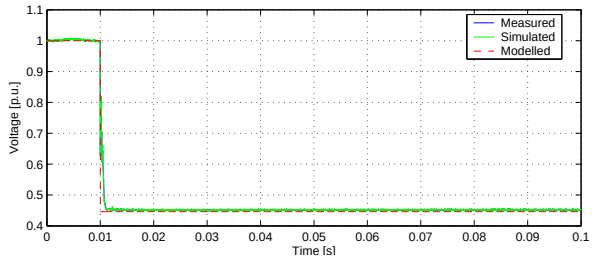

(g) Voltage - Step 4.

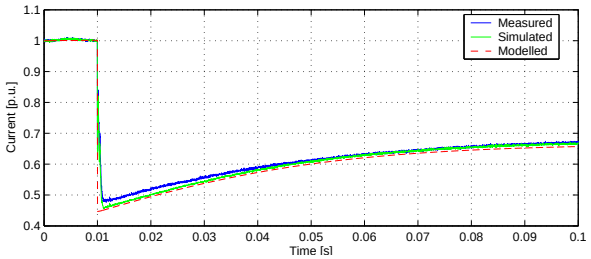

(h) Current - Step 4.

Figure H.20: Transient behavior of 60 W incandescent lamp 7.

60 W Incandescent Lamp 8

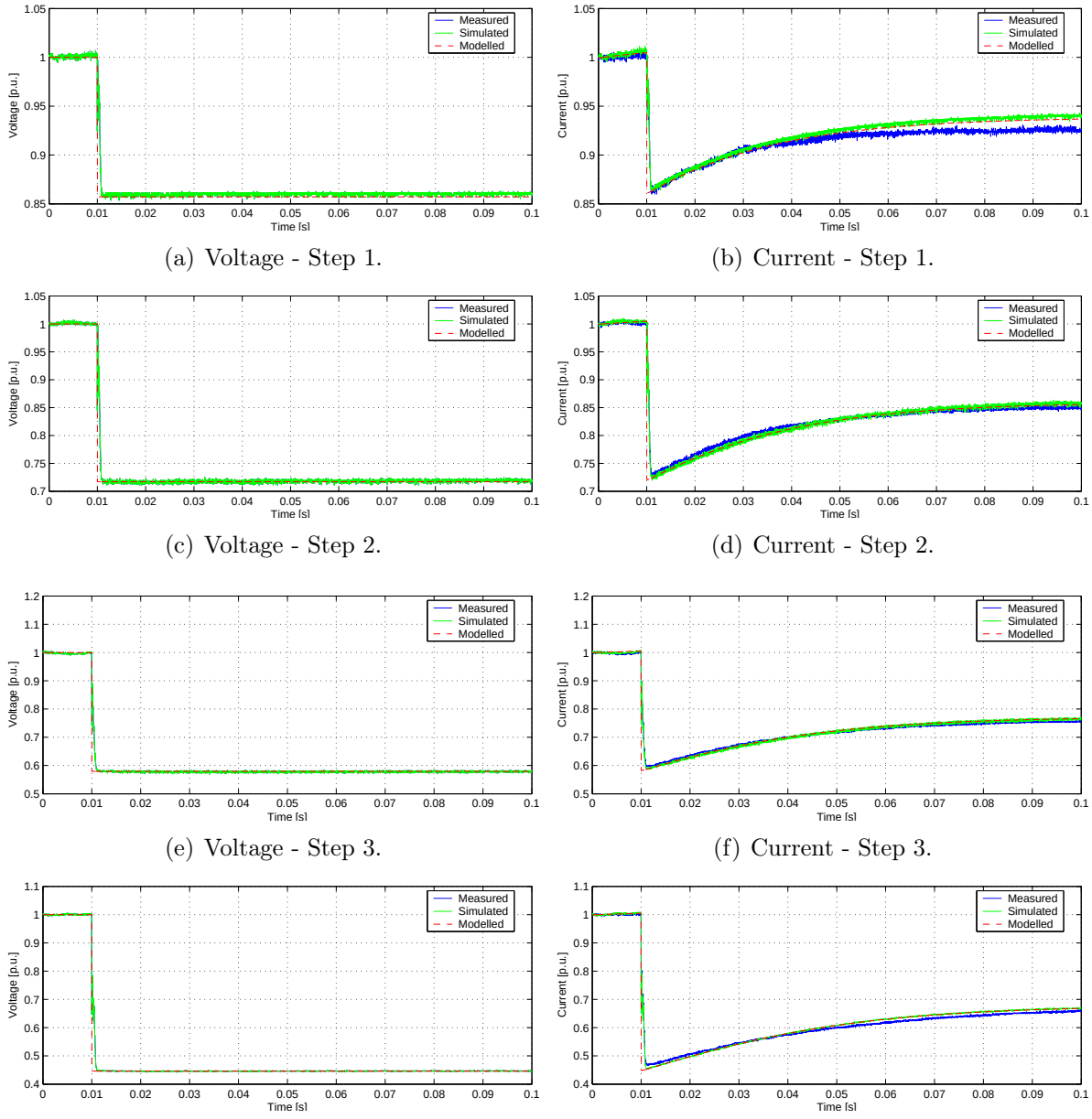

(a) Voltage - Step 1.

(b) Current - Step 1.

(c) Voltage - Step 2.

(d) Current - Step 2.

(e) Voltage - Step 3.

(f) Current - Step 3.

(g) Voltage - Step 4.

(h) Current - Step 4.

Figure H.21: Transient behavior of 60 W incandescent lamp 8.

75 W Incandescent Lamp 2

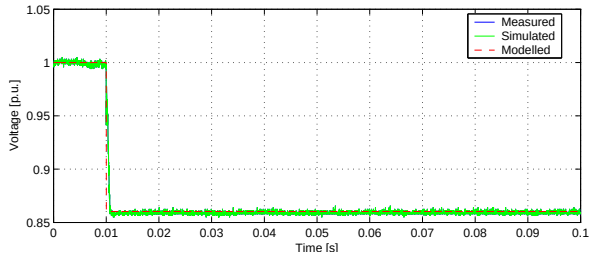

(a) Voltage - Step 1.

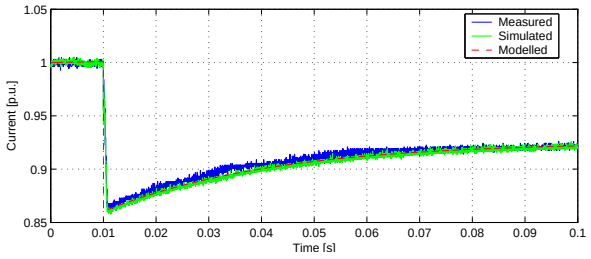

(b) Current - Step 1.

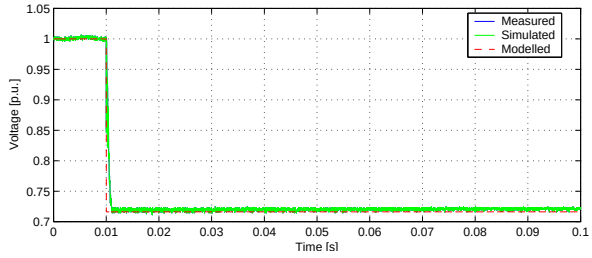

(c) Voltage - Step 2.

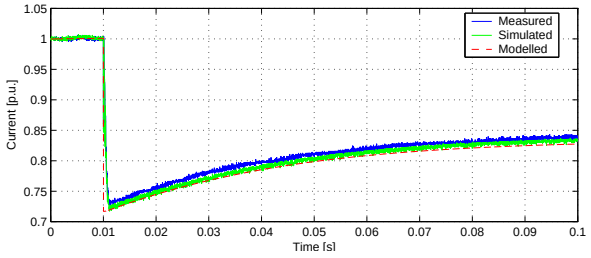

(d) Current - Step 2.

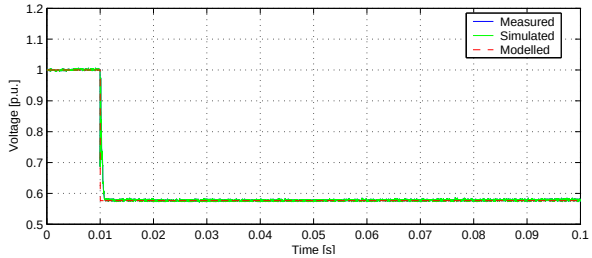

(e) Voltage - Step 3.

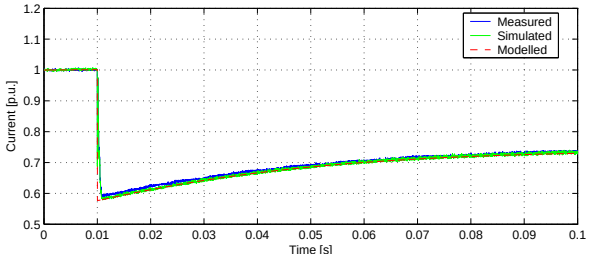

(f) Current - Step 3.

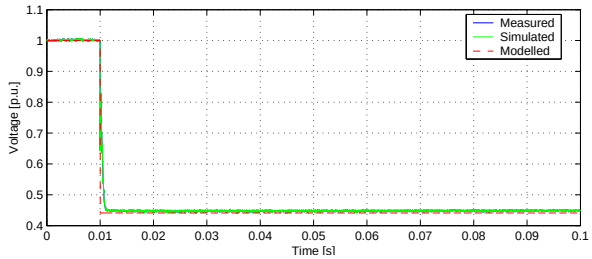

(g) Voltage - Step 4.

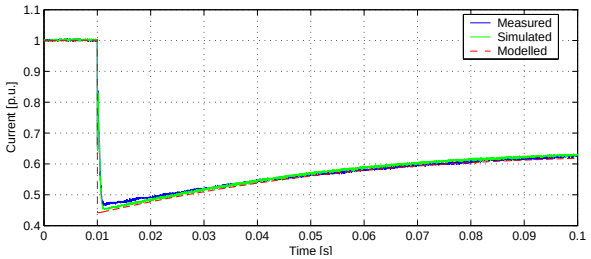

(h) Current - Step 4.

Figure H.22: Transient behavior of 75 W incandescent lamp 2.

75 W Incandescent Lamp 3

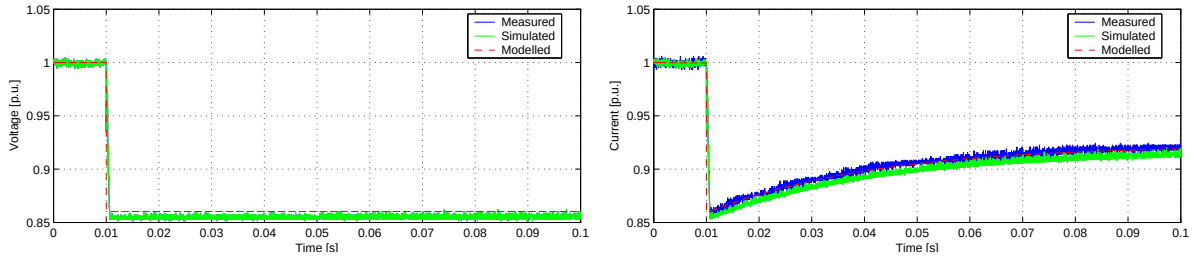

(a) Voltage - Step 1.

(b) Current - Step 1.

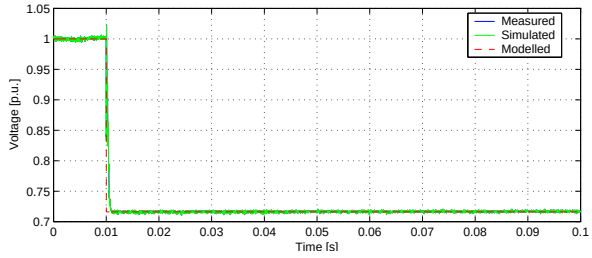

(c) Voltage - Step 2.

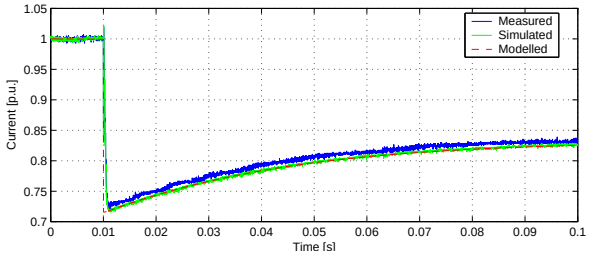

(d) Current - Step 2.

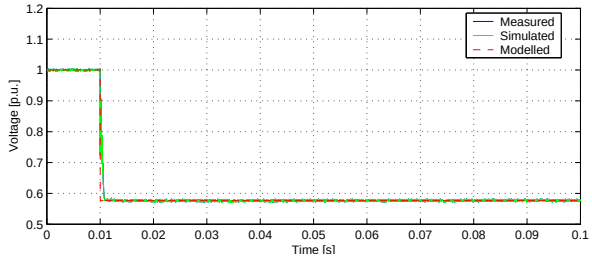

(e) Voltage - Step 3.

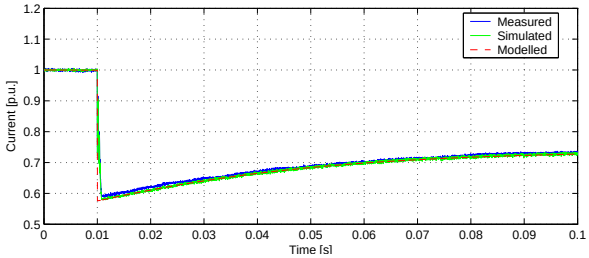

(f) Current - Step 3.

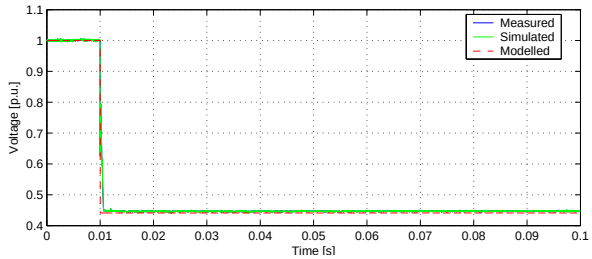

(g) Voltage - Step 4.

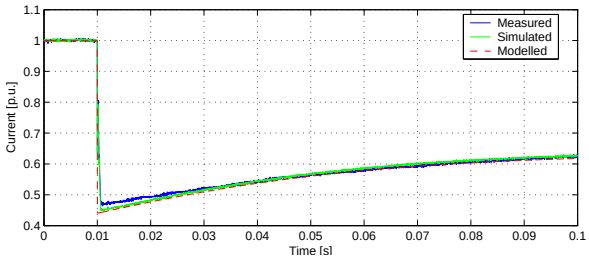

(h) Current - Step 4.

Figure H.23: Transient behavior of 75 W incandescent lamp 3.

100 W Incandescent Lamp 2

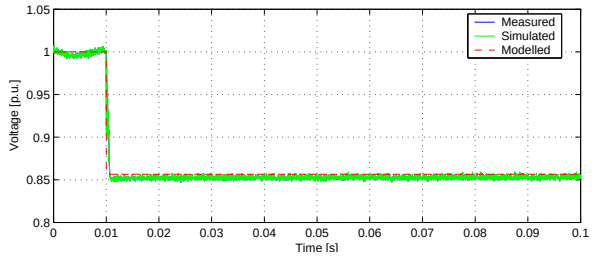

(a) Voltage - Step 1.

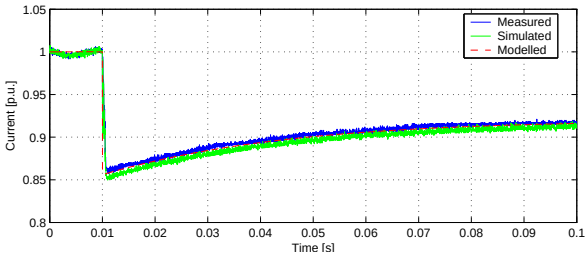

(b) Current - Step 1.

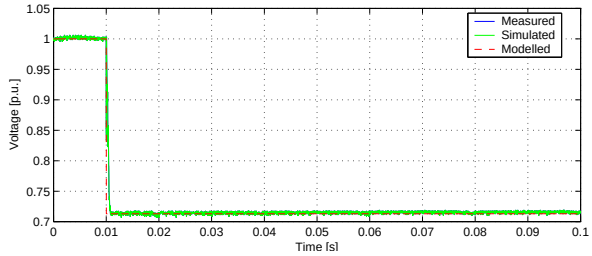

(c) Voltage - Step 2.

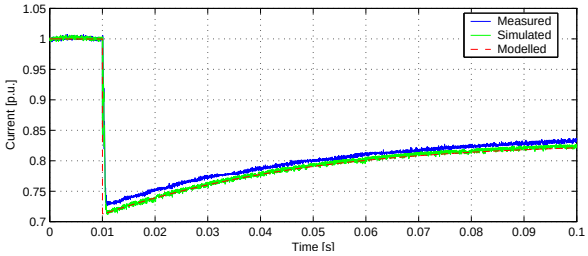

(d) Current - Step 2.

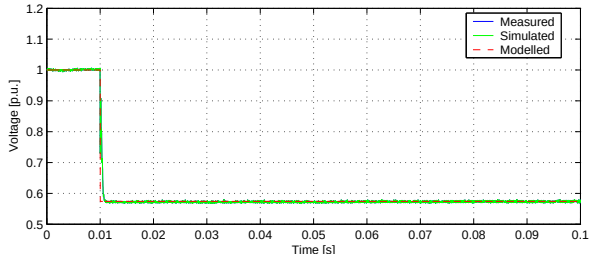

(e) Voltage - Step 3.

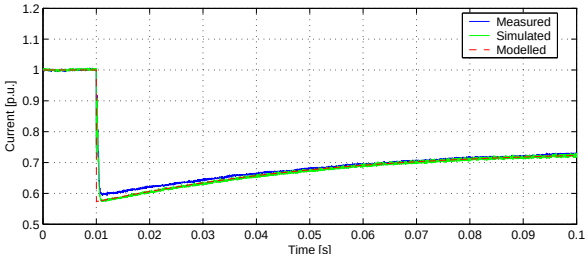

(f) Current - Step 3.

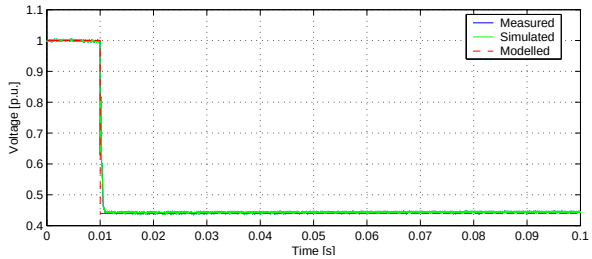

(g) Voltage - Step 4.

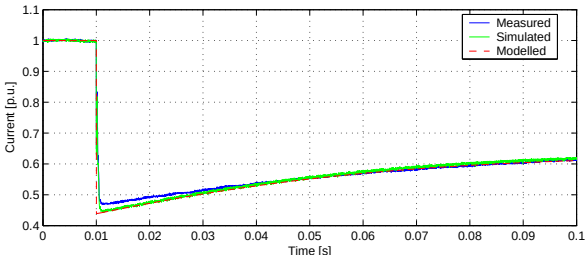

(h) Current - Step 4.

Figure H.24: Transient behavior of 100 W incandescent lamp 2.

100 W Incandescent Lamp 3

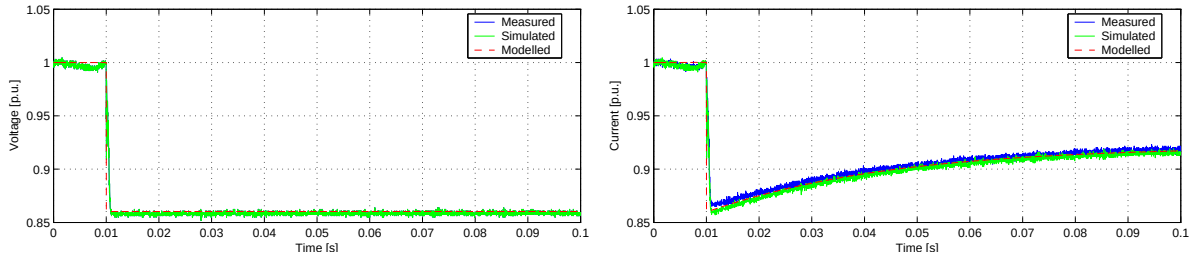

(a) Voltage - Step 1.

(b) Current - Step 1.

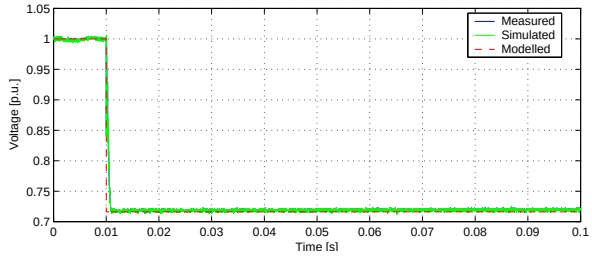

(c) Voltage - Step 2.

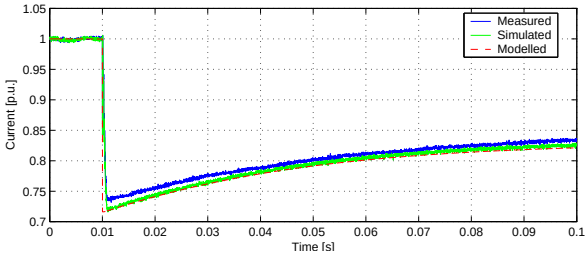

(d) Current - Step 2.

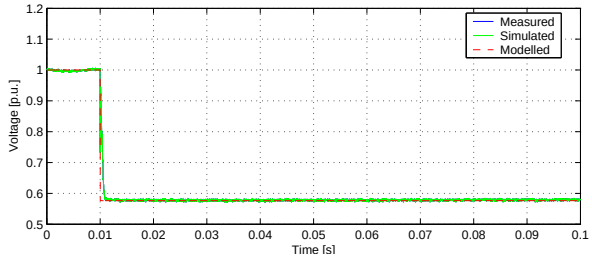

(e) Voltage - Step 3.

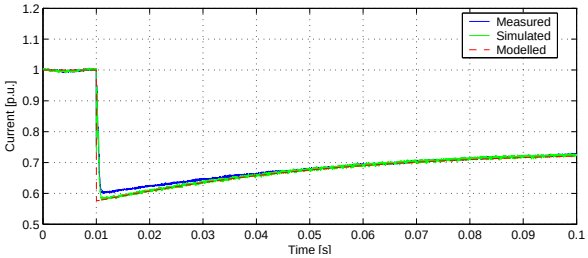

(f) Current - Step 3.

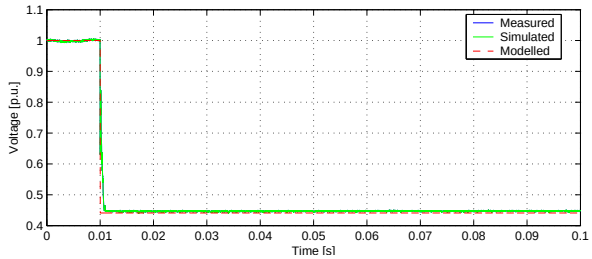

(g) Voltage - Step 4.

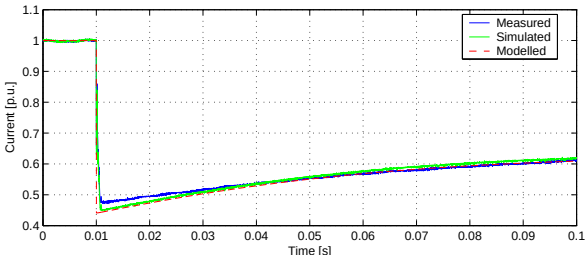

(h) Current - Step 4.

Figure H.25: Transient behavior of 100 W incandescent lamp 3.

100 W Incandescent Lamp 4

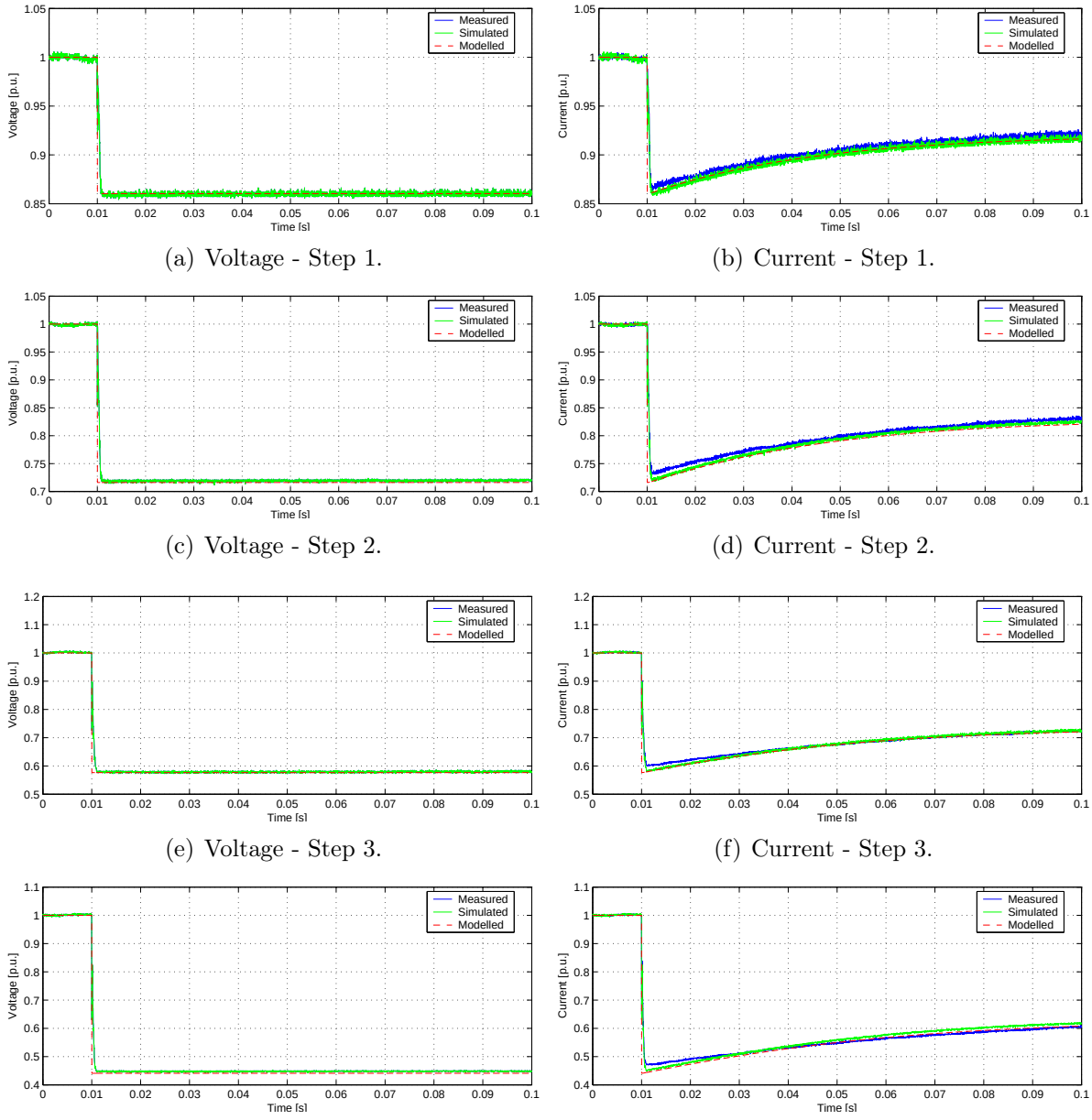

(a) Voltage - Step 1.

(b) Current - Step 1.

(c) Voltage - Step 2.

(d) Current - Step 2.

(e) Voltage - Step 3.

(f) Current - Step 3.

(g) Voltage - Step 4.

(h) Current - Step 4.

Figure H.26: Transient behavior of 100 W incandescent lamp 4.

150 W Tungsten Halogen Lamp 2

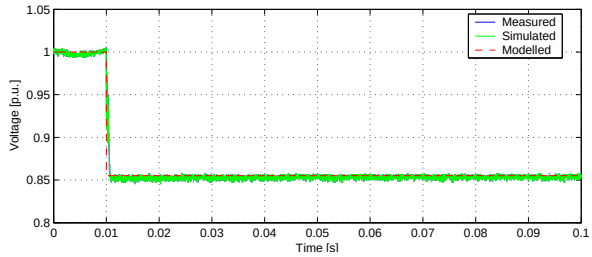

(a) Voltage - Step 1.

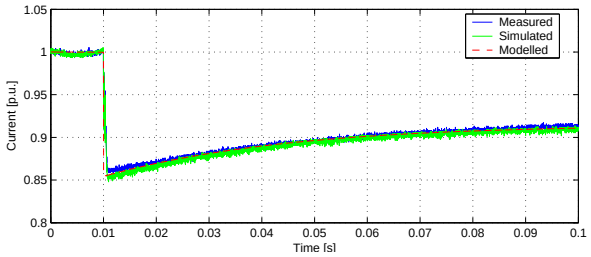

(b) Current - Step 1.

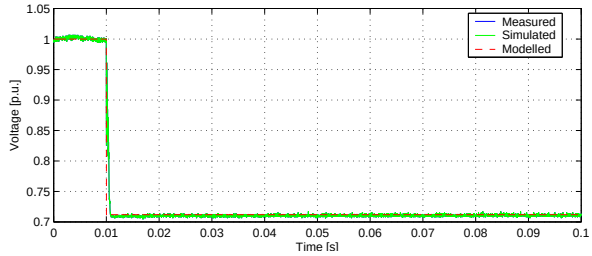

(c) Voltage - Step 2.

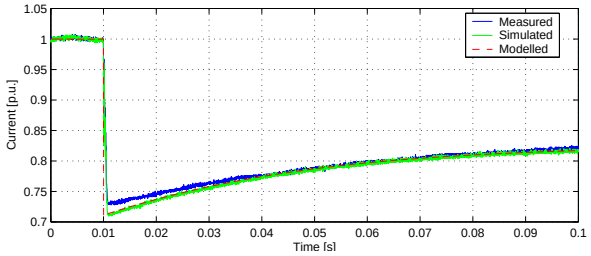

(d) Current - Step 2.

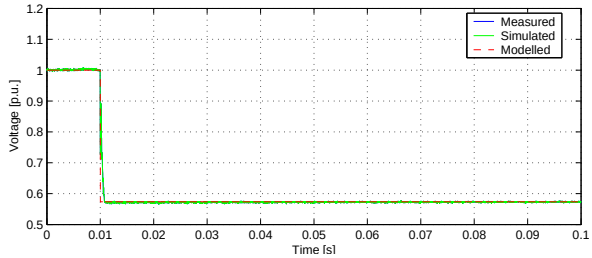

(e) Voltage - Step 3.

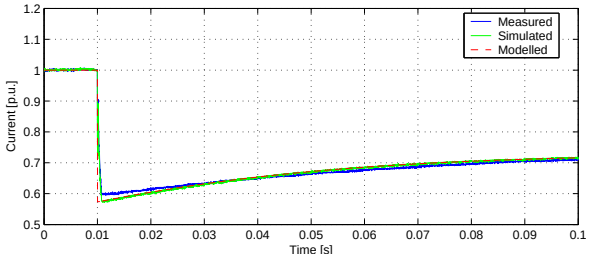

(f) Current - Step 3.

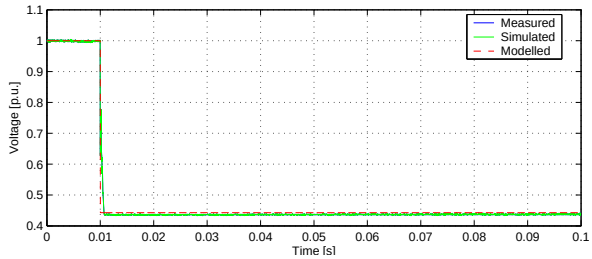

(g) Voltage - Step 4.

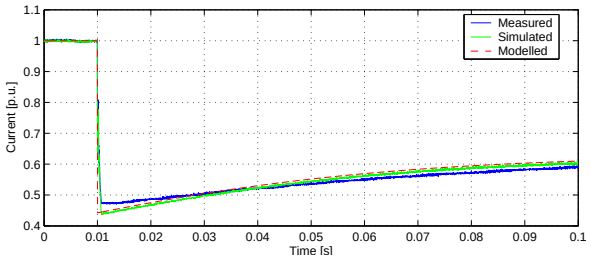

(h) Current - Step 4.

Figure H.27: Transient behavior of 150 W tungsten halogen lamp 2.